TORSIONAL VIBRATION ANALYSIS OF AUTOMOTIVE DRIVELINES

by

El-Adl Mohammed Aly Rabeih, BSc. & M.Sc.

Submitted in accordance with the requirements for the degree of PhD

Mechanical Engineering Department
The University of Leeds
Leeds, UK

March, 1997

The candidate confirms that the work submitted is his own and that appropriate credit has been given where reference has been made to the work of other

ABSTRACT

One of the most important source of noise and vibrations associated with vehicles is the vibration of driveline systems. Such phenomena are subjectively associated with customer complaints. In this study the torsional vibrations of driveline systems were investigated using discretised and lumped mass models of the system.

In the literature, many of the problems associated with torsional vibrations and refinement in drivelines have been tackled through relatively simple, lumped mass models combined with experimental measurements. However, some problems remain particularly where instabilities occur or complex coupling with other vehicle vibration modes exists. The review of previous work showed that although it is important to understand the dynamic behaviour of the individual driveline components; for example, engine, clutch, gearbox, etc., the whole system must be analysed together because of all the coupling which occurs.

The main source of excitation for torsional vibration of the driveline system is the engine fluctuating torque. A computer program using MATLAB subroutines was developed to obtain this fluctuation torque for different engine parameters for subsequent use in the modelling.

A substructure approach, using stiffness coupling technique with combined use of residual flexibility and modal synthesis, was used to analyse free and forced vibrations of the system, as a linear system. A computer program using MATLAB subroutines was designed to facilitate application of this technique. Good agreement between results for the overall system model and substructure model was found even for a few considered modes. This substructure technique offers significant computational advantages over other methods.

The effect of non-linear sources in the driveline system such as backlash, non-linear spring stiffness, Hooke's joint and angularity of the propeller shaft on the system torsional vibrations was investigated. The effect of backlash in the driveline system was significant and, as expected, vibration levels increased as backlash increased.

Hooke's joints caused an additional complex source of excitation but their significance is dictated by the details of the particular driveline design.

The modelling showed that instabilities commonly referred to a shunt or shuffle could occur during clutch engagement. The stick slip frictional properties of the clutch were crucial in this behaviour and the relative importance of various design features was quantified.

A mathematical model including torsional motion of the driveline system and other vehicle body motions was developed to analyse the ways in which the driveline couples with other dynamic components. Two running conditions were considered; steady state running and transient during clutch engagement. It was shown that the complete system was capable of self-excited oscillations under certain conditions during normal running as well as the instability which could occur during clutch engagement.

This comprehensive model represents an important contribution of the work in this area of research in two ways. First, it clarifies understanding of the dynamic coupling between the rotational and translational components of the whole vehicle system. Second, it provides design information to tackle instability problems and to lead to reductions in overall vibration levels.

TABLE OF CONTENTS

NOTATION

Because there are many symbols are repeated in different chapters, each chapter's notation is introduced individually in this section.

1-CHAPTER 2

A Piston area (m^2).

B Crank web width (m).

c Viscous damping coefficient (Ns/m or N.m.s).

D_1 Crank journal diameter (m).

D_2 Crankpin diameter (m).

D_e Diameter of the uniform equivalent crank (m).

F_d Damping force (N).

G Modules of rigidity of the crank shaft material (N/ m^2).

h Inclined crank web thickness (m).

i Gear speed ratio.

J_p Equivalent mass moment of inertia of the web and balance weight (kg m^2).

J_r Equivalent mass moment of inertia of the reciprocating parts (kg m^2).

J_j Equivalent mass moment of inertia of the crank journal (kg m^2).

J_{cp} Equivalent mass moment of inertia of the crank pin (kg m^2).

k Equivalent torsional stiffness (N.m/rad).

L Connecting rod length (m).

L_{cp} Crankpin length (m).

L_e Length of the uniform equivalent crank (m).

L_j Crank journal length (m).

m Reciprocating masses (kg).

m_c Connecting rod mass (kg).

m_p Piston mass (kg).

N Gears angular speed (rpm).

p Clutch clamp force (N).

P_g Indicated gas pressure (N/m^2).

r Mean clutch radius (m).

R Crank radius (m).

t Crank web thickness (m).

T Total engine torque (N.m).

T_i Reciprocating inertia torque (N.m).

T_g Indicating gas torque (N.m).

T_f Friction and pumping loss torque in engine (N.m).

α Hooke's joint angle (rad).

λ Crank radius to connecting length rod ratio.

ϕ Rotation crank angle (rad).

ω Uniform crankshaft speed (rad/s).

ρ Density of crankshaft material (kg/m^3).

μ Coefficient of friction between clutch faces.

2-CHAPTER 3

A Piston area (m^2).

c Cosine component coefficient of gas pressure harmonic components.

$g(\phi)$ Engine geometric function, see Eqn (3.2).

h_o Number of required harmonics.

m Reciprocating masses (kg).

N Engine revolution per minute.

n_c Number of cylinders.

n_s Number of strokes per cycle (2 or 4).

P_g Gas pressure (N/ m^2).

R Crank radius (m).

s Sine component coefficient of gas pressure harmonic components.

T Engine fluctuating torque (N.m).

α_{qk} Phase angle between q^{th} cylinder and 1^{st} cylinder for the k^{th} harmonic order (rad).

β_{kq} Total phase angle of k^{th} harmonic order and q^{th} cylinder, $\beta_{kq} = \gamma_{kq} + \alpha_{kq}$ (rad).

γ_k Phase angle due to sine and cosine combination of k^{th} harmonic order (rad).

ϕ Rotation crank angle (rad).

λ Crank to connecting rod length ratio.

ω Angular crank speed (rad/sec).

Suffixes

g Gas.

i Inertia.

k Harmonic order.

q Cylinder order.

3-CHAPTER 4

[A] A matrix defined by the Eqn (4.15).

[C] Damping matrix.

[K] Stiffness matrix.

$[k_c]$ Interface connection stiffness between substructures.

f_o Excitation force amplitude (N).

{F(t)} Excitation force vector.

[G] Compliance matrix or dynamic flexibility matrix.

[M] Mass matrix.

{Q} Generalised force vector.

n Number of lower modes.

N Number of total DOF of the system.

{x} Physical co-ordinate vector.

{y} Modal co-ordinate vector.

$\{\theta\}$ Torsional displacement vector.

$[\phi]$ Modal matrix.

ω System natural frequency (Hz).

Ω Excitation frequency (Hz).

$[\zeta]$ Damping ratio matrix.

Suffixes

n Number of substructures.

r Selected mode (rth mode).

l Lower modes.

h Higher modes.

i Internal degrees of freedom.

j Interface degrees of freedom.

ns Number of considered modes (retained modes).

s Substructure for superscript and static for subscript.

L Left substructure.

R Right substructure.

There are some variables with a multi-suffix, for example, ${}^{s}[\phi_{jL}]_{ns}$ is (jLxns) matrix of the retained normal modes, ns, of s th substructure corresponding to the left interface co-ordinates. Velocity and acceleration are denoted by a single and double dots respectively.

4-CHAPTER 5

[C] Damping matrix.

c Generalised damping coefficient or modal damping.

e Percentage deviation of natural frequencies, see Table (5.3).

h_o Number of considered harmonics of the engine fluctuating torque.

[K] Stiffness matrix.

K Connecting stiffness between substructures, see Fig (5.2a).

k Generalised stiffness coefficient or modal.

[M] Mass matrix.

m Generalised mass coefficient or modal mass.

N Number of degrees of freedom of the overall system.

n Number of retained modes of the overall system.

{Q} Excitation load vector.

β Phase angle of the excitation torque (rad).

ψ Total phase angle of the response (rad).

$\{\phi\}$ Eigenvector/mode shape.

$\{\Theta_o\}$ Steady state torsional vibration amplitude vector (rad).

Ω Angular speed of the engine (rad/sec).

ω Natural frequencies of the system (Hz).

$\{\theta\}$ Nodal displacement vector.

ζ Damping ratio.

Suffixes

i Internal degrees of freedom of substructures.

j Interface degrees of freedom of substructures.

r Particular mode, rth mode.

1,2 Refer to number of substructure (pre-superscript).

k Harmonic order of the engine fluctuating torque.

Velocity and acceleration are denoted by a single and double dots respectively.

5-CHAPTER 6

[C] System damping matrix.

ck_i Non-linear stiffness ratio of non-linear element i (k_n/k_{oi}), see Eqn (6.1).

{H} Fluctuating torque vector induced by Hooke's joint (N.m).

[K] System stiffness matrix.

k_i Total stiffness of i th element (N.m/rad), see Eqn (6.1).

k_n Non-linear stiffness coefficient.

k_{oi} Linear value of stiffness of i th element (N.m/rad), see Eqn (6.1).

M_f Friction torque induced by the clutch (N.m).

T Torque (N.m).

{y} State space vector.

α Hooke's joint angle (degree).

γ Angular backlash in the system (rad).

ϕ Angular displacement (rad).

ϕ_{maxi} Maximum angular deflection of the element i (rad).

ω_i Input angular velocity of the propeller shaft (rad/sec).

ω_o Output angular velocity of the propeller shaft (rad/sec).

Velocity and acceleration are denoted by a single and double dots respectively.

6-CHAPTER 7

A_o, A_2 Polynomial constants, Eqn (7.2).

A_1 Ingredient of friction coefficient.

[C] Damping matrix of the system.

F Clamping force (N).

[K] Stiffness matrix of the system.

[M] Mass matrix of the system.

M_f Friction torque induced by the clutch (N.m).

t_c Engagement time (sec).

r Mean friction radius of the clutch (m).

v Sliding speed (m/sec).

{y} State space displacement vector.

$\{\phi\}$ Angular displacement vector.

ω Angular mean sliding speed (rad/sec)

ω_e Angular engine speed (rad/sec).

ω_t Transmission speed (rad/sec).

μ_o Static friction coefficient.

$\mu(\phi)$ Coefficient of friction between the clutch friction plates.

7-CHAPTER 8

A_r Rolling resistance coefficient of the tyre.

c_{13} Longitudinal tyre tread to carcass damping coefficient (tyre longitudinal damping) (N.s/m).

c_{14} Vertical damping coefficient of the tyre (N.s/m).

J_{13} Mass moment of inertia of the road wheel including a large portion of the tyre (kg m^2).

J_t Mass moment of inertia of the tyre tread band (small portion) (kg m^2).

F_l Tyre longitudinal force (N).

F_r Rolling resistance force (N).

F_s Longitudinal slip force (N).

F_t Vertical tyre force (N).

k_{13} Longitudinal tyre tread to carcass stiffness (longitudinal tyre stiffness) (N/m).

k_{14} Vertical tyre stiffness (N/m).

m_u Mass of axle including wheels (unsprung mass) (kg).

m_b Mass of vehicle body (sprung mass) (kg).

M_a Restoring moment of the driving axles, $k_{12}(\theta_{13} - \theta_{12})$ (N.m).

{Q} Generalised force vector.

R Effective tyre rolling radius (assume it does not change with the tyre vertical displacement) (m).

S Longitudinal slip of tyre.

x_1, z_1 Longitudinal and vertical displacements of the axle or wheel centre respectively (m).

x_2, z_2 Longitudinal and vertical displacements of the vehicle body respectively (m).

θ_{13} Angular displacement of the wheel hub relative to the axle (rad).

θ_t Angular displacement of the tyre tread bands relative to the wheels (rad).

Note that all the variables are measured from a nominal equilibrium position i.e. only the perturbation motions are considered to linearise the system's equation of motion.

ACKNOWLEDGEMENT

First of all, I would like to express my sincere gratitude to **Prof. D. A. Crolla** and many thanks to him for his supervision of my work and his valuable guidance through this research.

Many thanks to all the department staff for their valuable advice and help during this work.

Also my thanks to technician staff of Dynamics and Control Laboratory for their help and advice using the Laboratory facilities.

I would like to thank all the people who have made this thesis feasible for me.

Many thanks to the people and government of my home country Egypt for their support.

Many thanks are reserved for all friends in the vehicle dynamics group. Also to the Egyptian community in Leeds who made the work circumstances enjoyable.

Finally my special thanks to my family, my wife and my children, for their endurance during this study.

To my family

My mother,

My wife and

My children Yara, Mohammed and Sarah

CHAPTER 1

INTRODUCTION AND LITERATURE REVIEW

1.1-INTRODUCTION

One of the most important subjects of current research is the reduction of vehicle weight, which helps improve vehicle performance and reduce fuel consumption as well as increasing overall efficiency. However, these improvements generally produce a negative effect in terms of noise and vibration. One of the most important problems concerning noise and vibration inside the vehicle is that associated with the driveline system because it is a major source of noise and vibration for vehicles ranging from automobiles to heavy trucks. Whenever these vibrations are transmitted to the chassis they cause a deterioration in the passenger comfort. Therefore, the vibrational properties of vehicle driveline systems are currently of considerable practical concern because they influence the subjective comfort ratings typically expressed in terms of "driveability", "smoothness", "refinement" etc. Overcoming these problems can significantly improve the customer's satisfaction and hence the manufacturer's success.

The automotive driveline system can be defined as the sum of the components starting from engine to the contact between tyres and road, Fig (1.1).

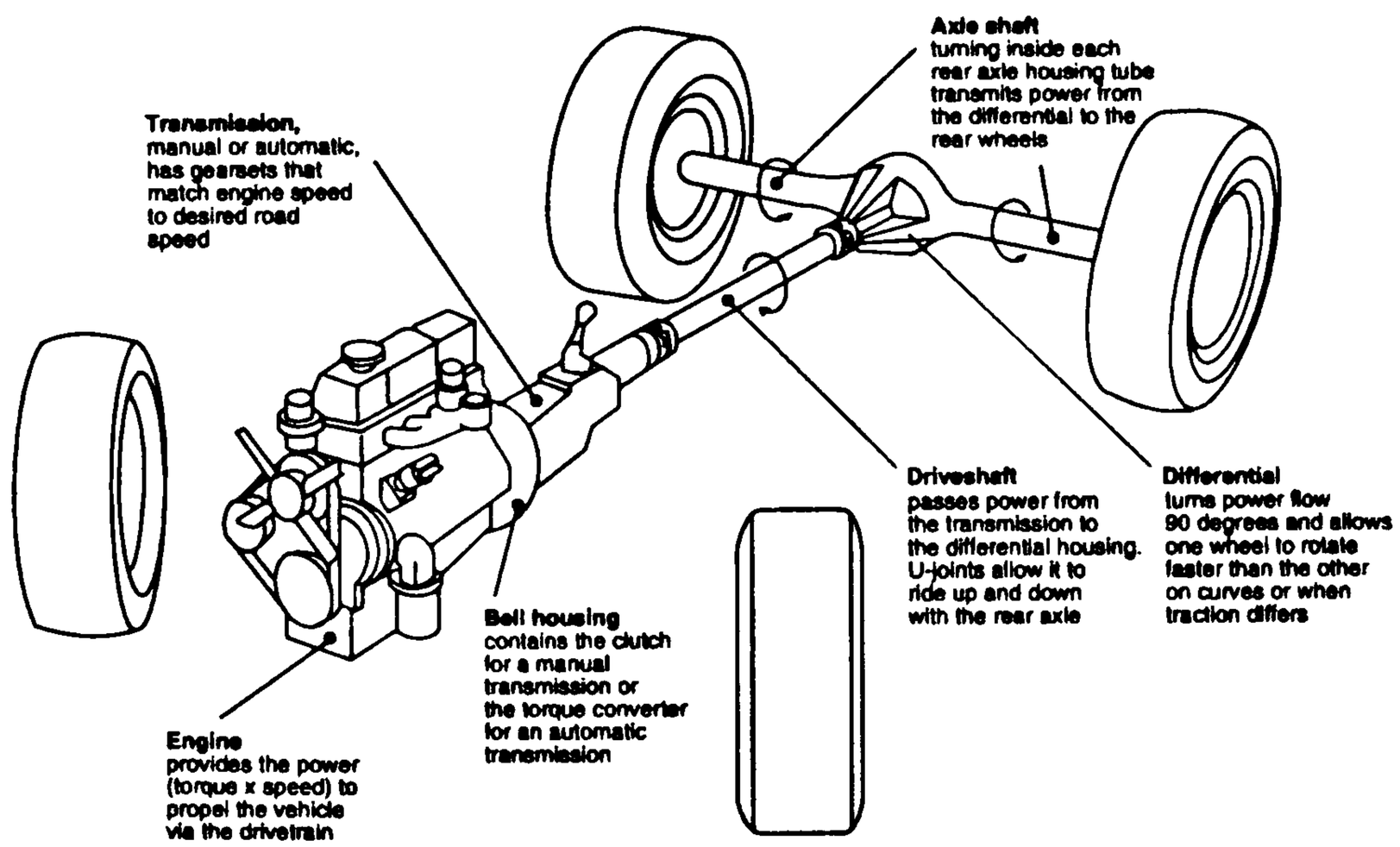

Fig (1.1) Automotive driveline system components [from 1]

Driveline systems that have been optimised for weight and efficiency tend to be highly sensitive to excitation. Table (1.1) shows an example of passenger car vibration caused by the driveline system, classified by frequency range and viewed in relation to physical phenomena [2].

Table (1.1) Classification of vibration noises caused by driveline system.

Frequency range (Hz)	*Exciting force*	*Type of vibration*	*Linear/ non-linear*	*Phenomenon*
2-10	Engine torque variation	Torsional	Linear	Surge (vibration)
2-10	Clutch non-linear	Torsional	Non-linear	Judder (vibration)
10-20	Propeller shaft joint angle	Torsional (Bending)	Non-linear	Vibration at start (vibration)
20-50	Engine torque variation	Torsional	Linear	Wind-up (vibration, boom noise)
20-50	Rotational unbalance	Bending	Linear	Wind-up (vibration, boom noise)
50-80	Engine torque variation	Torsional	Linear	Drive train torsional vibration (boom noise)
50-80	Propeller shaft joint angle	Torsional	Non-linear	Drive train torsional vibration (boom noise)
100-200	Engine reciprocating moment of inertia	Bending	Linear	Power plant/propeller shaft bending vibration (boom noise)
400-2000	Hypoid gear mesh	Bending (Torsional)	Linear	Power plant/propeller shaft bending vibration (differential gear noise)

Generally, driveline noises problems are associated with two categories, namely; idle gear rattle and driveline vibrations [3]. Idle gear rattle is a noise generated under low load conditions and is a direct result of gear tooth impacts. This problem predominantly occurs when the vehicle is stationary and the gearbox is hot. Components of the gearbox and gear train having a low inertia and lightly damping are susceptible to rattle when excited by the engine flywheel velocity fluctuations. The analysis of such problems requires detailed examination of the individual components within the driveline up to and including the gearbox. Driveline vibrations are noises emanating from the driveline system components such as engine, clutch and universal

joints, whilst the vehicle is in motion at different running conditions. In this study emphasis is placed on the driveline system vibrations.

There are many vibrational phenomena in the driveline which are important to study: (i) natural frequencies of the driveline in order to avoid coincidence of engine torque harmonics, and/or another excitation source, and driveline natural frequencies which could result in high stress level under load; (ii) forced response to the periodic excitation fluctuating torque from the engine, the torque fluctuation at the universal joints and the traction behaviour of the tyre; (iii) transient response of the driveline to any sudden change of the engine torque or gear shifting which cause so called 'shunt' phenomena and clutch judder phenomena which may occur during clutch engagement; (iv) torsional instability which could result a torsional failure of a driveline component due to severe torsional vibrations of the system.

There are many important components that introduce non-linear behaviour into the system such as the clutch, Hooke's joints, system free play and backlash. Also vibrations of the driveline system are coupled with other motions of the vehicle body like vertical and horizontal motions. In addition, the system may be subjected to transient input conditions when the vehicle is subjected to frequent stops and starts. All of these considerations make the analysis of the vibrational behaviour of the driveline system complicated and challenging to understand.

Generally, there have been two approaches to study vibration problems in driveline systems, experimental and computer simulation. The experimental approach which may lead to practical solutions to the problem, however, does not necessarily lead to an improved understanding of the vibration behaviour of a complex system like an automotive driveline system. Therefore, the advent of computer simulation applied to this problem has many claimed advantages, such as reduction in the development time, minimisation of the cost of the experimental work and achievement of optimal system design. In addition, experimental studies are typically expensive in terms of effort, cost and difficulty and they also require access to a production/prototype driveline.

Many of the previous published studies are quite elaborate and have been restricted to the study of individual components rather than the complete driveline system. However, many problems of driveline system design are the result of designer's combining components which are satisfactory when treated independently. Despite the great attention given to the study of this subject over the previous decades, further investigations are still needed to tackle the overall system problems.

1.2-Literature Review

1.2.1-Trucks and Tractors

Mazziotti in 1965, [4] reviews the functions, construction and operating characteristics of truck driveline systems. He studied the dynamic characteristics of constant velocity joints to show how they interact with the complete vehicle driveline. He outlined those factors that must be considered when engineering a driveline installation. These factors are; strength, life, torsional and transverse vibrations and response, its role as a transmitter or isolator and forces imposed on supports. This paper is helpful in the dynamic analysis of driveline systems and it is one of the most important references in this field although it does not contain any vibration results of these systems.

Several publications [5-10] modelled the automotive driveline systems as a set of inertia discs representing rotating masses linked by linear springs representing the torsional stiffnesses of the rotating shafts. Hui-Le et al in 1983, [5] developed a dynamic model for the driveline of a vehicle and all model parameters were evaluated experimentally. In this study, free vibrations for a torsional vibration discretized system for jeep, truck and coach driveline systems were performed and the steady state response of the system to the periodic excitation of the engine torque was calculated. The authors measured the oscillating torques on the input shaft of the gearbox, the propeller shaft and the rear axle shaft by strain gauges. Finally, they investigated the effect of the damper on reducing the vibration experimentally. They showed that it is necessary to incorporate a torsional vibration damper into the automotive driveline for improving its torsional vibration behaviour. Although the

findings are as expected and the model is simple, the approach is interesting particularly in representing the damping in the system components.

A general purpose program called (TORVIB) was used by Birket et al in 1991, [6] for a complete torsional analysis of the many unique drivelines specified by truck customers. In this program the driveline components, engine, flywheel, clutch, transmission, propeller shaft, and axle were modelled with equivalent inertias, stiffnesses and damping. A unique identification code was assigned to each component and all component data were stored in a database. Firing order and angles were used to assemble a multi-cylinder engine from the single cylinder torque data. The dynamic single cylinder torques were properly phased and applied to each cylinder inertia of the engine. TORVIB automatically assembled the equation of motion beginning with the engine and continues to the rear axle using components' data from the database. The authors have modified the program to include universal joint effects. They represented the joint in a simplified finite element model containing one rotational degree of freedom at each node. Each joint was separated into two degrees of freedom, one representing each yoke and a large torsional spring added between the two yokes. Universal joint effects were added by updating the mass and stiffness matrices to include degrees of freedom at each yoke on a universal joint. In this program, only one torque path was permitted while the branching of the torque to model the rear axle needs a special component model.

Lu in 1994, [7] focused attention on the analysis and control of torsional vibrations of a certain type of truck drivetrain. He generated a 41 DOF analytical model for torsional vibration of driveline systems. The driveline system was divided into four substructures. The authors used a physical coupling substructure, rather than modal coupling, for convenience of representation. The free vibration characteristics of this model were investigated and structural modifications to control the torsional vibration were performed. The structure dynamic modification analyses showed that torsional vibration damper in clutch driven plate, torsional vibration absorbers on engine crankshaft and propeller shafting, torsionally flexible coupling, etc. are useful components to control the torsional vibration of an automotive power driveline.

Discussions about the dominant substructure, the symmetrically branched driving axle substructure, advantages and disadvantages of simplification of the branched system were introduced. Since the high frequency modes are out of the operating range of the driveline system, the model may be simplified and some of the DOF could be removed, for example, the driving axle substructure because the moments of inertia of the axles are small.

Some of the useful work on driveline system analysis has been associated with tractor drivelines. Although, these systems include additional non-linear elements over and above those found in typical automobile driveline systems, such as overrun and overload clutches, nevertheless much of the modelling is relevant. Crolla in 1978 and 1979, [8, 9] described a theoretical analysis of a tractor and machine Power Take Off (PTO) driveline using a simplified three inertia model. The effect of Hooke's joints and non-linear elements such as backlash, overload and overrun clutches were studied, and the frequency response curves for the driveline of a typical tractor and drum mower were presented. He also described field measurements of the driveline torque loading. The model is simple but it gives a general idea about the torsional vibration behaviour of the system especially the method of modelling the non-linear elements of the tractor and machine's driveline system.

Drouin et al in 1991, [10] built an overall dynamic model of a driveline system of an agricultural tractor to analyse the torsional vibration behaviour of the driveline system using inertia discs and massless torsional springs equivalent to the various parts of the driveline. The model was tested by comparing the global torsional stiffness of the model to experimental measurements of the actual stiffness for different gears. The natural frequencies of the tractor were determined showing that a complex mechanical system such as an agriculture tractor driveline system could be idealised with regard to torsional vibrations to improve its design. The model can be used in the early stages of system design to provide a general idea about the system natural frequencies. The authors did not include any damping in the model and furthermore, the non-linearities of the non-linear components of the system were not considered. The system damping

and non-linear sources should be included to obtain the accurate vibrational response of the system.

1.2.2-Passenger Cars

Over the past three decades, the demand for increasing comfort where noise and vibration in passenger cars are concerned has enhanced the significance of the driveline, with its multitude of vibration exciting and transmitting components, to an ever increasing degree. Some authors have used simple models of driveline system to provide a general idea about the system vibration behaviour [11-13].

Sykes and Wyman in 1971, [11] calculated the frequency response and modes of vibration of a conventional automobile driveline, engine-gearbox assembly, propeller shaft and rear suspension, using receptance methods. They idealised the driveline into a single non-uniform beam and used a transfer matrix version of Myklestad's method to determine the receptance of the non uniform beam components. The complete driveline system was divided into only two subsystems, the first representing the engine-gearbox assembly and the second representing the propeller shaft-rear suspension assembly. This technique showed the difficulty of representing the driveline as a non-uniform beam because the dynamic characteristics of the system were strongly dependent on the joints between the individual components.

Ergun in 1975, [12] carried out a preliminary study of the torsional vibration of the driveline of a vehicle. He used the theory of vibrations to reduce the driveline to an equivalent system of inertias and torsional springs. The natural frequencies of the system were calculated by approximating it to a four inertia system. He performed test runs using a Zephyr passenger car which was instrumented by a torsiometer, an FM tape recorder and two magnetic transducers. The nodes of the 2nd and 3rd modes were found to be very close to the rear wheels. The capability of the model is limited since the driveline system was simplified into only four inertias and did not include all component details. However in many cases a simple model gives a good estimation of the natural frequencies of the system when the resonant frequencies of the torsional vibrations of a driveline are required.

Chikamori and Yoshikawa in 1980, [2] reported important results of noise and vibration of driveline system. Their study covered linear and non-linear vibration analysis of the system, engine surge and driveline vibrations, and differential and driveline vibrations. The effect of non-linear elements such as the clutch, free play and propeller shaft joints was studied. This study explained and introduced principles of many vibration problems in driveline systems such as clutch judder, engine surge and differential gear noise. The authors clarified the clutch judder as the self-excited vibration generated by the speed characteristics of friction torque when clutch engaged. They stated that the surge occurred due to the vibration of the vehicle body in longitudinal directions at low frequency by the characteristic vibration of the driveline system occurred by engine torque variation. They showed that the differential gear noise is generated as the vibration compelling force generated by the engagement of the hypoid gear is amplified by the resonance of the rear suspensions of the drivetrain. This paper is an important reference to provide models for the most important vibration phenomena in vehicle driveline systems such as clutch judder and engine surge. It provides a good outline of the studies in this field especially the classification of phenomena of driveline system and its type, causes and frequency range of each of these phenomena, see Table (1.1).

Reik in 1990, [13] presented a study of the torsional vibrations in vehicle drivetrain systems. He discussed the most important sources of torsional vibration of a vehicle driveline and analysed the gas forces in the engine suggesting them to be the main source of excitation for torsional vibrations in the system. Measuring procedures for the torsional vibrations causing gear rattle or boom were described. An example was provided showing how measurement and calculation complement each other during the system tuning process. A simple model consisting of three rotating inertias (engine, transmission and vehicle) linked together by linear springs was used. This simple model provides adequate information for many vibration problems, but it is important to emphasise that it can not be used to illustrate all problems of driveline vibration. In addition, the author ignored the inertia forces as an excitation source of the torsional vibration of the engine although they strongly affect the time-varying behaviour of the engine torque especially in high speed vehicles.

Zhanqi et al in 1992, [14] constructed a mathematical model including torsional, vertical and vehicle fore-aft vibrations to study the coupling of those vibrations together. Factors which effect on the vibration coupling of the system were introduced. These factors were; excitation source, tyre type, longitudinal stiffness of suspension and load vehicle conditions. Forced vibrations arising from the engine and road were simulated. Different road conditions and their effects on the system vibration behaviour were investigated. The study concluded that the major source of excitation of the driveline torsional vibration is the engine when a vehicle travels over a good asphalt road whereas the road excitation acted as a major source that excites the fore-aft vibration when the vehicle travels over a rough road. The study introduced a good approach to construct a comprehensive model which couples the different vehicle motions but the coupling associated with the suspension system was not exactly defined in this system. In addition, the authors concentrated all the vehicle mass on the rear suspension only. Furthermore they disregard the tyre/ road force although it is a function of the vertical motion of the vehicle.

The modelling of driveline vibration analysis posses the risk of incorrect projections because some times systems are oversimplified when defining the analytical model or masse, stiffness and damping coefficients do not accurately defined the system. Therefore it is very important to measure vibration of driveline systems. There are several publications concerned with experimental tests to investigate the driveline system vibrations [15-17]. Parkins in 1974, [15] conducted an experimental study of the driveline vibration modes and internal noise under normal road excitations of a car in which the driveline included the drive shaft, axle, semi-elliptic multi leaf spring and wheels. The author identified the driveline vibration modes in the laboratory by applying harmonic forces to various locations within the driveline system. Eleven resonant modes were identified in the range 10-200 Hz. Since the reduction of the internal noise inside a vehicle is a basic goal of vehicle design, this study attempted to establish the source of all contributions to the internal noise in order to decide which could be attributed to the driveline vibrations.

Healy et al in 1979, [16] used two vehicles as the basis of an experimental study of the driveline vibrations and their influence on the interior noise of the vehicles. Bending vibrations of the rear axle, torsional vibration of the rear axle casing and the gearbox vibrations were measured with accelerometers attached at suitable points. The displacements of the torsional vibrations of the rotating components were measured at three points along the driveline, at the front free end of the crankshaft, at the rear end of the propeller shaft and at the wheels. The interior noise level was measured by an omni-directional microphone positioned at the head height between the driver and the front seat passengers. These tests suggested that most of the peak levels of noise in the interior of a vehicle may be associated with resonance of the driveline vibrations. The analyses were carried out over the frequency range from 50 Hz to 500 Hz although in the range lower than 50 Hz there are many resonant frequencies of driveline system.

Exner and Amborn in 1991, [17] were concerned with a measuring system by which vibrations in rotating shafts and joints can be measured when the vehicle is in motion. They carried out measurements on rotating and non rotating components of the driveline of front wheel drive passenger cars. They used a laser system to measure lateral as well as torsional vibrations. As a source of vibration, the engine with the gas and inertial forces formed the most important exciter. In addition to that gear meshing in gearbox and differential for the most part higher frequency exciters can be superimposed. The individual excitations were transmitted to the car body through some components of the driveline system. In order to decrease the transmitted vibration by components that are linked directly with the car body, elastic units with damping should be used as mounts of these components. Using the laser system gave actual excitation measurements because the vehicle was in motion and therefore in a realistic running condition.

Although the experimental tests give direct measurements of the system behaviour, theoretical analyses are also required to understand the problem and to investigate effects of parameters on the system behaviour. On the other hand, analysis of experimental results is complicated and it is often difficult to distinguish between the

sources of excitation to know the individual effect of each source on the system behaviour. Therefore, there have been many driveline system simulation tools published in the past two decades to aid the design of vehicle driveline system and to minimise the cost of the experimental tests [3,18-20]. Hedges and Butler in 1979, [3] developed a 'CAD' system to study the idle gear rattle and vibration problems in vehicle drivelines. The authors adopted a modular approach to represent the driveline components. In this approach, the driveline system was broken down into a series of simple modules such as a clutch, gear pair, differential, etc. The driveline system was constructed from a set of these modules whose torsional vibration properties were definable. They used an interactive computer program to connect the individual modules together to represent any driveline configuration. The approach was used to recommend of clutch design capable of eliminating idle gear rattle and driveline vibration. This modular approach is adopted for the simulation analysis of the driveline system because it can be used for any configuration of the system. The CAD system was found to be successful in analysing driveline vibrations and idle gear rattle problems.

RENAULT formulated a driveline behaviour simulation tool (MOTRAN) several years ago in order to analyse, monitor and optimise drivelines. Tantot and Chapon in 1992, [18] have presented the basic principles and the generalised equations embodied with this program. The program deals with the simulation of the dynamic torsional behaviour of drivelines from the engine to the road wheels. The driveline system was modelled by a sequence of inertias and stiffnesses representing individual components of the system. The program user built the equivalent model using a catalogue of elementary and standard functions. An identity card was associated with each function of basic element in which appears the name and the characteristics necessary to define the element. Therefore, the program can be used for any driveline configuration. This approach and the modular approach described in [3] are similar and applicable for any configuration of driveline. In MOTRAN the input data are the system characteristics, inertia and stiffness, of each driveline component, while in the modular approach the input data are the types of modules which represent components of the system.

The work of Stuecklschwaiger et al in 1993, [19] was concerned with the optimisation of driveline components and their connections to the chassis. The model was generated by using measured input data particularly for elastic elements giving due consideration to non-linear characteristics. The main dynamic properties of the parts were determined by rough calculations or by experimental testing. A computer simulation for the layout of the automotive driveline was generated and this computer simulation was additionally utilised to simulate the experimental techniques and to identify and optimise the driveline component parameters and thus to reduce the number of tests. A subset of parameters such as engine mount stiffness was investigated. Two computer models of the driveline were represented; one of them for a front axle driven passenger car and another for a rear axle driven passenger car. The investigation of the effect of the engine mounts on the vibration behaviour of the driveline system proved interesting in that the hydraulic engine mounts could be used effectively to modify the system behaviour.

Hong in 1996, [20] focused attention on the dynamics and performance of road vehicles under transient accelerating conditions. This was accomplished through the combination of a dynamic engine model, a dynamic power train model and a dynamic road-load model. A computer package capable of a dynamic simulation of performance under transient accelerating conditions was developed to design the power train system. This work succeeded in appending mechanical inertia, thermal inertia and flow inertia effects on the original steady-state engine performance predictor so that a dynamic power train model was added to the model. This is important since the relation between the engine speed and the road speed under acceleration conditions is different to the steady-state relationships normally assumed. It is useful to study the performance under transient conditions because these are normally the main cause of unwanted emissions.

Some authors have used standard computer packages in order to analyse vehicle driveline systems. Ambrosi and Orofino in 1990 and 1992, [21,22] modelled driveline components using standard computer codes such as NASTRAN and ABAQUS to analyse a complete two and four wheel drive vehicle driveline dynamic behaviour. The

typical driveline model consisted of an assembly of finite elements simulating all the rotating shafts from engine to tyres. Modal and forced vibration analyses were used to identify natural frequencies and mode shapes. Steady state response, due to the second order harmonic excitation, was used to investigate the influence of the main driveline components on gear noise and forces transmitted to the car body by the power unit elastic mounts. A transient response was also performed in order to simulate the non linear effects due to clutch, engine mounts and tyres spring rate and damping coefficient. In these studies the harmonic orders other than the second have not been taken into account although they are significant in the engine fluctuating torque. Although the standard computer packages may be powerful, they are restricted to use certain function or mathematical algorithms which may not meet the designer's requirements.

Some authors have been concerned with ways of attenuation or damped the driveline vibration. Schwibinger et al in 1991, [23] described an experimental and theoretical approach to investigate vibration and noise problems in a driveline system of a passenger car. Vibration control products such as crankshaft damper, halfshaft damper and belt coupling damper were discussed. The authors compared the crankshaft vibrations for different damper designs that showed the potential for further vibration and noise reduction. Also, they provided two examples of the optimum tuning of crankshaft dampers. In the first, a dual mass torsional damper was used to reduce the coupled torsional and bending vibrations of the crankshaft, as well as the noise. In the other, a dual mass torsional-bending damper reduced the torsional and bending resonance vibrations of crankshaft. Two vibrations and noise problems in drivetrain were torsional vibration of a driveshaft, excited by gear mesh, and a bending resonance of a half shaft, excited by engine fluctuation. The authors showed how they can be solved by elastomer vibration dampers. Because there is a wide range of operating speed of vehicles and large number of excitation frequencies it is difficult to achieve vibration isolation in the driveline system over the entire speed range using a torsional damper. As a result, the tuning of torsional dampers always represents a compromise of acceptable vibration levels.

1.2.3-Driveline Vibrational Phenomena

Shunt/shuffle

Shunt or shuffle is the first torsional vibration mode of the driveline system. Fothergill and Swierstra in 1992, [24] developed a model for a whole driveline and suspension system of an automotive to allow simulation of shunt phenomenon. Ultimately, the objective was to understand shunt phenomenon and correlate the model to the test results from a special prototype in order that Audi could use it as a working tool with which to further investigate and solve of shunt problems. They found that shunt phenomenon in a front wheel drive (FWD) experimental vehicle was due to the excitation of a resonance of the system. The key flexible components were drive shafts and clutch. Also, the drive shaft and clutch damping influenced the shunt magnitude, but not enough to reduce it to acceptable level. A high level of damping in a device between the clutch and flywheel could effect a cure. Driveline mounting characteristics had only a limited influence on the nature of shunt. The engine torque rise/fall time was an extremely important parameter. The mathematical model was kinematically accurate but it was limited in the modelling of the vehicle dynamics. The authors removed the tyre stick/slip behaviour showing that this aspect of tyre behaviour was not relevant to shunt although the stick/slip motion produces a self excitation longitudinal force which is likely to affect the shunt.

Rooke et al in 1993, [25] were concerned with the shuffle or shunt phenomenon which results from driver throttle input. They discussed the shuffle response using a mathematical model of the driveline subsystems. In this model, the engine was represented as producing idealised torque profiles to represent the low order dynamic torques. The engine rotational dynamics were represented by a single lumped inertia. This is a satisfactory representation of the torsional dynamic of the drive train, however in order to make driveline mount recommendations, they developed a full six degree of freedom model. The transmission inertias were aggregated as a single lumped inertia located at the gearbox input shaft. The dynamics of the clutch were represented by a non linear spring and coulomb friction between the engine and transmission inertias. The axle dynamics were represented with a simple linear torque

displacement relationship. The tractive effort was represented as a non-linear function of tyre slip ratio based on experimental data obtained on a rig and only the fore-aft force was represented. Two key results from the parameters study were presented; the influence of the torque rise time and profile on the shuffle response and the importance of driveline stiffness control to influence both shuffle frequency and utilisation of available damping. The shunt may be caused by friction vibration induced from the clutch during the engagement, however this study was restricted to analyse the shunt resulting from driver throttle input only.

Engagement problems

There have been several attempts to explore various aspects of the engagement problems. Newcomb and Spurr in 1972, [26] described an experimental study to investigate the conditions under which the clutch judder occurs. Their investigation showed that judder is a mechanical resonance phenomenon caused by cyclic variations in the load on the clutch. They discussed the practical results with particular emphasis on how to reduce the tendency of clutch to judder. A complete description of the test machine and how the tests was carried out was presented. In the test rig the clutch was driven by an electric motor although it was recognised that in practice a vehicle engine produces a fluctuating torque which also affects the clutch behaviour.

Lucas and Mizon in 1978 and 1979, [27,28] presented a basic mathematical model of the engagement period to quantify the temperature reached during the engagement period. They introduced a mathematical model for engine, clutch, driveline and vehicle train as two subsystems. The authors showed that the heat generated during the engagement depends on the manner in which a driver manipulates the clutch and engine during take-off. They used an interesting expression for the friction coefficient in which the variation in the coefficient was described as a function of temperature, rubbing speed and contact pressure. However, the system was not assumed to have any flexibility, therefore it is not appropriate for a vibration study.

There have been other attempts to study the characteristics of the friction materials used in clutches and their effects on the engagement problems. Experimental and theoretical approaches to friction in wet clutches were studied by Risbet et al in 1982,

[29]. Two types of friction materials were used; sintered metals and impregnated paper. The authors monitored the effect of load, initial speed, oil temperature, disc inertia and friction material on friction torque. They developed three models to simulate the dynamic behaviour, isothermal, porous isothermal and thermal. Satisfactory agreement between theory and experiment was only obtained with the thermal model for sintered metals. In this model the coefficient of friction decreased with temperature and pressure and was practically independent of initial speed and inertia. From the previous studies, the characteristics of friction materials are the most important parameters to control and solve most of the engagement problems.

Maucher in 1990, [30] introduced a theoretical study of the clutch judder and discussed the effect of various parameters on the judder phenomenon. These parameters included the gradient of the friction coefficient, the damping value, the clamping load, the mass moment of inertia and the torsional spring rate of the driveline. However, he simplified the driveline vibration model effectively into a one degree of freedom system and so his conclusions are not widely applicable.

Kani et al in 1992, [31] determined experimentally that the gradient of friction coefficient, value of $d\mu / dv$, has a negative value when judder occurs and their theoretical modelling was able to show the same phenomenon. Factors which control the friction coefficient versus speed characteristic were clarified. They also determined that the $d\mu / dv$ value varies depending on the type and amount of a thin film formed on the friction surfaces and that a better characteristic can be obtained when a greater amount of superior carbon is added to the friction materials.

Szadkowski and Morford in 1992, [32] deal with clutch engagement problems. They used an engineering approach to performance level prediction of starting a vehicle without use of a throttle, based on a dynamic clutch engagement model. A computer simulation of engagement dynamics was used to study the lock-up mechanism and to develop proper prediction procedures. A mathematical model consisting of two inertias, elastic properties of the clutch damper, varying engine torque and clamping force was used. The mathematical model was used to determine sliding velocity, the torque transmitted through the clutch and the rate at which energy is dissipated during

engagement. For various loading conditions, they calculated lock-up parameters such as slip time, damper twist angle, total energy dissipated and transient torsional including clutch torque overshoot could be ascertained. Numerical examples were used to identify key design problems such as influence of engagement speed on vehicle performance and comfort. Some practical recommendations were made in the form of design specifications of clutch system to improve engagement quality. The model incorporated new features in comparison to similar models because it included not only elastic properties of the clutch damper but also varying engine torque and clamping force.

Axle tramp

Axle tramp (wind-up/axle pitch) is a rotary oscillation of rigid axles about the axis of rotation parallel to the longitudinal axis of the vehicle. The mode involves the wheels oscillating out of phase with each other. In other words, it is a self excited vibration occurring with automobile rear axles under braking and accelerating conditions. The axle tramp occurs particularly with vehicles those suspended on leaf springs, solid axle suspension or dependent suspension, under heavy braking or low gear, high accelerating torque conditions, [33].

Some attempts to study axle tramp and the coupling vibration of a vehicle driveline with the other motions of the vehicle body have been published. The axle tramping vibrations occurring with vehicle rear axles under braking and accelerating conditions have been studied by Sharp in 1969, [33]. The model of the system employed consisted of a rigid engine gearbox unit with longitudinal freedom restrained by the engine mountings, a splined coupling between the propeller shaft and this unit and the rigid axle with five degrees of freedom. Also included were the two wheels with vertically flexible tyres, torsionally flexible half shafts, a frictionless differential, the torsional flexibility of the propeller shaft, gearbox and clutch, the driven plate of the clutch, and the engine flywheel. The ways in which the stability of the system and the limit cycles are affected by changes in the system design were indicated, and the longitudinal axle mounting stiffness was identified as a critical parameter, having a major influence on the stability. The author concluded that the axle tramp can be

eliminated by suitable attention to the design of the axle to body mounting. Because this study was concerned with the behaviour of the rear axle, it emphasised the importance of the suspension system rather than the driveline system.

In 1981, [34], Sharp and Jones described a mathematical model of a truck tandem axle suspension and transmission system, with braking and the generation of longitudinal tyre/road forces. They derived the model employed from that described in [33]. They showed that the model is capable of producing a self excited oscillation, and conclusions were drawn regarding the conditions and design features which will promote the self-excited oscillations. The authors in this study represented details of the wheel modelling by considering the longitudinal tyre/road forces which are non-linear functions of wheel load and longitudinal slip. These forces may result is self-excited vibrations of the system.

A mathematical model of a vehicle axle suspended from a fixed chassis was set up and studied by Sharp in 1984, [35]. In the model, the axle has the freedom to translate longitudinally and vertically and to pitch or wind-up. The two wheels of the real vehicle were condensed into a single wheel having a spin freedom. In the three previous papers dissipative properties in the driveline system, which it is necessary to include in studies aimed at system behaviour and stability, were not included.

1.2.4-Driveline Components

There have been several attempts to study the vibration problems in particular components of a vehicle driveline system such as the engine, the gearbox and the propeller shaft.

Engine

Most predominant excitation forces in the engine structure and the driveline are induced by the crankshaft vibrations. Crankshaft vibrations are complex because of the 3-dimensional nature of the system. Several types of vibration for example, bending, axial and torsional are combined in a mode which includes displacements in all six degrees of freedom at any point along the crankshaft [36]. For sometime the

Finite Element Method (FEM) has been the only available technique for crankshaft analysis, however it remains time-consuming and expensive. It is also impractical when only a small number of modes need to be estimated [37]. In the FEM, the crankshaft is idealised by a set of different elements such as beam elements, journal and crank pin, rectangular elements, crank webs, and solid elements, balance weights. To simplify the analysis compared to a full FEM analysis, other techniques for crankshaft analysis such as Transfer Matrix Method (TMM) and Reduced Impedance Method (RIM) have been developed for analysis of the coupled torsional-bending and torsional-longitudinal vibrations of the crankshaft. In the analysis by TMM, the crankshaft is idealised by a set of equivalent mass and inertia matrices and the same set of field or stiffness matrices. The attached pulleys are idealised by an equivalent mass matrix. In the RIM analysis, the crankshaft is idealised by uniform circular bars and two crank arms corresponding to their real dimensions, however, the two crank arms are further idealised by a set of tetrahedrons using the FEM [38]. With the aim of simplifying the analysis by the RIM and eventually eliminating the FEM from the analysis, Okamura, et al [39] and Morita and Okamura [40] in 1995 idealised the crank arm and the counter weight as a set of jointed structures consisting of simple beam blocks along with modelling of the crank pin and crank journal as round bars. They presented Three-Dimensional free and forced vibration studies for the crankshaft system under firing conditions. They idealised the front pulley, timing gear and the flywheel as a set of masses and moments of inertia. The main journal bearings were idealised by a set of linear springs and dash-pots. The influence of the mass and moment of inertia of the front pulley on the crankshaft vibrational behaviour was calculated.

In the usual analysis of the crankshaft vibrations, only the torsional modes have been discussed, although the vibrations in a real crankshaft system are much more complicated and usually appear in a coupling of the torsional, bending and longitudinal vibrations [41].

Gearbox

Gearbox noise is one of the most important sources of vibration of driveline systems. Welbourn in 1979, [42] presented a comprehensive survey about the fundamental knowledge of gear noise. He stated that the fundamental cause of gear noise is the Transmission Error (TE), the difference between the actual angular position of the output shaft of the gear drive and the position which the shaft would be if the gear drive was perfect. This may be expressed as angular displacement or linear displacement at the pitch point. TE may be due to manufacturing errors or variation of teeth stiffness in the contact zone, where doubling the TE can increase noise by as much as 6 dB. There are other factors which affect gear noise such as system resonance, bearing, backlash, etc.

Daly and Smith in 1979, [43] measured the transmission error of gears using circular gratings to identify the noise and vibration in drivelines. The gratings were attached at input and output of the gear drive and the photocell signals generated were turned into pulse trains. The input pulse train was multiplied and divided electronically and compared with the output pulse train to show any relative movement between the theoretical and actual. The authors concluded that the gratings may be used to determine the manufacturing errors at low speed, where system resonance has not distorted the readings. Typical results from gearbox and back axle measurements were shown and discussed and advantages and limitations of this measurement were discussed. It should be emphasised that transmission error measurements are very useful for noise and vibration of gear systems. However, for closed gearboxes the noise may be determined by measuring the variation in forces at the gearbox bearings.

An extensive review of the literature on modelling of gears for gear dynamics and vibration studies has been given by Özgüven in 1991, [44]. He observed that the dynamic models suggested for gear systems may vary depending on the relative dynamic properties of the system. However, he used a six-degree of freedom model to analysis systems which have coupling between the torsional mode governed by mesh stiffness and torsional and transverse vibration modes governed by shaft and bearing compliances. In this study the Dynamic Transmission Error Program with a Multi

degree of freedom model (DYTEM) was used. From this study it has been concluded that the single degree of freedom non-linear model in which all the compliances except those of gear teeth are excluded may be adequate for an accurate dynamic analysis in some gear systems in which the mesh mode was uncoupled from other modes. However, extreme care is to be taken to be sure that the mesh mode can be uncoupled from the other modes before using a single degree of freedom model.

Idle gear rattle is a noise generated under low load conditions and is a direct result of gear tooth impacts, some authors concerned with the gear rattle considering it as a source of driveline vibrations. Brosey et al in 1986, [45] looked at the effect of transmission design on gear rattle. A theory that shows the relationship between gear rattle and the combined effects of the angular acceleration of the transmission input shaft, the effective transmission inertia and the transmission drag, was developed. A unique test stand to evaluate the gear rattle tendency of a transmission was described. A computer model to calculate the angular acceleration at the transmission input was presented. A typical driveline system model consisting of a set of concentrated inertias linked by torsional springs for system components from the engine to tyres was introduced. The factors affecting rattle were; backlash, pitch diameter and operating temperature. Free and forced vibrations analysis, due to harmonic excitations at any given point in the system, were performed. Drag inducing transmission designs to reduce gear rattle were undesirable due to their negative effects such as increasing shift effort, increasing operating temperature and reducing mechanical efficiency.

Fudala et al in 1987, [46] studied the torsional vibration of driveline systems for reducing gear rattle with particular emphasis on how system component inertias, spring rates and damping effect vibration level of the system and gear rattle. The authors used the same models of computer and driveline system published in reference [45]. They stated that the gear rattle was likely if the torsional vibration at gear/spline mesh location is sufficient to overcome the inertia and oil drag effects, where the teeth become completely unloaded. The severity of the rattle increases with amplitude of torsional activity at the gear mesh location because the relative impact velocity between the teeth increases. Furthermore, the amplitude of torsional oscillation at the

gear mesh point is a function of the system response of the total driveline from the flywheel to the tyres. Therefore, the clutch played an important part in minimising the rattle because its parameters (stiffness and damping) effect on torsional vibration of the gearbox input. Thus, rattle is related to the driveline dynamics. The last two papers introduced an interesting approach aimed at understanding the relation between the gear rattle and driveline system vibrations. However, gear rattle is a complex non-linear systems problem which requires an equally complex plan of attack.

Propeller shaft

The propeller shaft and its joints are another important source of driveline system vibration. Vibration effects of the universal joint may be categorised into two broad groups; vibrations about the axis of rotation (torsional vibrations) and vibrations about perpendicular axis (secondary couples). Kato et al in 1988 and 1990, [47,48] respectively, presented a study to analyse the coupled vibration of bending and torsion in the rotating shaft driven by a universal joint. They showed that the lateral-torsional vibrations become unstable in the same time. This instability occurred when the drive speed nearly coincided with the arithmetic mean of two natural frequencies about bending and torsional. The unstable region increased with increasing the joint angle and decreased with increasing the viscous damping coefficient of torsional vibration rather than bending vibration. The authors studied the excitation due to viscous and Coulomb frictions between cross-pin and yoke of the joints. The study confirmed that excitations due to viscous friction increased with increasing the joint angle but the excitation due to Coulomb friction was independent on the joint angle.

Otak et al in 1992, [49] were concerned with the test of the torsional fluctuation of the drive pinion due to the Hooke's joint using a digital simulation method. The backlash between spline sleeve of the output shaft of the gear box and the propeller shaft was taken into consideration to improve the accuracy of the method. A simulation of the drive train from the flywheel to the differential pinion was presented. The angular displacement caused by the angle of the Hooke's joint was assumed as the displacement input by means of conventional equations for this mechanical system.

Spring characteristics of the spline unit including the backlash were measured and found to have two stages, the first stage was the lower spring rate and the second stage having an increased spring rate. The fluctuation at the propeller shaft joints is a key parameter in studying the rattling and noise in the final gear because the gear rattle depends on the input fluctuating to the differential.

With the demands for higher shaft speeds and grater power transmission, the demands for a constant velocity joint become serious. Yamamoto et al in 1993, [50] dealt with the efficiency of the constant velocity universal joint (CVS) used for drive shafts. Two typical joints used for front-engine, front-drive passenger cars were considered. One of them is a Rzeppa joint, used on the wheel side of the drive shaft and the other is a Tripot joint, used on the differential side. The results were verified by experiment. They found that about 70 percent of frictional induced losses in a Rzeppa joint and a Tripot joint are due to internal friction caused by contact of the inner and outer surface with the case in the former and contact between the balls and the grooves of the housing in the later. However this joint proved difficult in maintenance aspects and is not efficient at the higher transmission torques.

1.3-SUMMARY

Many of the problems associated with torsional vibrations and refinement in drivelines have been tackled through relatively simple, lumped mass models combined with experimental measurements. More recently, it has become increasingly common to use multibody system dynamics codes to develop more sophisticated models to assist understanding in ensuring high levels of refinement.

However, some problems remain, for example, coupling of torsional vibration of the driveline with suspension motions may causes shunt/shuffle problems. Although some simple lumped mass models have been derived, this problem is not yet fully understood.

Some vibrational phenomena such as shunt have been investigated through simple models incorporating engine throttle variations, although many of these phenomena

arise due to clutch engagement. More understanding of the driveline system behaviour during clutch engagement is still required.

Although the transient operating condition of vehicles is one of the main causes of unwanted vibrations, publications concerned with the behaviour of driveline systems under these running conditions are relatively few. Therefore, more attention to the effects of transient behaviour is needed.

In the literature, parametric studies of the sensitivity of driveline system behaviour to changes of the design parameters have not proved satisfactory in providing guidelines for driveline designers in the early stages of the system design. Further work should performed to analyse the sensitivity of driveline vibration problems to design parameter changes.

1.4-AIMS OF THIS WORK

A substantial amount of research effort in the automobile industry is focused on the development of advanced control strategies. The success of these research efforts depends on the availability of validated dynamic models of the vehicle subsystems. Therefore, this study is concerned with a dynamic simulation model of the driveline system to investigate vibration problems and to study the sensitivity of the driveline behaviour resulting from changes in component design parameters. This is achieved using a comprehensive mathematical model for the driveline system vibration coupled with the vehicle body vibrations. It is implemented through computer programmes designed to be useful design tools for studying the torsional vibration problems in this system. Linear and non-linear models are used to study the free and forced vibrations and the steady and transient running conditions are considered. It is emphasised that the developed models and computer programmes are cabable of predicting the dynamic behaviour of vehicle driveline systems and investigating most of the vibration problems of these systems without inputting experimental data. Hence, through this study it is possible to perform parametric study of the vibrational behaviour of vehicle transmission system and body before a prototype vehicle is produced.

The principle aims of this work are;

1. To improve fundamental understanding of the dynamic interactions of components within a whole driveline system.
2. To understand the dynamic behaviour of the driveline and its coupling with longitudinal and vertical compliances in the vehicle suspension system.
3. To analyse the sensitivity of driveline vibration problems to design parameters changes.
4. To investigate how the mathematical models developed can be used in practice to lead to good design guidelines early in the design concept phase.

CHAPTER 2

DRIVELINE COMPONENTS AND MODELLING

2.1-INTRODUCTION

There are a large number of possible driveline configurations which result from different combination of the fundamental components, for example in-line and transverse engines, front and rear wheel drive, two and four wheel drive, direct and indirect gearbox, etc.,. However, the most common components of a driveline system, excluding rotating accessories are; the engine, flywheel and clutch, gearbox, propeller shaft and universal joints, differential and rear axle assembly and tyres. In this chapter, a mathematical model capable of simulating the torsional vibrational models of each of these components will be developed and explained. Certain components are discussed in more detail in later chapters such as the clutch and tyres.

2.2-ENGINE

The main sources of excitation for torsional vibrations of a driveline system are discrete engine ignition events. Because the main interest of this work is the driveline torsional vibration, the rotational dynamics of the engine is modelled by consideration of the crankshaft system. The engine mounts are not included in the model.

2.2.1-Equivalent System of a Crank

In [10], the crankshaft was represented by a simple system that was substantially equivalent in its torsional dynamic behaviour. The equivalent system consisted of concentrated rotors connected by massless, torsionally elastic springs. Each crank of the crankshaft was represented as a subsystem of 3 discs and 4 springs, Fig (2.1), where the distribution of inertia was as follows; two discs share the inherent inertias of the crank and rotational parts, denoted by J_w (journal + crank pin + webs) and central disc represents the equivalent inertia of the reciprocating parts, given by J_r, (piston + connecting rod + piston pin). For the complete crankshaft system model, inertias represent; torsional dampers, flywheels, propellers, etc. were added at planes of the actual of these components.

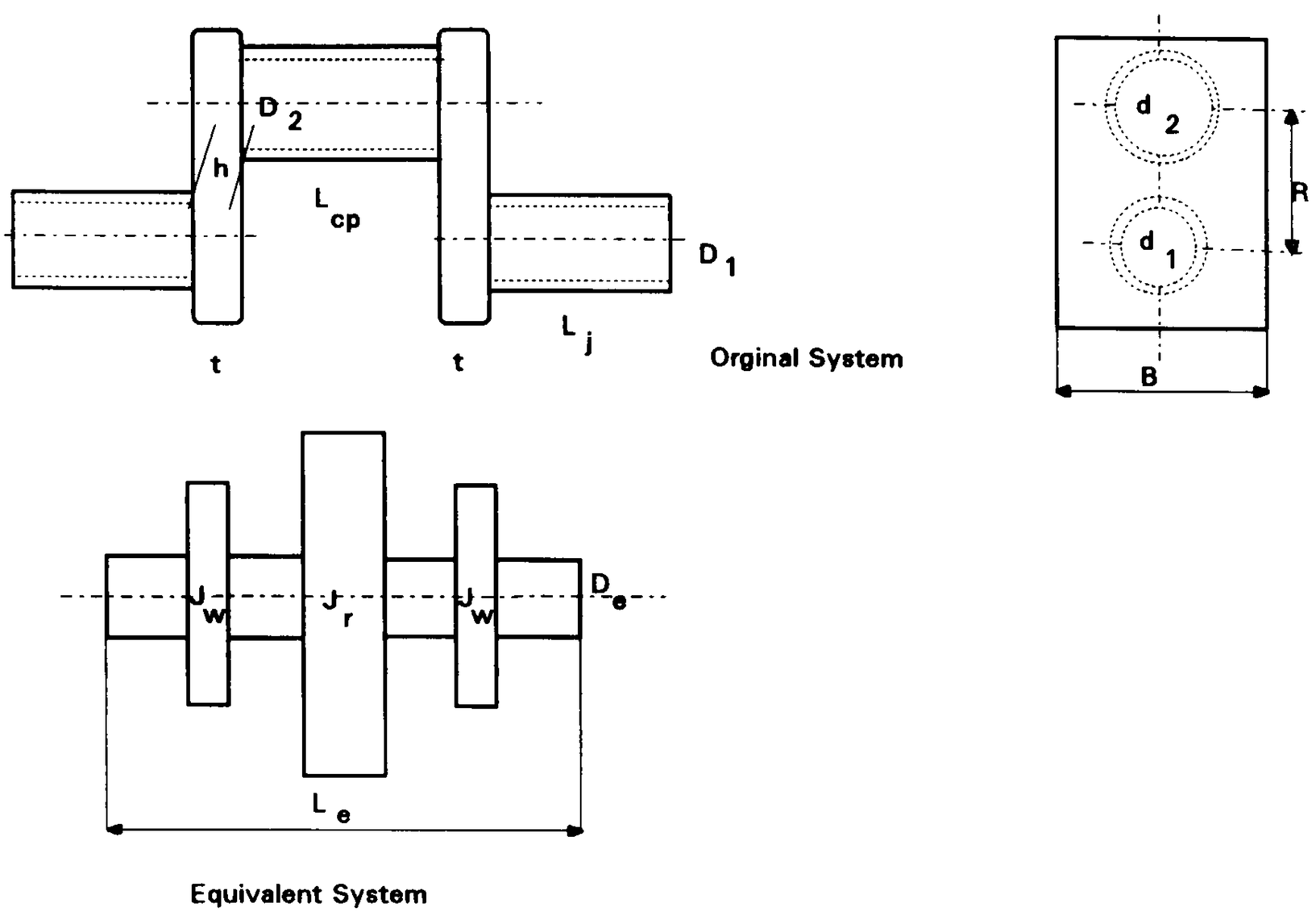

Fig (2.1) Equivalent and original system of a crank

2.2.2-Equivalent Mass Moment of Inertia of the Reciprocating Parts

The analytical analysis shows that the effect of the piston and connecting rod can be closely approximated by a concentrated rotor of mass moment of inertia J_r using this equation [10];

$$J_r = (0.5m_c + 0.75m_p)R^2 \qquad (2.1a)$$

Some researches [36] use a similar formula in terms of total reciprocating mass and crank radius to connecting rod length ratio (λ) to calculate J_r such as;

$$J_r = mR^2(0.5 + \lambda^2/8) \qquad (2.1b)$$

2.2.3-Equivalent Mass Moment of Inertia of the Rotating Parts

The rotating parts comprise the crank journal, crank pin, crank web and balance weight. The mass moment of inertia of the journal and the crank pin, respectively can be calculated from these relations [51];

$$J_j = \frac{\pi\rho L_j}{32}(D_1^4 - d_1^4) \quad \text{and}$$
$$J_{cp} = \frac{\pi\rho L_{cp}}{32}[(D_2^4 - d_2^4) + 8R^2(D_2^4 - d_2^4)] \qquad (2.2)$$

The determination of the mass moment of inertia of the crank webs and balance masses (J_b) is very complicated theoretically, so a graphical method has been used in [10].

The equivalent mass moment of inertia of the rotating masses, J_w Fig (2.1), is the sum of the inertias of the crank journal, crank pin, crank web and balance weight, i.e.;

$$J_w = 0.5(J_j + J_{cp} + J_b) \qquad (2.3)$$

2.2.4-Equivalent Torsional Stiffness

The torsional stiffness of the equivalent crankshaft can be calculated using this formula,

$$k = G\pi D_e^4 / 32L_e \qquad (2.4)$$

where L_e is the length of a uniform solid shaft of diameter D_e equal in torsional stiffness to the section of crankshaft between crank centres or between the middle of journals (equivalent crank length).

The equivalent length of the journal only is;

$$L_{ej} = D_e^4\left\{\frac{L_j}{D_1^4 - d_1^4}\right\} \qquad (2.5)$$

while the theoretical formula, [51], of the total equivalent length of the crank is;

$$L_e = D_e^4\left\{\frac{L_j}{D_1^4 - d_1^4} + \frac{L_{cp}}{D_2^4 - d_2^4} + \frac{0.9R}{tB^3}\right\} \qquad (2.6)$$

This formula has been derived assuming; no bearing constraint, no increment flexibility due to junctions of webs with crank pin and journal, the bending of the webs is from journal centre to crank pin centre and web stiffness is unaffected by chamfering and by overlap of crank pin and journal.

Empirical formulae

Many semi-empirical formulae have been proposed for calculation of the equivalent torsional stiffness of the crank. However, four formulae were recommended by Gironnet [10]. The average of these formulae gives results having a maximum deviation of less than 10% in comparison to experimental results [10]. They are given below associated with their author's name.

i-Carter's Formula

$$L_e = D_e^4 \left\{ \frac{L_j + 0.8t}{D_1^4 - d_1^4} + \frac{0.75L_{cp}}{D_2^4 - d_2^4} + \frac{1.5R}{tB^3} \right\} \qquad (2.7a)$$

ii-Wilson's Formula

$$L_e = D_e^4 \left\{ \frac{L_j + 0.4D_1}{D_1^4 - d_1^4} + \frac{L_{cp} + 0.4D_2}{D_2^4 - d_2^4} + \frac{R - 0.2(D_1 + D_2}{tB^3} \right\} \qquad (2.7b)$$

iii-Timoshenko's Formula

$$L_e = D_e^4 \left\{ \frac{L_j + 0.9t}{D_1^4 - d_1^4} + \frac{L_{cp} + 0.9t}{D_2^4 - d_2^4} + \frac{0.93R}{tB^3} \right\} \qquad (2.7c)$$

iv-Gironnet's Formula

$$L_e = D_e^4 \left\{ \frac{L_j + 0.5h}{D_1^4 - d_1^4} + \frac{L_{cp}}{D_2^4 - d_2^4} + \frac{1.4R}{hB^3} \right\} \qquad (2.7d)$$

2.2.5-Excitation Torque of the Crankshaft

The torsional vibration in a reciprocating engine is mainly due to excitation by the harmonics of the gas-pressure torque and the inertia torque. In this section, a brief description of the crankshaft excitation torque is presented and details will be discussed next chapter. The net torque acting on the crankshaft is composed of the sum of the inertia torque, T_i, friction and pumping loss torque, T_f, and the indicated gas pressure torque, T_g,. Only inertia and gas pressure torque are considered here because the value of the friction torque is small compared to the other two values, [52].

Inertia torque

The equivalent dynamic system for the connecting rod is based on dividing its total mass into two parts; reciprocating part, concentrated at the piston and rotating part, concentrated at the crank. Neglecting the torque due to dead weights of reciprocating and rotating parts and the inertia due to connecting rod couple, which arises due to the difference between its original moment of inertia and moment of inertia of its equivalent masses, the periodic inertia torque due to the reciprocating parts is related to the crank angle as [51];

$$T_i \cong m\omega^2 R^2 \left(\frac{1}{4}\lambda \sin\phi - \frac{1}{2}\sin 2\phi - \frac{3}{4}\lambda \sin 3\phi\right) \qquad (2.8)$$

where the terms of higher than 3rd order may be neglected.

Gas-pressure torque

The gas-pressure torque is related to the cylinder gas pressure by the geometry of the slider-crank mechanism and it can be expressed using this relation [53]; see Fig (2.2)

$$T_g \approx P_g \quad A \quad R \quad \sin\phi \quad (1+\lambda\cos\phi) \qquad (2.9)$$

where A is the lateral piston area.

$$F_{cr} = P_g A / \cos\varepsilon$$

$$F_t = F_{cr} \quad \sin(\varepsilon + \phi)$$

$$T_g = F_t \quad R$$

$$F_r = F_{cr} \cos(\varepsilon + \phi)$$

$$F_s = P_g A \tan\varepsilon$$

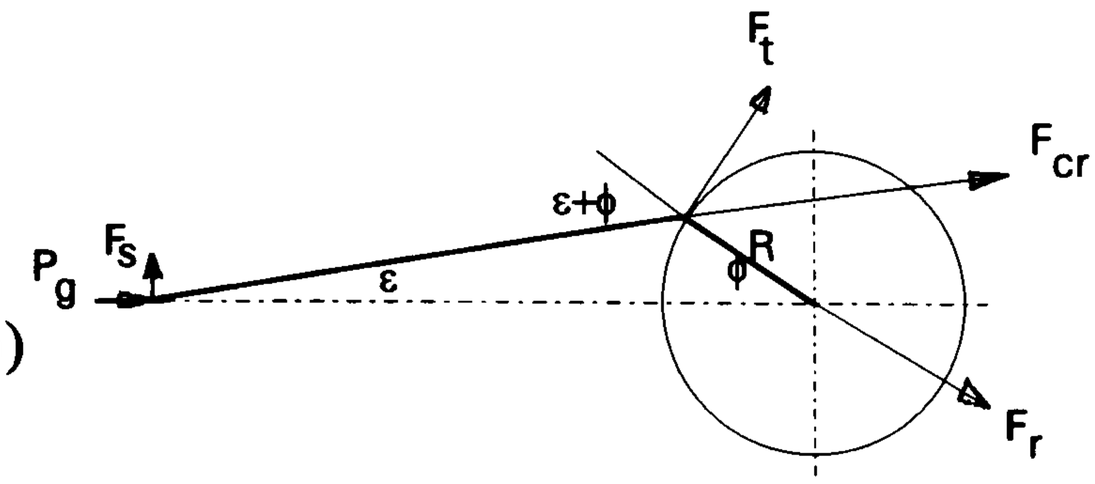

Fig (2.2) Slider-crank mechanism and its forces

The cylinder gas pressure corresponding to the crank-angle position, ϕ, can be taken from the engine P versus ϕ or P versus V diagrams. Details of this study will be provided in the next chapter.

The resultant excitation torque

The components of torque due to inertia are all sine($n\phi$) terms (where n is a positive integer) and they can be added to the sine terms due to gas pressure in order to obtain the resultant periodic excitation torque. This torque is a sum of a number of simple harmonic torques of various amplitudes and frequencies. The fundamental frequency of the excitation torque is equal to half the crankshaft speed for four-stroke engines and equal to the crankshaft speed for two-stroke engines. Harmonic components of a periodic torque have frequencies that are whole-number multiples of the fundamental frequencies. Details of the net torque is discussed in the next chapter.

2.2.6-Crankshaft System Model

Based on the previous presentation of crank modelling, the complete crankshaft system of a four cylinder engine is modelled as shown in Fig (2.3a). It includes, in addition to the inertias which represent each crank moving parts, inertias representing a torsional damper at the free end of the crankshaft, and a flywheel at the other end.

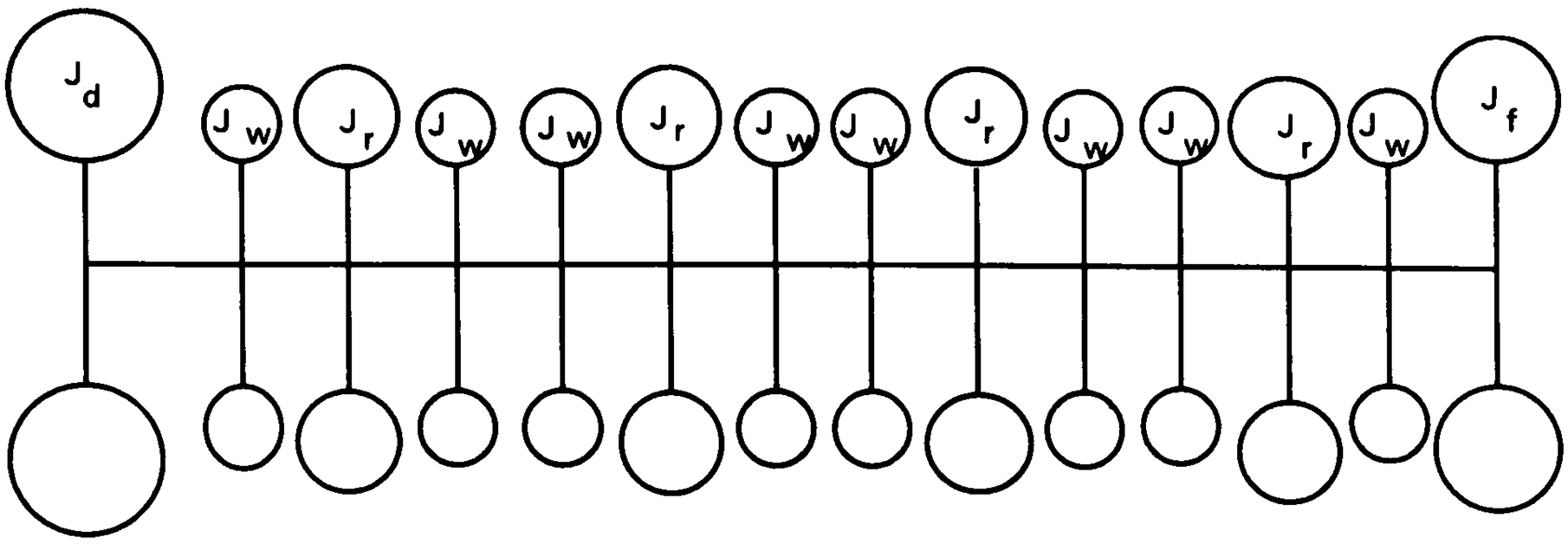

Fig (2.3a) Crankshaft system of a four cylinder engine

A compact crankshaft is very stiff therefore, the inertia of the rotating parts, J_w, are added to the inertia of the reciprocating parts, J_r, at the centre of the crank, i.e. each cylinder can be represented by a single concentrated inertia disc, $J_i = J_r + 2J_w$, i=1,2,3 and 4. Fig (2.3b) represents a model of a compact crankshaft system of a four-cylinder engine.

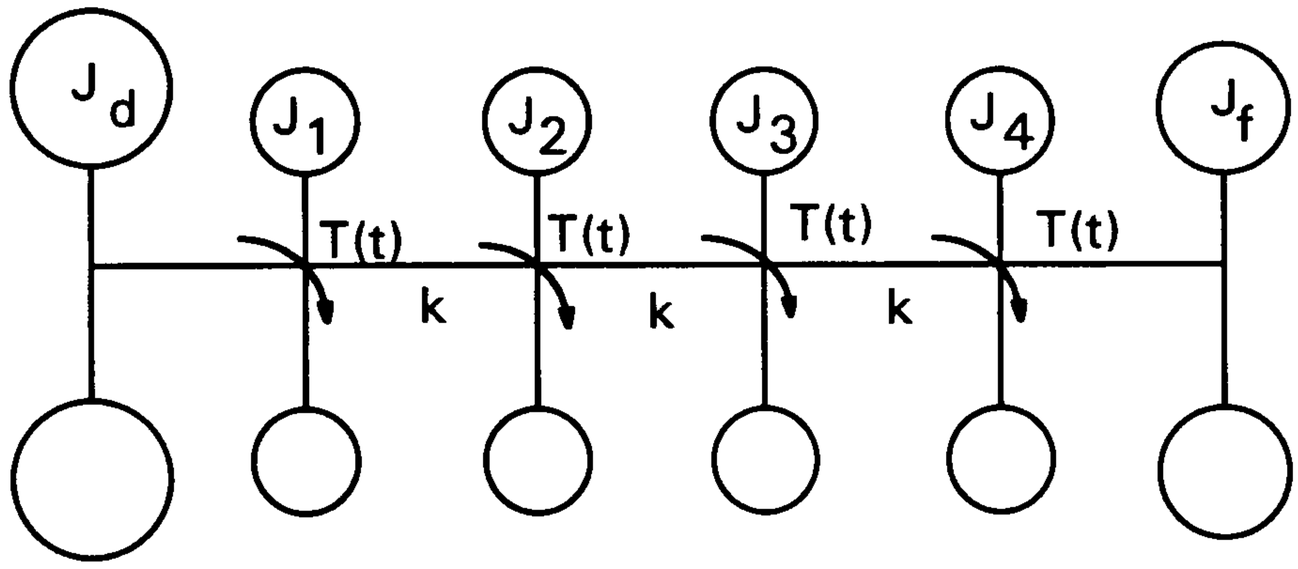

Fig (2.3b) Compact crankshaft system model of a four cylinder engine

2.3-CLUTCH

The clutch is a mechanism which enables the rotary motion of the engine to be transmitted to the gearbox. The frictional clutch is one of the main sources of a vehicle driveline system vibrations. The configuration of the modern automobile driveline system varies considerably from vehicle to vehicle. Some have long flexible propeller shafts while others have the short, stiff drive shafts typical of the front wheel drive vehicles. However, there are two common factors with all manual gearbox systems, namely; the dry friction clutch and the human operator. This study is

concerned with the dry friction clutch behaviour and its operation. The operation of the clutch may be described if the dimensions and physical characteristics of the frictional materials can be specified.

2.3.1-Clutch Models

Lucas and Mizon [27,28] presented a model for the analytical study of the take-up characteristics of an automotive clutch. They treated the engine-clutch-driveline-vehicle train as two subsystems, as shown in Fig (2.4). In this model, the flexibility of the driveline system was not considered. This model can be used to study the energy dissipated during engagement and the temperatures of the clutch components.

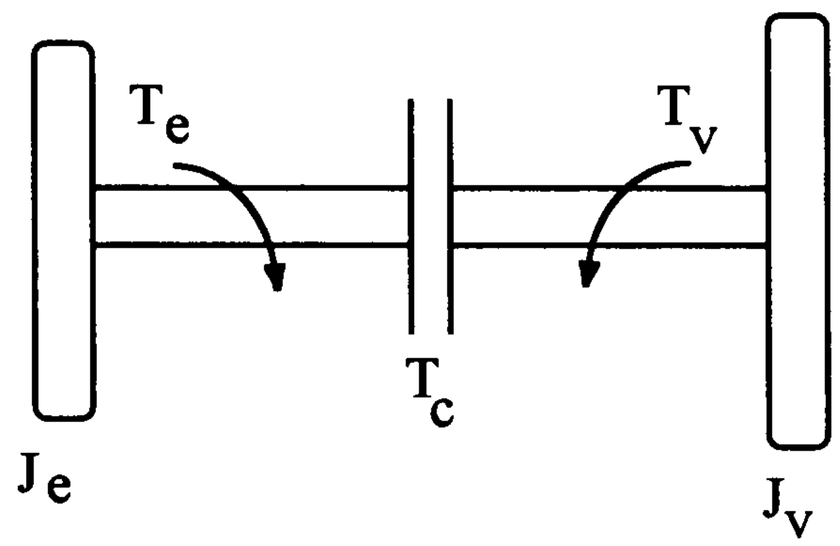

Fig (2.4) Clutch mathematical model

Equations of motion

The equations of motion during engagement period for the previous model are;

for the engine subsystem;

$$\frac{d\omega_e}{dt} = \frac{T_e - T_c}{J_e} \tag{2.11}$$

for the vehicle subsystem;

$$\frac{d\omega_v}{dt} = \frac{T_c - T_v}{J_v} \tag{2.12}$$

where subscript 'e' refers to the engine and 'v' refers to the vehicle. The clutch torque (T_c) is a function of the clamp load (p), mean clutch radius (r) and the coefficient of friction (μ) can be described as;

$$T_c = \mu \quad r \quad p \tag{2.13}$$

The previous differential equations (2.11) and (2.12) can be integrated using a numerical technique, such as the Runge-Kutta technique, with respect to time and at each time step the temperature distribution through the components can be evaluated. Note that, according to empirical observations, the coefficient of friction is a function of the temperature, clutch slip speed and the clamp force which is a function of driver's manner. More details of these considerations are discussed in chapter 7.

2.3.2-Clutch Representation

The study of clutch vibration is complex. The friction material is a complex, non-isotropic, composite material, which makes the prediction of its vibrational behaviour difficult. Therefore, for studying the dynamic behaviour of a vehicle driveline system the simplest representation for the clutch is considered because the prominent vibration mode is torsional. Rooke, et al [25] represented the dynamics of the clutch as a non linear spring and Coulomb friction was assumed between the engine and transmission inertia. Ambrosi [21,22] simulated the clutch using non linear characteristic curves for stiffness and damping when performing transient analysis, during clutch slipping, but for modal analysis and frequency response, after fully engagement, he evaluated linearized values of the stiffness and damping.

The torsional characteristic of a typical clutch is shown in Fig (2.5). This figure shows the two different torsional stiffnesses of the clutch for the range of torque. The low stiffness range provides a progressive loading of the transmission system and prevents damage due to rough driving. Once the clutch is engaged only the right hand part of the graph, characteristic by the high torsional stiffness, is used since the torque remains high. This means that the clutch has a non-linear torsional stiffness characteristic.

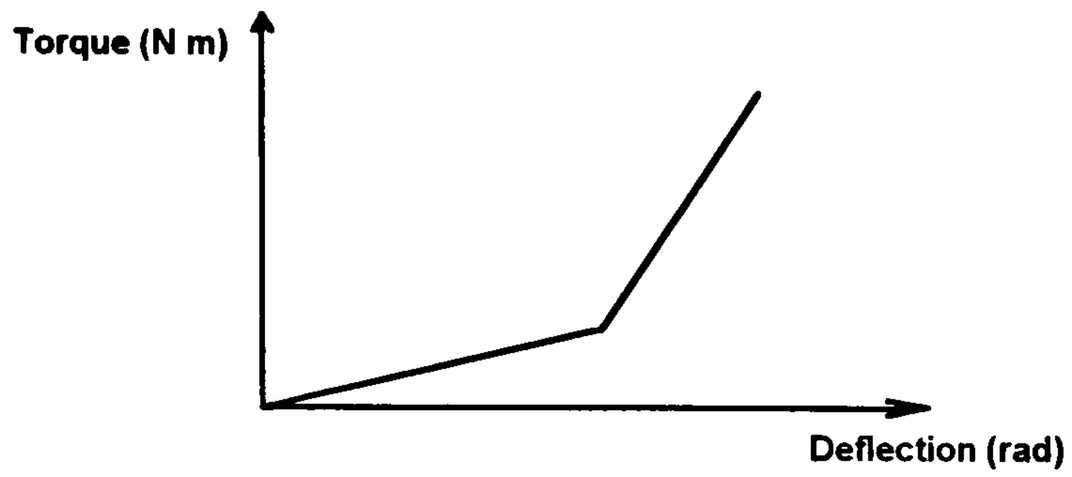

Fig (2.5) Typical torsional clutch characteristics [from 21,22]

When the clutch is completely engaged, only the high stiffness range need to be considered. Therefore, in this case, the analysis of the driveline system is based on representing the clutch by a concentrated inertia and a torsional stiffness equivalent to the stiffness of the high torque range and the inertia of the complete clutch mechanism is added to that of the engine's flywheel [10]. However, during clutch slipping, the clutch is represented as a source of non-linear excitation to the driveline system due to an induced friction torque in addition to a non-linear spring and a concentrated inertia representing the clutch disc.

2.3.3-Clutch Judder

Generally, a motor vehicle clutch contains; a flywheel, a pressure plate and a centre plate, which is usually blamed when a vehicle suffers from "clutch judder" [28]. Clutch judder is a phenomenon in which a vehicle is vibrated back and forth by a torsional vibration of the driveline system transmitted from the engine mount and suspension system of the vehicle during the clutch engagement process at the time of starting [31]. During the engagement period of the clutch, the vehicle driveline is subjected to self-excited vibrations due to the distributed frictional forces which are a function of relative slip velocity. The judder is significantly related to the friction-velocity characteristic of the friction material. The frequency of this vibration is reported to lie within the 5 to 20 Hz region [27-31]. These vibrations affect the driveline, the suspension, the tyres and the vehicle, together with the engine on its mounting system. The main parameters which affect clutch judder, in addition to the gradient of the friction-velocity coefficient are; the masses, inertias and stiffness of the components in the driveline, the suspension and tyre systems and the components in

mounting the engine. The clutch judder phenomenon is investigated in further detail in chapter 7.

2.4-GEARBOX

The principal function of the gearbox is to enable the driver to change the speed ratio between the engine and driving wheels and to get neutral or reverse. Gearboxes may be divided into two main groups; manual-change and automatic. The manual-change gearbox provides the driver with full control of the gearbox by means of a control lever and appropriate gear ratio can be selected to meet the driving conditions. The automatic gearbox covers the many systems in which the gear ratios are changed by the gearbox itself instead of relying on the driver. Once the driver has made the initial selection to determine the direction in which the vehicle is to move, and the gear range to be used, then other decisions concerning the chain of gear ration are made within the gearbox itself. The manual-change gearbox is probably the most common type in use especially in heavy vehicles. Gearbox noise and vibration constitutes a serious problem in the driveline system which is the concern of the study.

2.4.1-Dynamic Modelling

In general, gearboxes have a complex structure containing geometrical discontinuities, cavities and clearances. In addition the housing may have ribbed panels and bolted joints and the bearings may contribute non-linearities [54]. The major concern in dynamic modelling of gears considers; dynamic tooth stress, stability, noise radiation and rotor whirl. Therefore, it is not possible to construct the best model unless the purpose of the analysis and the relative dynamic properties of the gear system are known [38]. The purpose of this analysis is to construct a simple torsional vibration model and to use it in the investigation of the torsional vibration of vehicle driveline systems. Therefore the primary goal of this section is the modelling of gears and carrying shafts as a torsional vibratory system.

2.4.2-Gearbox Vibrations

In the first chapter, some attempts concerned with the gearbox noise and vibrations were reviewed. The noise and vibration of a gearbox have been investigated assuming

the shafts to be rigid for bending or at most torsion only, as a single degree of freedom (SDOF). However, the flexure of a shaft becomes more important when it is rotating at high speeds. Hence, it is necessary to consider the vibration of a shaft in a gearbox as a coupled one of torsion and flexure because the natural frequencies of the real system differ from the ones obtained without considering the effect of coupling [55]. Furthermore, the dynamic models for the gearboxes vary considerably and yet it may still be possible to obtain similar predictions by using completely different models for certain systems. However, this depends on the relative dynamic properties of the systems. For example, when the relative values of torsional and flexural stiffnesses of shafts and of the mesh stiffness are such that the mesh mode can be uncoupled from the other vibrational modes, it may be sufficient to use a SDOF model for obtaining accurate predictions. In this case, including the coupling between the torsional and transverse vibrations, a multi degree of freedom (MDOF) model, will not increase the accuracy of the predictions significantly. While the relative values of the dynamic properties cause a strong coupling among the mesh mode and other modes, however, a SDOF model cannot be useful for accurate predictions [38]. In other words, if the torsional compliances of the gear carrying shafts are much higher than that of the tooth mesh and, furthermore, if the system is carried on very stiff bearings, then the gear pair's torsional vibration mode controlled by mesh stiffness will be very lightly coupled with other vibrational modes. In such systems use of the SDOF model will not make much difference as far as the accuracy is concerned. It can be said that when the mesh mode is uncoupled from the other modes, there is no need to use a MDOF model for an accurate dynamic analysis.

On the other hand, when the torsional mode governed by mesh stiffness is coupled with the torsional and transverse vibration modes governed by shaft and bearing compliances, the coupling between these modes cannot be neglected and it is required to use a MDOF model including torsional and transverse vibration coupling. Generally, although several MDOF models have been developed for gearbox dynamics, only torsional vibrations are considered in most of them [38]. There are also many important factors which make the system non-linear such as, time varying mesh stiffness and damping, separation of teeth, backlash, single- and double- sides

impacts, various gear errors and profile modifications, [38,56]. In brief, in the analysis of the torsional dynamic behaviour of the total driveline system, only the torsional vibrational mode of the gearbox system will be considered and also, the non-linear parameters can be linearized.

2.4.3-Torsional Vibrations of a Gearbox

The determination of the torsional vibration characteristics of a gearbox is simplified if the actual system is firstly replaced by a dynamically equivalent one.

Equivalent system

In the torsional vibration equivalent system, all shafts and masses (gears) rotate with the same mean angular velocity. It is usual to select one of the shafts of the original system as the reference shaft and to refer all quantities to the speed of this shaft. The energies in every element in the equivalent system must be equal to that in the corresponding element in the original system. This means that corresponding to any mass moment of inertia "J" of a rotor (gear) on a shaft running at "i" times the speed of the reference shaft, there is a mass moment of inertia "Ji^2" in the equivalent system, obtained by the equating the kinetic energy of the original system to that of the equivalent one. The equation of the strain energies of the actual system and the equivalent system means that the torsional stiffness of the equivalent shaft must be "i^2" times that of the original shaft.

Certain parts in the gearbox revolve without transmission torque and thus are not subjected to torsional load and these parts are considered as inertias only. Therefore, the model contains an equivalent inertia disc for any gear transmitting torque, or driving one or several idling gears. The inertia of the equivalent disc also embodies the inertia of the idling gears, reduced to the speed of the driving gear. For the calculation of the intermediate stiffness, the portions of shaft considered were those transmitting torque and located between the inertia discs [10] as shown in Fig (2.6).

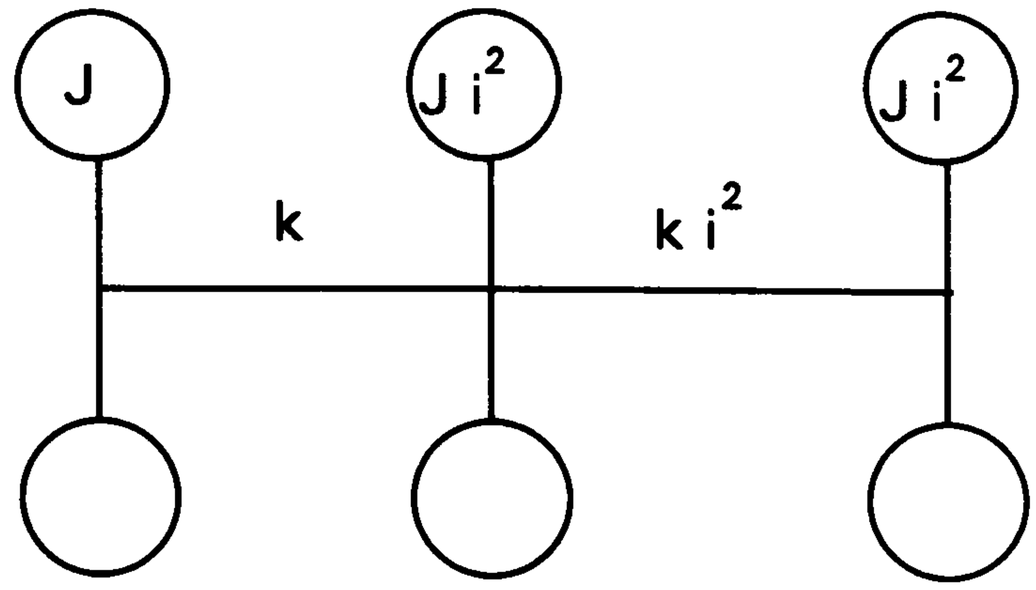

Fig (2.6) Gearbox mathematical model for torsional vibration

The oscillating torque and displacement of the equivalent system can be obtained by solving the governing equations of motion of the equivalent system. Then by recovery, the corresponding values of the original system can be obtained by dividing the equivalent values by the factor "i^2".

2.5-PROPELLER SHAFT AND UNIVERSAL JOINTS

The propeller shaft, or the Cardan shaft in vehicles, drive the road wheels through the final drive (differential). The propeller shaft is an another major source of excitation to the vehicle driveline system due to either mass imbalance or Hooke's joints. Several Hooke's joints (universal joints) are usually present because the output gearbox shaft and the rear axle drive (driving shaft) are not necessarily in the same plane.

2.5.1-Hooke's Joints

For each complete revolution of a Hooke's joint operating at a specified angle of inclination, there are four distinct phases of motion, two in which the output shaft rotates faster than the input shaft and two in which it rotates more slowly. As the joint angle or angularity is increased these changes in velocity become more pronounced. Fig (2.7) shows the input to output velocity ratio versus the input shaft angular position, Eqn (2.15), for different angles of inclination of the input shaft joint.

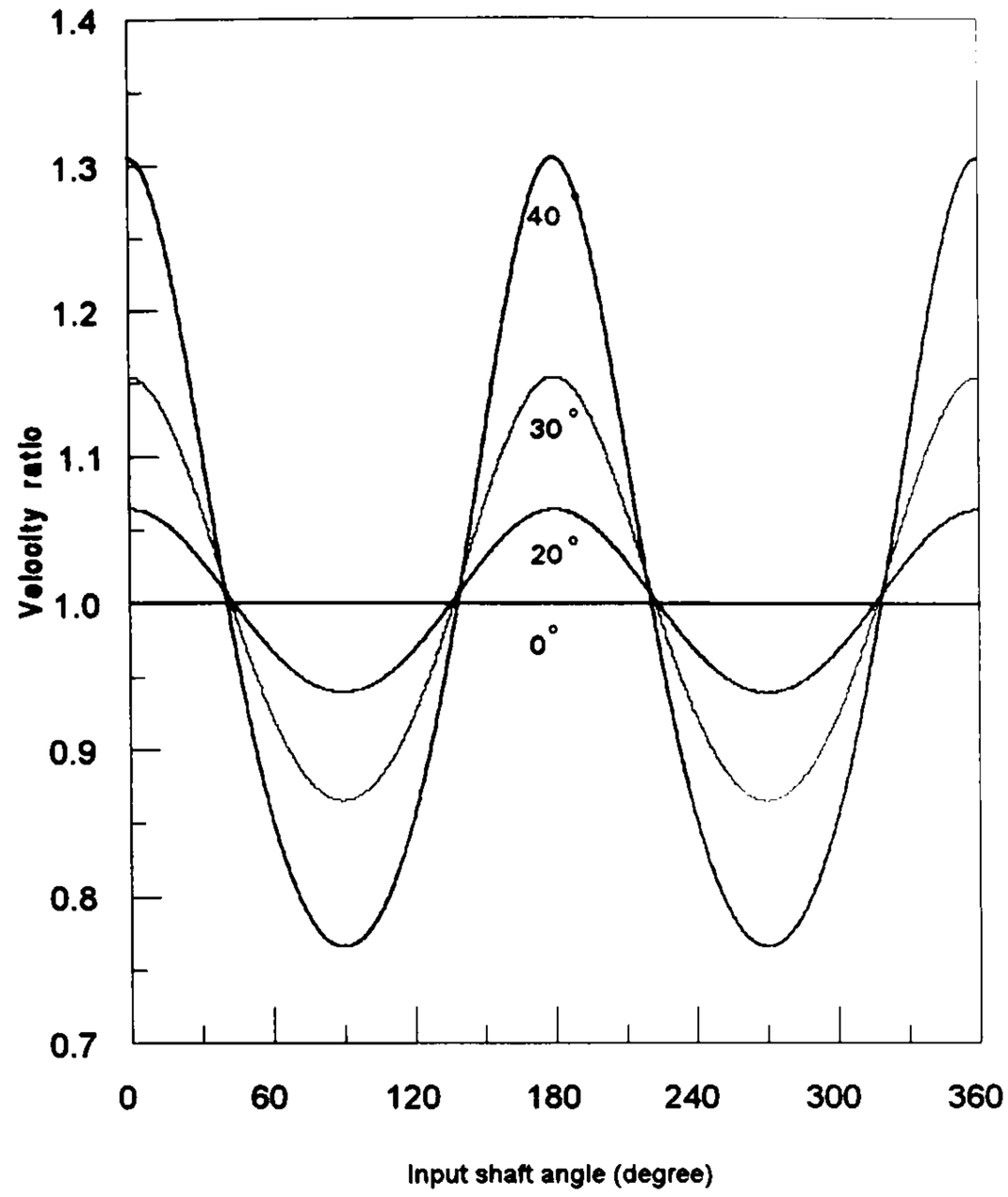

Fig (2.7) Velocity ratio of a Hooke's joint for different angle of inclination

Also, the rate of velocity change or acceleration fluctuation increases with angle of inclination. As mentioned before, the universal joint is not a constant-velocity device. That means, when the input shaft rotates with a constant angular velocity, the output shaft is subjected to the fluctuation of angular velocity. Therefore, even for small shaft angles, the high speeds common modern vehicles can cause unacceptable level of vibration and noise [57]. The angular velocity of the output shaft (ω_o) and the input one (ω_i) is related by the well known relation [8,58] ;

$$\frac{\omega_o}{\omega_i} = \frac{\cos\alpha}{1-\sin^2\alpha\ \sin^2\phi_i} \approx 1 - A_1\cos 2\phi_i + A_2\cos 4\phi_i \qquad (2.15)$$

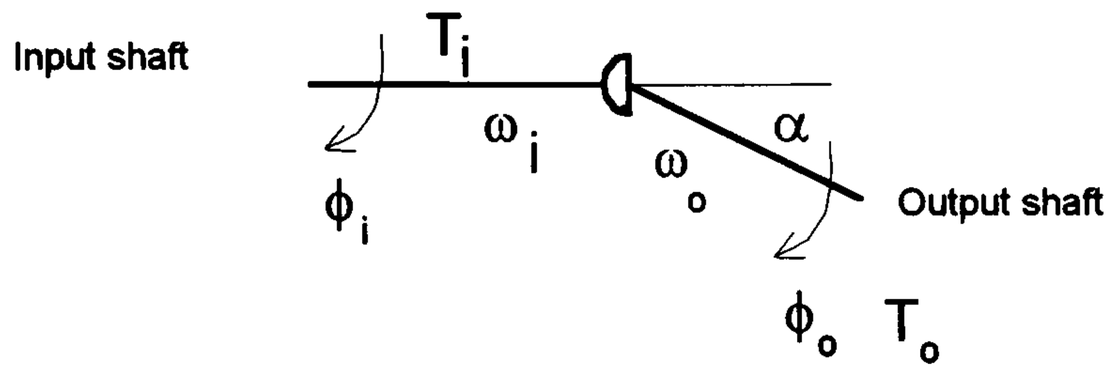

Fig (2.8) Hooke's joint representation

where

ϕ_i is the angular displacement of the input shaft, $\phi_i = \omega_i t$,

ω_i is the angular velocity of the input shaft,

ω_o is the angular velocity of the output shaft and

A_1 and A_2 are constants involving α.

From this relation, it can be proved that the rotating speed ω_o of the propeller shaft will change within the range of ($\omega_o \cos\alpha$) to ($\omega_o \sec\alpha$).

The combination of two universal joints, with the same angularity, may be arranged in such away that one joint balances the fluctuations of the other to produce a constant velocity ratio, also a constant torque, but the intermediate shaft (propeller shaft) still continues to fluctuate [57]. Due to these fluctuations any resonance of the driveline system may be excited. The pair of universal joints introduces a fundamental forcing frequency of twice the input shaft speed into the propeller shaft. Similarly, there is a fluctuating relationship between the transmission torques of the input and output shafts.

2.5.2-Torsional Vibrations of the Propeller Shaft

The propeller shaft is subjected to torsional vibrations due to torque fluctuation with fundamental frequency of twice input shaft speed. Since the torque is inversely proportional with the speed, the torque relation can be written as;

$$T_o = \left(\frac{1 - \sin^2\alpha \ \sin^2\phi_i}{\cos\alpha} \right) T_i \approx (A + B\cos 2\phi_i) T_i \qquad (2.16)$$

where

$$A = \frac{1 - 0.5\sin^2\alpha}{\cos\alpha} \quad \text{and} \quad B = \frac{0.5\sin^2\alpha}{\cos\alpha}$$

Two general approaches are used in analysing torsional vibration of such systems. The first approach considers that the mass of the propeller shaft and stiffness are

distributed over the whole length while the universal joints are concentrated at the ends of the shaft as a concentrated mass moment of inertia. In this case a continuous system model can be developed and the governing equation of motion is a partial differential equation. The second approach is to approximate the propeller shaft as an equivalent discrete system. In this model, the moments of inertia of the attached masses (universal joints) and the shaft elements between two nodal points are summed and lumped at a chosen location corresponding to the approximate centre of gravity. The governing equation of motion of this model is an ordinary differential equation. Because this study is based on lumped masses for the driveline system components, the second approach is used, Fig (2.9).

2.5.3-Coupled Lateral-Torsional Vibrations of the Propeller Shaft

Universal joint vibration can be categorised into two broad groups: vibrations about the axis of rotation (torsional vibrations) and vibrations about any other axis (secondary couples) [6]. In other words, a universal joint gives a moment of force in shaft axis direction and also one in the direction perpendicular to this axis, which is called the secondary moment and this moment is caused a transverse vibration of the propeller shaft. As mentioned before, when the input shaft rotates with a constant angular velocity, the output shaft is subjected to the angular velocity fluctuation governed by a joint angle between the drive shaft and the driven one. However, when the driven shaft vibrates laterally and causes bending in itself, the joint angle is slightly changed and the rotating speed deviates. This is why the coupled lateral and torsional vibrations become unstable at the same time [47].

2.5.3-Propeller Shaft Model

This section is concerned with the torsional vibration modelling of the propeller shaft and Hooke's joints in the whole driveline system. The practical effect of a Hooke's joint between shafts is equivalent to a gearbox connecting two shafts in which the gear ratio varies sinusidally with input rotation and, therefore, input and output shafts can be replaced by a dynamically equivalent non-linear system. However, this representation makes the model complicated in this study because the model is based on lumped masses. Assuming the mass moment of inertia of the joints is relatively

large compared to the propeller shaft, the system can be considered as an elastic massless shaft between two mass moment of inertias excited by fluctuating torques provided by the joints located at the ends of the propeller shaft, Fig (2.9). Details of the fluctuating torque, $T(\phi)$, are covered in chapter 6.

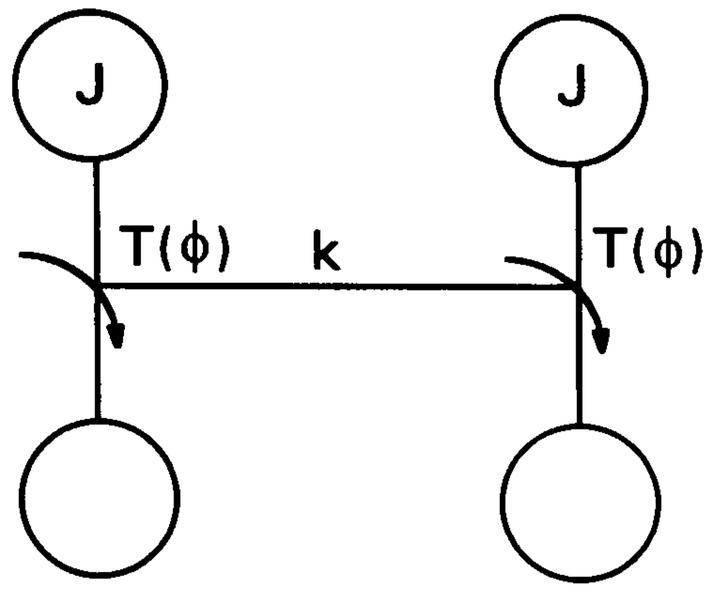

Fig (2.9) Propeller shaft and joints mathematical model

2.6-FINAL DRIVE SYSTEM

The function of turning the drive from the propeller shaft through 90° to distribute it to the wheels, reducing the speed of rotation and increasing the torque, is performed by the differential unit and the final axles. In other words, the differential is the device that divides the torque from the propeller shaft between the two output shafts to the wheels, regardless of the fact that they may be rotating at different speeds, for instance on rounding a corner [59].

The final drive system, Figs (2.10), consists of two similar axles 'b' which carry at their ends the road wheels, with mass moment of inertia J_w for each. These axles are driven by differential bevel gears, with mass moment of inertia J_d, and fixed to a crown wheel driven by a bevel pinion, with mass moment of inertia J_g. The bevel pinion, with mass moment of inertia J_p, is integrated with the differential input shaft 'a'. This shaft is coupled by means of a universal joint to the propeller shaft.

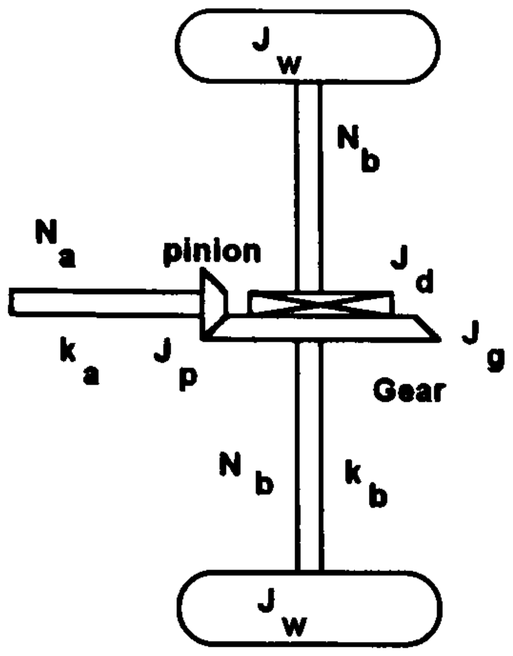

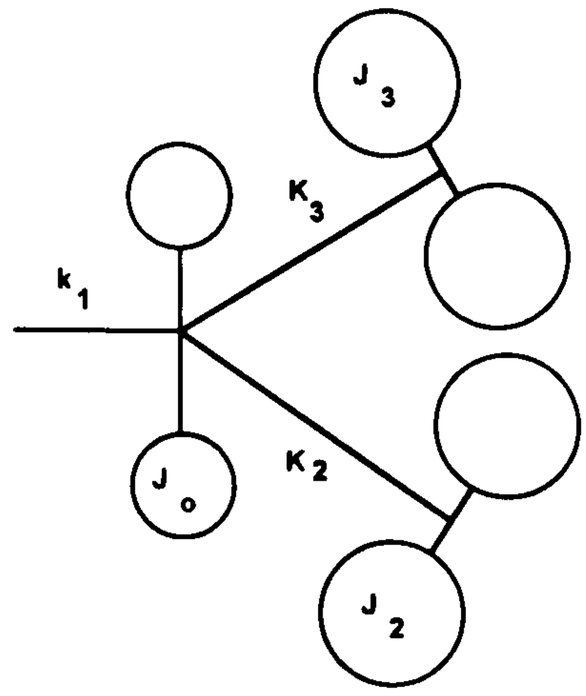

Original system Equivalent system

Figs (2.10) Arrangement of the final drive system and its equivalent system

2.6.1-Torsional Vibration of Equivalent System

In many early studies of the torsional vibration of vehicle driveline systems, this kind of substructure was simplified to a single branch. In reference [7], the comparison between the computed results of branched system and single branch one showed that the single branch model only reserves the symmetrical modes of the branched substructure and loses all the un-symmetric modes. However, the antisymmetrical 4th, 6th ,8th, 10th and 12th modes possess approximately equal frequencies and nearly identical mode shapes, for each of both branches, with the symmetrical 5th, 7th, 9th, 11th and 13th ones, respectively. Therefore, symmetrical branches of analytical models of torsional vibrations of such systems can not, in general, be simplified to a single branch. However, if the high-frequency modes need not be considered, the branched model can be reduced into single one.

Equivalent system

In the final drive system, there is one junction point with more branches each carrying one or more masses connected by lengths of elastic shafting. Therefore, the system can be reduced to an equivalent system referred to the propeller shaft speed, N_a, Fig (2.10). This figure shows the equivalent system where its characteristics are as follows:

$$\left.\begin{aligned} J_o &= J_p + (J_g + J_d)(N_b / N_a)^2 \\ J_2 &= J_3 = J_w (N_b / N_a)^2 \\ k_1 &= k_a \qquad \text{and} \\ k_2 &= k_3 = k_b (N_b / N_a)^2 \end{aligned}\right\} \tag{2.18}$$

Vibration analysis

For the individual vibrational analysis of this system, the natural frequencies of the equivalent system can be determined from the free vibration solution of the system model. Note that, since the branches J_3 on k_3 and J_2 on k_2 are identical (J_2=J_3 and k_2=k_3) then one of the natural frequencies of the system is ($\omega^2 = k_3/J_3 = k_2/J_2$) [51]. The remaining frequencies can be determined after simplifying the equivalent system by duplicating the identical branches and replace them by a single one consisting of 2J on 2k as shown, Fig (2.11). Thus the system reduces to a two-mass arrangement.

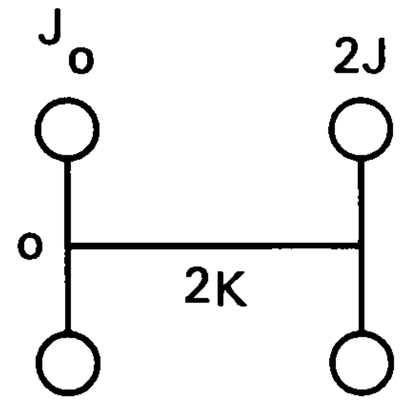

Fig (2.11) Simplified equivalent system

Mode shape

In such branched systems, each branch consists of a single mass connected by a flexible shaft to a single common point, the modes of the complete system can be divided into two categories. The first group of i similar branches (ω_i of similar branches are equal), having common frequency ($\omega_i^2 = k_i / J_i$) vibrates with a node at the common point, o, and other parts of the system remain at rest, i.e. only the similar branches share in the motion and the remainder of the system including the mass at the common point remain at rest. In the second group, the system vibrates without a node at the common point. For this type of motion all the branches in a given group of similar branches vibrate in phase and with the same amplitude [51]. Note that the

calculated mode shapes values are equivalent values; the original values are obtained by making due allowance for the gear ratios as;

$$\left.\begin{aligned} \theta_p &= \theta_o, \\ \theta_g &= \theta_o (N_b/N_a) \quad \text{and} \\ \theta_w &= \theta_2 (N_b/N_a) \end{aligned}\right\} \tag{2.19}$$

2.7-DAMPING

The general reason for including some damping in a vibratory system is to suppress the vibration peaks and control the generated noise. In this section, the well known general ideas about vibration damping and its application to driveline systems are introduced.

2.7.1-Introduction

Damping is the term used to define the non conservative forces acting on a vibratory system that dissipate energy. The correct mathematical form used to model damping for a given mechanical system is difficult to determine. However, for most mechanical systems, damping is categorised by one or more of the following types [36];

1. Damping proportional to the velocity or viscous damping ($F_d = c\ \dot{x}$), typically that due to shearing of a laminar and viscous fluid or the resistance of viscous fluid flow through an orifice.
2. Damping proportional to the velocity square ($F_d = c\ \dot{x}^2$), typically that due to the drag of a turbulent fluid-a high speed phenomena in the case of viscous fluids.
3. Damping constant or Coulomb damping ($F_d = c$), typically that due to dry friction with constant friction coefficient with respect to sliding speed
4. Hysteresis damping/structure damping, typically that due to internal friction between various planes of material as the material is deformed.

2.7.2-Damping in Driveline Systems

All the driveline system components include some damping with different types and different levels. For the engine, energy is dissipated in the plain bearings and piston rings. As mentioned in [36], an interesting exercise was carried out to assess the effect

of the piston rings on the magnitude of the damping in the engine torsional vibration system. It would appear that a fairly high proportion of the whole damping of torsional vibrations is provided by the piston rings. This is to be expected because damping at the main bearings is unlikely to be significant whereas torsional displacements of the crankpin are transferred through the connecting rod to give linear vibration of the piston and rings.

There is also energy dissipated in the gearbox and the final transmission, in the mesh and bearings. An internal or structure damping exists and depends on the material of each component of the driveline system. Also, the equivalent damping of the tyres is significant in the study of the torsional vibration behaviour of the driveline system.

Torsional vibration dampers

Research has indicated that various types of vibration dampers could more or less damp the torsional vibrations. For example, to reduce torsional vibrations, a vibration rubber damper may be mounted at the free-end of the engine crankshaft since the vibration amplitude at this point is considerable for all modes of vibration and this is an accessible position. In this type of damper, the torsional vibrations are absorbed in friction in the same way as in the case of a spring damper. However, the rubber dampers are limited to small engines in their application.

An alternative damper is the viscous type which, though more expensive than the rubber type, is extremely reliable [53]. The theoretical treatment of the viscous-shear damper is similar to that of the rubber dampers, but with the simplification that the stiffness of the damping material is zero.

Moreover, the elastic-friction torsional vibration damper is usually incorporated into the driven plate of the transmission clutch. It consists of elastic elements (springs) and damping elements (friction rings). Generally, the torsional damper in the clutch disc has the task of influencing the torsional vibration behaviour of the complete driveline in the required manner.

General considerations

In modelling vehicle driveline systems, the following considerations should be taken into account.

1. The journal bearings possess considerable damping arising from viscous shearing of the oil film and, the viscous type damping is a good approximation to represent the damping torque of the journal bearing of the system.
2. The torsional dampers at the front end of the crankshaft and in the clutch disc can be represented by viscous damping type.
3. The torsional damping of the tyre can be represented by hysteresis damping type; this value must be obtained from the experiment.
4. The internal damping of the driveline component's material can be represented by hysteresis damping.
5. The drag torque in the gearbox and differential can be approximately represented by a viscous damping torque.

However, the damping coefficients in the different components of the driveline system model considered in this study are represented by the viscous damping type. The hysteresis damping of the driveline segments and the dry friction damping caused by engine accessories such as the camshaft, water pump, fan generator, air compressor and so on are neglected. Note that the latter damping term introduces non-linearities into the driveline system.

In the suggested driveline system model, Fig (2.13), the following damping coefficients are defined as;

c_1 The equivalent viscous damping coefficient of the torsional vibration damper at the front end of the crankshaft.

c_2-c_5 The equivalent viscous torsional damping coefficients in the engine for each piston-rod-crank unit; for a given engine, these data may be obtained by standard experiments.

c_6 The equivalent viscous damping coefficient of the torsional damper of the clutch disc.

c_7-c_9 The equivalent viscous torsional damping coefficient in the gearbox.

c_{10}-c_{12} The equivalent viscous torsional damping coefficients in the propeller shaft and the differential units.

c_{13} and c_{14} The equivalent viscous torsional damping coefficient of tyres.

2.8-Overall Driveline System Model

The overall equivalent torsional vibrating model of a vehicle driveline system is based on discretisation and lumping of the masses. It consists of idealising the complete driveline system as a set of inertia discs linked together by torsional, linear and massless, springs which reproduce the dynamic behaviour of all constituent parts; the engine and torsional damper, the clutch, the gearbox, the propeller shaft and Hooke's joints, the differential and the rear axle assembly. Wheels and tyres are simply modelled by concentrated mass moments of inertia, linearised torsional stiffness and viscous damping coefficients. The driving wheels are considered connected to the ground because the effect of the tyre slip is neglected and the mass moment of inertia of the vehicle body is relatively large. Discrete values of viscous damping for each components are included. Figure (2.13) shows the 14 DOF torsional vibration model of the overall driveline system of a four-cylinder, rear-drive vehicle which is used in this thesis.

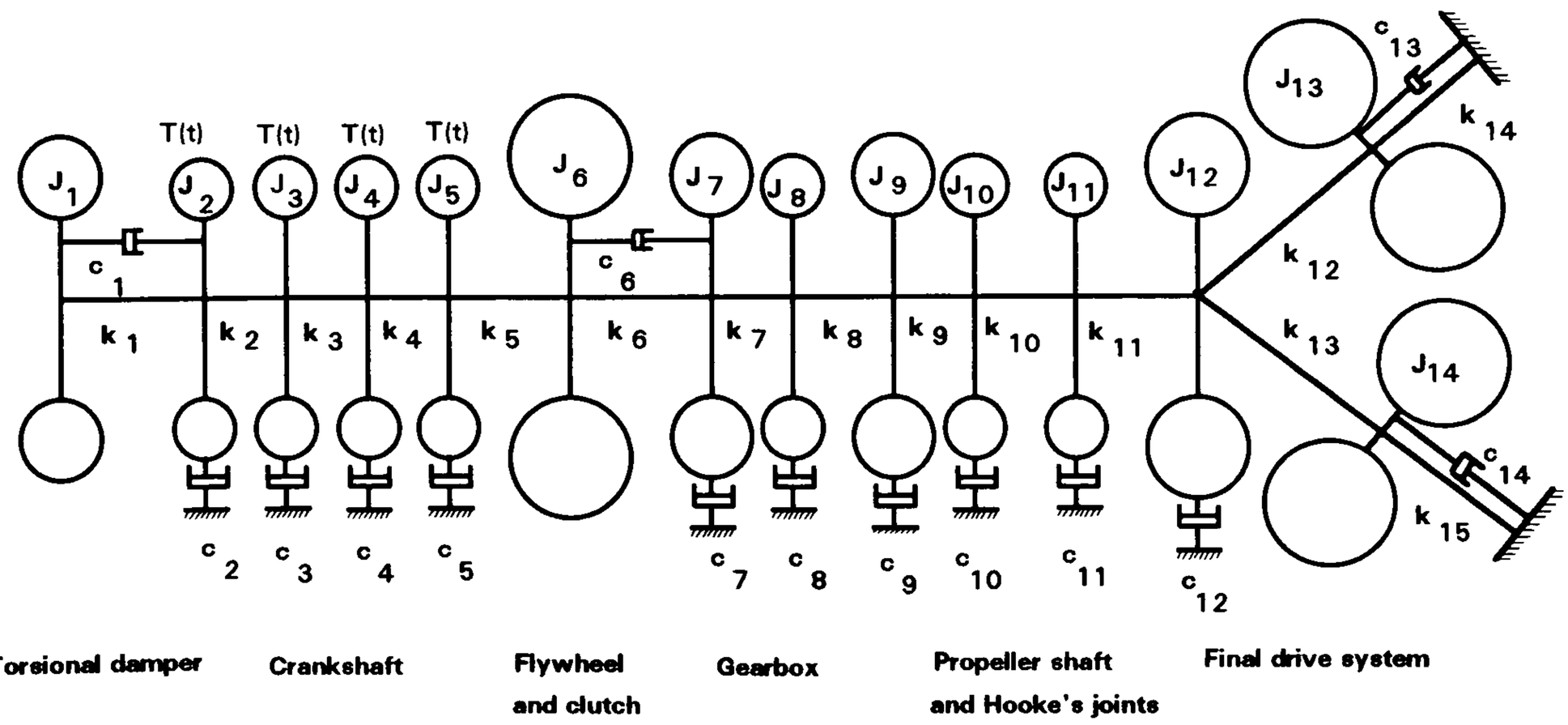

Fig (2.13) Damped torsional vibration model of the driveline system

2.9-SUMMARY

A review of the torsional vibration properties of each component of the driveline system including elements of a vibration system (mass, stiffness and damping) was presented. The overall equivalent torsional vibration model of a vehicle driveline system based on discretisation and lumping of the masses was constructed. The sophistication of this model was based on the requirement of accurately representing the low frequency behaviour of the driveline for the purpose of this study. It consists of idealising the complete driveline system as a set of inertia discs linked together by torsional, linear and massless, springs which reproduce the dynamic behaviour of all constituent parts; the engine and torsional damper, the clutch, the gearbox, the propeller shaft and Hooke's joints, the differential and the rear axle assembly. Discrete values of viscous damping representation for each component were included.

The torsional vibration problems in the whole driveline system are closely related to the torsional vibration problems in the individual system components such as fluctuating engine torque, clutch judder, gearbox noise and fluctuating torque due to Hooke's joints. Therefore, it was concluded that it is not possible to understand the total system behaviour based on the behaviour of the individual component because they are all interacted dynamically. Hence it is required to model the entire system to capture all the coupling effect.

CHAPTER 3

ENGINE EXCITATION OF DRIVELINE SYSTEM

3.1-INTRODUCTION

Many sources of excitation of vehicle driveline systems should be considered with respect to torsional vibrations analysis of the system. These sources may be divided into linear and non-linear excitations. Table (3.1) lists major causes, without claiming to be all-inclusive [13].

Table (3.1) Excitation sources of a vehicle driveline torsional vibration

Excitation Source	**Phenomenon**	**Linear/non**
Engine	Ignition, irregular ignition, torque change, friction and inertia of moving masses.	Linear
Clutch	Judder due to induced friction torque.	Non-linear
Torsion damper	Periodic change in the damping characteristics.	Linear
Transmission	Gear meshing, gear pitch error and torque spikes due to shifts	Non-linear
Propeller shaft	Fluctuating torque due to bending angle	Non-linear
Tyres	Road surface conditions, longitudinal slip forces	Non-linear

For the engine, the main source of the excitation is the torque fluctuation arising from the four stroke and two stroke cycles. Irregular ignition or even misfiring can also lead to serious vibration problems, but these factors will not be treated in this study because they represent fault conditions.

Clutch judder can also become an additional source of driveline excitation and a detailed study of this phenomenon is presented in a separate section.

Gear meshing and gear pitch error in the transmission itself can also excite torsional vibrations of driveline system. In automatic transmissions, gear shifts can have an effect similar to a change in engine torque. Propeller shafts with Hooke's joints can also be excited by induced fluctuating torque due to the angularity of joints. Irregular road surfaces are capable of exciting the driveline system, as can tyre slippage resulting from small changes in friction coefficient between the tyre and the road surface.

This chapter is concerned with the excitation torque arising from the engine only, while other excitation sources such as clutch, Hooke's joints and tyres are discussed in other chapters.

3.2-ENGINE FLUCTUATING TORQUE

Reciprocating piston engines, typically 2 or 4 stroke inevitably involve cyclical processes and so the torque delivered by the engine is not constant in magnitude. At the crankshaft the torque delivered consists of a series of pulses corresponding to the power stroke of each cylinder. Fig (3.1) shows torque variations against the crank angle for a typical four-stroke, four-cylinder engine [1].

The flywheel inertial acts so as to smooth the torque output which consists of a steady-state component plus superimposed torque variations. Because of compliances in the engine/transmission mounts, the system typically vibrates in six directions, three transitional directions and three rotations around the transitional axes. Therefore, the engine may produce forces and moments on the vehicle body in directions other than roll as a result of the inherent imbalances in the reciprocating / rotating masses. However, this study is restricted to a study of the torque variations at the transmission which produce excitation in the rotational direction of the driveline system.

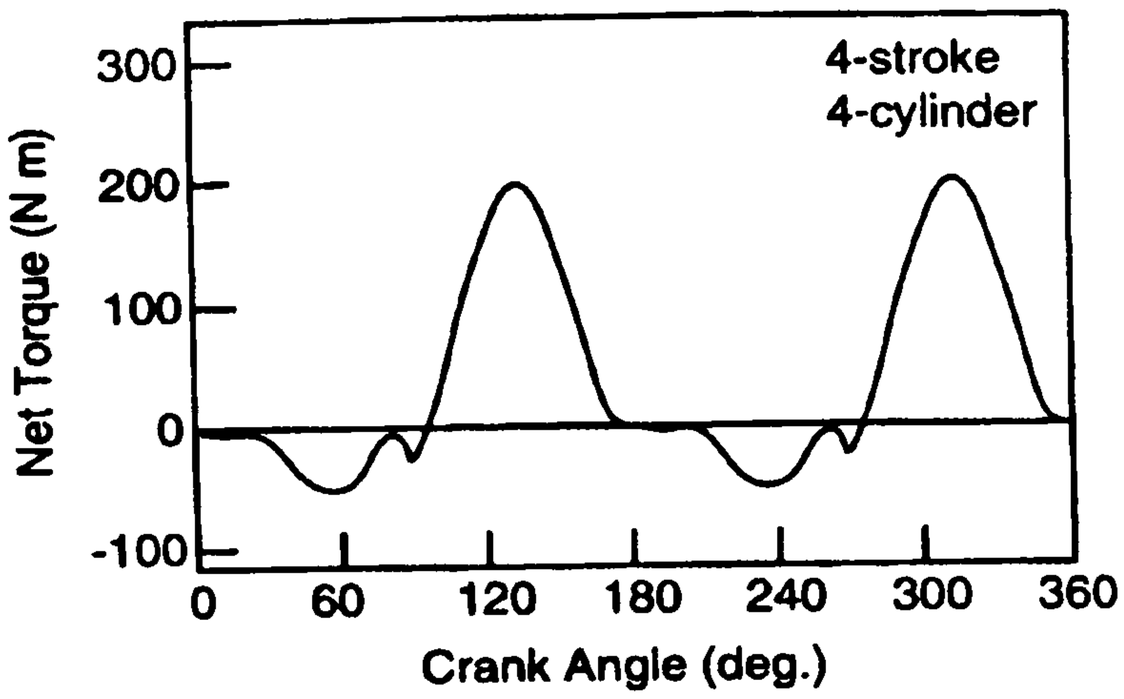

Fig (3.1) Typical torque variations at the output of a four-stroke, four-cylinder engine

Although the speed spectrum of the engine was used in [14], it is the engine fluctuating torque which is required for accurate modelling. In this chapter a method for describing the engine fluctuation torque is introduced and used as an excitation load vector for the driveline system vibrations.

As the engine cycle progresses, there are three forces which act together on the connecting rod and ultimately produce a torque on the crankshaft. These are the gas pressure, inertia and friction forces which all add together to produce the periodically varying rotational torque on the crank. However, the friction force is a relatively unimportant contribution to the net force [52], so it is not considered in this study. Therefore, the engine fluctuating torque, arising only from the combined effect of the varying gas pressure in the cylinders and the motion of the reciprocating masses, is the principle cause of forced torsional vibrations of the driveline system. A detailed study of gas pressure and inertia torques are presented in the next sections.

3.2.1-Gas Pressure Torque and its Harmonics

The torque generated by the gas pressure forces, T_g, is usually referred to as indicated torque. The relationship between the indicated pressure for each cylinder, P_g, and the resulting indicated torque contribution for that cylinder is a function of engine geometry. This function $g(\phi)$ may be found in many publications such as [60], where;

$$T_g(\phi) = P_g(\phi).g(\phi) \quad \text{and} \qquad (3.1)$$

$$g(\phi) \approx AR \sin\phi \quad (1 + \lambda \cos\phi) \qquad \text{(see also Eqn 2.9)} \qquad (3.2)$$

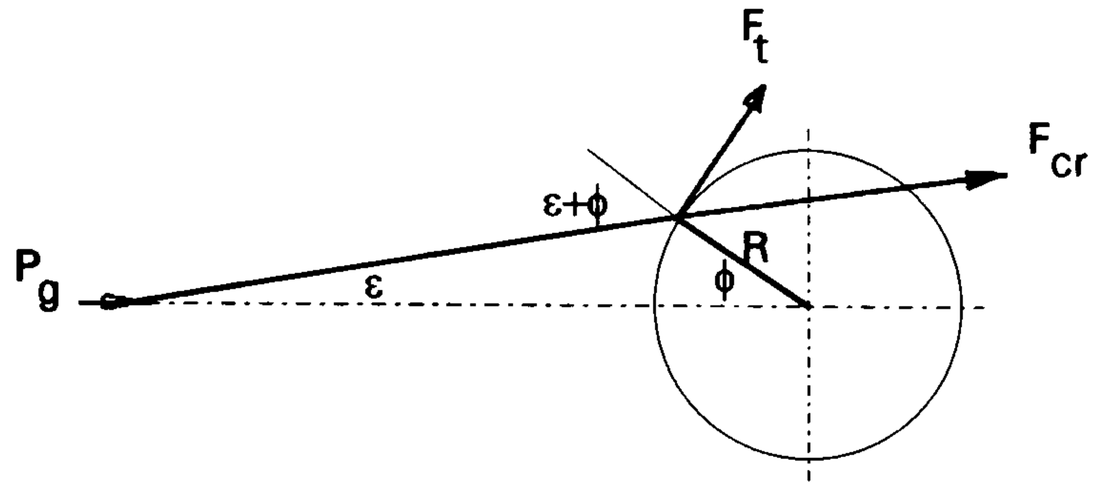

From the figure shown;

$F_{cr} = P_g A / \cos\varepsilon$

$F_t = F_{cr} \quad \sin(\varepsilon + \phi)$

$T_g(\phi) = F_t \quad R$

Fig (3.2) Schematic diagram of slider-crank mechanism

Since ϕ is a function of time, T_g and P_g are also, in general, functions of time; however, the geometry of the engine imposes a periodicity with respect to the crank angle on the fluctuating torque, as indicated by the function $g(\phi)$. The crank angle ϕ is directly related to time by a factor equal to engine speed, $d\phi = \omega dt$, and for constant engine speed; $\phi = 2\pi Nt / 60$, where N is the engine revolution per minute.

To obtain the gas pressure, it is possible to construct theoretical cylinder-pressure diagrams with the aid of thermodynamic charts. However, such diagrams are of limited value for torsional-vibration investigations and it is preferable, wherever possible, to base design-stage calculations on reliable experimental data because the fluctuations in cylinder-pressure diagrams vary from cylinder to cylinder and even from one engine cycle to another as a result of a variety of thermal factors. In view of these variations, it is not surprising that it is difficult to assign accurate values of harmonic components to a particular engine, unless these values are based on tests of the particular engine considered. These inaccuracies may reach 100% in some cases. Hence, this is one of the main reasons why formulae for predicting vibration amplitudes can only give very approximate estimated values [60].

Therefore, the true gas pressure has to be determined for the different speeds and load conditions on an engine test bed by use of a pressure transducer inside the combustion chamber [19]. However, it is beyond the scope of this study to investigate the

phenomenon of combustion. So, typical data of the gas pressure at a particular engine speed were taken from reference [61].

The gas pressure torque obtained from Eqn (3.1) is in numerical form and has discretized values corresponding to crank angle and gas pressure. In the next section, the gas torque is analysed into its harmonic components.

Harmonic components of the gas pressure torque

The gas pressure torque of an internal combustion engine, Eqn (3.1), repeats after every complete working cycle. For a four-stroke cycle, single acting engine, the interval of repetition is two revolutions of the crankshaft (4π) and the period is $4\pi/\omega$. For a two-stroke cycle, single-acting engine the internal is one revolution (2π) and the period is $2\pi/\omega$, where ω is the angular velocity of the crankshaft. Therefore, the gas pressure torque, T_g, can be represented by a Fourier series which consists of a steady part, T_o, and fluctuating part. The steady part determines the useful mean output power from the engine, but does not excite torsional vibration, therefore it is omitted in the system vibration analysis. The form of the Fourier series of the gas torque is;

$$T_g(t) = T_o + \sum_{k}^{h_0} c_k \cos(k\omega t) + \sum_{k}^{h_o} s_k \sin(k\omega t) \qquad \begin{matrix} k=0.5,\ 1,\ 1.5,\ldots \text{for 4stroke-cycle} \\ k=1,\ 2,\ 3,\ldots\ldots\ldots \text{for 2stroke-cycle} \end{matrix} \qquad (3.3)$$

where, h_o is the maximum number of required harmonic orders; in practice h_o is from 8 to 12 orders. The mean torque and the amplitude of harmonic components are numerically determined by these following expressions;

$$\left.\begin{aligned} T_o &= \frac{1}{ni}\sum_{n=1}^{ni} T_{gn}, \\ c_k &= \frac{2}{ni}\sum_{n=1}^{ni} T_{gn}\cos\left(\frac{2\pi nk}{ni}\right) \qquad \text{and} \\ s_k &= \frac{2}{ni}\sum_{n=1}^{ni} T_{gn}\sin\left(\frac{2\pi nk}{ni}\right) \end{aligned}\right\} \qquad (3.4)$$

where ni is the number of equal intervals into which the given periodic gas pressure torque curve for one period is divided and T_{gn} is the gas pressure torque at each interval [62].

The number of excitations received by the system during one revolution of the crankshaft is called the order number or harmonic order, k. For a four-stroke-cycle, single acting engine, the harmonic component orders are half multiple, i.e. k= 1/2, 1, 3/2, 2, etc. While for a two-stroke-cycle, single acting engine, there are no half orders, the harmonic component orders are integer multiple i.e. k=1, 2, 3,.. etc. For instance, the 4^{th} order component of the fluctuating torque repeats itself four times in each revolution of the crankshaft in the two-stroke-cycle engine, while it repeats itself two times in the four-stroke-cycle engine [60].

High levels of vibration will occur when the frequency of a peak in the excitation specimen coincides with one of the natural frequencies of the system. Since the excitation frequencies change with engine speed, it is clear that a wide range of excitation condition will occur throughout the engine speed range.

3.2.2-Inertia Torque

The inertia torque does not contribute any net energy to the system but strongly affects the time-varying behaviour of the engine torque and consequently the system vibrations [63]. The inertia torque is assumed as sum of three terms [60] namely; torque due to inertia of reciprocating and rotating masses, torque due to dead weights of reciprocating and rotating masses and the inertia torque due to the connecting rod couple, which arises due to the difference between its original moment of inertia and moment of inertia of its equivalent lumped masses (assuming lumped mass model). In the majority of practical cases the effect of the inertia torque due to the dead weight and connecting rod couple are small and can be disregarded. Therefore, the most important effect from the point of view of torsional vibration is the inertia torque arising from the motion of the reciprocating masses only.

As in the case of gas pressure torque, the inertia torque due to reciprocating parts can be analysed to obtain a series of harmonic components, which for both two-stroke and four-stroke cycle engines contains the integer order only, 1, 2, 3, etc., and each order is represented by a sine term only i.e., there are no half-orders and no cosine terms. The inertia torque T_i due to the reciprocating parts in terms of time can be calculated correctly as long as the crank-train kinematics are modelled properly. Assuming the crankshaft angular velocity ($\dot{\phi}$) is constant, the inertia torque, as mentioned in Eqn (2.8) is [60];

$$\left.\begin{aligned} &T_i(t) \approx s_1 \sin\omega t - s_2 \sin 2\omega t - s_3 \sin 3\omega t + \ldots. \\ &\text{where} \\ &s_1 = m\omega^2 R^2 \lambda / 4, \\ &s_2 = m\omega^2 R^2 / 2, \\ &s_3 = 3m\omega^2 R^2 \lambda / 4, \\ &\lambda = R / l_{cr} \end{aligned}\right\} \qquad (3.5)$$

where m is the reciprocating masses.

It is assumed that the terms of higher than 3rd order can be disregarded since they have an insignificant effect on the inertia torque.

3.2.3-Total Fluctuating Torque

The total fluctuating torque applied to the crankshaft is the sum of the gas pressure torque, Eqn (3.3), and the reciprocating masses inertia torque, Eqn (3.5). Since the gas pressure components contain both sine and cosine terms, while the inertia torque components contain sine terms only it is necessary to add the sine terms in both equations independently, before combining them with the cosine terms in Eqn (3.3) to obtain the resultant fluctuating torque. As a general rule, the gas pressure components of the integer orders 1 to 3 in the case of both two-stroke cycle and four-stroke cycle engines should be added vectorially to the corresponding terms of the reciprocating masses inertia torque, while no additions need be made to all the remaining orders, including the half-orders associated with four-stroke cycle engine.

The resultant fluctuating torque for one cylinder for a four stroke-cycle engine becomes;

$$T(t) = T_g(t) + T_i(t)$$

Substituting in Eqs (3.3) and (3.5) gives;

$$T(t) = \sum_{k=0.5}^{h_o} s_k \sin(k\omega t) + \sum_{k=0.5}^{h_o} c_k \cos(k\omega t) = \sum_{k=0.5}^{h_o} T_k \sin(k\omega t + \gamma_k) \qquad (3.6)$$

where

T_k is the amplitude of k^{th} order fluctuating torque,

$$T_k = \sqrt{s_k^2 + c_k^2} = \sqrt{(s_g + s_i)_k^2 + c_{gk}^2}\,, \qquad (3.7)$$

γ_k is the phase angle of the k^{th} order fluctuating torque (due to combination of the cosine and sine terms),

$$\gamma_k = \tan^{-1}\frac{c_k}{s_k} = \tan^{-1}\frac{c_{gk}}{(s_g + s_i)_k}, \qquad (3.8)$$

c_g: cosine coefficient of the gas torque,

s_g: sine coefficient of the gas torque, and

s_i: sine coefficient of the inertia torque.

The subscripts g and i referred to gas and inertia terms respectively.

It is clear from Eqn (3.6) that, for a four stroke-cycle engine, the fundamental frequency of the fluctuating torque is equal to half the crankshaft speed and the harmonic components have frequencies which are whole-number multiples of the fundamental frequencies. That means that the harmonic components of the torque applied to the crankshaft have frequencies equal to crankshaft speed multiplied by 1/2, 1, 3/2, 2,....etc. for a four stroke engine and have frequencies equal to crankshaft speed multiplied by 1, 2, 3,...etc. for a two-stroke-engine.

3.2.4-Multi Cylinder Engine

Eqn (3.6) gives the fluctuating torque emanating from a single cylinder engine. In the case of a multi-cylinder engine it can be assumed that, in general operating conditions, all cylinders have substantially the same output, i.e. T(t) is the same for all cylinders [60]. However, there is a phase difference between the fluctuating torque in each cylinder. The phasing of the fluctuating torque of the individual cylinder is related to the firing order, the type of the engine (two or four stroke-cycle), the harmonic order and the angle between the various cranks. The phase angle α_{qk} between cylinder number q and the first cylinder for the k^{th} harmonic order can be calculated from these expressions, [62];

$$\left.\begin{aligned} \alpha_{qk} &= (q-1)\Delta\alpha_k \qquad \text{where} \\ \Delta\alpha_k &= \frac{k.n_s\pi}{n_c} \end{aligned}\right\} \tag{3.9}$$

where $\Delta\alpha_k$ is the phase angle between two fluctuating torques with k^{th} harmonic order developed by two successively firing cylinders, n_s is the number of strokes per cycle (2 or 4), n_c is the number of cylinders and k is the harmonic order. The expressions (3.9) are derived based on a fact that the cylinders of the engine are arranged so that all the fluctuating torques developed for one revolution (2π) of the crankshaft will be uniformly distributed within a 2π angle.

The fluctuating torque of the q^{th} cylinder acting on the crankshaft in the q^{th} plane becomes;

$$\{T(t)\}_q = \left\{\sum_{k=.5}^{h_o} T_k \sin(k\omega t + \beta_k)\right\}_q \tag{3.10}$$

where

β_{kq} is the phase angle of k^{th} harmonic order of q^{th} cylinder, $\beta_{kq} = \gamma_{kq} + \alpha_{kq}$.

Thus a total fluctuating torque vector, with length, n_c, for a multi cylinder engine in terms of the time and engine speed is formed by adding the individual fluctuating torque of each cylinder.

3.3-COMPUTER PROGRAM

The previous mentioned mathematical operations have been translated into a computer program using the mathematical library subroutines in MATLAB to obtain the numerical form of the fluctuating torque vector for different engine types (two / four stroke-cycle), different firing orders, different numbers of harmonic order, different engine speeds and different cylinder numbers. The program has been designed to be interactive allowing the user to specify the engine specifications by answering a series of questions such as, what is the number of strokes per cycle?, what is number of cylinders?, how many harmonics need to be considered?, which orders are required to be considered?, what is the engine speed?, what is the firing order?,.... etc. See the program flow chart steps in Fig (3.3).

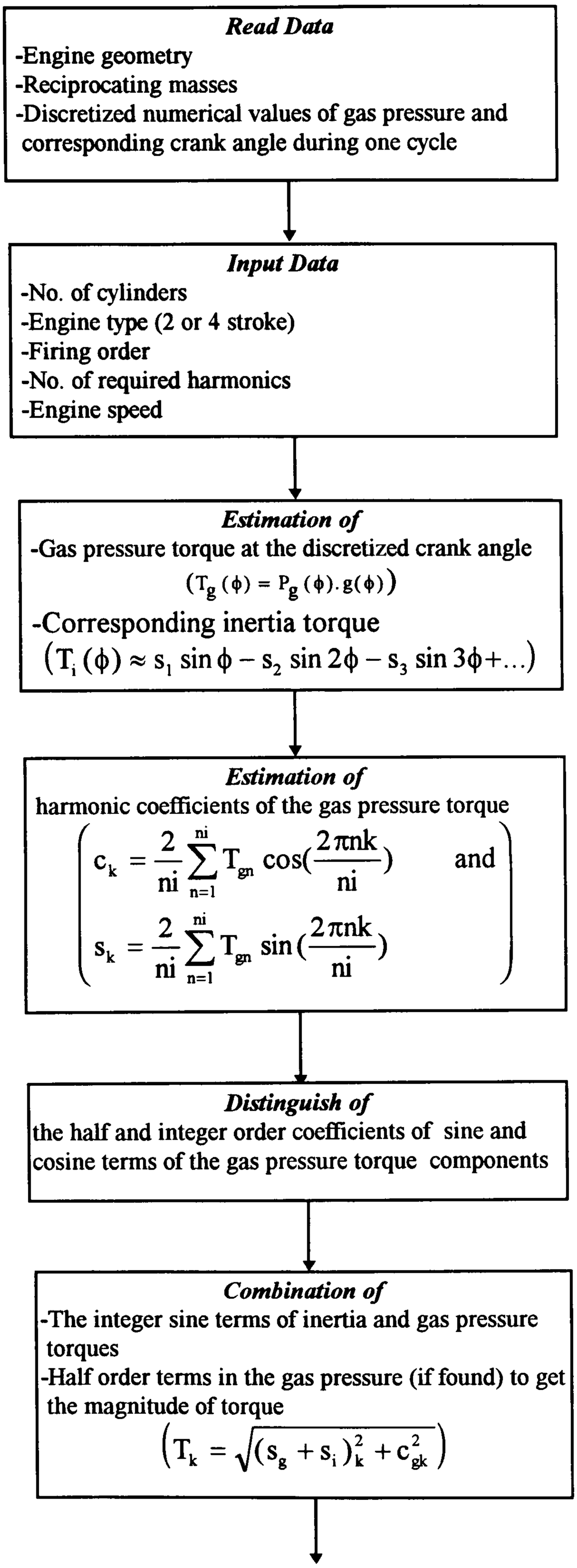
Read Data
-Engine geometry
-Reciprocating masses
-Discretized numerical values of gas pressure and corresponding crank angle during one cycle
Input Data
-No. of cylinders
-Engine type (2 or 4 stroke)
-Firing order
-No. of required harmonics
-Engine speed
Estimation of
-Gas pressure torque at the discretized crank angle
$(T_g(\phi) = P_g(\phi).g(\phi))$
-Corresponding inertia torque
$(T_i(\phi) \approx s_1 \sin\phi - s_2 \sin 2\phi - s_3 \sin 3\phi + \ldots)$
Estimation of
harmonic coefficients of the gas pressure torque
$c_k = \frac{2}{ni}\sum_{n=1}^{ni} T_{gn} \cos(\frac{2\pi nk}{ni})$ and
$s_k = \frac{2}{ni}\sum_{n=1}^{ni} T_{gn} \sin(\frac{2\pi nk}{ni})$
Distinguish of
the half and integer order coefficients of sine and cosine terms of the gas pressure torque components
Combination of
-The integer sine terms of inertia and gas pressure torques
-Half order terms in the gas pressure (if found) to get the magnitude of torque
$(T_k = \sqrt{(s_g + s_i)_k^2 + c_{gk}^2})$

Flow chart steps, continue

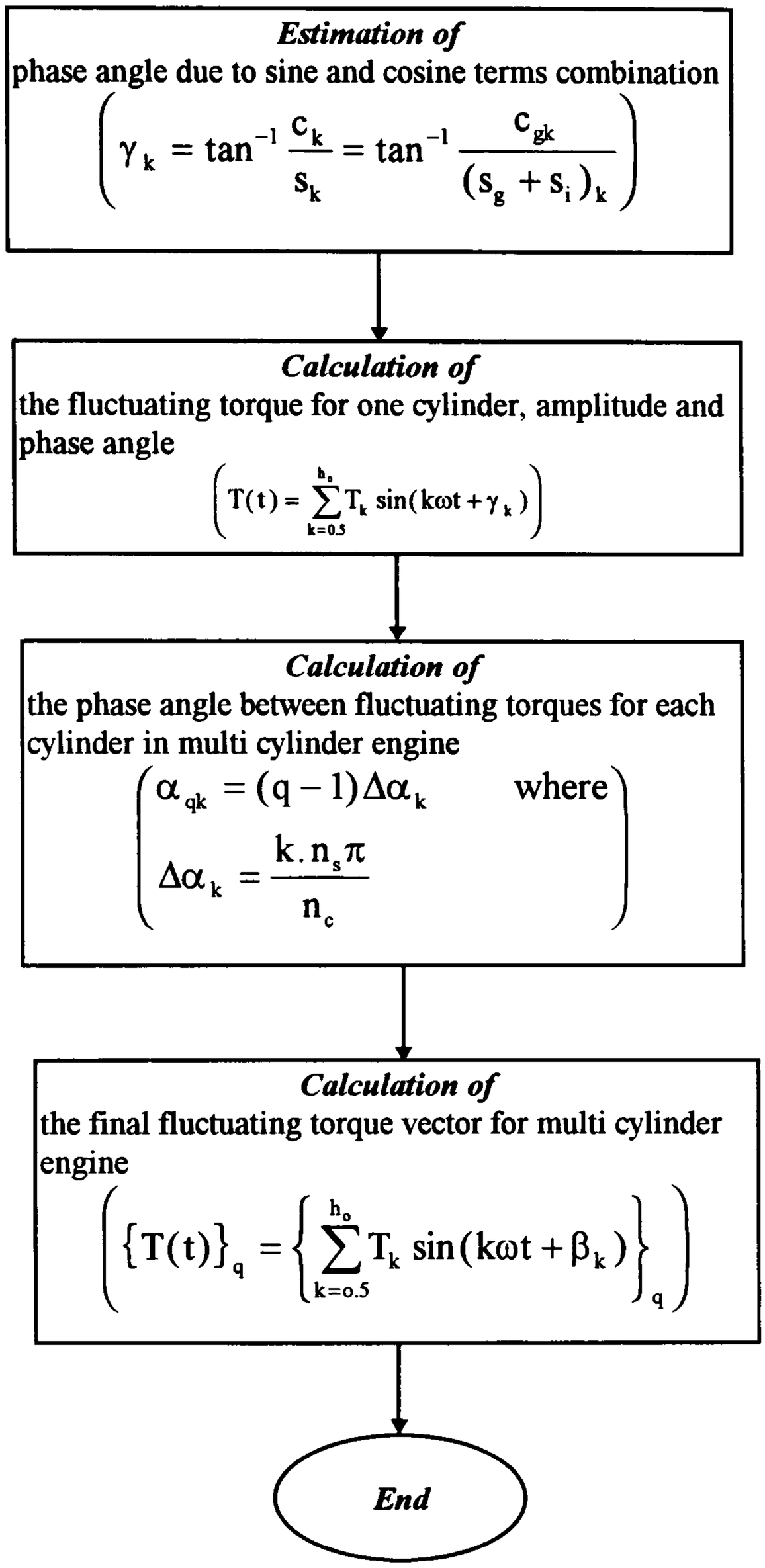

Fig (3.3) Flow chart steps of fluctuating engine torque using MATLAB

The resultant fluctuating torque in numerical form is used for further analysis of the driveline system vibrations. The output of the program for a typical engine is shown, in Fig (3.4).

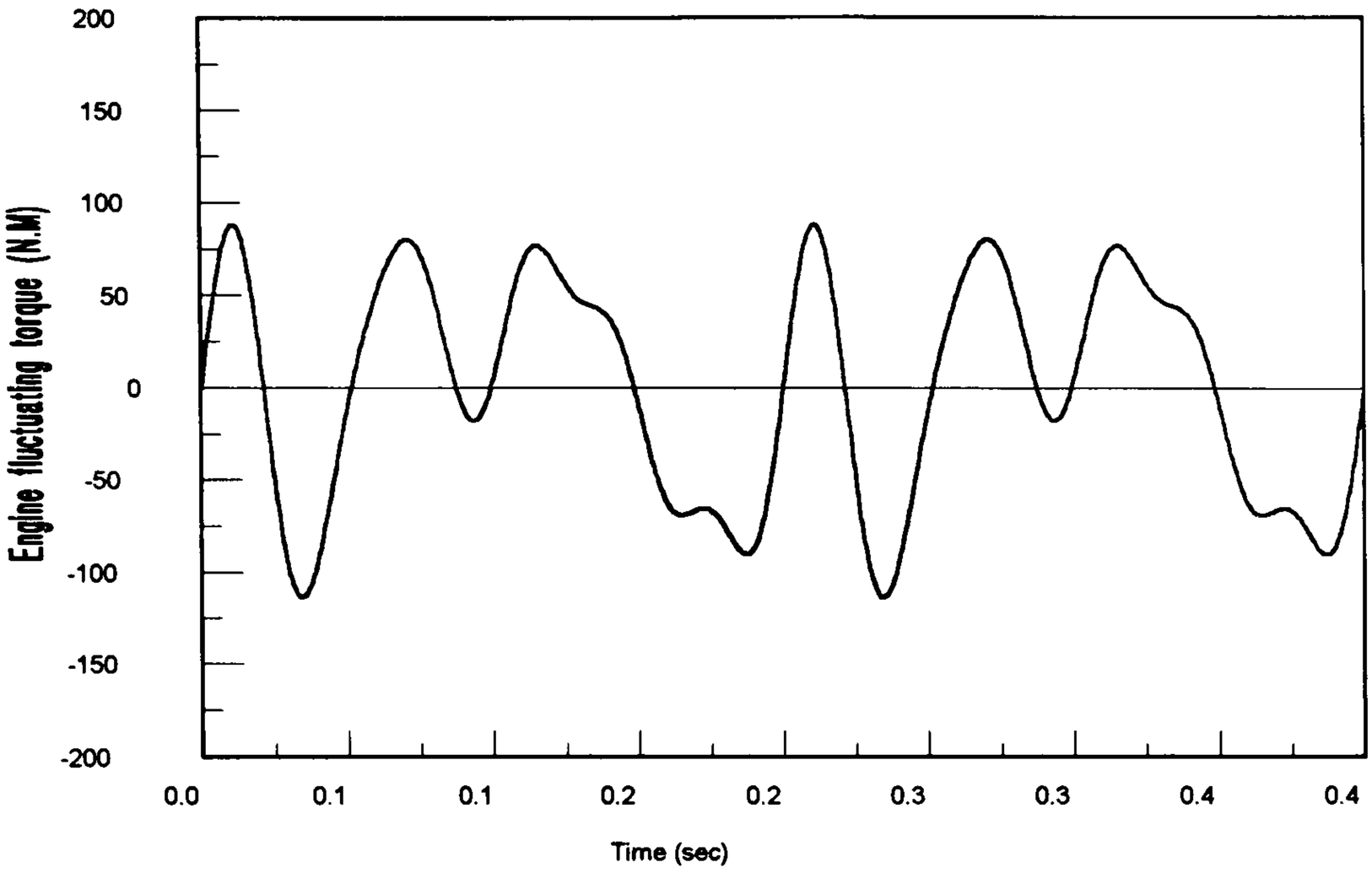

Fig (3.4) Fluctuating torque from one cylinder for typical engine data

3.4-SUMMARY

The most important sources of excitation for torsional vibrations in the vehicle driveline have been discussed. Because it is crucial to the prediction of driveline behaviour since it is provides the main forcing, a computer programme using MATLAB subroutines was developed to obtain this fluctuating torque for different engine parameters. The computer program was used throughout all later chapters for further study of the dynamic behaviour of the automotive driveline system.

CHAPTER 4

SUBSTRUCTURE APPROACH AND MODAL ANALYSIS

4-1-INTRODUCTION

The past few decades have seen the development of several techniques for the dynamic analysis of large structures. It is desirable to have a method for dynamic analysis which permits the study to be simple and allow as much independence as possible in the design and analysis of substructures. Some of these methods are constructed based on dividing the complex structure into components or substructures. Therefore, the substructure synthesis method has been developed for the vibration of complex structures for which the usual method, e.g. finite element method or transfer matrix method is either difficult or impossible to apply. A large amount of literature has been published on the development and applications of modal synthesis and substructure technique and a detailed review is given in [64] and [65].

The driveline system usually involves non uniform distributed parameters and complicated boundary conditions. Hence, the analysis of the vibrational behaviour of a such system is usually complicated and tedious. A technique is required which allows any driveline configuration to be studied without having to write the equation of motion of the complete system. A substructure approach satisfies this requirement. Any driveline model can be constructed from the vibrational characteristics of each component which can be found analytically or from experimental tests. Another advantage of using substructure techniques is that the analysis and design of different components can be carried out independently at different organisations. Also, the effect of a modification in one of the components on the whole system is more easily incorporated in the model. Because a new design in one component need only modify the modal data of that changed component, the modified modal data can then simply be coupled with the remaining unchanged components. However, the analysis using substructure technique depends on modal analysis and superposition principles which require the system to be linear and therefore, in this chapter, the driveline system is modelled as being linear.

The aim of this chapter is to present efficient and simple procedures to deal with the dynamic behaviour of a vehicle driveline system. The procedures are based on substructure and mode synthesis techniques. The substructure approach is explained

in point of view of basic concepts and the mathematical derivation for coupling of substructures is described in the context of the vehicle driveline problem.

4.2-BASIC CONCEPTS

The main basic concept of the substructure technique is to treat the structure as an assembly of connected components or substructures, each of which is analysed separately to derive a set of modes or displacement shapes from which a set of modal co-ordinates applicable to the complete structure is synthesised.

The procedure of the substructure synthesis technique is as follows; the modal parameters, natural frequencies, mode shapes and damping ratios of all the component parts are obtained either experimentally by vibration tests or theoretically by any appropriate method depending on complexity of each substructure. If the frequency response functions of some or all parts are obtained experimentally, the modal parameters of these parts can be extracted by curve fitting techniques. Then, the modal parameters of all substructures are combined to construct an equation for the total system, and this equation can then be solved, and natural frequencies, natural modes and dynamic response can be obtained [66]. The vibration modes of the total system can be obtained by either partial, or full modal coupling of the substructure modes.

Some of the basic concepts which are required to understand the principles of the substructure approach are introduced here without details.

4.2.1-Modal Analysis

The well known equation of motion of a vibratory system with NDOF is;

$$[M]\{\ddot{x}\} + [C]\{\dot{x}\} + [K]\{x\} = \{F(t)\} \qquad (4.1)$$

where [M], [C] and [K] are (NxN) mass, damping and stiffness matrices respectively, $\{x\}$, $\{\dot{x}\}$ and $\{\ddot{x}\}$ are (Nx1) vectors of nodal displacements, velocities and accelerations respectively and $\{F(t)\}$ is an (Nx1) vector of applied time-varying

external load $\{f_o\}e^{j\Omega t}$, where $\{f_O\}$ is the amplitude of the excitation load vector and Ω is the excitation load frequency.

The equations of motion of the NDOF substructure can be changed into uncoupled ones in terms of modal co-ordinates, or principal co-ordinates, using this transformation;

$$\{x\} = [\phi]\{y\} \tag{4.2}$$

where $[\phi]$ is the (NxN) modal matrix whose columns are the normal modes of the system which is obtained from undamped eigenvalue problem of the equations of motion and $\{y\}$ is the (Nx1) vector of modal co-ordinates.

The uncoupled transformed equation in terms of modal co-ordinates is then ;

$$[m][\ddot{y}] + [c][\dot{y}] + [k][y] = \{f(t)\} \tag{4.3}$$

where

$$\left.\begin{aligned} [m] &= [\phi]^T[M][\phi] \\ [c] &= [\phi]^T[C][\phi] = 2[\xi][\omega] \\ [k] &= [\phi]^T[K][\phi] \quad \text{and} \\ \{f(t)\} &= [\phi]^T\{F(t)\} \end{aligned}\right\} \tag{4.4}$$

[m], [c] and [k] are (NxN) diagonal modal mass, damping and stiffness matrices respectively. $\{f(t)\}$ is the (Nx1) modal load vector; $[\omega]$ is the (NxN) diagonal matrix formed by the natural frequencies of the system and $[\xi]$ is the(NxN) diagonal matrix formed by the damping ratios in each normal mode. The diagonal property of the [m], [c] and [k] is a consequence of the orthogonality of the normal modes.

The equation of motion relative to mode r is then given by;

$$m_r\ddot{y}_r + c_r\dot{y}_r + k_r y_r = f_r(t) \tag{4.5}$$

where;

m_r is the generalised mass coefficient corresponding to mode r, $\{\phi\}_r^T[M]\{\phi\}_r$

k_r is the generalised stiffness coefficient corresponding to mode r, $\{\phi\}_r^T[K]\{\phi\}_r$

c_r is the generalised damping coefficient corresponding to mode r,

$\{\phi\}_r^T[C]\{\phi\}_r = 2\xi_r\omega_r$

$f_r(t)$ is the modal load corresponding to mode r, $=\{\phi\}_r^T\{F(t)\}$ and

$\{\phi\}_r$ is the r th mode shape

The amplitude of the total response of a system for harmonic excitation, in complex form, can be expressed as the linear combination of a system modal parameters as follows;

$$\{x\} = \sum_{r=1}^{N} \frac{\{\phi\}_r\{\phi\}_r^T\{f_o\}}{k_r\{1-(\Omega/\omega_r)^2+2j\xi_r(\Omega/\omega_r)\}} = [G]\{f_o\} \qquad (4.6)$$

where

[G] is the compliance matrix or dynamic flexibility matrix which is defined as;

$$[G] = \sum_{r=1}^{N} \frac{\{\phi\}_r\{\phi\}_r^T}{k_r\{1-(\Omega/\omega_r)^2+2j\xi_r(\Omega/\omega_r)\}} \qquad (4.7)$$

ω_r is the natural frequency of the r th mode

ζ_r is the damping ratio of the r th mode

4.2.2-Mode Truncation

If a system of NDOF is subjected to exciting forces in the lower frequency range, the modes may be split into two groups, one of them containing the lower modes ,n, and the other containing, (N-n), higher modes. Thus the total response of the system can be written as follows;

$$\{x\} = \sum_{r=1}^{n} \frac{\{\phi\}_r\{\phi\}_r^T\{f_o\}}{k_r\{1-(\Omega/\omega_r)^2+2j\xi_r(\Omega/\omega_r)\}} + \sum_{r=n+1}^{N} \frac{\{\phi\}_r\{\phi\}_r^T\{f_o\}}{k_r\{1-(\Omega/\omega_r)^2+2j\xi_r(\Omega/\omega_r)\}}$$

$$= ([G]_l + [G]_h)\{f_o\} \qquad (4.8)$$

where

$[G]_l$ is the dynamic flexibility matrix corresponding to the lower modes (n) and

$[G]_h$ is the dynamic flexibility matrix corresponding to the higher modes (N-n).

Many authors have shown that the response of the complete system can be found, within the low frequency range from the free vibration modes of the system if a sufficient number of modes are retained to represent the system. If only n modes are retained to describe the system then the modal transformation is;

$$\underset{(Nx1)}{\{x\}} = \underset{(Nxn)}{[\{\phi\}_1 \quad \{\phi\}_2 \quad \{\phi\}_3 \ldots\ldots \{\phi\}_n]} \quad \underset{(nx1)}{\{y\}_n}$$

The modes from (n+1) to N have been truncated and are not used in the system. The physical interpretation of this truncation means that of the original NDOFs to describe the state of the system,{x}, only nDOFs remain. Clearly, the n modes retained for a system must have sufficient modal definition to provide an accurate system dynamic representation in the required range of frequency.

4.2.3-Residual Flexibility

In order to eliminate the need to include a large number of modes, residual flexibilities can be introduced to approximate the effect of omitted higher modes. In the experimental modal analysis, the influence of the residual flexibility can be estimated using curve fitting methods [67]. However, for the theoretical approach, there are several methods to calculate the residual flexibility and some of them are discussed in the following sections.

Usual method

In this method the residual flexibility can be estimated from equation (4.7), corresponding to the higher modes only [67];

$$[G] = \sum_{r=n+1}^{N} \frac{\{\phi\}_r \{\phi\}_r^T}{k_r \{1-(\Omega/\omega_r)^2 + 2j\xi_r(\Omega/\omega_r)\}} \qquad (4.9)$$

In this method, all the higher modes must be calculated to obtain the exact residual flexibility matrix. However, it is difficult to use all the natural modes because, in many

systems, the number of degrees of freedom are very large and hence it is difficult to obtain an accurate residual flexibility matrix by this method.

Static residual flexibility

For the higher frequency range, the masses of the system have the dominant effect on the system response, so only the static residual flexibility will be estimated in this method [68].

Since for higher modes the frequency ratio (Ω/ω_i) is sufficiently small, the response given by the equation (4.8) may be simplified into;

$$\{x\} = \sum_{r=1}^{n} \frac{\{\phi\}_r \{\phi\}_r^T \{f_o\}}{k_r \{1-(\Omega/\omega_r)^2 + 2j\xi_r(\Omega/\omega_r)\}} + \sum_{r=n+1}^{N} \frac{\{\phi\}_r \{\phi\}_r^T \{f_o\}}{k_r} \qquad (4.10)$$

$$= ([G]_l + [G]_{sh})\{f_o\}$$

where

$[G]_{sh}$ is the static residual flexibility corresponding to higher omitted modes (N-n)

$$[G]_{sh} = \sum_{r=n+1}^{N} \frac{\{\phi\}_r \{\phi\}_r^T}{k_r} = \sum_{r=n+1}^{N} \{\phi\}_r (\{\phi\}_r^T [K] \{\phi\}_r)^{-1} \{\phi\}_r^T \qquad (4.11)$$

The static residual flexibility matrix can be obtained without calculation of the higher modes from the total static flexibility matrix, $[G]_S$, and the static flexibility matrix corresponding to the retained lower modes, $[G]_{Sl}$, using the following relation;

$$[G]_s = [G]_{sl} + [G]_{sh} \quad \text{i.e.}$$
$$[G]_{sh} = [G]_s - [G]_{sl} \qquad (4.12)$$

where the total static flexibility matrix, $[G]_S$, is equal to the inverse of the stiffness matrix of the system, [K], i.e. $[G]_s = [K]^{-1}$

The lower static flexibility matrix can be obtained from the following relation;

$$[G]_{sl} = \sum_{1}^{n} \frac{\{\phi\}_r \{\phi\}_r^T}{k_r} = \sum_{1}^{n} \{\phi\}_r \ (\{\phi\}_r^T [K] \{\phi\}_r)^{-1} \ \{\phi\}_r^T \text{ i.e.}$$

$$[G]_{sh} = [K]^{-1} - \sum_{1}^{n} \{\phi\}_r \ (\{\phi\}_r^T [K] \{\phi\}_r)^{-1} \ \{\phi\}_r^T \qquad (4.13)$$

As this method does not need the higher modes, it is more efficient than the usual method but it cannot be applied to structures with Free-Free boundary conditions directly because the inverse of the stiffness matrix of such structures cannot be obtained since it is not positive definite (singular matrix).

Residual flexibility for Free-Free structure

Since many substructures with Free-Free boundary conditions appear in the analysis by the substructure synthesis method, it is important to propose an efficient method which enables an accurate estimate of the static residual flexibility of such substructures.

The so called pseudo-flexibility matrix will be calculated [68] as;

$$[G] = [A]^T [G_c][A] \qquad (4.14)$$

where

$$[A] = [I] - \sum_{r=n+1}^{n_r} [M]\{\phi\}_r (\{\phi\}_r^T [M]\{\phi\}_r)^{-1} \{\phi\}_r^T \qquad (4.15)$$

is a transfer matrix which filters the rigid body modes, n_r and $[G_c]$ is the flexibility matrix of the structure obtained by introducing isostatic boundary conditions to prevent rigid body motion.

4.3-COUPLING OF SUBSTRUCTURES

In order to demonstrate the idea of the substructure synthesis technique, it is supposed first that the coupling of two substructures which was published in [68] is used. This is described in detail in appendix-A. Then, to generalise this technique for

any number of substructures, the coupling of three substructures is presented in the next section using same method as described in [68].

4.3.1-Coupling of three substructures

Complex structures usually are divided into more than two substructures, so some of these substructures are interfaced with two substructures at least. To generalise the stiffness coupling, with combined use of residual flexibility and modal synthesis, technique, the coupling of three substructures is represented in this section. It is supposed that a structure composed of three substructures, Fig (4.2), namely; sub-L, sub-s and sub-R. The degrees of freedom of s-th substructure, sub-s, are divided into three parts, left interface "jL", interior "i" and right interface "jR" degrees of freedom.

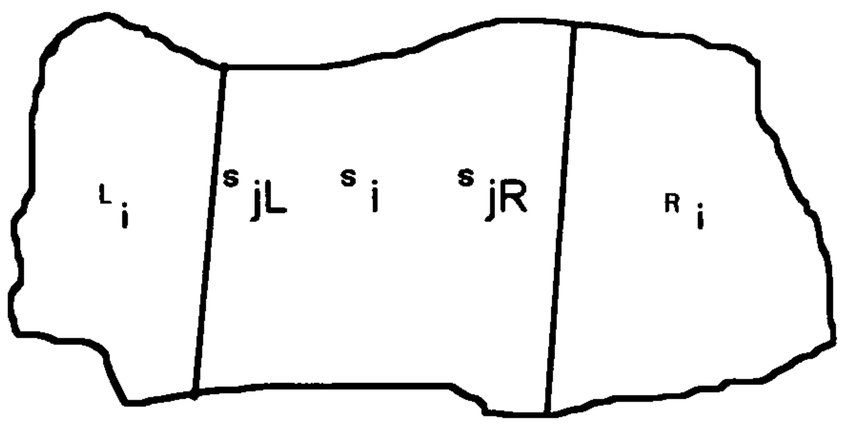

Fig (4.2) Structure composed of three substructures

where;

^{s}jL Interface DOFs of s-th substructure with the left substructure, sub-L.

^{s}jR Interface DOFs of s-th substructure with the right substructure, sub-R.

^{s}i Interior DOFs of s-th substructure, sub-s.

^{L}i Interior DOFs of left substructure, sub-L.

^{R}i Interior DOFs of right substructure, sub-R

The mass, damping and stiffness matrices for s-th substructure can be split into sub matrices corresponding to interior and interface DOFs as follow;

$$
{}^{s}\begin{bmatrix} [M_{jLL}] & [M_{jLi}] & [M_{jLR}] \\ [M_{iL}] & [M_{ii}] & [M_{iR}] \\ [M_{jRL}] & [M_{jRi}] & [M_{jRR}] \end{bmatrix} {}^{s}\begin{Bmatrix} \ddot{x}_{jL} \\ \ddot{x}_{i} \\ \ddot{x}_{jR} \end{Bmatrix} + {}^{s}\begin{bmatrix} [C_{jLL}] & [C_{jLi}] & [C_{jLR}] \\ [C_{iL}] & [C_{ii}] & [C_{iR}] \\ [C_{jRL}] & [C_{jRi}] & [C_{jRR}] \end{bmatrix} {}^{s}\begin{Bmatrix} \dot{x}_{jL} \\ \dot{x}_{i} \\ \dot{x}_{jR} \end{Bmatrix} + {}^{s}\begin{bmatrix} [K_{jLL}] & [K_{jLi}] & [K_{jLR}] \\ [K_{iL}] & [K_{ii}] & [K_{iR}] \\ [K_{jRL}] & [K_{jRi}] & [K_{jRR}] \end{bmatrix} {}^{s}\begin{Bmatrix} x_{jL} \\ x_{i} \\ x_{jR} \end{Bmatrix} = {}^{s}\begin{Bmatrix} [F_{jL}(t)] \\ [F_{i}(t)] \\ [F_{jR}(t)] \end{Bmatrix}
$$

(4.16)

The uncoupled equations corresponding to the interface DOFs, jL, and, jR, respectively are;

$$^{s}[m_{jL}]_{ns}\ ^{s}\{\ddot{y}_{jL}\}_{ns}+^{s}[c_{jL}]_{ns}\ ^{s}\{\dot{y}_{jL}\}_{ns}+^{s}[k_{jL}]_{ns}\ ^{s}\{y_{jL}\}_{ns}=^{s}[\phi_{jL}]_{ns}^{T}\ ^{s}\{F_{jL}(t)\} \qquad (4.17a)$$

$$^{s}[m_{jR}]_{ns}\ ^{s}\{\ddot{y}_{jR}\}_{ns}+^{s}[c_{jR}]_{ns}\ ^{s}\{\dot{y}_{jR}\}_{ns}+^{s}[k_{jR}]_{ns}\ ^{s}\{y_{jR}\}_{ns}=^{s}[\phi_{jR}]_{ns}^{T}\ ^{s}\{F_{jR}(t)\} \qquad (4.17b)$$

where $^{s}[m_{jL}]_{ns}$, $^{s}[c_{jL}]_{ns}$ and $^{s}[k_{jL}]_{ns}$ are generalised mass, damping and stiffness matrices corresponding to left interface DOFs, jL, and the remaining modes, ns and $^{s}[m_{jR}]_{ns}$, $^{s}[c_{jR}]_{ns}$ and $^{s}[k_{jR}]_{ns}$ are generalised mass, damping and stiffness matrices corresponding to the right interface DOFs, jR, and the remaining modes, ns.

Solution of the equations (4.17) gives the interface displacements $^{s}x_{jL}$ and $^{s}x_{jR}$ as follows;

$$^{s}\{x_{jL}\} = {}^{s}[\phi_{jL}]_{ns}\ ^{s}\{y\}_{ns} + {}^{s}[G_{jL}]_{ns}\ ^{s}\{F_{jL}\} \text{ and} \qquad (4.18a)$$

$$^{s}\{x_{jR}\} = {}^{s}[\phi_{jR}]_{ns}\ ^{s}\{y\}_{ns} + {}^{s}[G_{jR}]_{ns}\ ^{s}\{F_{jR}\} \qquad (4.18b)$$

where

$^{s}[G_{jL}]_{ns}$ and $^{s}[G_{jR}]_{ns}$ are the (jLxjL) and (jRxjR) static residual flexibility matrices corresponding to the left and right interface co-ordinates respectively due to the omitted higher modes of the s th substructure,

$^{s}[\phi_{jL}]_{ns}$ and $^{s}[\phi_{jR}]_{ns}$ are (jLxns) and (jRxns) matrices of the remaining normal modes, ns, of s th substructure corresponding to the left and right interface co-ordinates respectively and, $^{s}\{y\}_{ns}$ is the (nsx1) vector of the remaining modal modes, ns, of the s th substructure.

Both compatibility and equilibrium conditions at the interface regions jL and jR of the left and right substructures respectively must be satisfied for the modal coupling.

Compatibility conditions:

$$\left.\begin{aligned} {}^{s}X_{jL} &= {}^{L}X_{jL} \\ {}^{s}X_{jR} &= {}^{R}X_{jR} \end{aligned}\right\} \qquad (4.19)$$

Equilibrium conditions

$$\left.\begin{aligned} {}^{s}F_{jL} + {}^{L}F_{jL} &= 0 \\ {}^{s}F_{jR} + {}^{R}F_{jR} &= 0 \end{aligned}\right\} \qquad (4.20)$$

Applying the displacement vector expressions, (4.18), for the left interface (between sub-L and sub-s) and the right interface (between sub-s and sub-R) in the compatibility and equilibrium equations (4.19) and (4.20) gives;

For the left interface

$${}^{L}[\phi_{jL}]_{nL}\ {}^{L}\{y\}_{nL} + {}^{L}[G_{jL}]_{nL}\ {}^{L}\{F_{jL}\} = {}^{s}[\phi_{jL}]_{ns}\ {}^{s}\{y\}_{ns} + {}^{s}[G_{jL}]_{ns}\ {}^{s}\{F_{jL}\} \quad \text{or}$$

$$\left.\begin{aligned} {}^{L}[\phi_{jL}]_{nL}\ {}^{L}\{y\}_{nL} - {}^{s}[\phi_{jL}]_{ns}\ {}^{s}\{y\}_{ns} &= ({}^{L}[G_{jL}]_{nL} + {}^{s}[G_{jL}]_{ns})\ {}^{s}\{F_{jL}\} \quad \text{and} \\ {}^{s}[\phi_{jL}]_{ns}\ {}^{s}\{y\}_{ns} - {}^{L}[\phi_{jL}]_{nL}\ {}^{L}\{y\}_{nL} &= ({}^{L}[G_{jL}]_{nL} + {}^{s}[G_{jL}]_{ns})\ {}^{L}\{F_{jL}\} \end{aligned}\right\} \qquad (4.21a)$$

For the right interface

Similar relations for substructures sub-R and sub-s can be automatically obtained by replacing the suffix R instead of L in the two previous relations, Eqns (4.21a), i.e.;

$$\left.\begin{aligned} {}^{R}[\phi_{jR}]_{nR}\ {}^{R}\{y\}_{nR} - {}^{s}[\phi_{jR}]_{ns}\ {}^{s}\{y\}_{ns} &= ({}^{R}[G_{jR}]_{nR} + {}^{s}[G_{jR}]_{ns})\ {}^{s}\{F_{jR}\} \quad \text{and} \\ {}^{s}[\phi_{jR}]_{ns}\ {}^{s}\{y\}_{ns} - {}^{R}[\phi_{jR}]_{nR}\ {}^{R}\{y\}_{nR} &= ({}^{R}[G_{jR}]_{nR} + {}^{s}[G_{jR}]_{ns})\ {}^{R}\{F_{jR}\} \end{aligned}\right\} \qquad (4.21b)$$

From the previous four relations, Eqns (4.21a) and Eqns (4.21b), the interface forces in terms of substructure parameters are;

$${}^{L}\{F_{jL}\} = [k_{jL}]\ ({}^{s}[\phi_{jL}]_{ns}\ {}^{s}\{y\}_{ns} - {}^{L}[\phi_{jL}]_{nL}\ {}^{L}\{y\}_{nL}), \qquad (4.22a)$$

$$^{s}\{F_{jL}\} = [k_{jL}]\,(^{L}[\phi_{jL}]_{nL}\ ^{L}\{y\}_{nL} - {}^{s}[\phi_{jL}]_{ns}\ ^{s}\{y\}_{ns}), \tag{4.22b}$$

$$^{s}\{F_{jR}\} = [k_{jR}]\,(^{R}[\phi_{jR}]_{nR}\ ^{R}\{y\}_{nR} - {}^{s}[\phi_{jR}]_{ns}\ ^{s}\{y\}_{ns}) \quad \text{and} \tag{4.22c}$$

$$^{R}\{F_{jR}\} = [k_{jR}]\,(^{s}[\phi_{jR}]_{ns}\ ^{s}\{y\}_{ns} - {}^{R}[\phi_{jR}]_{nR}\ ^{R}\{y\}_{nR}) \tag{4.22d}$$

where

$[k_{jR}] = (^{R}[G_{jR}]_{nR} + {}^{s}[G_{jR}]_{ns})^{-1}$ is the static residual stiffness matrix corresponding to right interface DOFs and the omitted higher modes of substructures sub-s and sub-R and $[k_{jL}] = (^{L}[G_{jL}]_{nL} + {}^{s}[G_{jL}]_{ns})^{-1}$ is the static residual stiffness matrix corresponding to left interface DOFs and the omitted higher modes of substructures sub-s and sub-L.

Note that if there is an elastic connection with stiffness matrix, $[k_c]$, between the substructures, the total equivalent flexibility connection matrix is the sum of the residual flexibility corresponding to the higher modes and the physical interface connection flexibility i.e.,

$$\left.\begin{aligned} [k_{jR}] &= (^{R}[G_{jR}]_{nR} + {}^{s}[G_{jL}]_{ns} + [k_{cR}]^{-1})^{-1} \\ [k_{jL}] &= (^{L}[G_{jL}]_{nL} + {}^{s}[G_{jL}]_{ns} + [k_{cL}]^{-1})^{-1} \end{aligned}\right\} \tag{4.23}$$

Replacing the expressions (4.22) for the interface forces in the following uncoupled equations of motion, corresponding to equation (A.4) in appendix-A, of the left, right and s-th substructures gives,

$$^{L}[m]_{nL}\ ^{L}\{\ddot{y}\}_{nL} + {}^{L}[c]_{nL}\ ^{L}\{\dot{y}\}_{nL} + {}^{L}[k]_{nL}\ ^{L}\{y\}_{nL} = {}^{L}[\phi_{jL}]^{T}_{nL}\ ^{L}\{F_{jL}\} + {}^{L}[\phi_{i}]^{T}_{nL}\ ^{L}\{F_{i}\},$$

$$^{s}[m]_{ns}\ ^{s}\{\ddot{y}\}_{ns} + {}^{s}[c]_{ns}\ ^{s}\{\dot{y}\}_{ns} + {}^{s}[k]_{ns}\ ^{s}\{y\}_{ns} =$$

$$^{s}[\phi_{jL}]^{T}_{ns}\ ^{s}\{F_{jL}\} + {}^{s}[\phi_{jR}]^{T}_{ns}\ ^{s}\{F_{jR}\} + {}^{s}[\phi_{i}]^{T}_{ns}\ ^{s}\{f_{i}\} \quad \text{and}$$

$$^{R}[m]_{nR}\ ^{R}\{\ddot{y}\}_{nR} + {}^{R}[c]_{nR}\ ^{R}\{\dot{y}\}_{nR} + {}^{R}[k]_{nR}\ ^{R}\{y\}_{nR} = {}^{R}[\phi_{jR}]^{T}_{nR}\ ^{R}\{F_{jR}\} + {}^{R}[\phi_{i}]^{T}_{nR}\ ^{R}\{F_{i}\}$$

Arranging the equations in matrix form, the total system equations are then;

$$\begin{bmatrix} {}^{L}[m]_{nL} & [0] & [0] \\ [0] & {}^{s}[m]_{ns} & [0] \\ [0] & [0] & {}^{R}[m]_{nR} \end{bmatrix} \begin{Bmatrix} {}^{L}\{\ddot{y}\}_{nL} \\ {}^{s}\{\ddot{y}\}_{ns} \\ {}^{R}\{\ddot{y}\}_{nR} \end{Bmatrix} + \begin{bmatrix} {}^{L}[c]_{nL} & [0] & [0] \\ [0] & {}^{s}[c]_{ns} & [0] \\ [0] & [0] & {}^{R}[c]_{nR} \end{bmatrix} \begin{Bmatrix} {}^{L}\{\dot{y}\}_{nL} \\ {}^{s}\{\dot{y}\}_{ns} \\ {}^{R}\{\dot{y}\}_{nR} \end{Bmatrix} +$$

$$\begin{bmatrix} \left({}^{L}[k]_{nL} + {}^{L}[\phi_{jL}]^{T}_{nL}\ [k_{jL}]\ {}^{L}[\phi_{jL}]_{nL}\right) & \left(-{}^{L}[\phi_{jL}]^{T}_{nL}\ [k_{jL}]\ {}^{s}[\phi_{jL}]_{ns}\right) & [0] \\ \left(-{}^{s}[\phi_{jL}]^{T}_{ns}\ [k_{jL}]\ {}^{L}[\phi_{jL}]_{nL}\right) & \begin{pmatrix} {}^{s}[k]_{ns} + {}^{s}[\phi_{jL}]^{T}_{ns}\ [k_{jL}]\ {}^{s}[\phi_{jL}]_{ns} \\ + {}^{s}[\phi_{jR}]^{T}_{ns}\ [k_{jR}]\ {}^{s}[\phi_{jR}]_{ns} \end{pmatrix} & \left(-{}^{s}[\phi_{jR}]^{T}_{ns}\ [k_{jR}]\ {}^{R}[\phi_{jR}]_{nR}\right) \\ [0] & \left(-{}^{R}[\phi_{jR}]^{T}_{nR}\ [k_{jR}]\ {}^{s}[\phi_{jR}]_{ns}\right) & \left({}^{R}[k]_{nR} + {}^{R}[\phi_{jR}]^{T}_{nR}\ [k_{jR}]\ {}^{R}[\phi_{jR}]_{nR}\right) \end{bmatrix}$$

$$\begin{Bmatrix} {}^{L}\{y\}_{nL} \\ {}^{s}\{y\}_{ns} \\ {}^{R}\{y\}_{nR} \end{Bmatrix} = \begin{Bmatrix} {}^{L}[\phi_i]_{nL}\ {}^{L}\{F_i\} \\ {}^{s}[\phi_i]_{ns}\ {}^{s}\{F_i\} \\ {}^{R}[\phi_i]_{nR}\ {}^{R}\{F_i\} \end{Bmatrix} \tag{4.24}$$

These now represent the model for the three coupled substructures in matrix form. The generalisation for any number of substructures is straightforward and the dimension of these matrices can be extended automatically according to the number of substructures. The total physical modal matrix corresponding to equation (A.10) is

$$[x] = \left[{}^{1}[x] \quad {}^{2}[x] \quad {}^{3}[x]\right]^{T} \tag{4.25}$$

4.4-SUBSTRUCTURED DRIVELINE SYSTEM

The overall driveline system model under consideration, mentioned in section 2.9, is a 14 DOF system, Fig (4.3). To study the efficiency of the substructure technique to analyse this system, it may be divided into four substructures as shown in Fig (4.4). The first substructure, sub-1, represents the engine, the second substructure, sub-2, represents the clutch and gearbox, the third substructure, sub-3, represents the propeller shaft and joints and the fourth substructure, sub-4, represents the final drive system.

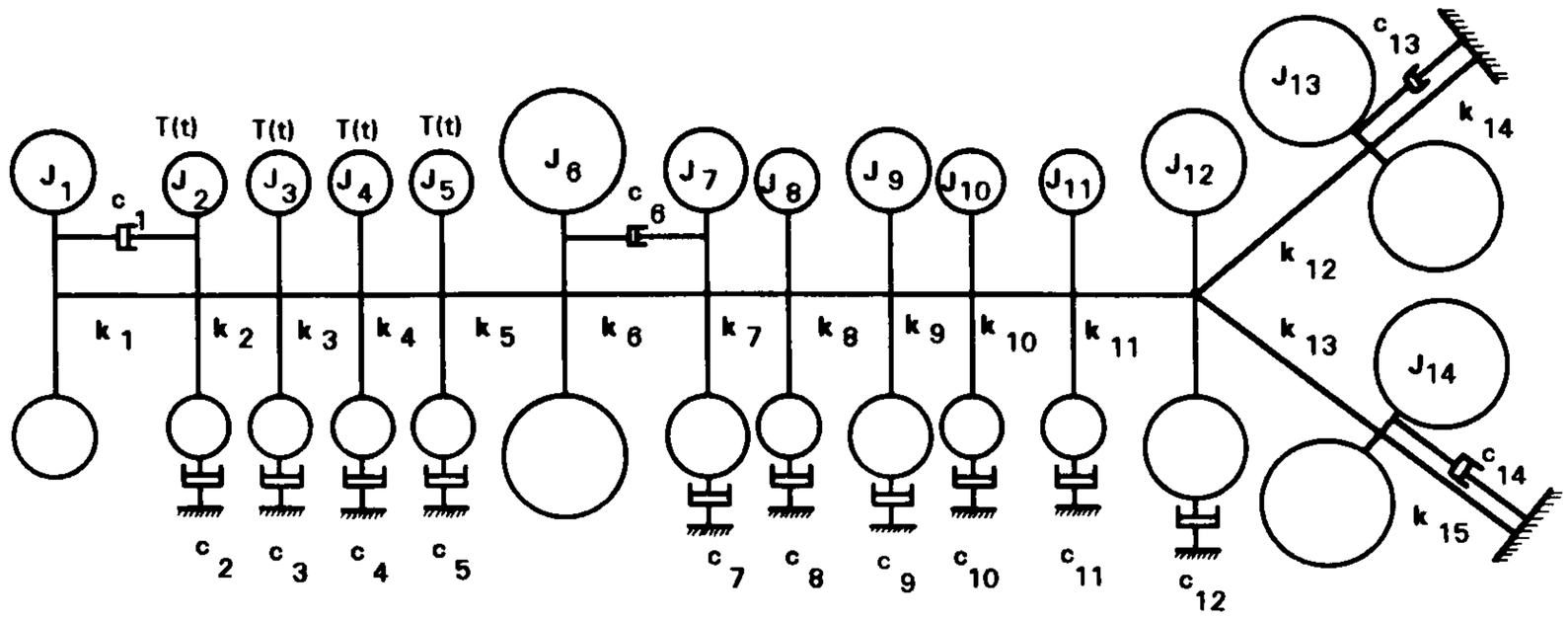

Fig (4.3) Whole driveline system model (14 DOF)

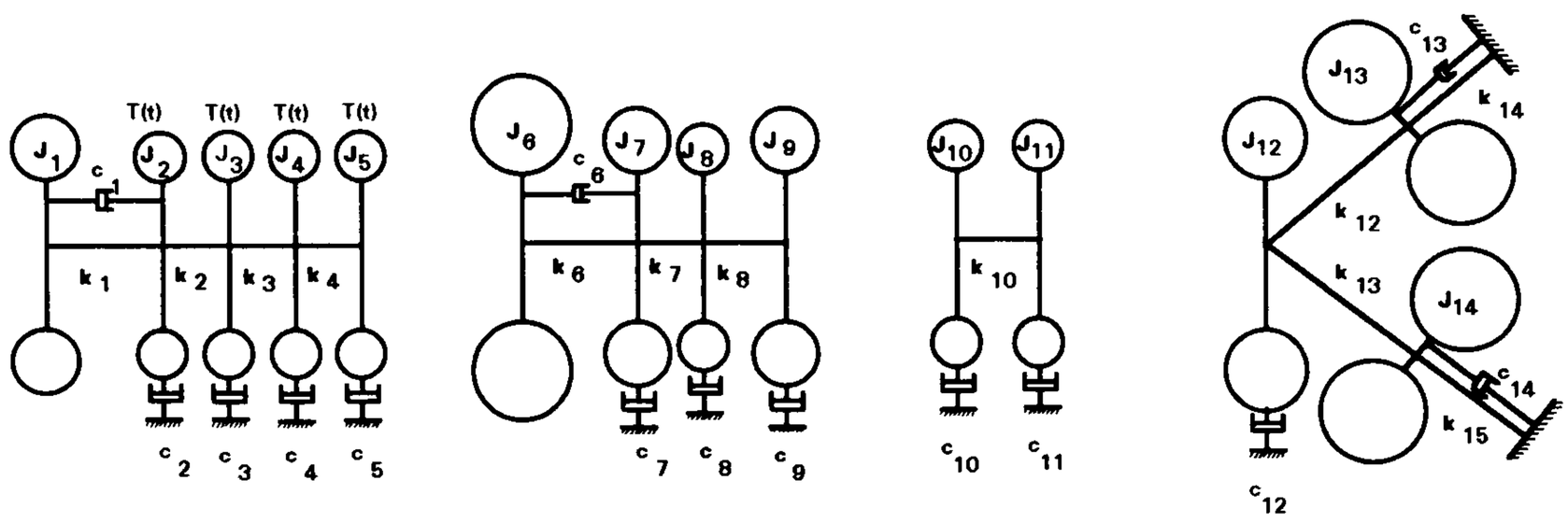

Fig (4.4) Four substructures model

The equation of motion of the whole driveline system, Fig (4.3), in matrix form is;

$$[M]\{\ddot{\theta}\}+[C]\{\dot{\theta}\}+[K]\{\theta\}=\{Q\} \qquad (4.26)$$

The vibrational characteristics of this system may be obtained from the free vibration solution of this equation. The equation of motion and the vibrational characteristics of each set of substructure are obtained individually from free vibration theory. The equation of motion of the total system is constructed from the combination of each substructure modal parameters. The size of the total equation of motion depends on the number of retained modes of each substructure.

4.5-COMPUTER PROGRAM

From the previous published work, there are two different methods for the analysis of the dynamic behaviour of vehicle drivelines. The first uses experimental techniques only and the second uses computer simulation in addition to the experimental

investigations. The experimental method provides direct solutions but it is difficult to understand the vibration behaviour of a complex system such as an automotive driveline by measurements only. On the other hand, the number of tests typically has to be restricted because of the high cost and effect of experimental modifications. Therefore, development a computer program to investigate the dynamic behaviour of driveline systems will be useful. One of the intrinsic advantages of a computer simulation is the possibility to investigate many variants covering a much wider range of parameters [19].

The mentioned mathematical model of substructure approach has been translated into a computer program using MATLAB software suitable for vibration of automobile driveline systems. The program has been designed for many investigation purposes such as the efficiency of the substructure technique for the system under consideration, the effect of the omitted higher modes on the accuracy of the system natural frequencies, the effect of the residual flexibility of the omitted modes and modes which have a dominant effect on the system behaviour. It is designed to be interactive program allowing the driveline designer to specify the vehicle driveline by answering a series of questions such as; how many substructures? how many modes of each substructure should be considered? do you want consider the residual flexibility or not?,..... etc. The answers to the questions build up the simulation program in a step by step way. The user also should specifies the output required, having a choice of tabular and/or graphical output. See the programme flow chart steps in Fig (4.5). In the chapter 5, typical numerical data for the driveline system model are introduced to analyse free and forced vibrations of this system using the mentioned substructure approach.

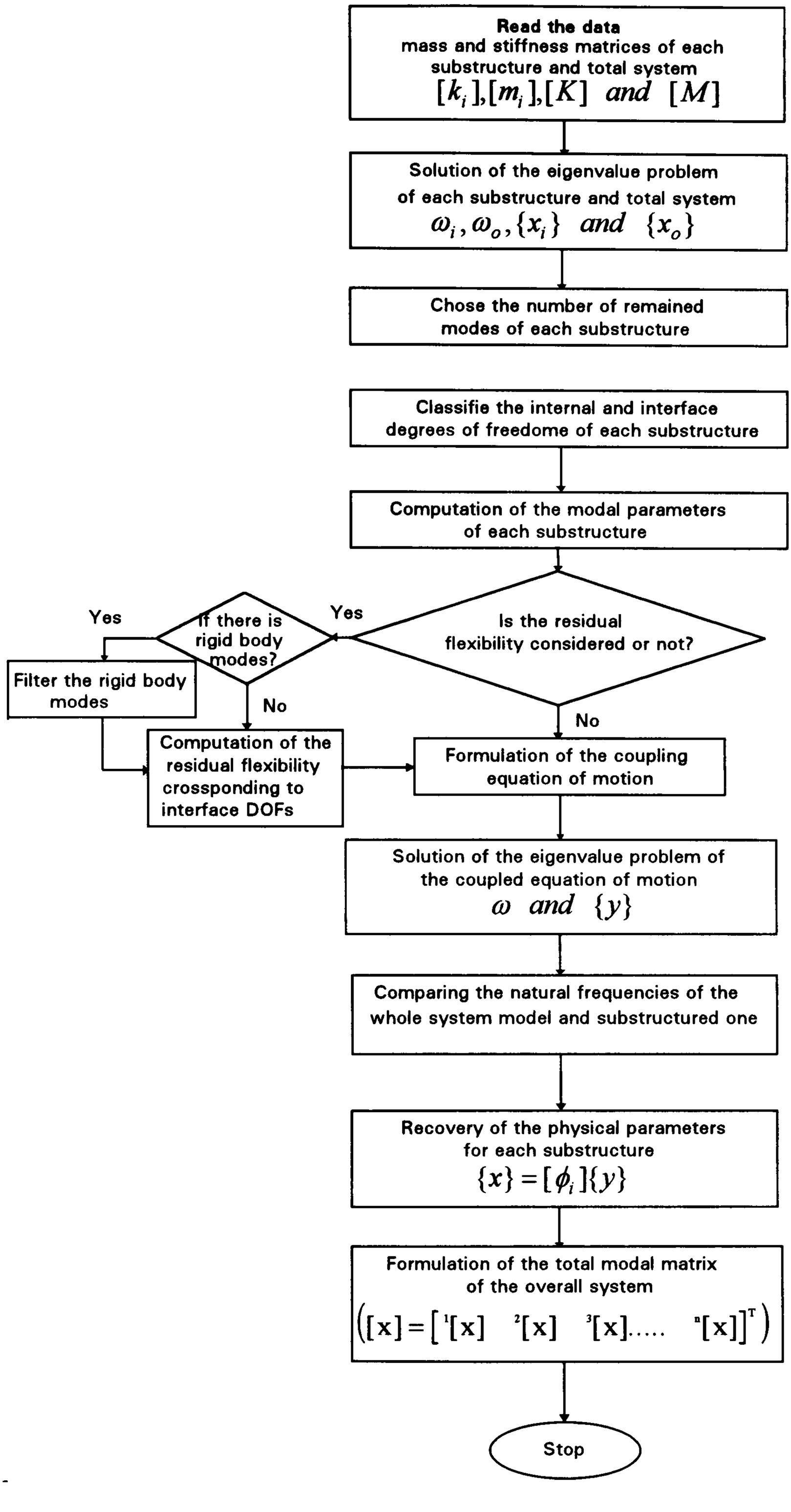

Fig (4.5) Flow chart steps of substructure approach using MATLAB

4.6-SUMMARY

The substructure approach using the stiffness coupling technique, with combined use of residual flexibility and modal synthesis, was extended from two substructures to treat the general case with any number of substructures. The generalisation of this technique represents an important contribution to the study of complex, linear dynamic systems because it reduces the computational effort and time. This technique was embodied in a computer program, again using MATLAB subroutines, to facilitate its application to dynamic systems. This programme was subsequently used to study the driveline system vibration problems.

CHAPTER 5

LINEAR VIBRATION OF DRIVELINE SYSTEM

5.1-INTRODUCTION

Although practical automotive driveline systems typically include non-linear components, the driveline system is considered first as a linear system in this chapter in order to use the substructure technique. Non-linear effects are considered in a later chapter.

A model of the driveline system, Fig (5.1), with typical numerical values for the parameters of the system, see Table (5.1), is used in this chapter to study its free and forced torsional linear vibrations behaviour using the substructure technique that was described in chapter 4. The aims of this chapter is to investigate the fundamental torsional vibrational behaviour of the driveline system and in addition to investigate the efficiency of the substructure technique for analysing this system.

5.2-FREE VIBRATIONS

One of the aims of studying the free vibration of automotive driveline systems is to avoid coincidence of engine harmonics, and/or another excitation sources, with system natural frequencies which could result in high stress level under loads. Also, it provides information of the positions at which large displacements occur so that an appropriate solutions to attenuate the vibration problems at these positions may be proposed.

5.2.1-Mathematical Model

The typical model, Fig (5.1), is used with typical numerical values, Table (5.1), to establish the range of the system natural frequencies and in addition, to investigate the substructure technique. There are three aspects ; firstly , to investigate the efficiency of the substructure technique for the torsional dynamic behaviour of a vehicle driveline system analysi ; secondly, to study the effect of the omitted higher modes on the accuracy of the computed values of the natural frequencies and the mode shapes and thirdly; to study the effect of the residual flexibilities of the omitted modes on

these values. Lastly, to investigate the modes which have a dominant effect on these values.

For these purposes, the eigenvalue problem of the overall 14 DOFs system is solved. Then the system is divided into four substructures, Figs (5.2) and each of them is analysed as a separate system. Coupled equations of motion for the system are then constructed from the modal parameters of each substructure and the eigenvalue problem of this equation is solved. Finally, the percentage deviation of the natural frequencies computed from the substructure model from the corresponding values computed from the overall system model is estimated for different numbers of considered modes of each substructure.

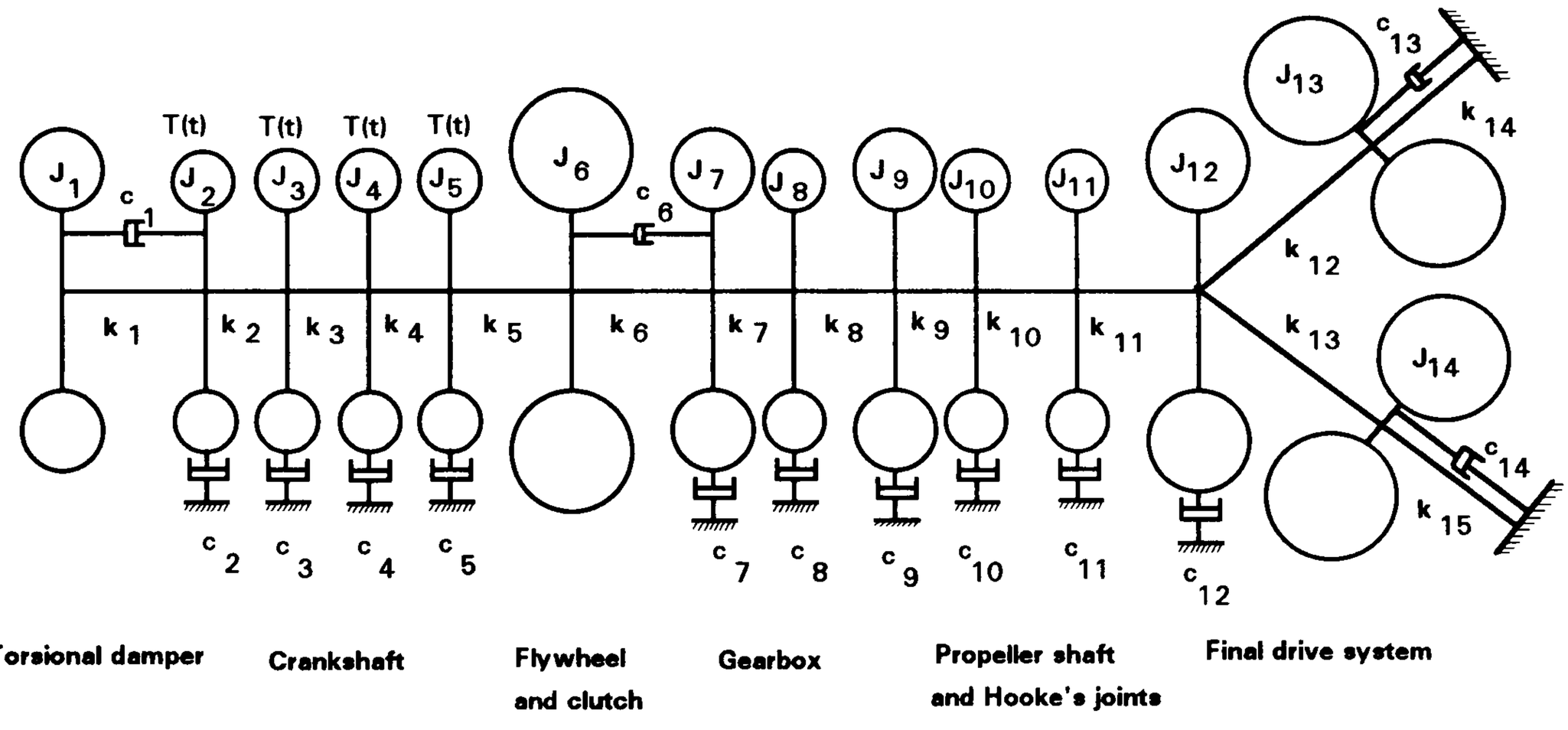

Fig (5.1) Overall system model for a driveline system (14 DOF)

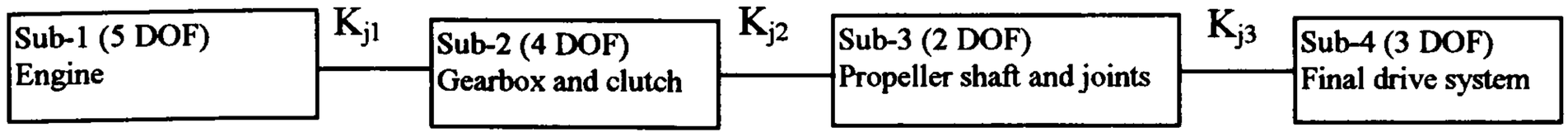

Fig (5.2a) Layout of the substructured system

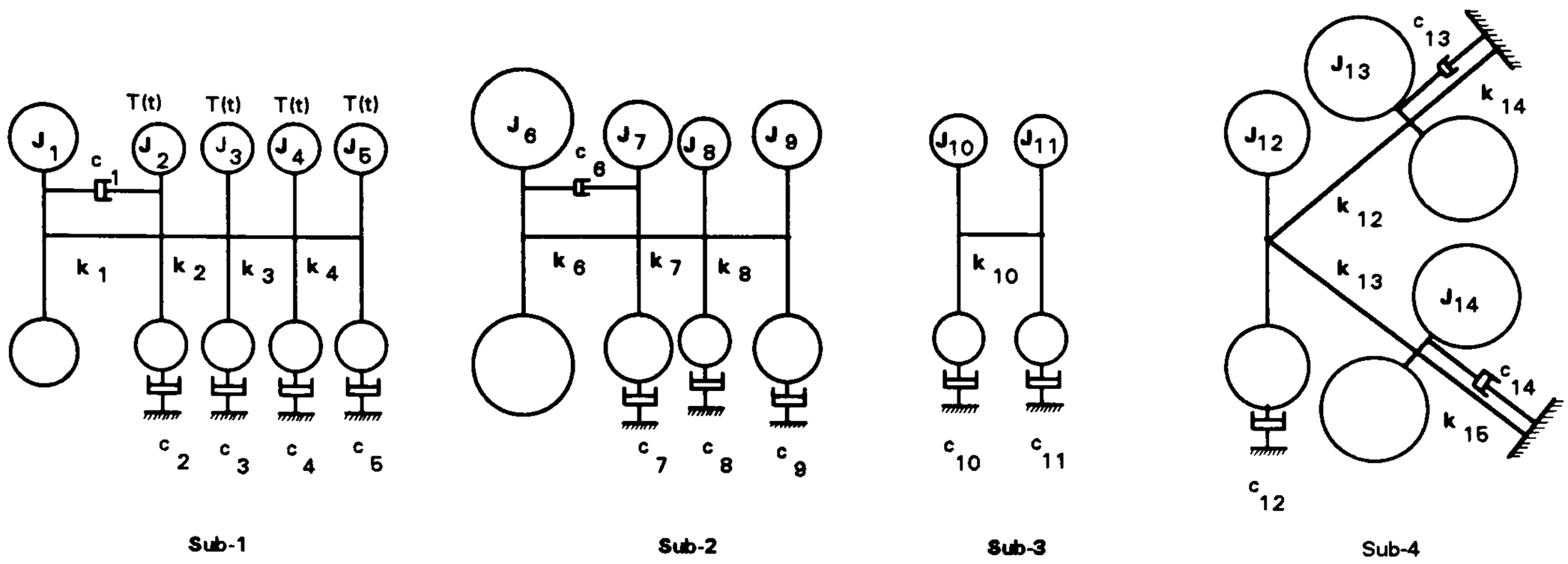

Fig (5.2b) Four substructure model of driveline system

Typical numerical values of the equivalent system parameters, shown in Table (5.1), were chosen from previous publications and have been taken as nominal values to investigate the torsional vibration behaviour of the system.

Table (5.1) Typical data of equivalent parameters of a vehicle driveline system (nominal values)

Equivalent stiffness (N/m or N.m/rad)		Equivalent mass and moment of inertia (kg or kg m^2)		Equivalent system damping (N.s/m or N.m s/rad)	
Parameter	value	Parameter	value	Parameter	value
k_1	0.2×10^6	J_1	0.3	c_1	3
k_2	1×10^6	J_2	0.03	c_2	2
k_3	1×10^6	J_3	0.03	c_3	2
k_4	1×10^6	J_4	0.03	c_4	2
k_5	1×10^6	J_5	0.03	c_5	2
k_6	0.05×10^6	J_6	1.0	c_6	4.42
k_7	2×10^6	J_7	0.05	c_7	1
k_8	1×10^6	J_8	0.03	c_8	1
k_9	0.1×10^6	J_9	0.05	c_9	1
k_{10}	0.1×10^6	J_{10}	0.02	c_{10}	1.8
k_{11}	0.2×10^6	J_{11}	0.02	c_{11}	1.8
k_{12}	0.5×10^4	J_{12}	0.3	c_{12}	2
k_{13}	0.5×10^4	J_{13}	2	c_{13}	10
k_{14}	0.2×10^4	J_{14}	2	c_{14}	10
k_{15}	0.2×10^4				

5.2.2-Mathematical Analysis

The equation of motion of the overall driveline system model may be written in matrix form as follows;

$$[M]\{\ddot{\theta}\}+[C]\{\dot{\theta}\}+[K]\{\theta\}=\left\{\sum_{k=0.5}^{h_o} T_k \sin(k\omega t+\beta_k)\right\} \qquad (5.1)$$

The equations of motion of the substructure system model, with dimensions depending on the number of retained modes of each substructure (n1, n2, n3, and n4), may be obtained in a corresponding form of Eqn (4.23), chapter 4, which is formed from the modal parameters of each substructure as follows;

$$[\mathbf{M}]\{\ddot{y}\}+[\mathbf{C}]\{\dot{y}\}+[\mathbf{K}]\{y\}=\{\mathbf{Q}\} \qquad (5.2)$$

where

$\{y\}$ is the modal nodes displacement vector;

$$\begin{Bmatrix} {}^{1}\{y\}_{n1} \\ {}^{2}\{y\}_{n2} \\ {}^{3}\{y\}_{n3} \\ {}^{4}\{y\}_{n4} \end{Bmatrix}$$

[M] is the mass matrix of substructured model;

$$\begin{bmatrix} {}^{1}[m]_{n1} & & & [0] \\ & {}^{2}[m]_{n2} & & \\ & & {}^{3}[m]_{n3} & \\ [0] & & & {}^{4}[m]_{n4} \end{bmatrix}$$

[C] is the damping matrix of substructured model;

$$\begin{bmatrix} {}^{1}[c]_{n1} & & [0] & \\ & {}^{2}[c]_{n2} & & \\ & & {}^{3}[c]_{n3} & \\ & [0] & & {}^{4}[c]_{n4} \end{bmatrix}$$

$[\mathbf{K}]$ is the stiffness matrix of substructured model ;

$$\begin{bmatrix} \left({}^{1}[k]_{n1}+{}^{1}[\phi_{j12}]_{n1}^{T}\ [k_{j1}]\ {}^{1}[\phi_{j12}]_{n1}\right) & \left(-{}^{1}[\phi_{j12}]_{n1}^{T}\ [k_{j1}]\ {}^{2}[\phi_{j21}]_{n2}\right) & [0] & [0] \\ \left(-{}^{2}[\phi_{j21}]_{n2}^{T}\ [k_{j1}]\ {}^{1}[\phi_{j12}]_{n1}\right) & \left(\begin{array}{l}{}^{2}[k]_{n2}+{}^{2}[\phi_{j21}]_{n2}^{T}\ [k_{j1}]\ {}^{2}[\phi_{j21}]_{n2} \\ +{}^{2}[\phi_{j23}]_{n2}^{T}\ [k_{j2}]\ {}^{2}[\phi_{j23}]_{n2}\end{array}\right) & \left(-{}^{2}[\phi_{j23}]_{n2}^{T}\ [k_{j2}]\ {}^{3}[\phi_{j32}]_{n3}\right) & [0] \\ [0] & \left(-{}^{3}[\phi_{j32}]_{n3}^{T}\ [k_{j2}]\ {}^{2}[\phi_{j23}]_{n2}\right) & \left(\begin{array}{l}{}^{3}[k]_{n3}+{}^{3}[\phi_{j32}]_{n3}^{T}\ [k_{j2}]\ {}^{3}[\phi_{j32}]_{n3} \\ +{}^{3}[\phi_{j34}]_{n3}^{T}\ [k_{j3}]\ {}^{3}[\phi_{j34}]_{n3}\end{array}\right) & \left(-{}^{3}[\phi_{j34}]_{n3}^{T}\ [k_{j3}]\ {}^{4}[\phi_{j43}]_{n4}\right) \\ [0] & [0] & \left(-{}^{4}[\phi_{j43}]_{n4}^{T}\ [k_{j3}]\ {}^{3}[\phi_{j34}]_{n3}\right) & \left({}^{4}[k]_{n4}+{}^{4}[\phi_{j43}]_{n4}^{T}\ [k_{j3}]\ {}^{4}[\phi_{j43}]_{n4}\right) \end{bmatrix}$$

$\{\mathbf{Q}\}$ is the generalised force vector of the substructure model;

$$\begin{Bmatrix} \left\{{}^{1}[\phi_i]_{n1}^{T}\{F_i\}_{n1}\right\} \\ \left\{{}^{2}[\phi_i]_{n2}^{T}\{F_i\}_{n2}\right\} \\ \left\{{}^{3}[\phi_i]_{n3}^{T}\{F_i\}_{n3}\right\} \\ \left\{{}^{4}[\phi_i]_{n4}^{T}\{F_i\}_{n4}\right\} \end{Bmatrix}$$

Free vibration solution of Eqs (5.1) and Eqs (5.2), in homogenous form, is performed to obtain the vibrational characteristics, natural frequencies and mode shapes, of the overall and substructured models respectively. All the mathematical operations are performed using the computer program which has been described in section 4.6 (chapter 4). The coupled equations of motion are formulated and solved considering different numbers of retained modes, with and without consideration of the residual flexibilities of the omitted higher modes. The results are tabulated in Tables (5.2) to (5.4).

Table (5.2) Damped natural frequencies of overall and substructure system models in Hz

Mode No.	*Overall system model*	*Substructured System, n=14*	*Sub-1*	*Sub-2*	*Sub-3*	*Sub-4.*
1	***3.997***	***3.997***	0.000	0.000	0.000	4.832
2	***9.407***	***9.407***	222.550	103.932	503.241	9.4o7
3	***12.572***	***12.572***	755.785	815.215		30.153
4	***50.849***	***50.849***	1317.014	1844.979		
5	***109.686***	***109.686***	1701.827			
6	***138.941***	***138.941***				
7	427.352	427.352				
8	432.342	432.342				
9	679.948	679.948				
10	838.848	838.848				
11	955.585	955.585				
12	1421.346	1421.346				
13	1730.070	1730.070				
14	1845.524	1845.524				

Table (5.3) Comparison between substructured and overall system models with and without considering the residual flexibility (N1=5, N2=4, N3=2 and N4=3)

m o d e	$\omega_{o(Hz)}$ Overall system model	Percentage deviation between substructured system and overall system models								
		All modes n=14	n1=5, n3=2,	n2=4, n4=2	n1=3, n3=1,	n2=3, n4=3	n1=2, n3=1,	n2=2, n4=3	n1=1, n3=1,	n2=1, n4=3
		e	e (rs=0)	e (rs≠0)	e (rs=0)	e (rs≠0)	e (rs=0)	e (rs≠0)	e (rs=0)	e (rs≠0)
1	3.997	0	1.457	0. 0 27	0. 169	0. 0 84	0.177	0. 0 84	0.469	0. 104
2	9.407	0	0. 0	0. 000	0. 0	0. 000	0. 0	0. 000	0. 0	0. 0
3	12.572	0	79.851	6.456	2.883	1.414	3.022	1.414	8.763	1.823
4	50.849	0	113.83	85.96	6.591	3.111	7.065	3.113	65.650	11.250
5	109.686	0	20.904	4.16	1.644	0.497	5.019	0.566	162.76	7.551
6	138.941	0	206.05	91.94	17.207	7.124	18.312	7.145	223.57	144.17
7	427.352	0	0.017	0.005	2.675	10.538	6.794	10.378		
8	432.342	0	56.14	33.536	4.5	0.896	31.567	5.028		
9	679.948	0	23.37	23.32	22.86	22.179				
10	838.848	0	13.919	13.92	20.788	16.975				
11	955.585	0	48.737	48.74						

Table (5.3), Continue

12	1421.35	0	21.719	21.72						
13	1730.07	0	6.673	6.67						
14	1845.52	0								

Table Key

N_S Number of total DOFs of s th substructure.

n_S Number of remained modes of the s th substructure.

rs Switch for considering the static residual flexibility, due to the omitted higher modes, or not (rs≠0 for considering and rs=0 for non considering the residual flexibility).

ω_o The natural frequencies which calculated from the overall system model.

ω The natural frequencies which calculated from the substructure model.

e The percentage deviation due to using the Substructured model, $e = 100\ (\omega - \omega_o) / \omega_o$

Table (5.4) The first six eigenvectors for overall system and substructured system models

Overall system model					**Substructured system model, 8 modes retained (n1=2, n2=2, n3=1 and n4=3)**				
1st	2 nd	3 rd	4 th	5 th	1st	2 nd	3 rd	4 th	5 th
1	0	1	1	1	1	0	1	1	1
0.9990	0	0.9906	0.8468	0.2876	0.9890	0	0.9889	0.8147	0.2024
0.9988	0	0.9886	0.8136	0.1410	0.9987	0	0.9872	0.7849	0.0738
0.9986	0	0.9863	0.7779	-.0076	0.9986	0	0.9859	0.7639	-0.0164
0.9983	0	0.9839	0.7398	-.1560	0.9985	0	0.9853	0.7531	-0.0629
0.9981	0	0.9813	0.6994	-.3023	0.9981	0	0.9807	0.6804	-0.3129
0.9799	0	0.8062	-1.5362	-.3560	0.9795	0	0.7974	-1.6836	-0.2390
0.9794	0	0.8017	-1.5882	-.3531	0.9792	0	0.7945	-1.7204	-0.2378
0.9785	0	0.7926	-1.6873	-.3423	0.9789	0	0.7909	-1.7668	-0.2364
0.9686	0	0.6986	-2.5919	-.1531	0.9660	0	0.6666	-2.9602	-0.0007
0.9586	0	0.6037	-3.4436	.05077	0.9660	0	0.6666	-2.9602	-0.0007
0.9535	0	0.5558	-3.8343	.1503	0.9584	0	0.5922	-3.5557	0.1360
0.8337	-0.7071	-0.5049	0.0972	-.00079	0.8383	-0.7071	-0.5052	0.0846	-0.0007
0.8337	0.7071	-0.5049	0.0972	-.00079	0.8383	0.7071	-0.5052	0.0846	-0.0007

5.2.3-Results and Discussion

Table (5.2) shows the natural frequencies of the torsional vibration of the overall system model and substructured model. There are about five torsional natural frequencies which lie within the operating range of the driveline system and three of them below the typical nominal speed. From this table, the natural frequencies computed by substructure technique (3rd column) considering all modes are identical to the corresponding ones computed from the overall system model (2nd column).

Table (5.3) shows the percentage deviation of the natural frequencies computed using the substructure technique from the corresponding computed values from the overall system model for different numbers of considered modes of each substructure, with and without considering the residual flexibilities of the omitted modes. The percentage deviation is zero if all modes are considered (3rd column). Even if only a few lower modes are considered, the percentage deviations in the lower modes can be neglected and they are not significant until the normal working range of frequency, especially if the residual flexibilities were considered (last column). The lower modes of each substructure which lie in the operating range of the frequency are more effective on the substructure model results than the other modes. The inclusion of the residual flexibilities of the omitted higher modes has a great effect on the results of the substructure model in minimising the deviation of the natural frequencies. Table (5.4) contains the first 5th eigenvectors obtained from the overall system model and substructured model considering only lower modes of each substructure. From this table, only slight differences in the first five modes and one slight change of a node position of the fifth mode are seen.

Based on the previous discussion, only the lower modes which lie in the normal operating range of the frequency may be considered in the system steady state response because they have the dominant effect on the total response. These modes are marked as bold italic in the Table (5.2).

5.3-STEADY STATE RESPONSE

The same mathematical model used in the free vibration analysis, Eqs (5.1) and (5.2), is used in this section. The persistent system response to the fluctuating engine torque, T(t), has been obtained for the overall system model and the substructured model. It relies on the principle of linear superposition being valid, i.e. in a linear elastic system the motion produced by two or more sets of periodically varying forces, acting simultaneously, is equal to the sum of the motions which would be produced by separate forces acting alone, due regard being given to the phase relations between the respective components. Thus the motion produced by the fluctuating torque of a

single cylinder is the sum of the motions which would be produced by the separate harmonic components of the torque curve if these were assumed to be acting alone; and the motion produced by a group of cylinders is the sum of the motions produced by the separate cylinders.

The modal superposition method is used to solve the equations of motion, (5.1) for the overall system model. For substructure model, the same technique is used to solve the equations of motion constructed from the modal parameters of each substructure, Eqn (5.2). Only the dominant modes in the operating range of frequency, first 8 modes, of 14 modes of the substructured system are considered.

The response of individual harmonic order, k, can be obtained using a limited number of the vibration modes, n, using this equation, see section (4.3);

$$\{\theta_k(t)\} = \{\Theta_o\}_k \sin(k\Omega t + \Psi_k) \qquad (5.3)$$

where $\{\Theta_o\}_k$ is the amplitude vector of the kth harmonic order, (14x1);

$$\{\Theta_o\}_k = \sum_{r=1}^{n} \frac{\{\phi\}_r \{\phi\}_r^T \{T_k\}}{k_r \{1-(k\ \ \Omega/\omega_r)^2 + (2\xi_r(k\ \ \Omega/\omega_r))^2\}} \qquad (5.4)$$

$\{\phi\}_r$ The rth natural mode shape corresponding to rth natural frequency, ω_r, obtained from the undamped free vibration system analysis,

ζ_r Damping ratio corresponding to the rth natural vibration mode,

k_r The generalised stiffness coefficient corresponding to rth mode, $\{\phi\}_r^T[K]\{\phi\}_r$

Ω The angular speed of the engine, and

Ψ_k The total phase angle of the kth harmonic order, where;

$\beta_k - \Psi_k = \sum_{r=1}^{n} \tan^{-1} \frac{2\xi_r k\ \ \Omega/\omega_r}{1-(k\ \ \Omega/\omega_r)^2}$ is the response phase angle of kth harmonic order.

β_k is the phase angle of k th harmonic order, see section (3.3).

The total steady state time history response of the system to the periodic fluctuating engine torque can be obtained by repeating these calculations for each harmonic order torque and accumulating all results, i.e.

$$\{\theta(t)\} = \sum_{k=0.5}^{ho} \{\Theta_o\}_k \sin(k\Omega t + \Psi_k) \qquad (5.5)$$

$\{\theta(t)\}$ is the vector of the steady state time history response.

In order to identify the frequency components in the steady state time history system response, Eqn (5.5), at particular engine speed, the time response is converted to the frequency domain by taking the discrete Fast Fourier Transform of this response (FFT). This transformation gives frequency-domain information about a given time response.

The responses at the key points of the driveline system, such as the torsional damper, the clutch, the differential and the driving wheels are presented for both the overall system and substructure models, Figs (5.7) to (5.19).

5.4-COMPUTER PROGRAM

Computer programs using mathematical library subroutines from MATLAB have been implemented to obtain the frequency response for any number of harmonic order of the engine fluctuating torque, Eqn (5.4), the total time response of this torque, Eqn (5.5), and its transformation into the frequency domain. The programmes are designed to deal with both the overall and substructured system models. Choices of number of selected modes of each substructure and overall system, required harmonic order, engine speed range, firing order and required harmonic order are available in the programmes. Programmes are designed to be interactive allowing the user to input the required system parameters. Programmes flow charts are shown in Figs (5.3) and (5.4).

Read Data
-Natural frequencies and natural modes of each substructure and overall system (from free vibration analysis program)
-Gas torque vector (from special program for this purpose)

↓

Input Data
-Required harmonic order
-Engine speed range (sweeping range)
-Number of required modes of overall system and Substructured models
-Firing order of the engine

↓

Calculation of
-the modal parameters for the overall system and each substructure (modal mass, modal stiffness, modal damping and modal load)

↓

Calculation of
-the inertia torque for the particular engine speed
-the phase angle between each successive cylinders based on firing order
-the total excitation torque from gas and inertia torques

↓

Calculation of
-the frequency ratio of the first harmonic order and first considered mode
-the frequency response for that mode in terms of modal co-ordinates for overall system and substructured system models

↓

Sum of
the previous two steps for all considered modes

$$\left(\{\Theta_o\}_k = \sum_{r=1}^{n} \frac{\{\phi\}_r \{\phi\}_r^T \{T_k\}}{k_r \{1-(k\ \ \Omega/\omega_r)^2 + (2\xi_r(k\ \ \Omega/\omega_r))^2\}} \right)$$

↓

Repeat
the previous three steps for the required engine speed range

↓

Transfer
-the response from modal co-ordinates into physical co-ordinates for overall system model and substructured model

↓

Plot
-the angular perturbation at different points against the engine speed for overall and substructured system models

↓

End

Fig (5.3) Frequency response flow chart steps using MATLAB

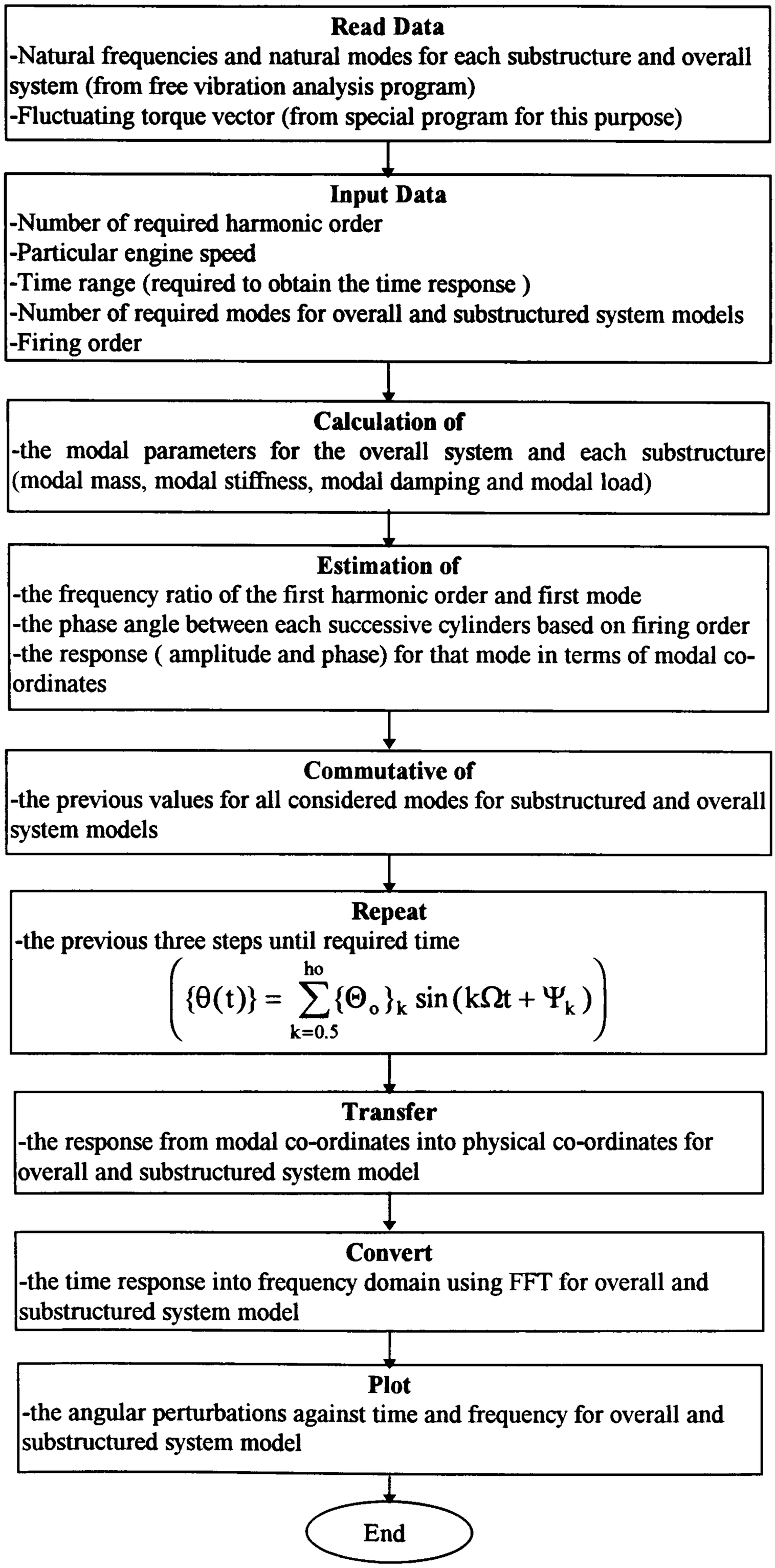

Fig (5.4) Time history response and its FFT flow chart steps using MATLAB

Typical results from the programmes are plotted in Figs (5.5) to (5.19). A four-cylinder, four-stroke engine with firing order 1-3-2-4 has been assumed throughout the analysis. All results are obtained for the overall system model as a 14 DOF system and substructured system with dimension depending on the number of retained modes of each substructure. The dominant modes in the operating frequency range of each substructure are considered, the higher modes are omitted and the residual flexibilities of the omitted modes have been considered, i.e., the substructured system has been reduced from 14 DOF into 8 DOF. Figs (5.7) to (5.15) show the system frequency responses for individual harmonic orders at various points and for various system parameters. Figs (5.16) to (5.19) present the steady state time responses of the system and its FFT at different engine speeds, different number of harmonic orders and different points on the driveline system.

5.5-Results and Discussion

From the frequency response curves, Figs (5.7) to (5.15), resonances occur when the engine speed multiplied by the harmonic order of the fluctuating torque coincides with any natural frequency of the system. For example, for the component of the fluctuating torque with harmonic order 0.5, there are resonances when half engine speed coincides with any natural frequency of the system i.e. at 8, 18.8, 25, 101.7,...Hz, Figs (5.7) to (5.9), while for the fluctuating torque with harmonic order 1, there are resonances when the engine speed coincides with any natural frequency of the system i.e. 4, 9.4, 12.5, 50.8,... Hz of the engine, Figs (5.10) to (5.12). Also, when the harmonic order 2 is considered, resonances occur when double engine speed coincides with any natural frequency of the system i.e. 2, 4.7, 6.3, 25.4, 54.9, 69... Hz, Figs (5.13) to (5.15), and so on. Therefore, the system is excited by multiple frequencies at a particular engine speed and there is resonance when a half multiple of the engine speed coincides with any torsional natural frequency of the system. The design principle is that natural frequencies of the system should not coincide with engine torque excitation frequencies, although in practice this is not feasible in the normal operating speed range.

From these figures, it is noticed that the second mode resonance (9.4 Hz) has not appeared in the frequency response function. Because in the branched system has two similar branches (equal stiffnesses and masses) having common frequency vibrate with a node at common point (differential) and other parts of the system remain at rest, i.e. only the similar branches share in the motion (out of phase) and the rest of the system remain at rest, see the second mode shape in the free vibration analysis, Table (5.4). For this reason this mode (2nd mode) has never excited by any excitation torque applied at any point of the driveline system from the torsional damper until the differential.

The time responses, Figs (5.16) to (5.19), have been obtained for different engine speeds and different numbers of harmonic order. These results confirm the ability of the computer program to obtain the system response to any number of harmonic order and they illustrate that the system may be excited by many frequencies at a particular engine speed, for example, at engine speed 3000 rpm (50 Hz) the excitation frequencies are; 25, 50, 75, 125, ... and so on, Fig (5.18).

From the previous figures, there is good agreement between the results of the overall system model and substructure model even for a few considered modes. This provides evidence for the effectiveness of the analysis technique (substructure technique) and the computer programs.

5.6-SUMMARY

1. The total vehicle driveline system was analysed by deriving a model for the overall system based on an analysis of the separate components using the substructure approach. Using overall and substructured system models to study the behaviour of driveline systems indicated good agreement between results of the two models.

2. Using the substructure approach has shown that the natural frequencies and response of the vehicle driveline system in the range of normal vehicle operation may be obtained from considering only a few lower modes and residual flexibility

of the higher modes of each component without significant error. This is very useful in reducing both the computational effort and time.

3. There is good agreement between results for the overall system model and substructure model even for a few considered modes. This finding supports the effectiveness of the analysis technique (substructure technique) and feasibility of the computer programs for efficiently tackling problems of the dynamic behaviour of vehicle drivelines.

4. Unlike many other dynamic systems in which the forcing frequencies are fixed, by a constant running speed, the driveline vibration problem is more complicated because the engine speed varies over a wide range. Even at any given engine speed there are a range of forcing frequencies. Therefore, structural modifications aimed at changing the system natural frequencies to change the resonance of the torsional vibration of the driveline system are not really feasible in practice.

5. Because the system response is predictable, it opens up the opportunity in future to control this vibration using some sort of intelligent control system to control overall driveline system vibrations.

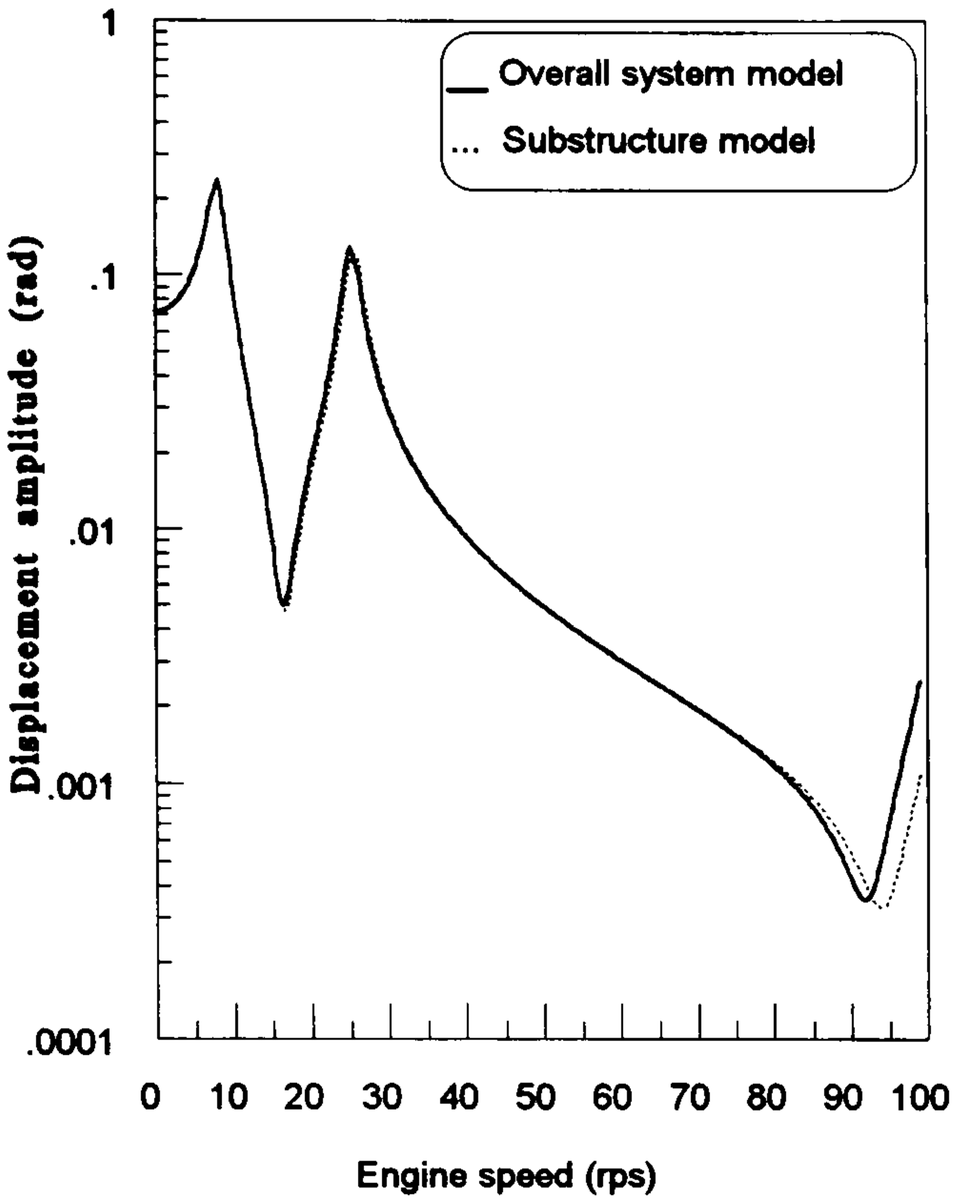

Fig. (5.7) System response at the torsional damper for harmonic order 0.5

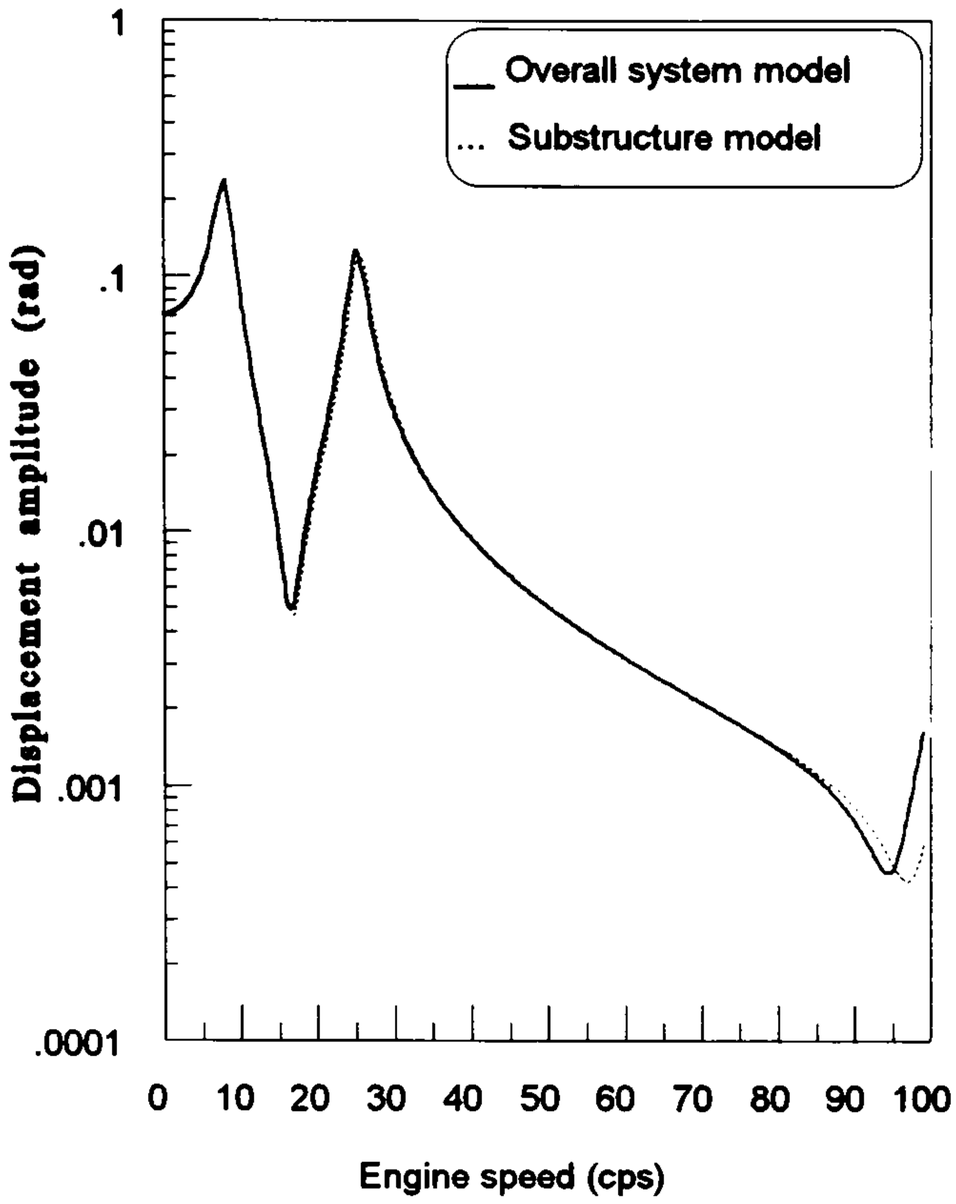

Fig (5.8) System response at the clutch for harmonic order 0.5

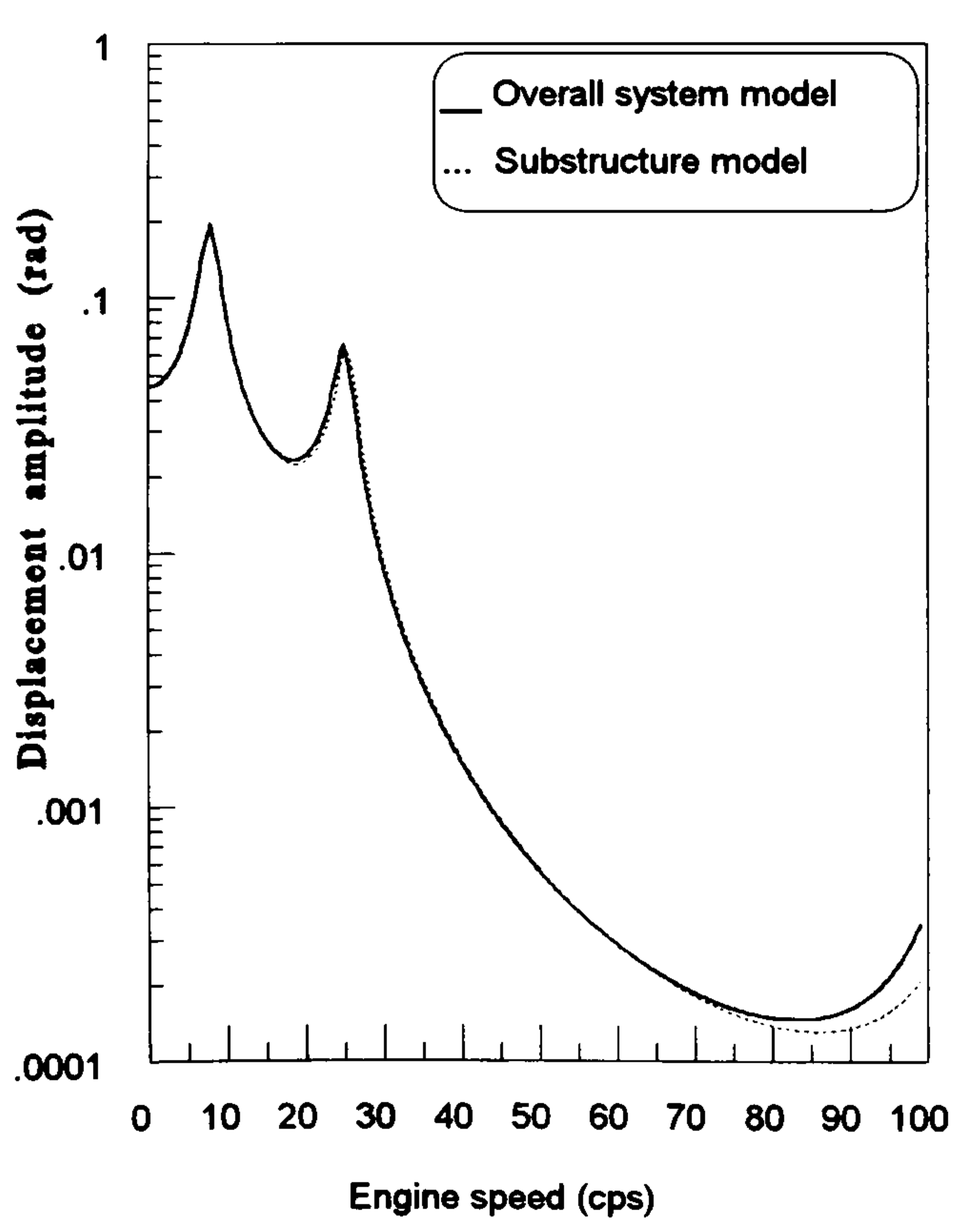

Fig (5.9) System response at the driving wheels for harmonic order 0.5

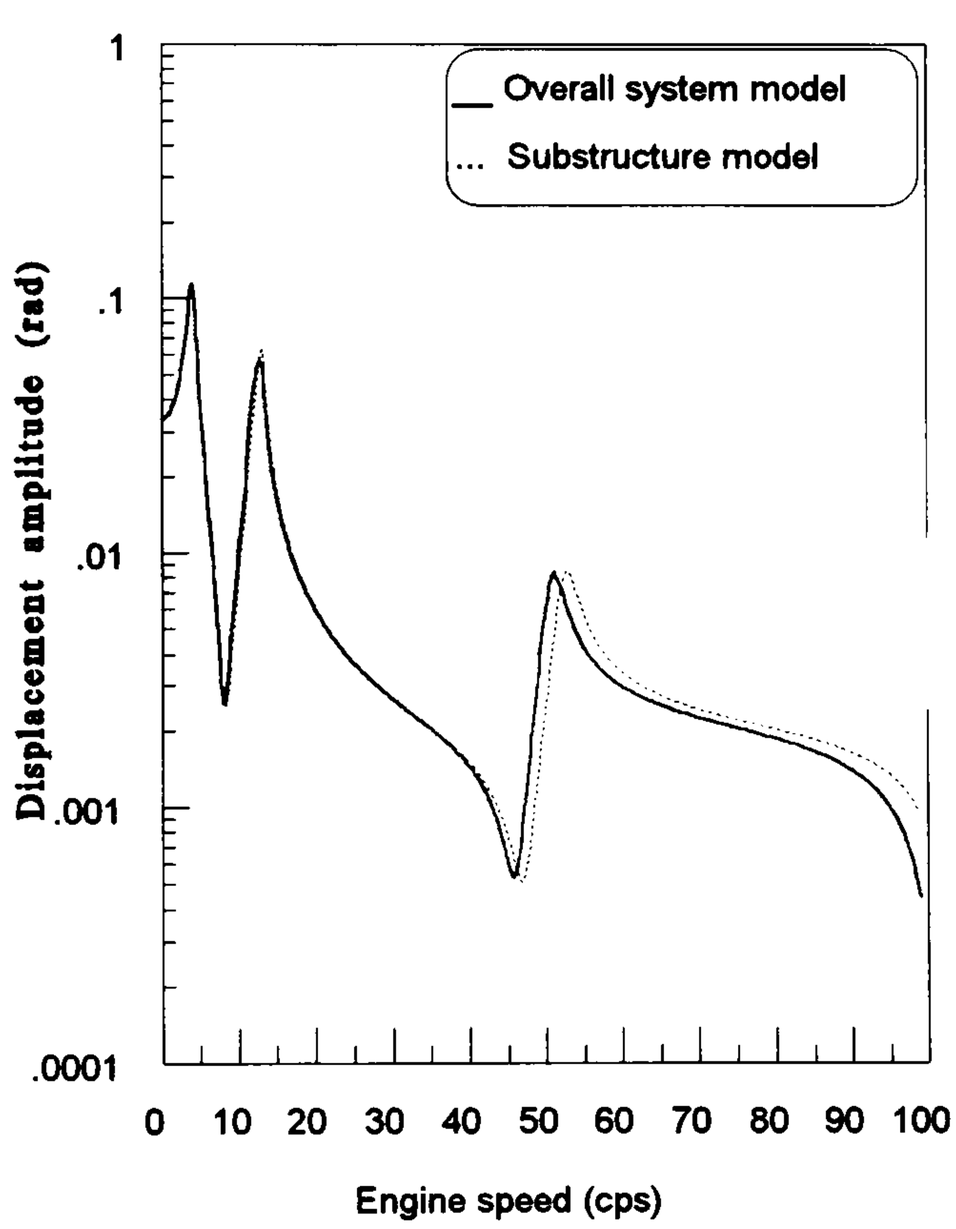

Fig (5.10) System response at the torsional damper for harmonic order 1

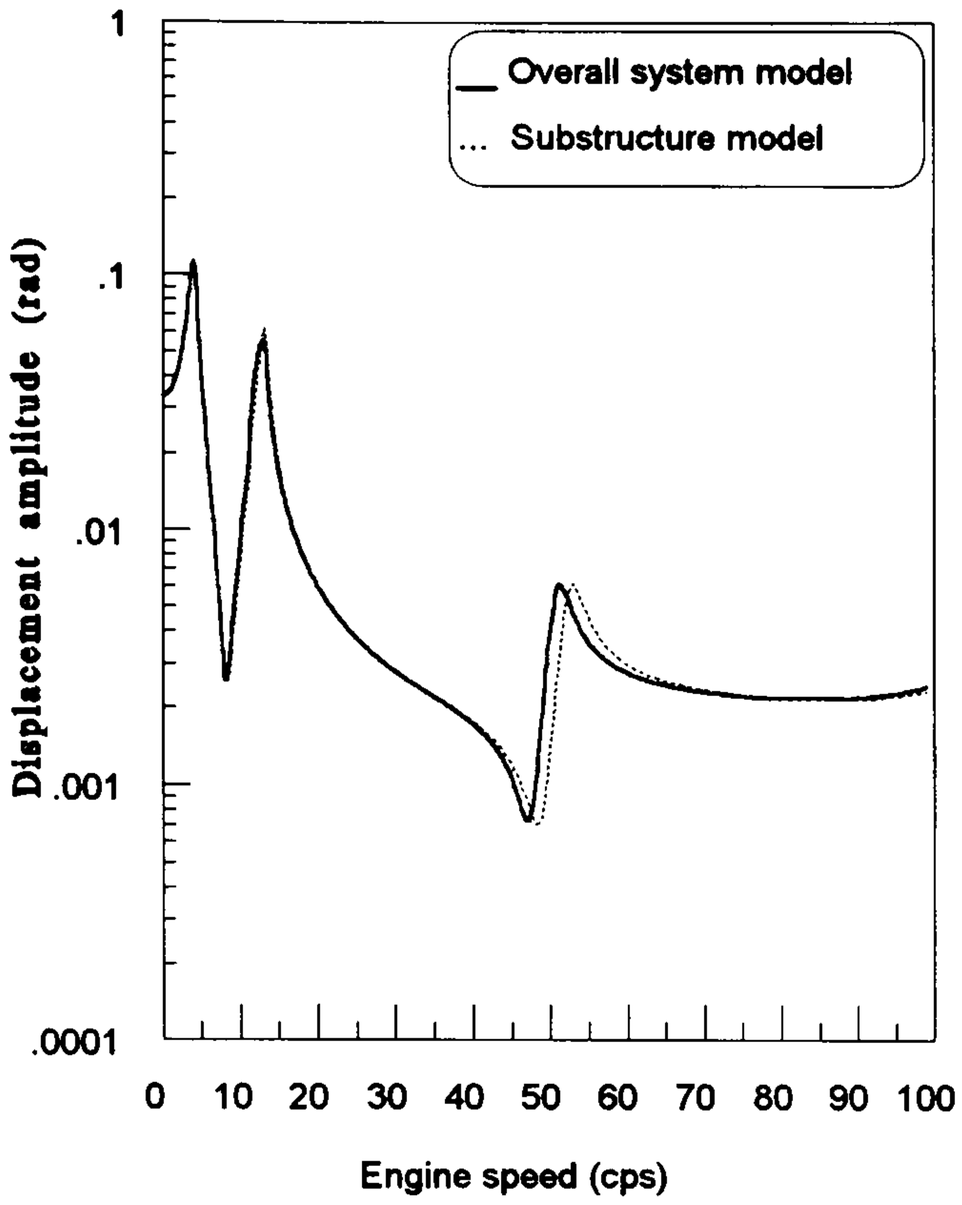

Fig (5.11) System response at the clutch for harmonic order 1

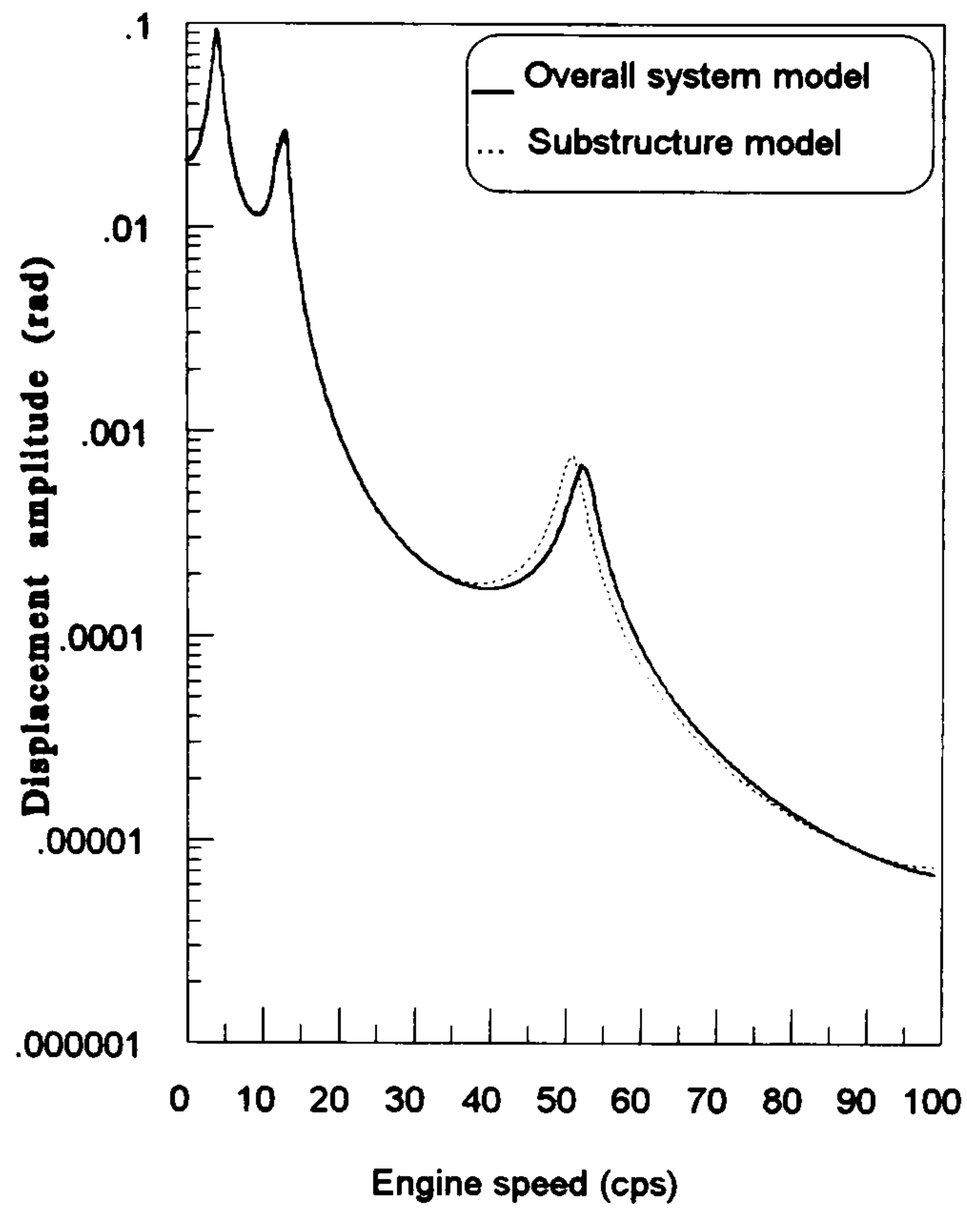

Fig (5.12) System response at the driving wheels for harmonic order 1

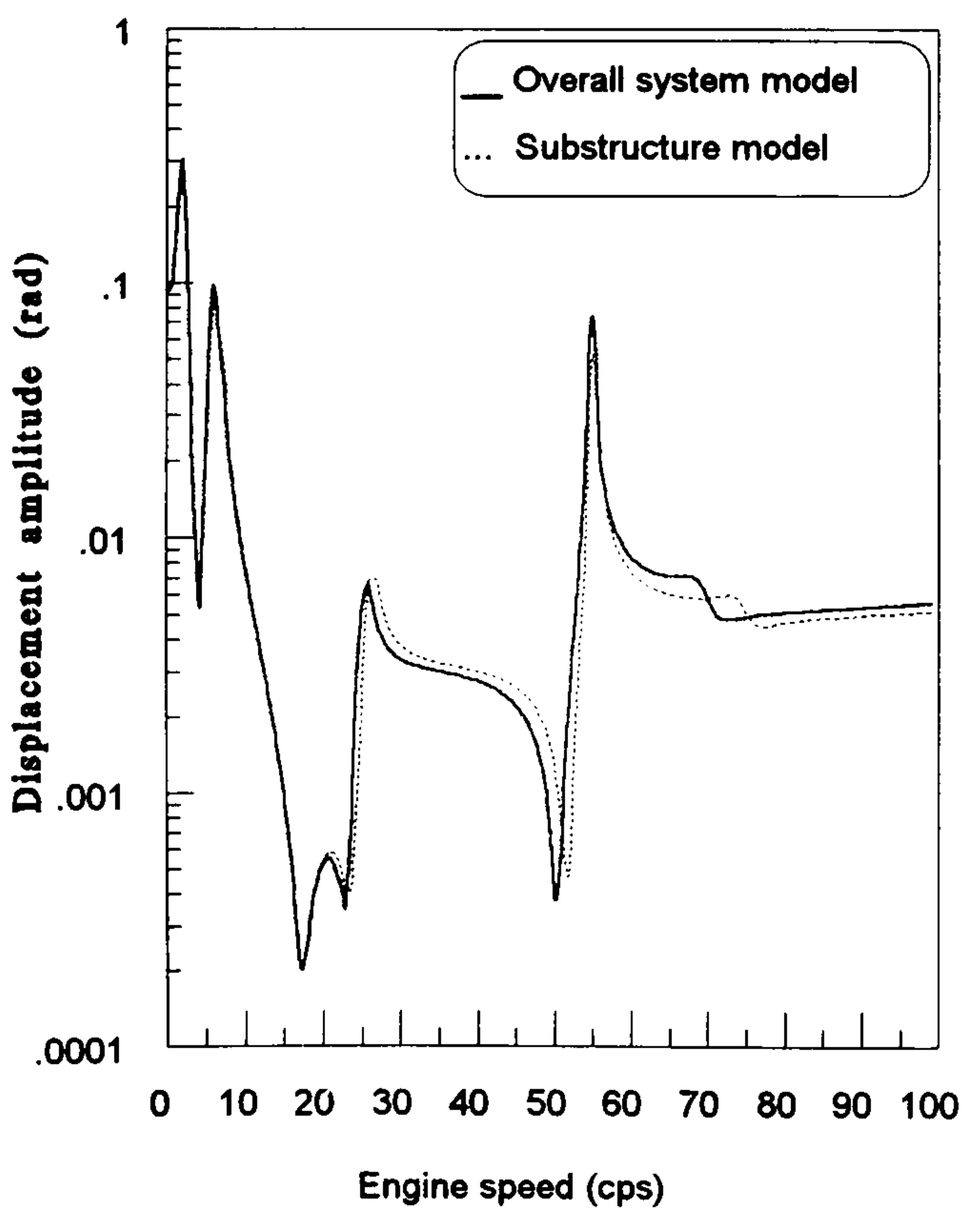

Fig (5.13) System response at the torsional damper for harmonic order 2

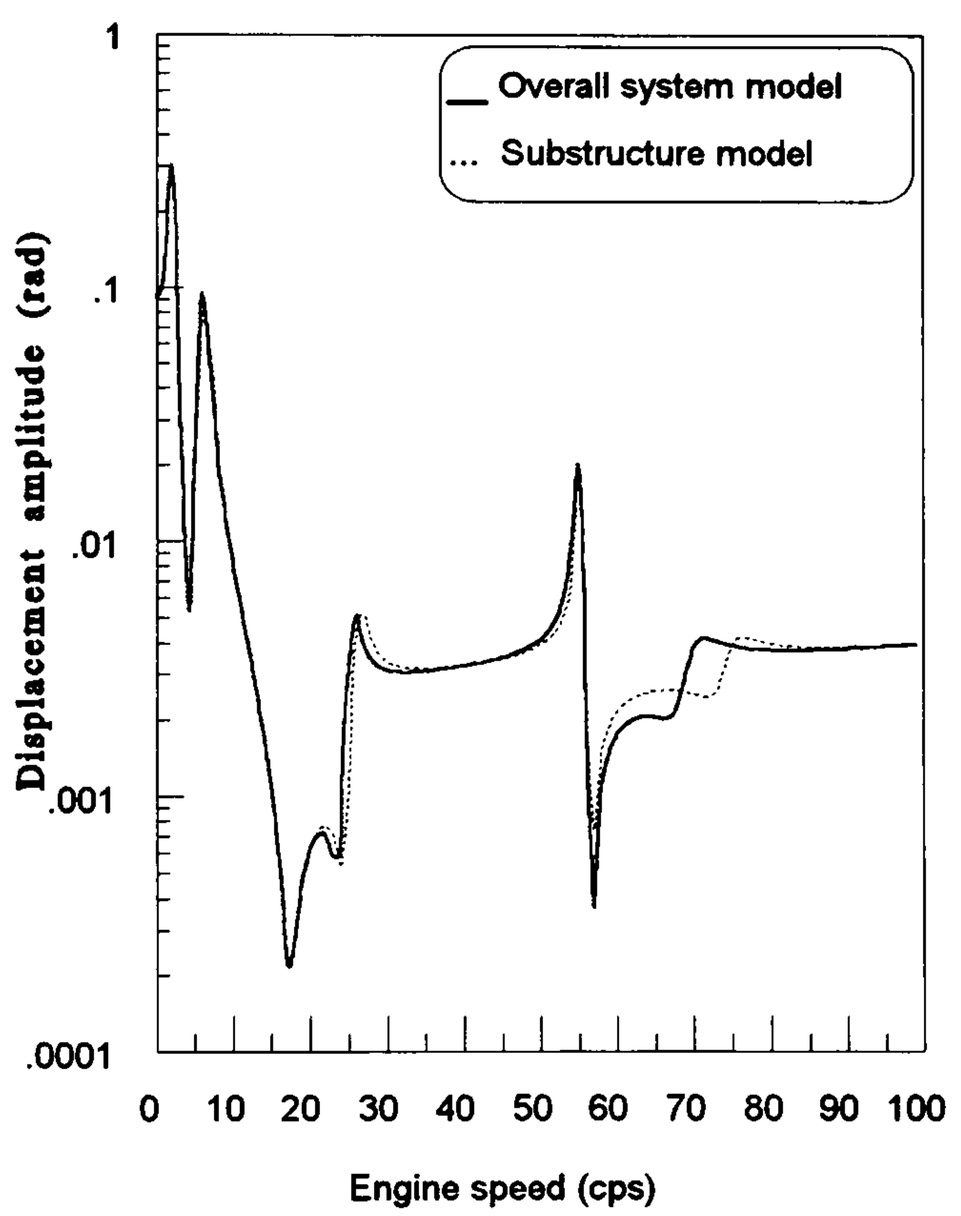

Fig (5.14) System response at the clutch for harmonic order 2

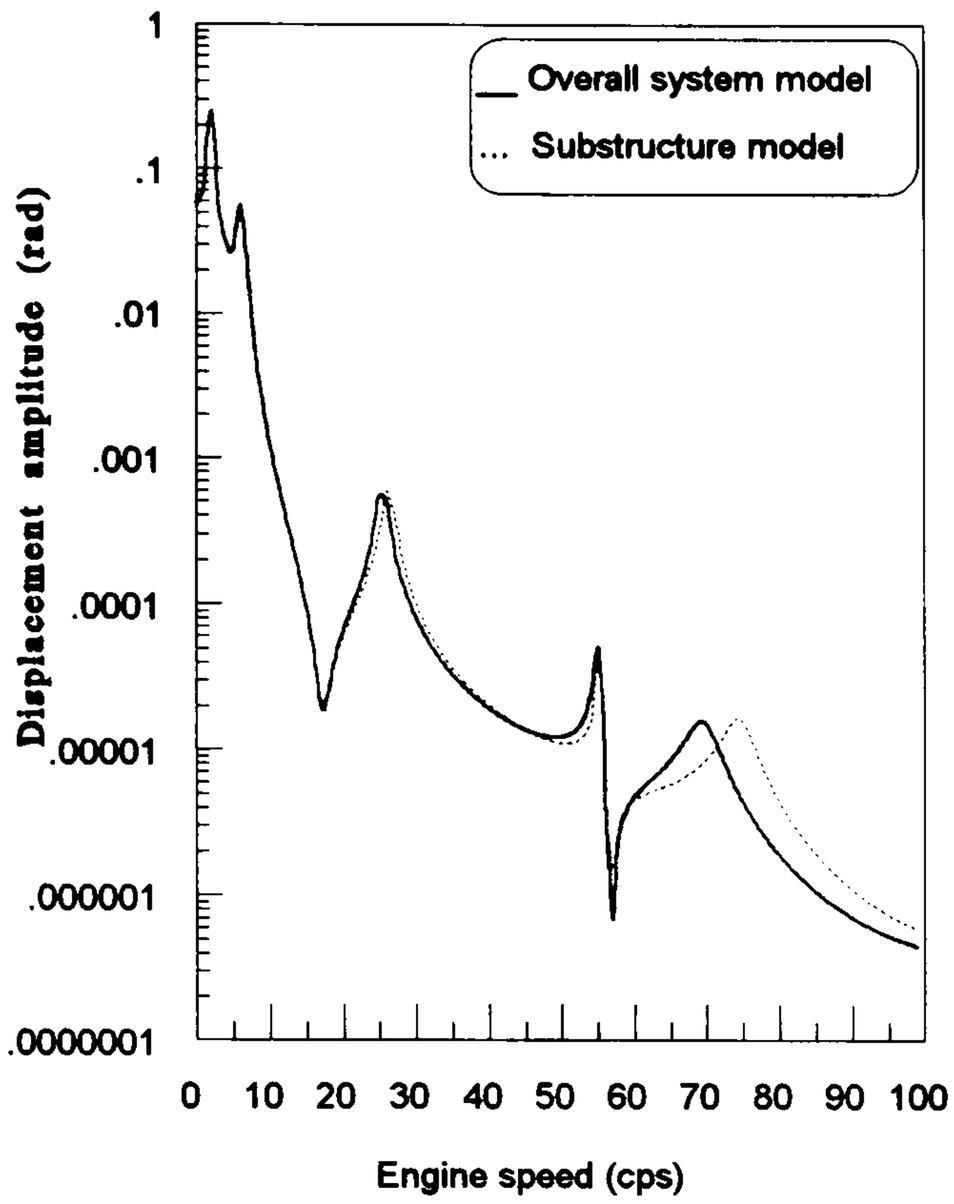

Fig (5.15) System response at the driving wheels for harmonic order 2

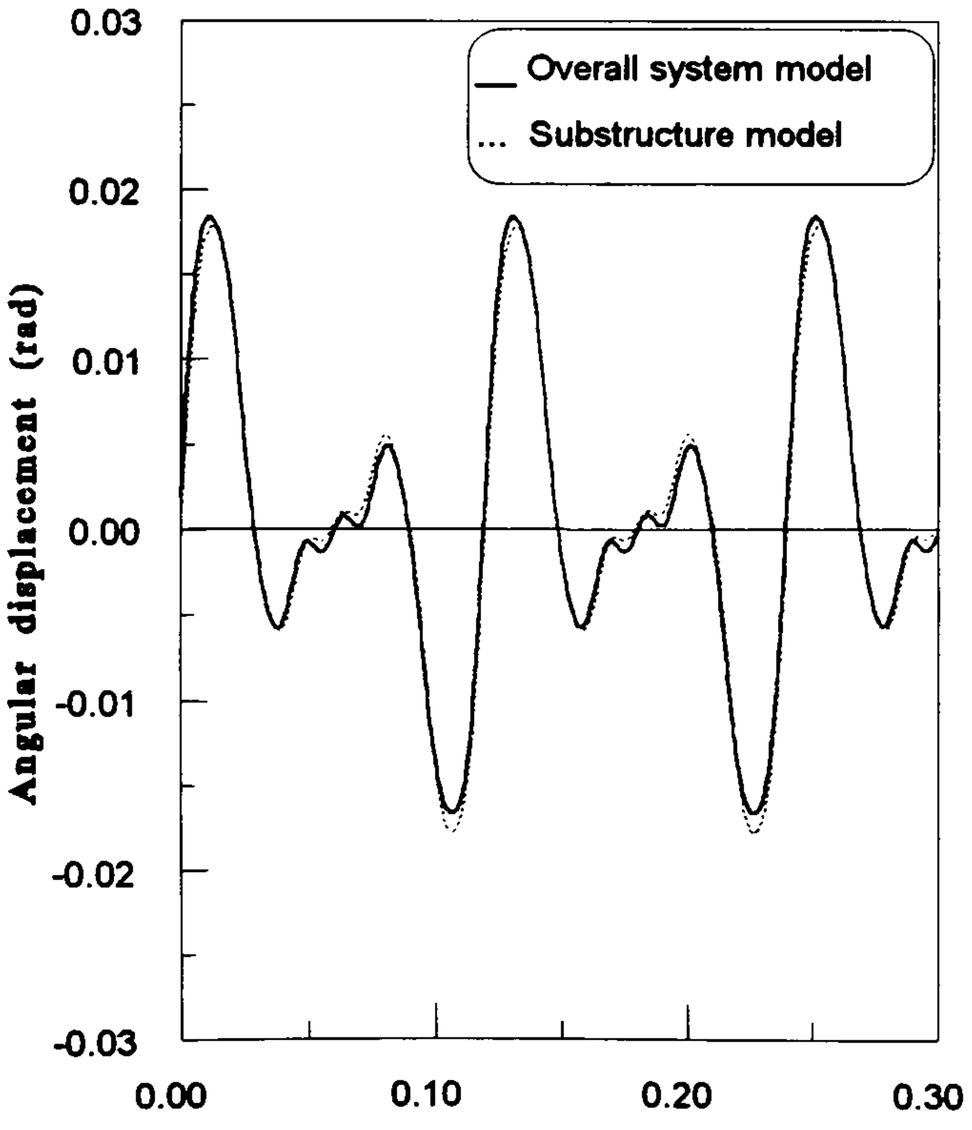

Fig (5.16a) Time response behaviour at the torsional damper, engine speed 1000 rpm and the number of harmonics is 8

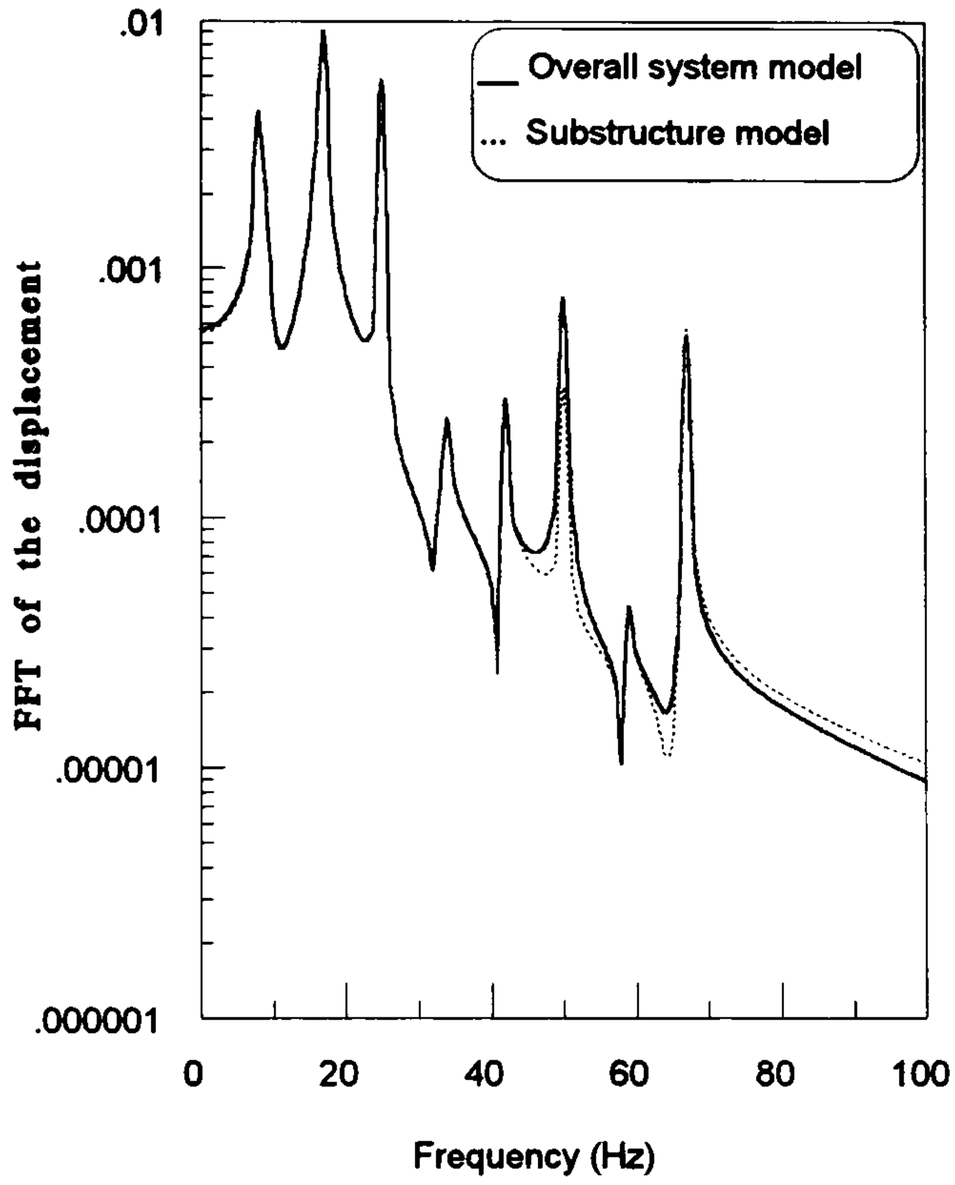

Fig (5.16b) FFT of the time response behaviour at the torsional damper, engine speed 1000 rpm and the number of harmonics is 8

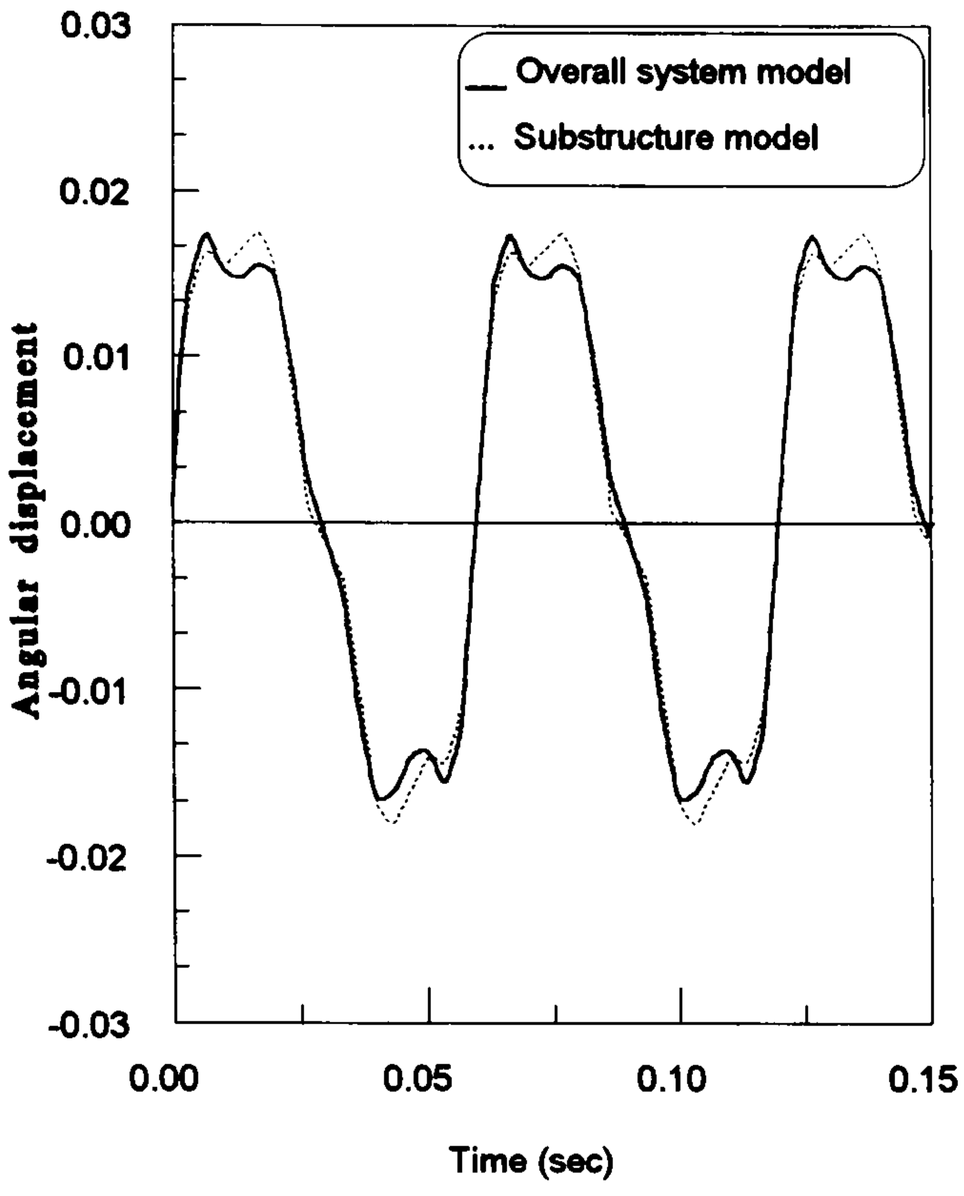

Fig (5.17a) Time response at the clutch, engine speed 2000 rpm and the number of harmonics is 6

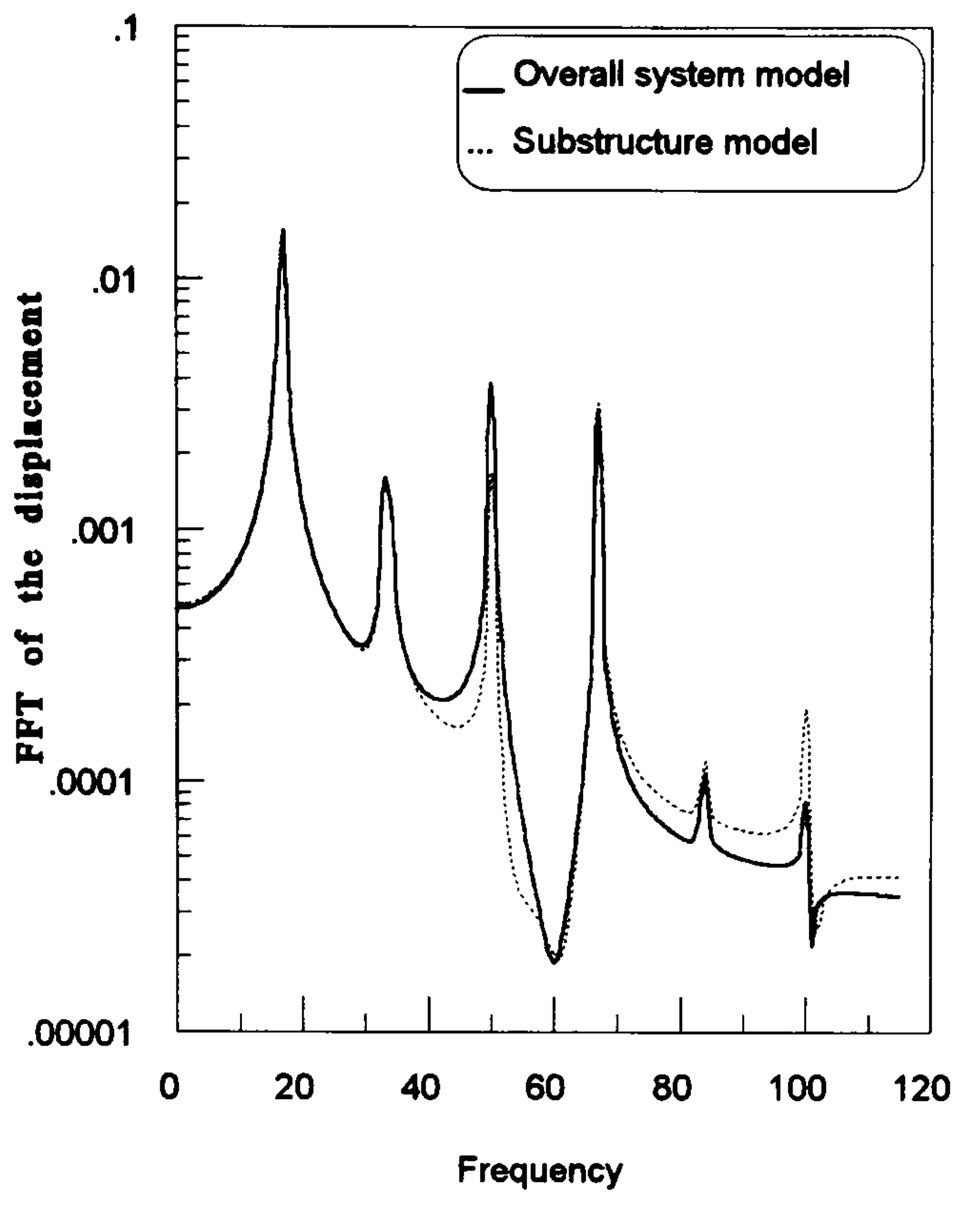

Fig (5.17b) FFT of the time response at the clutch, engine speed 2000 rpm and the number of harmonics is 6

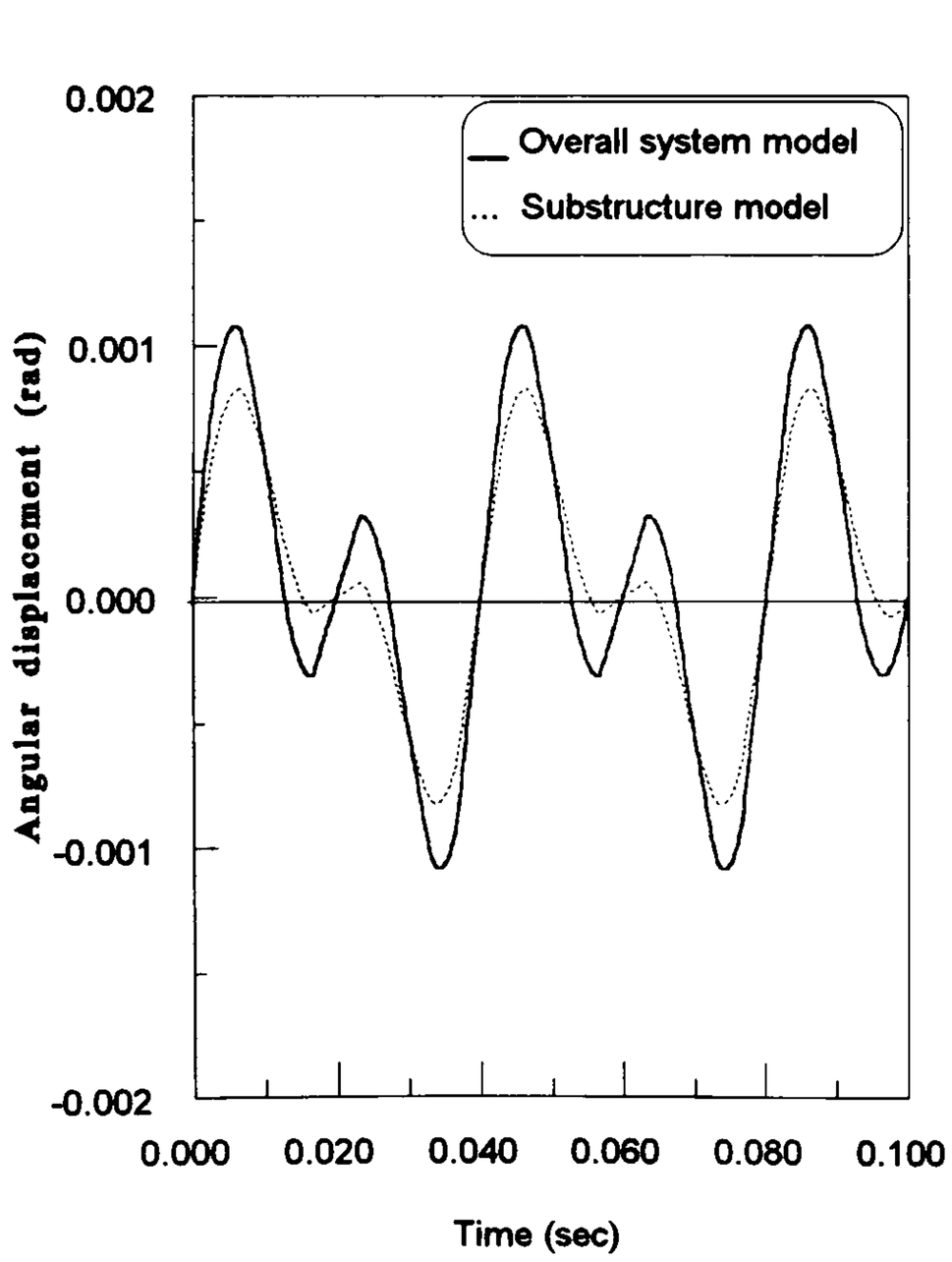

Fig (5.18a) Time response at the driving wheels, engine speed 3000 rpm and the number of harmonics is 8

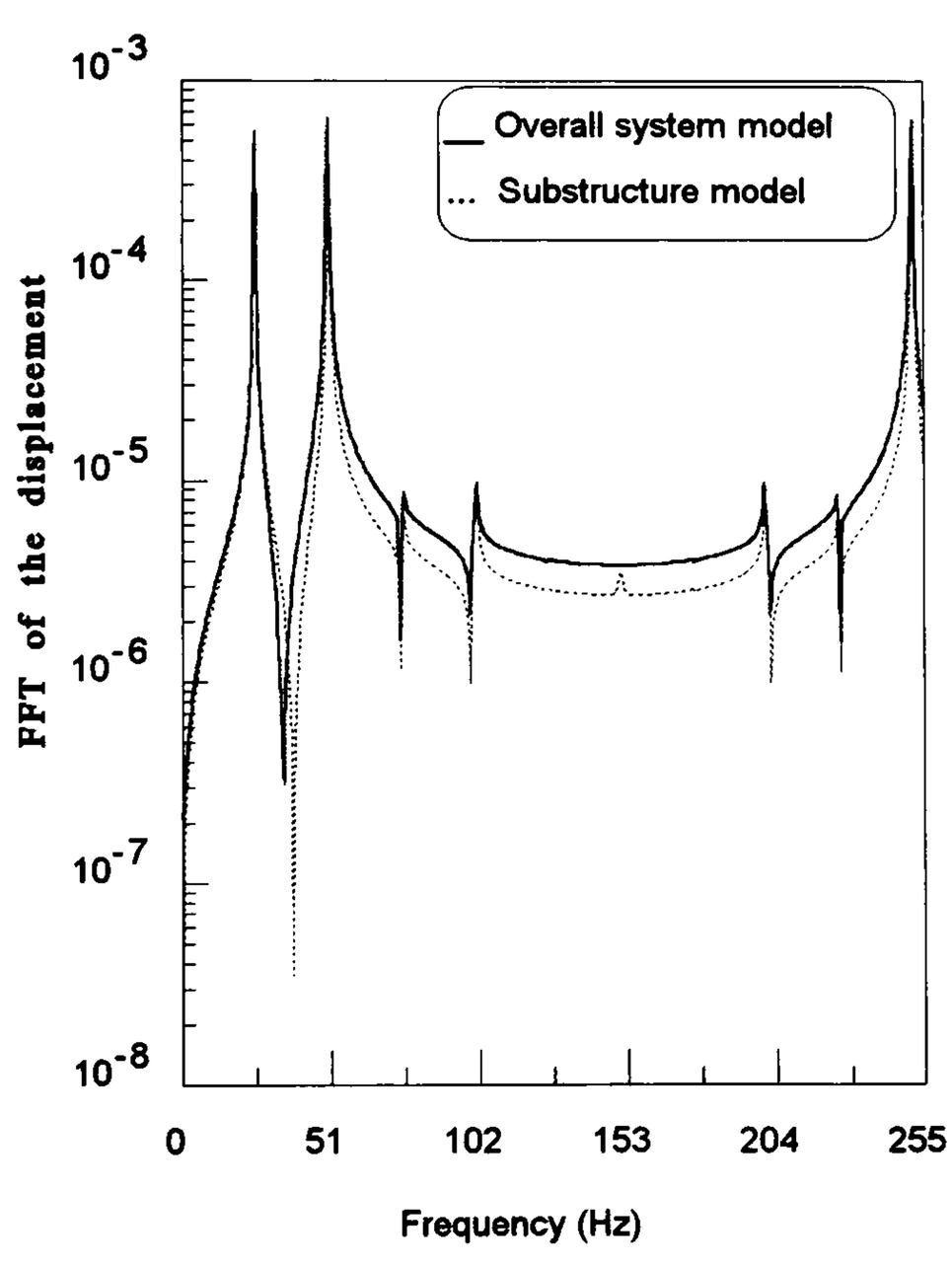

Fig (5.18b) FFT of the time response at the driving wheels, engine speed 3000 rpm and the number of harmonics is 8

.

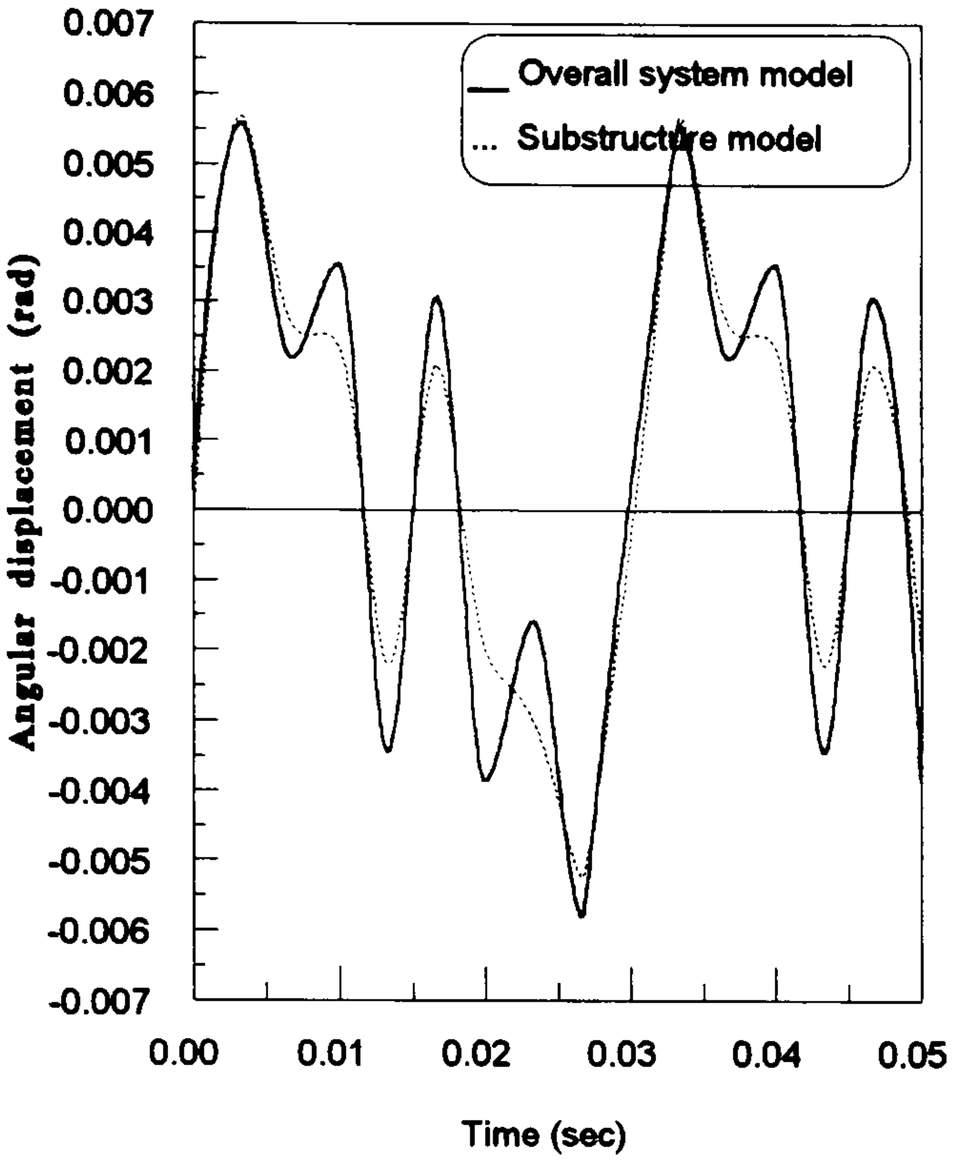

Fig (5.19a) Time response at the differential, engine speed 4000 rpm and the number of harmonics is 6

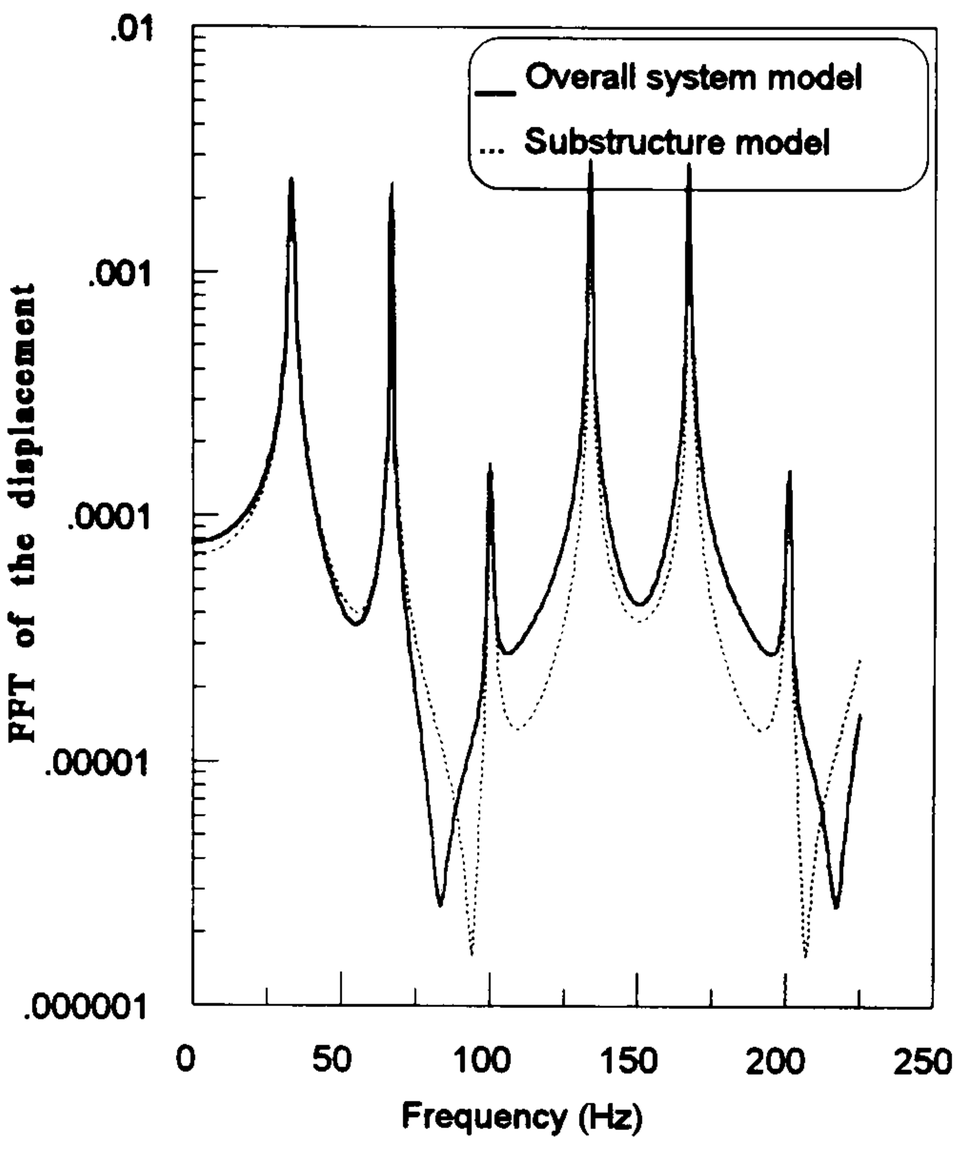

Fig (5.19b) FFT of the time response at the differential, engine speed 4000 rpm and the number of harmonics is 6

CHAPTER 6

NON-LINEAR TORSIONAL VIBRATION OF DRIVELINE SYSTEM

6.1-INTRODUCTION

Whereas some features of the driveline are amenable to linear analysis, most of the problem areas are probably associated with non-linear characteristics introduced, for example, by backlash, Hooke's joints, non-linear stiffness properties and hysteretic damping, etc. In order to investigate the transient dynamic response of vehicle driveline systems, it is necessary to simulate the phenomena in which the non-linear components play an important part. This chapter concerned with the non-linear components in the driveline system and their effect on its torsional vibration behaviour.

Non-linear systems are difficult to analyse and need relatively complicated mathematical steps; however, non-linear analysis can be used to improve the practical design of driveline systems. For non-linear systems, the superposition principle does not apply and so the modal analysis and substructure techniques described in chapter 5 can not be used.

In this chapter, the effect of the non-linear components on the torsional vibration behaviour of the driveline system is investigated to identify the differences between the behaviour of the linear and non-linear system and to clarify the most significant effects of the non-linearities on the system behaviour.

The aims of this chapter are:

(i) to devise mathematical models of the non-linear dynamics of the drivelines of typical passenger cars.

(ii) to use these mathematical models to understand the sensitivity of driveline response to design parameters.

(iii) to optimise driveline refinement by controlling susceptibility to torsional oscillation.

6.2-NON-LINEAR SPRING STIFFNESS

In the vehicle driveline system, the most important non-linear stiffness elements are the clutch and tyre. The stiffness of the clutch or the tyre has a torque vs. deflection characteristic which has a non-linear relationship, see Fig. (6.1a).

$$T(\phi) = T_o\phi + T_n\phi^2$$

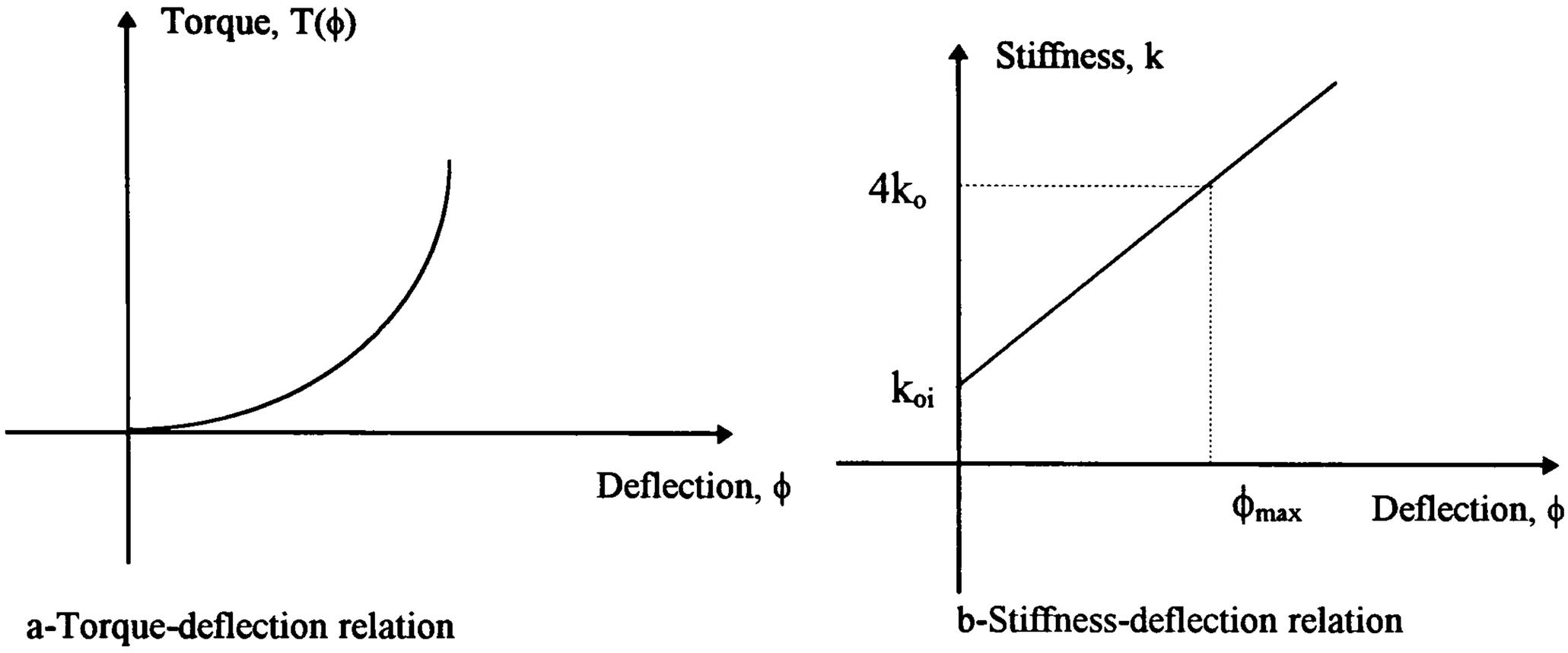

Fig (6.1) Model of non-linear spring stiffness

The non-linear stiffness of an element i can typically be described by the general following equation ;

$$k_i(\phi) = k_{oi} + k_n\phi_i$$
or
$$k_i(\phi) = k_{oi}(1 + ck_i \ |\phi_i|) \qquad (6.1)$$

where;

k_i is the total stiffness of an element i.

ϕ_i is the angular displacement of the element i.

k_{oi} is a constant (linear) value of the stiffness of the element i.

ck_i is a non-linear stiffness ratio of element i (k_n/k_{oi})

ϕ_{max} is the maximum angular displacement of the non-linear element, Fig. (6.1b).

In practice, Eqn (6.1) can vary considerably but it will generally result in an increasing spring stiffness as element twist increases [8]. In this study, the value of the maximum stiffness was assumed to be four times of the basic value, k_{oi}, Fig (6.1b).

6.3-BACKLASH

Impacts in power transmission systems occur where backlash is present at points in the system, such as gear teeth, splines and the mating surfaces of flexible couplings of the toothed-ring and claw types. In a vibrating system, repeated impacts will occur if the amplitude at the mating surfaces due to the vibratory torque is greater than the deflection due to the mean torque transmitted by the mating surfaces, i.e. if there is torque reversal. In systems with angular backlash, natural frequencies may vary depending on the variation of the ratio (mean torque/vibrating torque) with operating conditions. The backlash also tends to widen the range of speed over which severe vibration may be experienced in each resonant zone. In severe cases of clearance and backlash the impacts become audible as rattles or thumps, a condition which may result in significant noise and fatigue failures due to fretting at high dynamic loading.

Thus from the point of view of the response of the system to vibratory loading the effect of clearance and backlash is detrimental and it is desirable to adjust the characteristics of the system so that the amplitude of the vibratory torque is less than the mean transmitted torque, at least over the normal operating range of speeds. In cases of system operation at various speeds under both full and no-load conditions, nominal values of natural frequency may fluctuate significantly. Note that because the system is non-linear, it does not have unique modal frequencies as for a linear system. Although some backlash is almost inevitable it is an accepted principle that it should be kept to the minimum permitted by functional requirements. A model of the transmitted torque characteristics through a component which includes backlash, spline shaft for example, is shown in Fig (6.2).

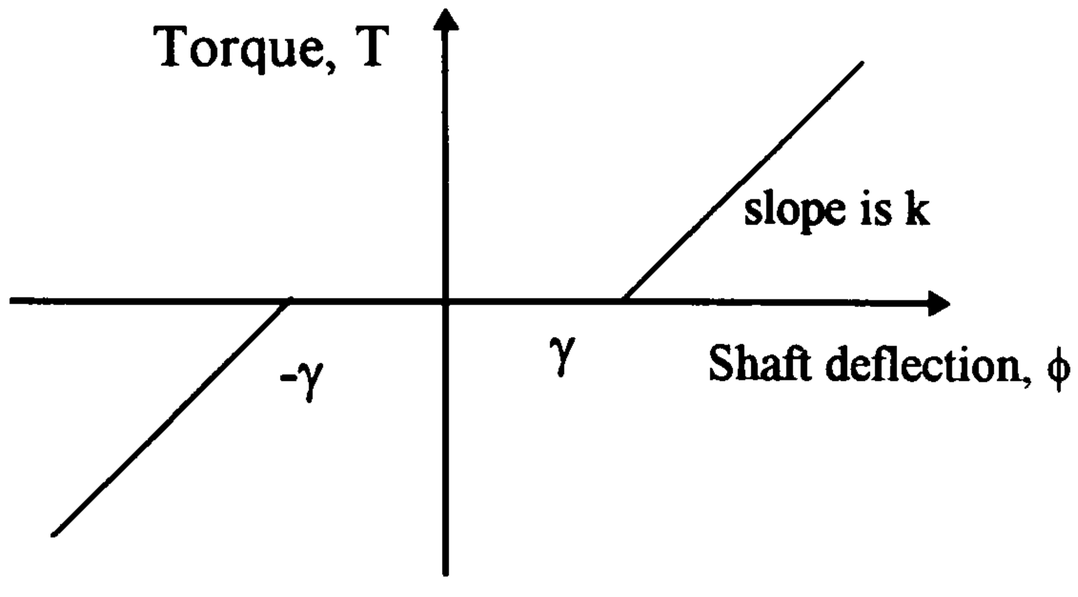

Fig (6.2) Torque characteristic of a shaft with backlash

This model has a backlash/free play of $\pm\gamma$ rad and therefore has non-linear characteristics such that its torsional rigidity is zero when its angular displacement lies between $\pm\gamma$ but is k when its angular displacement is outside that range [2].

The characteristics of the backlash can be represented mathematically by;

$$\begin{aligned} T &= 0 && -\gamma \le \phi \le \gamma \\ T &= k(\phi - \gamma) && \text{elsewere} \end{aligned} \qquad (6.2)$$

where

T is the transmitted torque,

γ is the angular backlash in the system, and

$\phi = (\phi_1 - \phi_2)$ is the twist of the spline shaft.

For clarification, assume there is a constant mean driving torque imposed on the driveline, then normal operation will occur on the right-hand slope of this characteristic and for small amplitude fluctuations about this mean the system will be linear. Obviously, if during vibration $(\phi_1 - \phi_2)$ falls below γ, then the behaviour is non-linear and the shaft torque suddenly drops to zero until $(\phi_1 - \phi_2)$ reaches $-\gamma$ when the shaft again operates as a torsional spring [8]. If non-linear operation occurs then the actual behaviour is more complicated than that shown in Fig (6.2) because severe impacts occur each time a torque reversal occurs as the teeth or splines re-engage but for simplicity such impacts are ignored in this study.

6.4-EFFECT OF HOOKE'S JOINTS

Hooke's joints are used to connect shafts which are not in line, e.g. the propeller shaft connecting the engine gearbox to the back axle of the vehicle driveline system typically has a Hooke's joint at each end, see section 2.6. As mentioned before, the Hooke's joint is not a constant-velocity device, that means, when the input shaft rotates with a constant angular velocity, the output shaft is subjected to the angular velocity fluctuation, see Fig (2.7). Similarly, there is a fluctuating relationship between the transmission torques of the input and output shafts. Even for small angles, the high speeds common on modern vehicles can result in unacceptable vibration and noise, Fig (6.3).

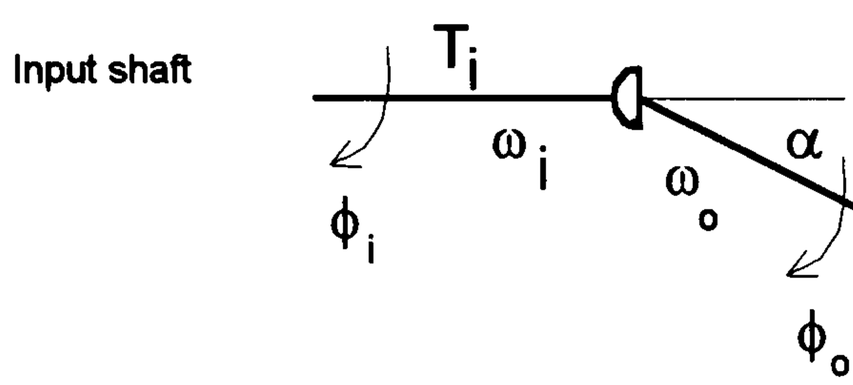

Fig (6.3) Hooke's joint representation

The angular velocity ratio of the output shaft (ω_o) and input shaft (ω_i) is described by Eqn (2.15);

$$\frac{\omega_o}{\omega_i} = \frac{\cos\alpha}{1 - \sin^2\alpha \ \sin^2\phi_i} \tag{6.3}$$

where

α is the Hooke's joint angle,

ϕ_i is the angular displacement of the input shaft, $\phi_i = \omega_i t$,

ω_i is the angular velocity of the input shaft, and

ω_o is the angular velocity of the output shaft.

The practical effect of a Hooke's joint between shafts is equivalent to a gearbox connecting shafts where the gear ratio varies sinusidally with input rotation and, therefore, input and output shafts can be replaced by a dynamically equivalent system.

However, this representation makes the model complicated because the model in this study is based on lumped masses. Assuming the mass moment of inertia of the joints is relatively large compared to the propeller shaft, the system considered as an elastic massless shaft between two mass moment of inertias excited by fluctuating torques provided by the joints acting at the ends of the propeller shaft.

For a single Hooke's joint, the amplitude of the torsional fluctuation acceleration of the output shaft is [50];

$$\ddot{\phi}_o(t) = \omega_i^2 (2a \sin 2\phi_i + 2a^2 \sin 4\phi_i) \tag{6.4}$$

where 'a' is a constant depending on the joint angle α,

$$a = \frac{\sin^2 \alpha}{2 - \sin^2 \alpha} \tag{6.5}$$

From Eqn (6.4), the value of a is always less than 1, and is less than 0.15 for the practical range of values of α, i.e. up to about $\alpha=30^o$.

The magnitude of the fluctuating acceleration is $\pm 2\omega_i^2 a$ for the 2nd order component, and $\pm 2\omega_i^2 a^2$ for the 4th order component, so that even for an angle as large as $\alpha = 30^o$, the 4th order component is less than 15% of the 2nd order component. There are also disturbances of the 6th, 8th, etc., orders but amplitudes of these components tend to be insignificant.

The vibratory torque associated with the Hooke's joint, $T(\phi)$, is $J\ddot{\phi}_o$ where J is the mass moment of inertia of the output shaft and joint assuming that the input shaft speed is constant. Thus the fluctuation torque induced by Hooke's joint in terms of the angular displacement is;

$$T(\phi) = J\omega_i^2 (2a \sin 2\phi_i + 2a^2 \sin 4\phi_i) \tag{6.6}$$

Therefore, the effect of Hooke's joints is to impose a non-linear excitation torque dominated by a frequency of twice shaft speed on to the output shaft.

Two Hooke's joints can be combined in such away that one joint balances the fluctuation of the other to produce a constant velocity ratio between input and output and hence constant torque, but the intermediate shaft (propeller shaft) still continues to fluctuate [57]. Due to these fluctuations any resonance of the driveline system may be excited. The advantage of confining the irregular motion to the propeller shaft is that this member can be made light and stiff so that vibratory torque due to its periodic acceleration is minimised.

6.5-Clutch Friction Torque

An another non-linear excitation source is the friction torque induced from clutch during the engagement. Since this only affect the system intermittently i.e. during clutch operation, it is discussed separately in chapter 7.

6.6-Mathematical Model

The same mathematical model of the driveline system used in chapter 5, is modified here to include the non-linear components.

The equations of motion which describes the torsional vibration of this model are;

$$[M]\{\ddot{\phi}\}+[C]\{\dot{\phi}\}+[K]\{\phi\}=\{T(t)\}+\{H(\phi)\}+\{M_f(\phi)\} \qquad (6.7)$$

where [M], [C] and [K] are mass, damping and stiffness matrices of the system respectively and $\{\phi\}$ is the angular displacement vector.

$\{T(t)\}$ is the excitation torque vector emanating from the engine, see chapter 3;

$$T(t)\} = \{0 \quad T_1(t).... \quad T_i(t).... \quad T_j(t) \quad ...0\}^T$$

where $T_i(t)$ is the linear periodic excitation torque due to reciprocating inertia and gas forces from a cylinder i and j is the number of engine cylinders. Eight harmonic terms have been considered in this analysis.

$\{H(\phi)\}$ is the non-linear fluctuating torque vector from Hooke's joints, Eqn (6.6).

$$H_i(\phi) = J_i \ddot{\phi}_{oi}(t)$$

where J_i and ϕ_i are the mass moment of inertia and angular acceleration of the joint i respectively, i= 10 or 11, i.e.;

$$\{H(\phi)\} = \{0.... \quad H_{10}(\phi) \quad H_{11}(\phi) \quad ....0\}^T$$

$M_f(\phi)$ is the friction torque induced from the friction clutch only during clutch engagement. A detailed study of this torque is introduced in chapter 7.

Fig (6.4) shows the idealisation of the driveline system as a set of inertia discs linked by torsional massless springs.

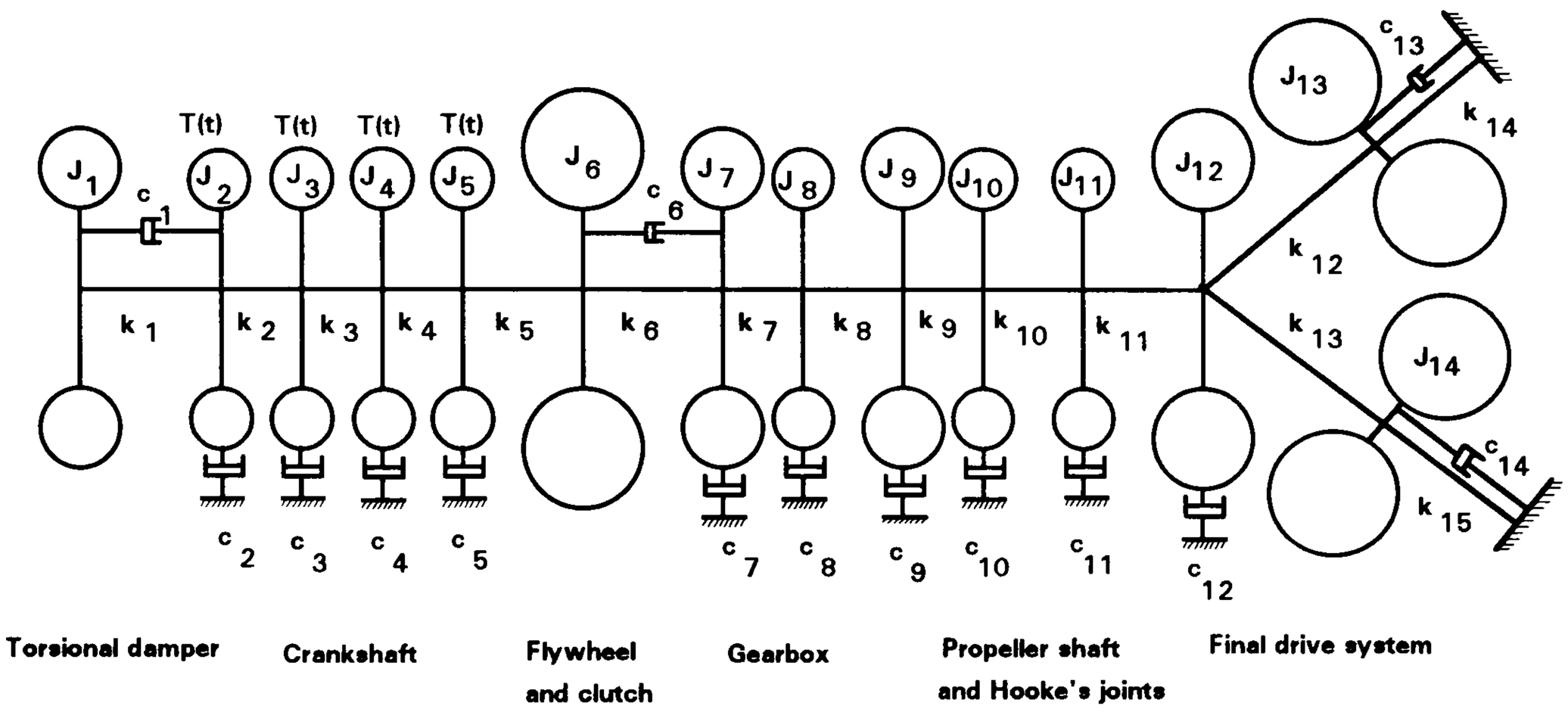

Fig (6.4) Vehicle driveline system mathematical model

6.7-NUMERICAL DATA AND SOLUTION

Two approaches to solving the non-linear differential equations are possible; (i) use a standard computer package e.g. MATLAB which is restricted to the number of numerical integration routines available. (ii) write a purpose-designed program to deal with the particular problem and , therefore, optimise the integrator for this particular type of problem. A purpose-designed FORTRAN program has been developed to

integrate the system equation of motion because the MATLAB routines are relatively slow.

The Runge-Kutta numerical method has been used to integrate the non-linear differential equations of motion (6.7) with respect to the time to obtain the time response of the system for values of different parameters. Eqn (6.7) was transferred into a first order form by defining two (nx1) vectors $\{y_1\} = \{\phi\}$ and $\{y_2\} = \{\dot{\phi}\}$, where $\{y_1\}$ is the displacement vector and $\{y_2\}$is the velocity vector. Differentiating these two vectors yields;

$$\{\dot{y}_1\} = \{\dot{\phi}\} = \{y_2\} \qquad \text{and}$$

$$\{\dot{y}_2\} = \{\ddot{\phi}\}$$

The equation of motion can be recognised as first-order vector differential equations ;

$$\begin{Bmatrix} \dot{y}_1 \\ \dot{y}_2 \end{Bmatrix} = \begin{Bmatrix} \{y_2\} \\ M^{-1}(\{T(t)\} + \{H(y)\} + \{M_f(y)\} - [K]\{y_1\} - [C]\{y_2\}) \end{Bmatrix} \qquad (6.8)$$

with initial conditions $\begin{Bmatrix} y_1(o) \\ y_2(o) \end{Bmatrix} = \begin{Bmatrix} \phi_o \\ \dot{\phi}_o \end{Bmatrix}$

Eqn (6.8) is a first-order differential matrix equation which can be solved numerically to find the response vector $\{y(t)\}$. Here $\{y(t)\}$ is the (2nx1) state vector, where the first (nx1) elements correspond to the displacement vector, $\{\phi(t)\}$, and the second (nx1) elements correspond to the velocity vector, $\{\dot{\phi}(t)\}$.

The fluctuating velocity and displacement at points of interest in the driveline system were plotted versus time using a typical numerical data. The typical numerical values of the equivalent system parameters were those quoted in chapter 5, Table (5.1). However, the values of the stiffnesses of the non-linear elements, such as the torsional spring stiffness of the clutch and the torsional stiffness of the tyre, were assumed to increase as angular displacement (twist) increases from constant value, k_o, (linear value) up to four times of the constant value.

Backlash in the input and output of the propeller shaft splines was taken to represent a typical example of existing backlash in the system. Three discretized values of the backlash were used in the numerical computations. These values were 0 (no backlash), 0.02 and 0.05 rad.

The Hooke's joints angle were changed through three values, 0^o,15^o and 30^o to investigate the effect of the fluctuating torque emanating from non constant velocity joints on the system behaviour.

As the driveline system, under normal conditions, runs at essentially constant speed, the excitation torque emanating from the engine is retained as the unique linear source of the driveline excitation during this analysis. This fluctuating torque was obtained at a particular engine speed, see chapter 3,. The effect of the friction torque due to clutch engagement was not included here since the clutch does not slip during normal running conditions.

6.8-RESULTS AND DISCUSSION

Results were generated for the time history responses of the system due to engine forcing and an attempt made to investigate the system sensitivity to several key design parameters.

Figs (6.5) to (6.12) show the system time responses at the gearbox input and the rear wheels (driving wheels in the model). Torsional vibrations of gearbox input are assumed to be related to a measure of the noise level of the gearbox. The torsional vibrations of the driving wheels are related to a measure of the longitudinal vibration of the vehicle body.

The individual effect of the non-linearity of the clutch spring stiffness is shown in Figs (6.5) and (6.6). From these figures, there is no significant effect on the system behaviour due to non-linearity of the clutch spring stiffness within the considered range of the torsional stiffness of the clutch spring (four times of the basic value, k_{oi}, Fig (6.1b)).

Figs (6.7) and (6.8) show the effect of the tyre torsional stiffness non-linearity on the system torsional behaviour at the gearbox input and the driving wheels. Again, from these curves, there is no significant effect on the system behaviour due to the non-linearity of the torsional tyre stiffness. The non-significant effect of the non-linearity of the torsional stiffness of the clutch spring and tyre may be because these values are relatively small compared to the torsional stiffness values of the other components of the driveline system.

Because the constant natural frequencies and mode shapes only exist for linear system, the non-linearity of the torsional stiffness of the clutch spring and the tyre cause change of the effective natural frequencies of the system but this can not be seen in the time response. This change of the effective natural frequencies depends on the vibration torque.

The significant effect of the backlash of the propeller shaft splines on the system behaviour is shown in Figs (6.9) and (6.10). From these figures, the fluctuations of the driveline vibrations increase as the backlash of the propeller shaft splines increases.

Figs (6.10) and (6.12) show the effects of the system fluctuation due to the excitation torque of the Hooke's joints at different values of the joint's angles. From these figures, it is clear that the vibration level of the driveline increases as the Hooke's joints angle increase and it becomes sever when the joint angle exceeded 15^{o}. Increasing the vibration level with the angularity refereed to joints fluctuating torque that becomes more pronounced with the large angularity of the joints. However this torque may be sever also at any joint angle when it excites any resonance of the driveline system.

In general these results confirm the findings from the linear model and provide additional information to the system behaviour, see chapter 5.

6.9- SUMMARY

1. A mathematical model of a vehicle driveline system including the important non-linear effects such as; backlash, non-linear spring stiffness, Hooke's joint and angularity of the propeller shaft was developed.

2. The effect of backlash in the driveline system on the system torsional vibration levels is significant and, as expected, vibration levels increase as backlash increases.

3. Hooke's joints in the driveline system were found to cause additional torsional vibration, however at the considered engine speed this vibration only became severe if the joint angle exceeded 15^{o}.

4. The developed computer program may be used as a design tool to investigate the torsional vibrations of vehicle driveline systems including the effect of non-linear components.

5. The predicted results can be used to quantify the relative effects of different non-linearities and to rank their relative effects from a design viewpoint.

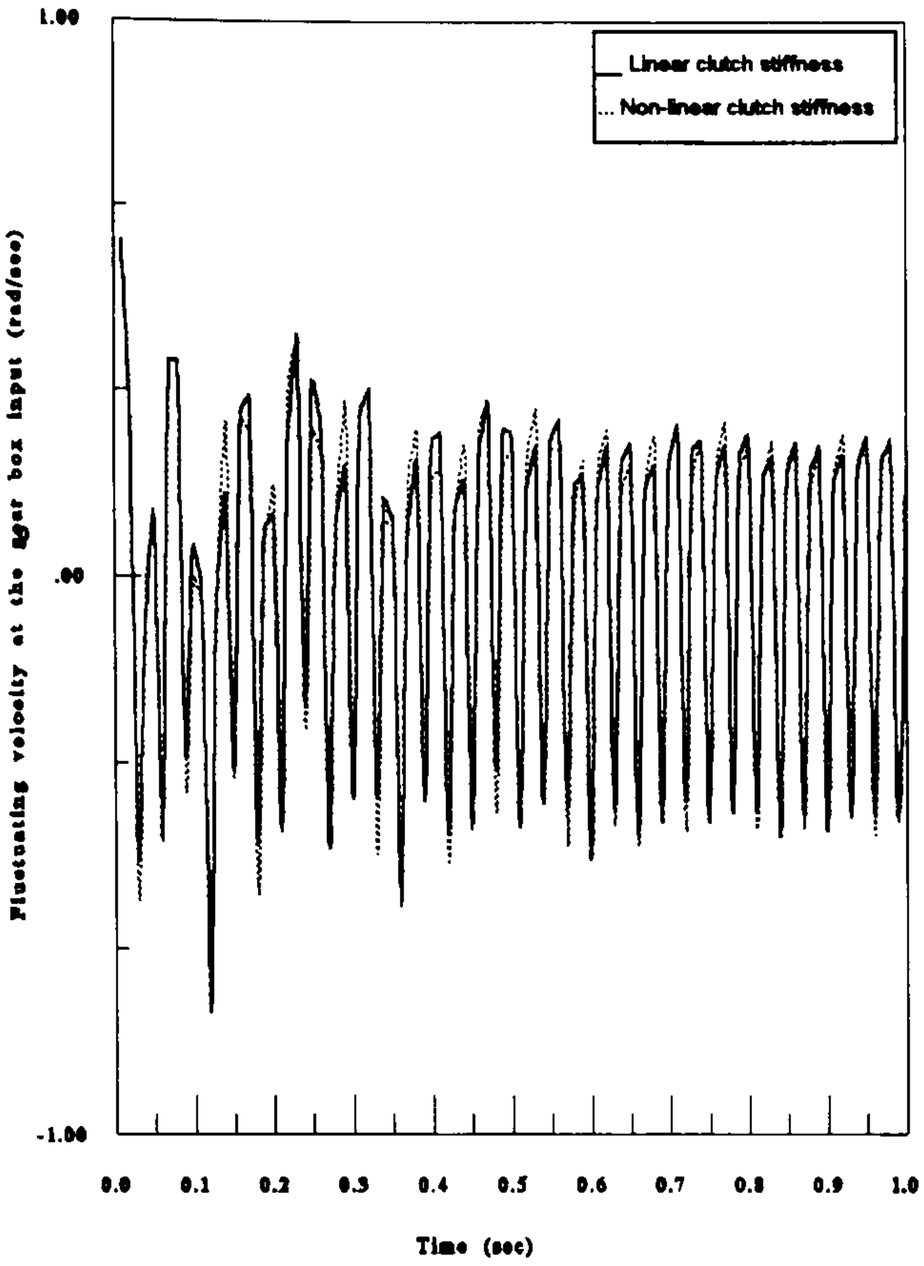

Fig (6.5) Effect of the clutch spring non-linearity on the gearbox input

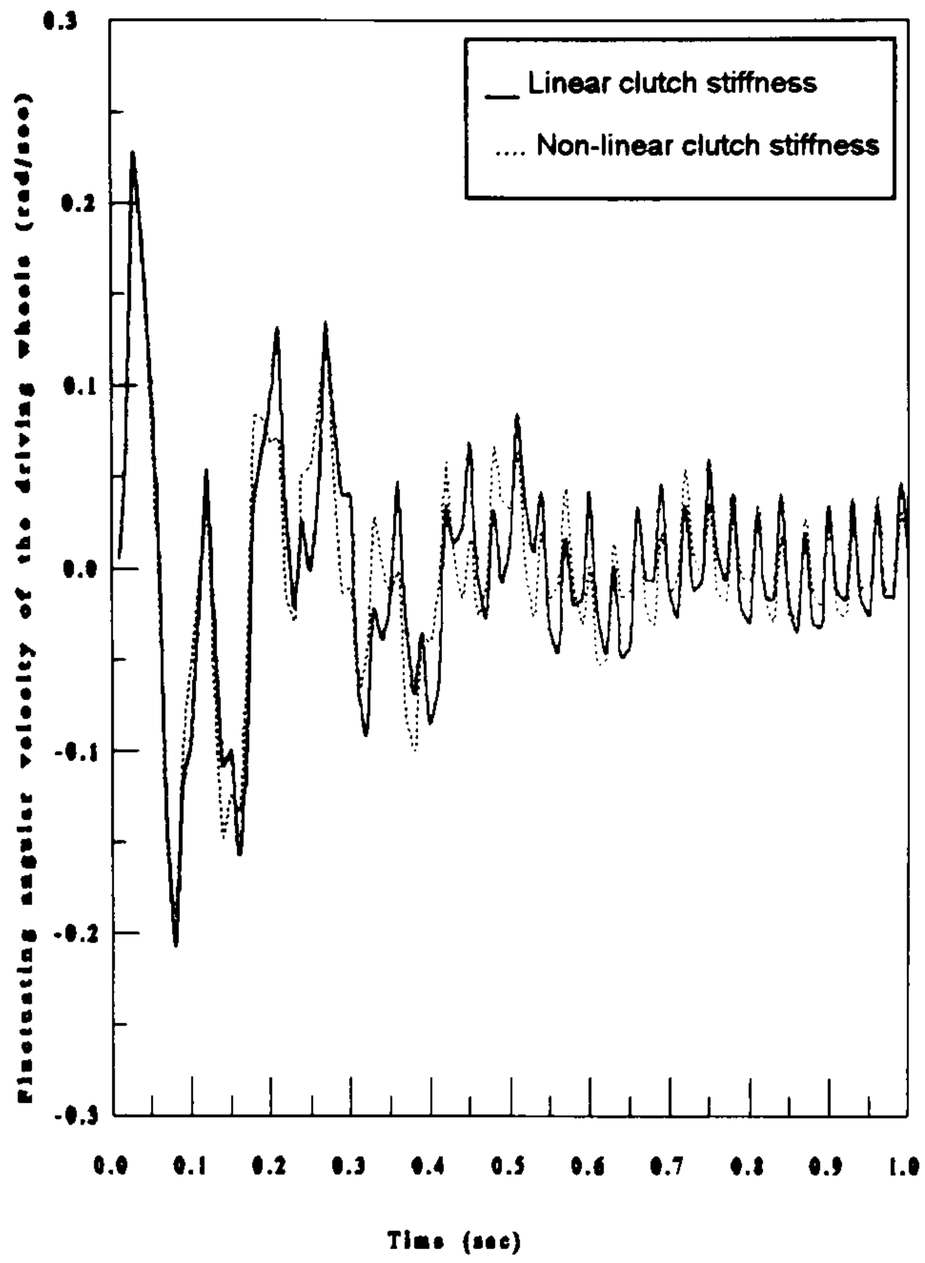

Fig (6.6) Effect of the clutch spring non-linearity on the driving wheels

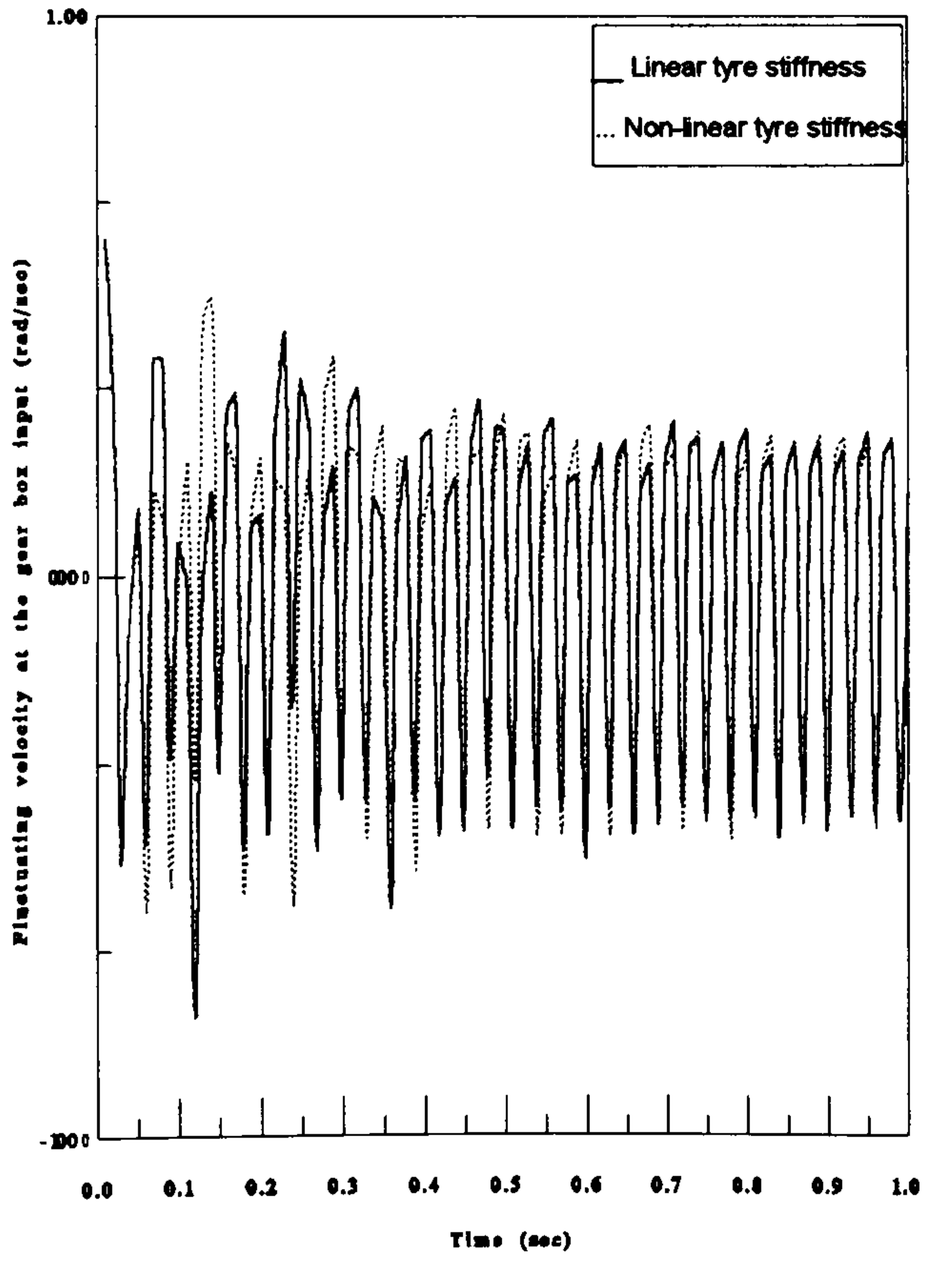

Fig (6.7) Effect of the tyre stiffness non-linearity on the gearbox input

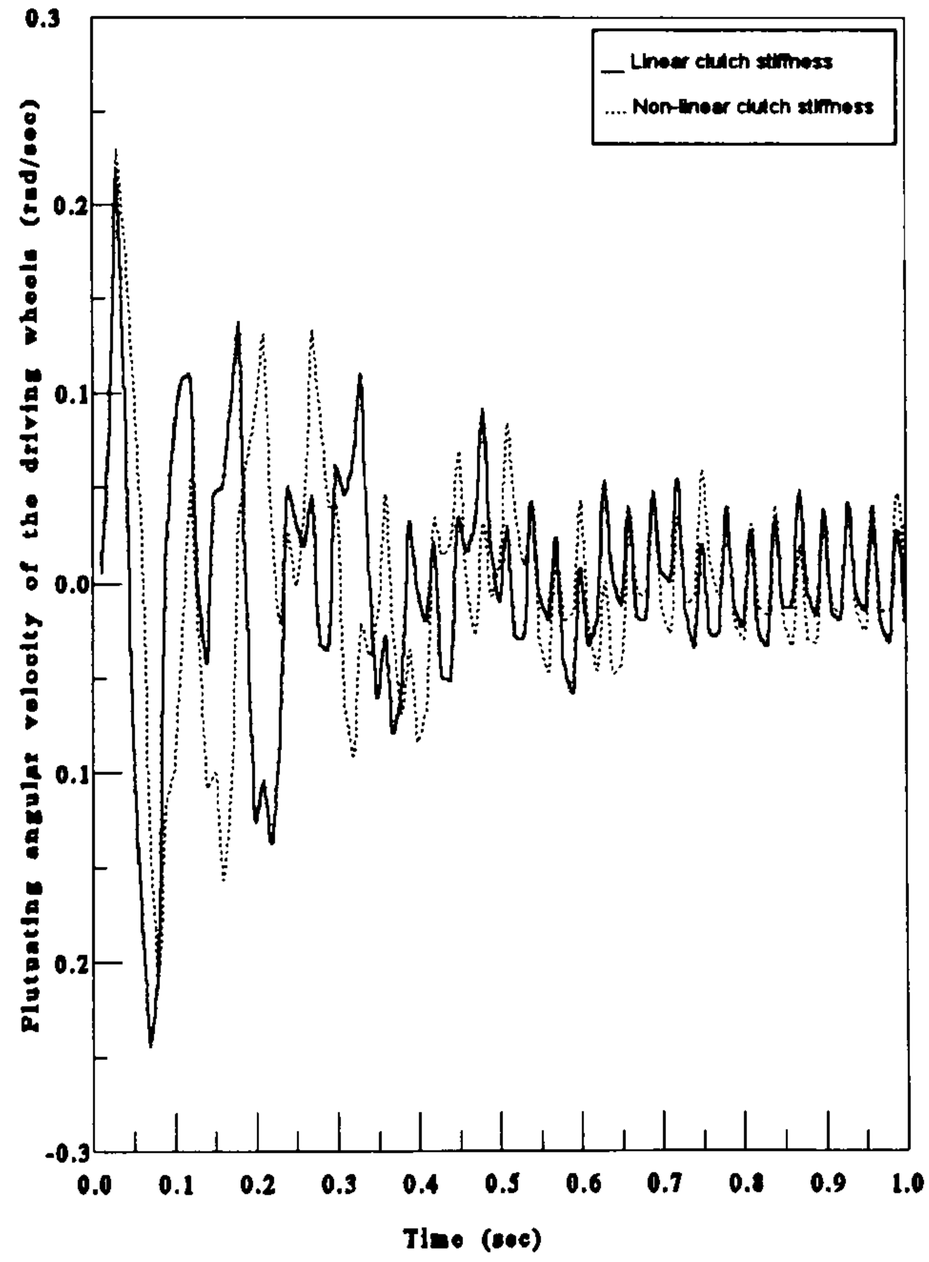

Fig (6.8) Effect of the tyre stiffness non-linearity on the driving wheels

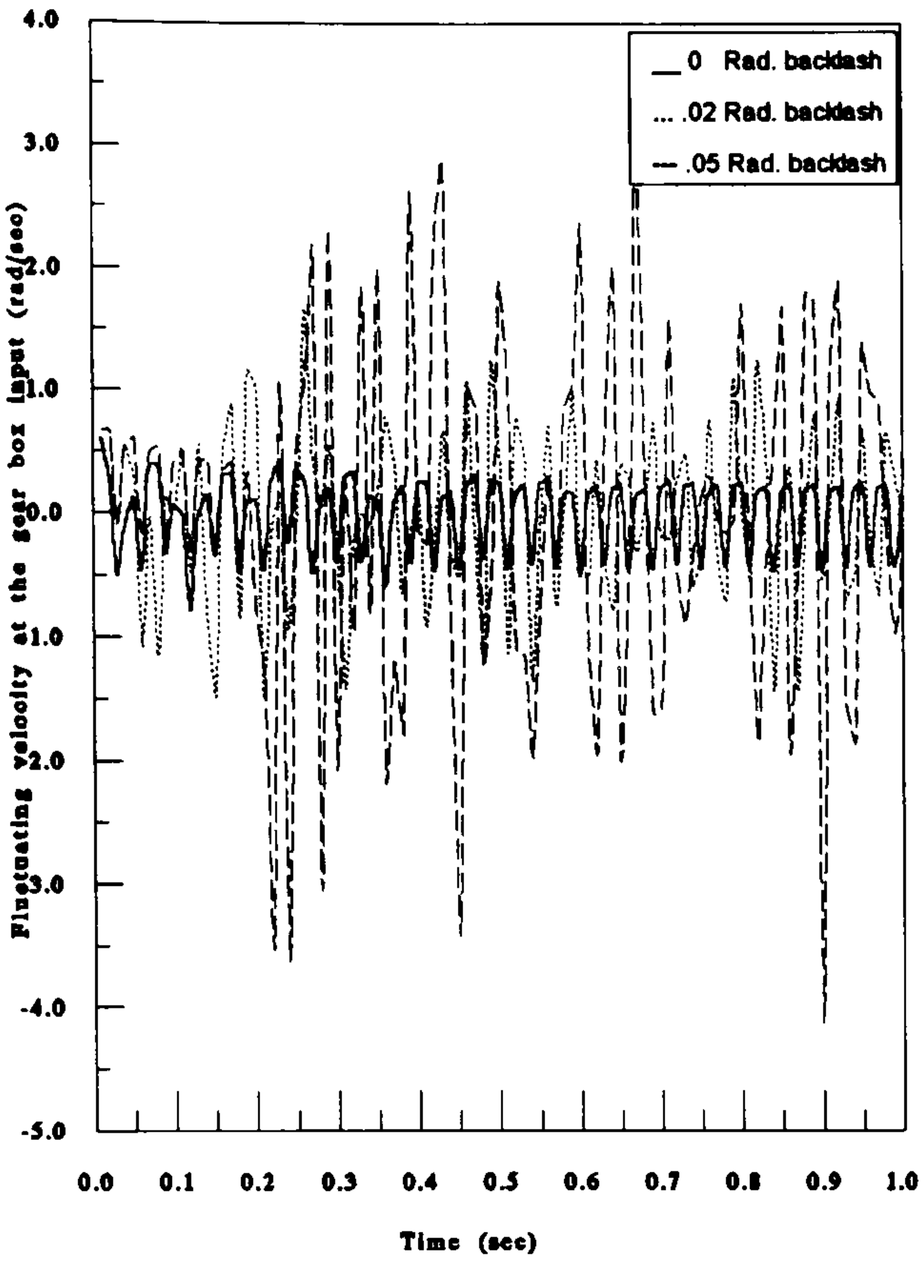

Fig (6.9) Effect of the backlash in the spline on the gearbox input

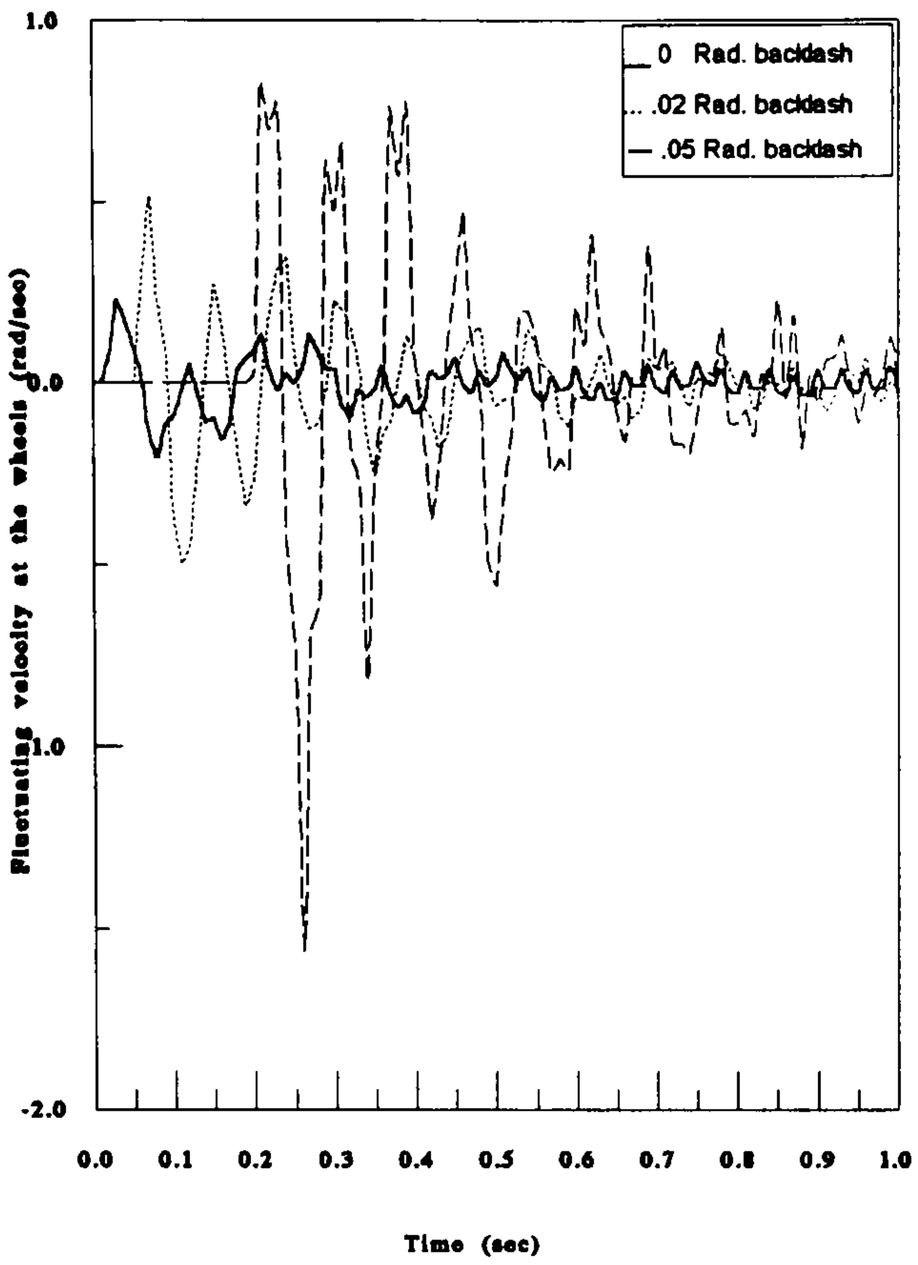

Fig (6.10) Effect of the backlash in the splines on the driving wheels

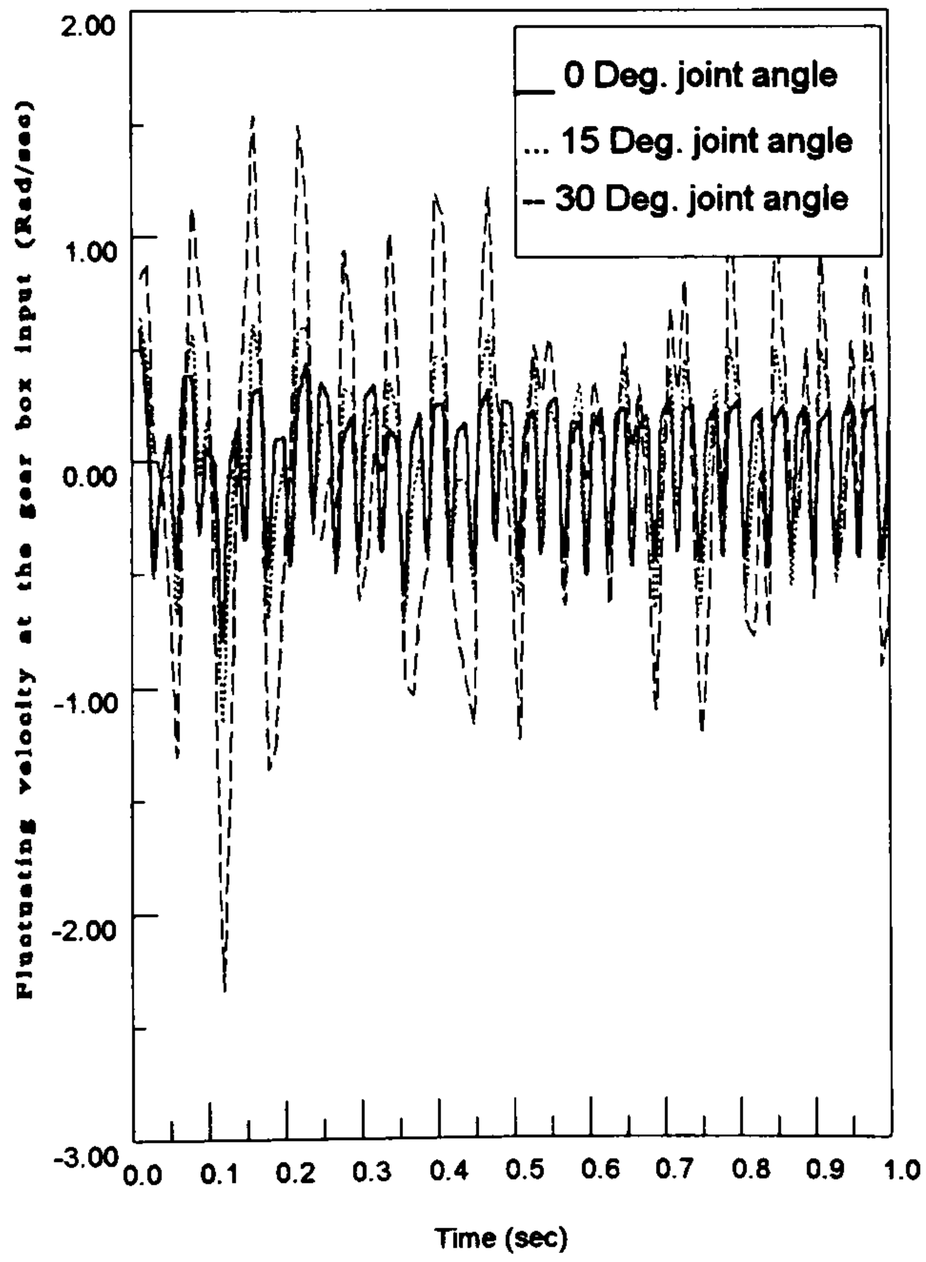

Fig (6.11) Effect of the Hooke's joint angle on the gearbox input

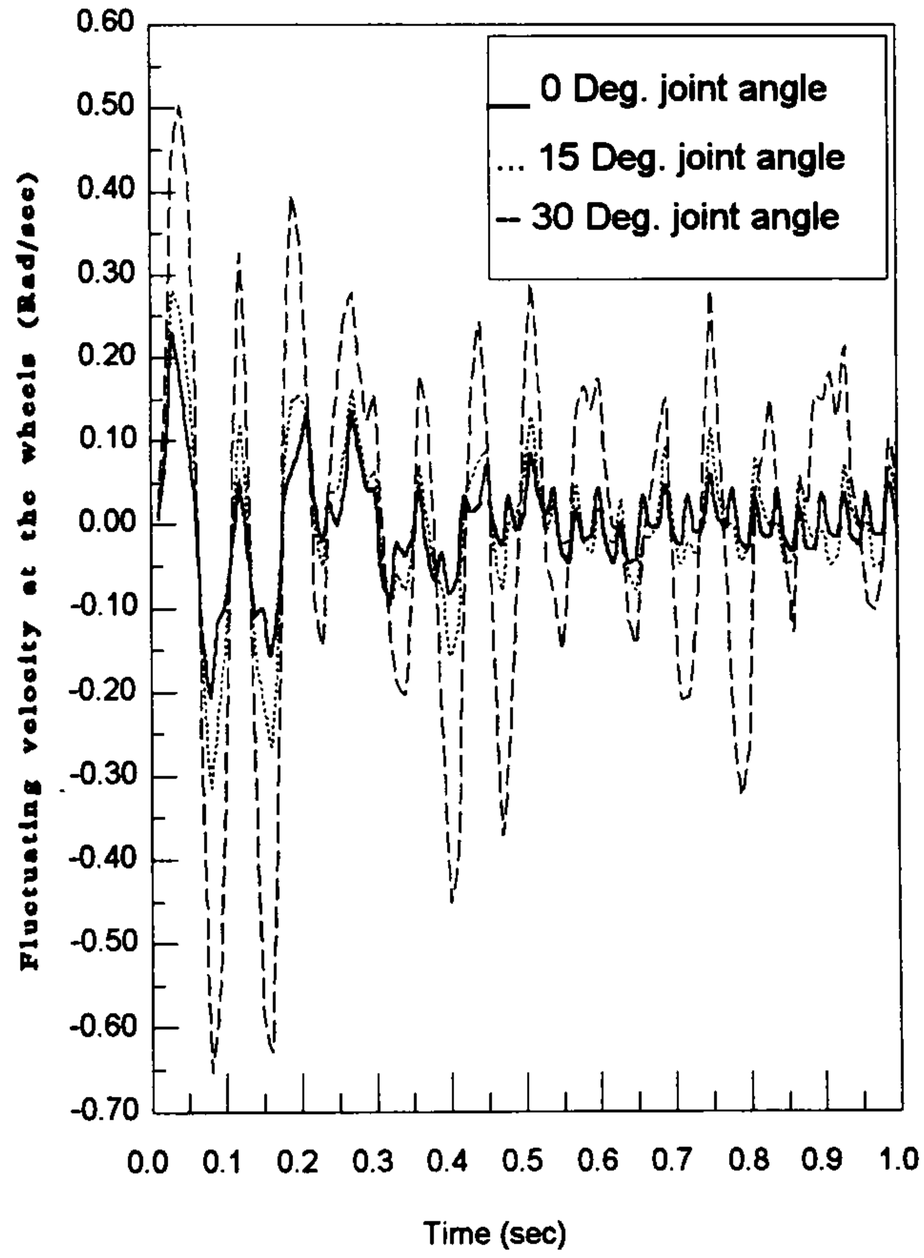

Fig (6.12) Effect of the Hooke's joint angle on the driving wheels

CHAPTER 7

DRIVELINE SYSTEM BEHAVIOUR DURING CLUTCH ENGAGEMENT

7.1-INTRODUCTION

One of the most important sources of torsional vibration of vehicle driveline systems is during clutch engagement in manual gearbox systems. The study of torsional vibrations of vehicle driveline systems during clutch engagement is quite complex and it is not well covered in the literature, although, there have been several attempts to explore various aspects of the engagement problem, see chapter 1.

For every configuration of driveline systems there are two common factors with all manual shift systems; namely, the dry friction clutch and human operator. Both play an important part in the torsional vibration of driveline systems. Human behaviour cannot be predicted precisely but can often be generalised for a particular event and set of given conditions. Hence, this chapter concentrates on the torsional vibration behaviour of driveline systems during the engagement of the dry friction clutch.

A manual transmission vehicle with a friction clutch may generate an unwanted vibration in the longitudinal direction of the vehicle when starting the vehicle or shifting the gear because torsional vibration develops in the driveline system to an unacceptable level; this phenomenon is called *shunt* or *shuffle*. It is felt by the passenger as fore-aft vibration of the vehicle body. An extreme shunt referred to as the 'Kangaroo start' is commonly experienced by learner drivers following a severe clutch engagement. In some cases when this vibration is extreme, it may result in vehicle stall. However, it is the former shunt and shuffle conditions which influence refinement that are of main concern here.

Shunt, as defined in literature, is the first torsional vibration mode of the driveline system of a vehicle. This oscillation can be excited by any torsional perturbation in the driveline system due to, for example, engine throttle, *clutch judder* or road disturbances. *Clutch judder* is probably one of the most important issues associated with the shunt phenomenon and harshness complaints.

Clutch judder can be explained as the self-excited vibration generated by the speed characteristics of frictional force during clutch engagement. This phenomenon is often

due to the stick-slip phenomenon caused by the difference between static and dynamic friction forces or the negative slope of the friction force vs. sliding velocity curve. It is an additional source of torsional vibration of the driveline system of a vehicle. It is sensed partly by its noise and partly by feel. Controlling the shunt and the judder phenomena to subjectively acceptable levels results in a vehicle which is inherently easy to drive and is rated highly by both the driver and passengers.

The aims of the study described here are; (i) to model the torsional vibration of the entire driveline system during clutch engagement (ii) to investigate the effect of various design parameters on the engagement problem phenomena (iii) to analyse whether driveline problems could be avoided by clutch modulation strategies.

7.2-MATHEMATICAL MODELLING

The driveline system associated with a vehicle which may suffer from clutch judder is shown diagrammatically in Fig (7.1). This model is a modification of simple models described in previous publications, see chapter 1. It incorporates important features in comparison with other models, for example, dynamic characteristics of the driveline system components, introduction of the clamping load and the mean sliding speed as time dependent functions. This dynamic model is similar to that used in previous torsional analysis which basically idealises the driveline system as a set of inertia discs linked together by torsional, massless springs.

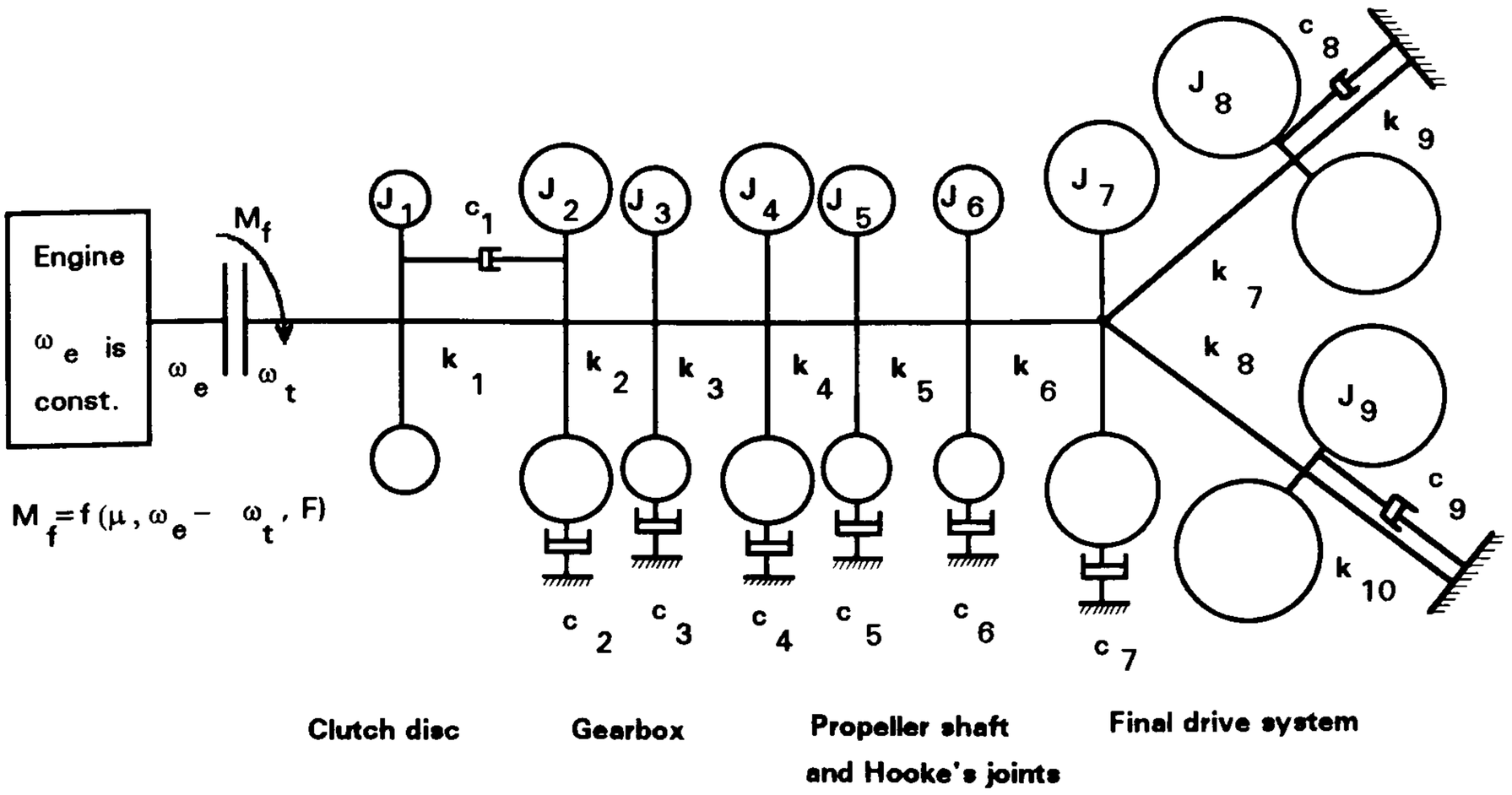

Fig (7.1) Model of the driveline system during clutch engagement

In this model, the input torque and speed from the engine are assumed constant and a fluctuating friction torque acts as the source of excitation of the system's torsional vibration during the clutch engagement. The typical numerical values of the equivalent system parameters, used in previous chapters, Table (7.1), were used here.

Table (7.1) Typical data of equivalent parameters of a vehicle driveline system (nominal values)

Equivalent stiffness (N/m or Nm/rad)		Equivalent mass and moment of inertia (kg or kg m^2)		Equivalent system damping (N.s/m or N.m s/rad)	
Parameter	value	Parameter	value	Parameter	value
k_1	0.05×10^6	J_1	0.01	c_1	4.42
k_2	2×10^6	J_2	0.05	c_2	1
k_3	1×10^6	J_3	0.03	c_3	1
k_4	0.1×10^6	J_4	0.05	c_4	1
k_5	0.1×10^6	J_5	0.02	c_5	1.8
k_6	0.2×10^6	J_6	0.02	c_6	1.8
k_7	0.5×10^4	J_7	0.3	c_7	2
k_8	0.5×10^4	J_8	2	c_8	10
k_9	0.2×10^4	J_9	2	c_9	10
k_{10}	0.2×10^4				

The equations of motion which describe the torsional vibration of this model are;

$$[M]\{\ddot{\phi}\} + [C]\{\dot{\phi}\} + [K]\{\phi\} = \{M_f(\phi)\} \qquad (7.1)$$

where [M], [C] and [K] are mass/inertia, damping and stiffness matrices of the model respectively and $M_f(\phi)$ is the friction torque which is defined as $2Fr\mu(\phi)$ where F is the time dependent clamping force, r is the friction radius of the clutch, ϕ is the angular displacement of the torsional vibration of the system and $\mu(\phi)$ is the coefficient of friction between the friction plates which depends on the characteristics of the friction and mating material properties.

7.2.1-Friction Coefficient

Various mathematical expressions have been used to represent the friction coefficient. The method suggested by Heap, see [28] considers that the friction coefficient is a function of the clamping force, temperature and the sliding speed as follows;

$$\mu(F,T,v) = \mu_o \frac{\mu(F).\mu(T).\mu(v)}{\mu_f \mu_t \mu_v} \tag{7.2}$$

where $\mu(F)$, $\mu(T)$ and $\mu(v)$ are functions describing the variation of coefficient of friction with clamping force, temperature and sliding speed respectively, each applying when the other two variables remain constant. μ_f, μ_t and μ_v are the normalised coefficients of friction at a reference condition and μ_o is the static friction coefficient.

Since the judder is significantly related to the μ-v characteristic of the friction material [31] this study concentrates on the variation of the friction coefficient as a function of sliding speed, v, only i.e.;

$$\mu = A_o + A_1 v + A_2 v^2 \tag{7.3}$$

The sliding speed, v, is the difference between the engine speed and the transmission speed. The angular engine speed is assumed to be constant, ω_e, and the angular transmission speed will be assumed as a steady state value, ω_t, with a perturbation value, ϕ, superimposed upon it i.e.;

$$v = r[\omega_e - (\omega_t + \dot{\phi})] = r(\omega - \dot{\phi}) \tag{7.4}$$

where $\omega=\omega_e - \omega_t$ is the mean sliding speed, and Eqn (7.3) therefore leads to;

$$\mu(\phi) = A_o + A_1 r(\omega - \dot{\phi}) + A_2 r^2 (\omega - \dot{\phi})^2 \tag{7.5}$$

Thus the friction torque in terms of angular perturbation is;

$$M_f(\phi) = 2Fr\left[A_o + A_1 r(\omega - \dot{\phi}) + A_2 r^2 (\omega - \dot{\phi})^2\right] \tag{7.6}$$

7.2.2-Engagement Rate

The value of the maximum clamping force is related to the maximum torque to be transmitted by the clutch but this force can be applied at different rates. Low loading rates can cause very slow engagements which may overheat the clutch. On the other hand, high loading rates cause fast engagements that could overload and stall the

engine or, if the engine is resistant enough, cause the vehicle to lurch. Knowing this, the ideal operator would select the optimal loading rate which would ensure minimum engagement time but not stall the engine or lurch the vehicle. The no-stall condition for the engine indicates that the clutch must lock-up when the engine torque is large enough to exceed the resisting torques. The no-lurch condition for the vehicle is determined by the maximum vehicle acceleration characterised by the lurch coefficient (typically ≤ 0.14 g). The fastest possible engagement must satisfy these two conditions simultaneously.

Suggested relationships for the clamping force, F, and the mean sliding speed, ω, with the time can be described as shown in Figs (7.2), where t_c is the engagement time and F_o is the maximum clamping force. The mean sliding speed decreases continuously during the engagement period from engine speed, ω_e , at the start of engagement to zero at complete engagement where the clamping force is maximum. For simplicity, linear reduction in the mean sliding speed is assumed. The mathematical expressions for the clamping force and the mean sliding speed are;

$$\left.\begin{aligned} F(t) &= F_o(t/t_c) \qquad \text{and} \\ \omega(t) &= \omega_e(1-t/t_c) \end{aligned}\right\} \tag{7.7}$$

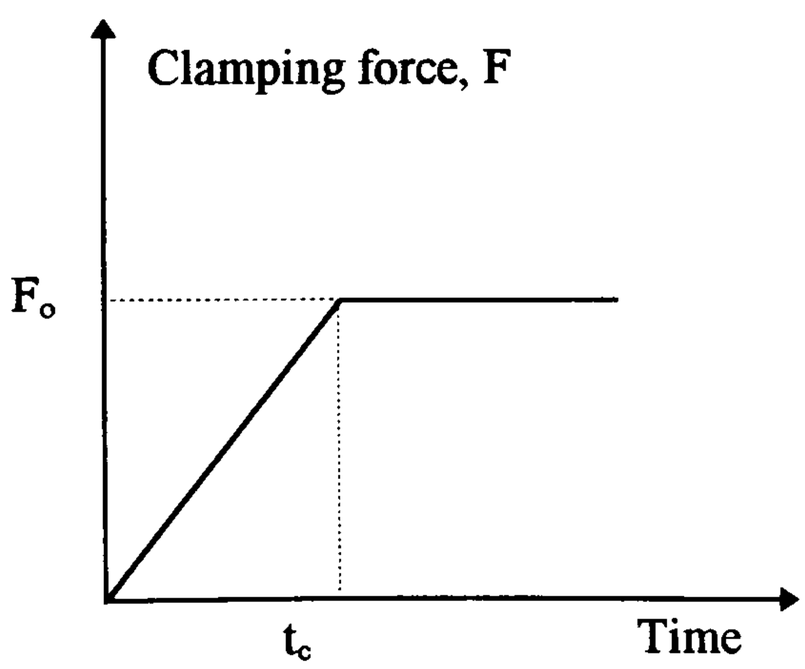

Fig. (7.2-a) Clamping force model

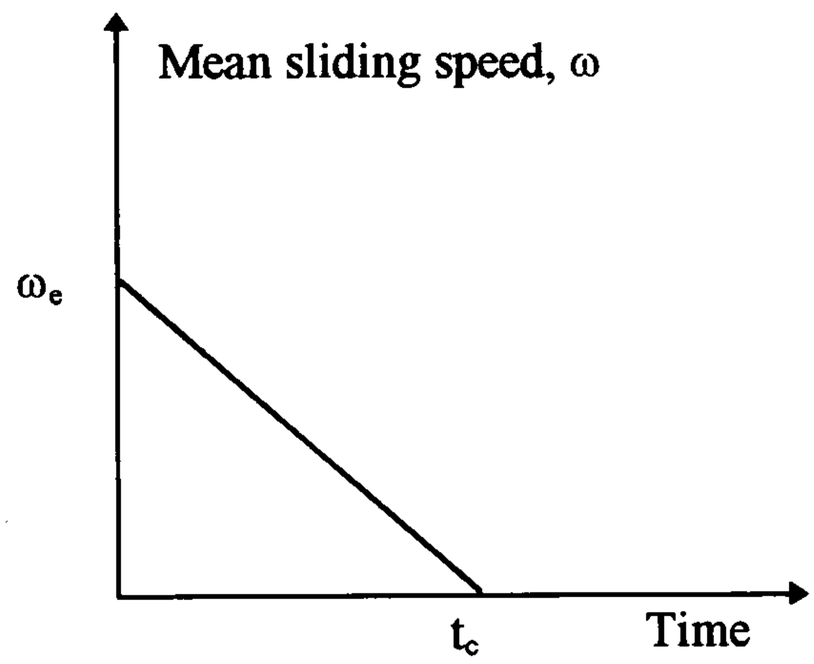

Fig. (7.2-b) Mean sliding speed model

Substituting the expression for the friction torque, Eqn (7.6), in the equation of motion, (7.1) gives;

$$[M]\{\ddot{\phi}\}+[C]\{\dot{\phi}\}+[K]\{\phi\} = \{B_o\}+[B_1]\{\dot{\phi}\}+[B_2]\{\dot{\phi}^2\} \tag{7.8}$$

where;

$$\left.\begin{aligned} B_o(1) &= 2Fr(A_o + \omega r A_1 + \omega^2 r^2 A_2) \\ B_1(1,1) &= -2Fr^2(A_1 + 2\omega r A_2) \\ B_2(1,1) &= 2Fr^3 A_2 \end{aligned}\right\} \qquad (7.9)$$

and the other values of elements of the matrices $[B_o],[B_1]$ and $[B_2]$ are zeros.

The gradient of friction coefficient is assumed to be constant with respect to the sliding speed i.e.; A_2 =0 in Eqn (7.9) leads to;

$$\left.\begin{aligned} B_o(1) &= 2Fr(A_o + \omega r A_1) \\ B_1(1,1) &= -2Fr^2 A_1 \\ B_2(1,1) &= 0 \end{aligned}\right\} \qquad (7.10)$$

7.2.3-Stability Analysis

From Eqns (7.8) and (7.10), the stability of the driveline system during clutch engagement can be explained as follows; if A_1 is positive, i.e. the value of $(-2Fr^2A_1)$ is negative the system must be stable, while if the value of A_1 is negative, i.e. the value of $(-2Fr^2A_1)$ is positive, the system may be stable or not depending on the value of $(-2Fr^2A_1)$ and the damping level in the system. The value of A_1 represents the gradient of the friction coefficient, so the stability of the driveline system is related to the gradient of the friction coefficient in addition to the clamping force and the system damping. These principles will be discussed in detail in section 7.5.

7.3-Numerical Solution

The Runge-Kutta numerical method has again been used to integrate the non-linear differential equation (7.8) with respect to time to obtain the time response of the system for values of different parameters. Eqn (7.8) was transferred into a first order form by defining two nx1 vectors,

$\{y_1\} = \{\phi\}$ and $\{y_2\} = \{\dot{\phi}\}$, where $\{y_1\}$ is the displacement vector and $\{y_2\}$ is the velocity vector. Differentiating these two vectors yields ;

$\{\dot{y}_1\} = \{\dot{\phi}\} = \{y_2\}$ and

$\{\dot{y}_2\} = \{\ddot{\phi}\}$

The equations of motion can be written as first-order vector differential equations,

$$\begin{Bmatrix} \dot{y}_1 \\ \dot{y}_2 \end{Bmatrix} = \begin{Bmatrix} \{y_2\} \\ M^{-1}\left(\{B_o\} + ([B_1] - [C])\{y_2\} + [B_2]\{y_2^2\} - [K]\{y_1\}\right) \end{Bmatrix} \qquad (7.11)$$

with initial conditions $\begin{Bmatrix} y_1(o) \\ y_2(o) \end{Bmatrix} = \begin{Bmatrix} \phi_o \\ \dot{\phi}_o \end{Bmatrix}$

Eqn (7.11) is a first-order matrix differential equation which can be solved numerically to find the response vector {y(t)}. Here {y(t)} is the (2nx1) state vector, where the first (nx1) elements correspond to the displacement vector, $\{\phi(t)\}$, and the second (nx1) elements to the velocity vector, $\{\dot{\phi}(t)\}$.

The typical numerical values of the system parameters, Table (7.1), were used in the numerical analysis in order to investigate the trends of the design variables. The gradient of friction coefficient and the system damping values have been translated in matrix form. The gradient of friction coefficient, A_1, was varied from +0.05 to -0.45. (s/m). The damping level of the system was varied between 50% and 150% of the baseline value (nominal values). For each damping level (high, medium and low levels) the gradient of friction coefficient was changed from a positive value to a negative value through the considered range (+0.05 to -0.45). To change the clamping force rate, three values of engagement time (1, 0.5 and 0.2 second) with a constant maximum clamping force, 1500 N, were considered. To study the effect of the driving axle stiffness and the clutch stiffness on the system behaviour, the driving axle stiffness was changed from ten times to one tenth of the baseline value. The clutch stiffness was changed from three times to one third of the baseline value. During all

the previous calculations, the mean clutch radius was 84.5 mm and the engine speed was kept constant at 1000 rpm.

The angular velocities of the torsional vibration of the clutch disc and the driving wheels vs. the engagement time have been plotted for different cases, Figs (7.3) to (7.14). The torsional vibration behaviour of the clutch disc was interpreted as a measure of the clutch judder. Because the torque variations at the axle will vary the drive forces at the ground and thus may act directly to generate longitudinal vibrations in the vehicle body, the torsional vibration behaviour of the driving wheels was considered as an indirect measure of the shunt phenomenon.

7.4-Results and Discussion

Generally, the torsional vibration behaviour of the clutch disc and the driving wheels due to the clutch friction torque variation during the engagement is related to the physical parameters of the system, damping and stiffness, gradient of friction coefficient and the loading rate, see Table (7.2) and Figs (7.3) to (7.14).

The system oscillates as a free damped vibratory system for the positive values of the gradient of the friction coefficient as shown in Figs (7.3) and (7.4), while for the negative gradient of the friction coefficient, the system is subjected to self excited vibrations and becomes unstable at certain value of the gradient, as shown in Figs (7.5) and (7.6). This instability occurs at the end of the engagement time. The instability level of the system increases with further increases in the negative value of the gradient of the friction coefficient. This instability happens due to increasing the provided energy by the clutch friction torque and decreasing the dissipated energy by the damping of the system. The system oscillations occur at a frequency equal to the fundamental frequency of the torsional vibration of the system (4.7 Hz) in the stable range. However, in the unstable range, the maximum vibration response is at higher natural frequency of the system, Figs (7.5) and (7.6).

The value of the negative gradient that causes the clutch judder (instability of the clutch disc) is less than that which causes the shunt phenomenon (instability of the

driving wheels), see Table (7.2). The negative value of the gradient which causes instability depends on the system damping level, Table (7.2) and Figs (7.7) and (7.8) , the rate of the clamping load, Figs (7.9) and (7.10), the axle shaft stiffness, Figs (7.11) and (7.12), and the clutch spring stiffness, Figs (7.13) and (7.14).

Table (7.2) Gradient of friction coefficient (A_1) that causes driveline instability

Damping Level	High damping		Medium damping		Low damping	
	Clutch disc	Driving wheels	Clutch disc	Driving wheels	Clutch disc	Driving wheels
Values of A_1	-0.53	-0.57	-0.37	-0.42	-0.23	-0.26

Figs (7.7) and (7.8) show that the clutch disc and the driving wheels are subjected to torsional instability at low system damping particularly at the end of the engagement time. Figs (7.9) and (7.10) show that the angular oscillation amplitudes of the clutch disc and the driving wheels increase as the engagement rate increases, to a point at which it could stall the engine. Hence, the engagement rate can not be decreased significantly; however, the low engagement rate has a negative effect from point of view of the generated heat.

Figs (7.11) and (7.12) show the effect of the axle shaft stiffness on the judder and the driving wheel's behaviour. From these figures, the axle shaft stiffness is seen to have opposing effects on the judder and the driving wheel's behaviour. Clutch disc angular fluctuations are almost inevitable at low axle stiffnesses, while high axle shaft stiffnesses may result in high fluctuation of driving wheels at the end of the engagement time. However, during about 95% of the engagement time, the variation of the stiffness does not have a critical effect on the driving wheel's behaviour because the response of the driving wheels and the rest of the system are nearly decoupled.

Figs (7.13) and (7.14) show the effect of the clutch stiffness on the judder and the driving wheel behaviour. From these figures, the torsional fluctuation of the clutch disc is likely to be unstable at low clutch spring stiffness, while the torsional fluctuation of the driving wheels is likely to be unstable at high clutch spring stiffness. From Figs (7.11) to (7.14), decreasing the clutch spring stiffness and the axle shaft

stiffness causes judder. Thus, the design of the driveline involves a number of difficult design compromises.

From the mathematical analysis, it can be seen how friction gradient coefficient, effective system damping, clutch and driveline compliances, clutch engagement details and other driveline parameters affect the overall driveline behaviour. Particular problems are associated with clutch judder and torsional vibration instabilities during start-off or gear change manoeuvres. Therefore, although the severity of clutch judder is influenced significantly by the manner in which the vehicle is driven, there are several desirable design features which minimise the likelihood of its occurrence.

7.5-SUMMARY

1. Clutch judder and shunt phenomena due to self excited torsional vibrations arising from the stick-slip phenomenon during engagement of the dry friction clutch were investigated.

2. It was found that these phenomena could be avoided by increasing the system damping or by decreasing the negative gradient of the friction coefficient.

3. By increasing the axle shaft torsional stiffness and the clutch spring torsional stiffness, judder could be avoided.

4. Because the dynamics of the system are predictable, it should in future be possible to control the torsional vibration instability during the engagement period using some sort of intelligent control system sensing information related to the system and taking control action to modify the response into a subjectively acceptable form.

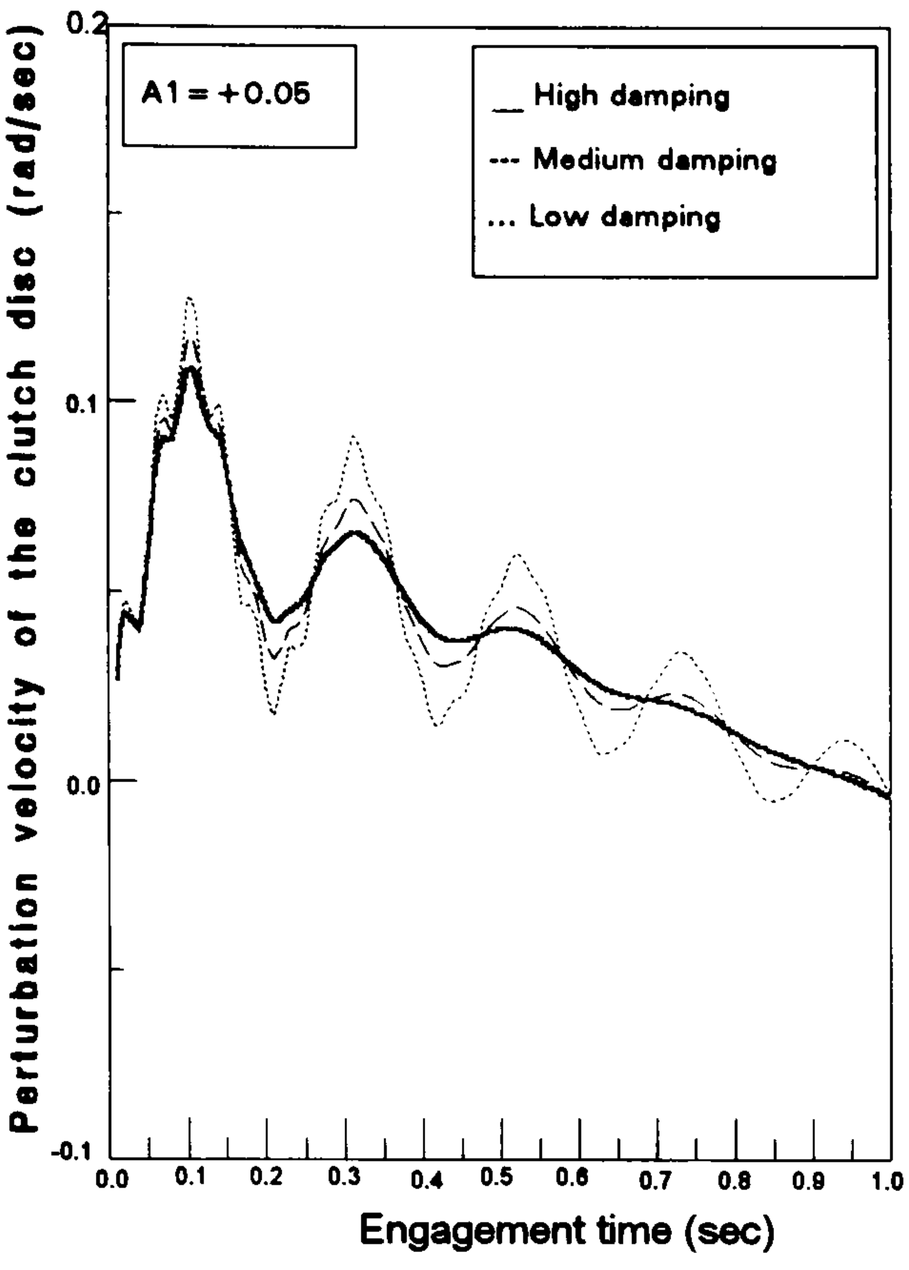

Fig (7.3) Effect of damping level on the clutch disc due to clutch's friction torque at positive gradient of friction coefficient.

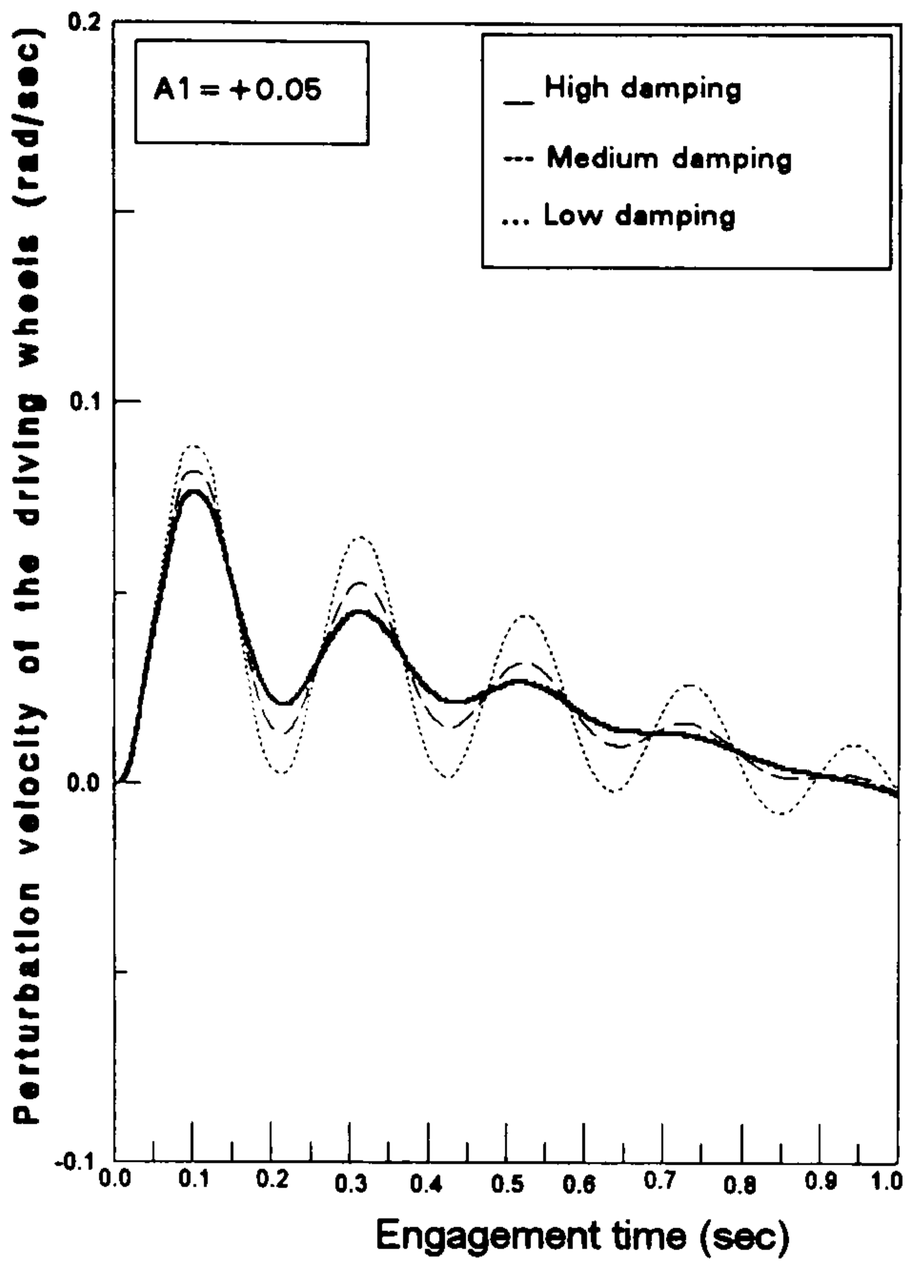

Fig (7.4) Effect of damping level on the driving wheel due to clutch's friction torque at positive gradient of friction coefficient.

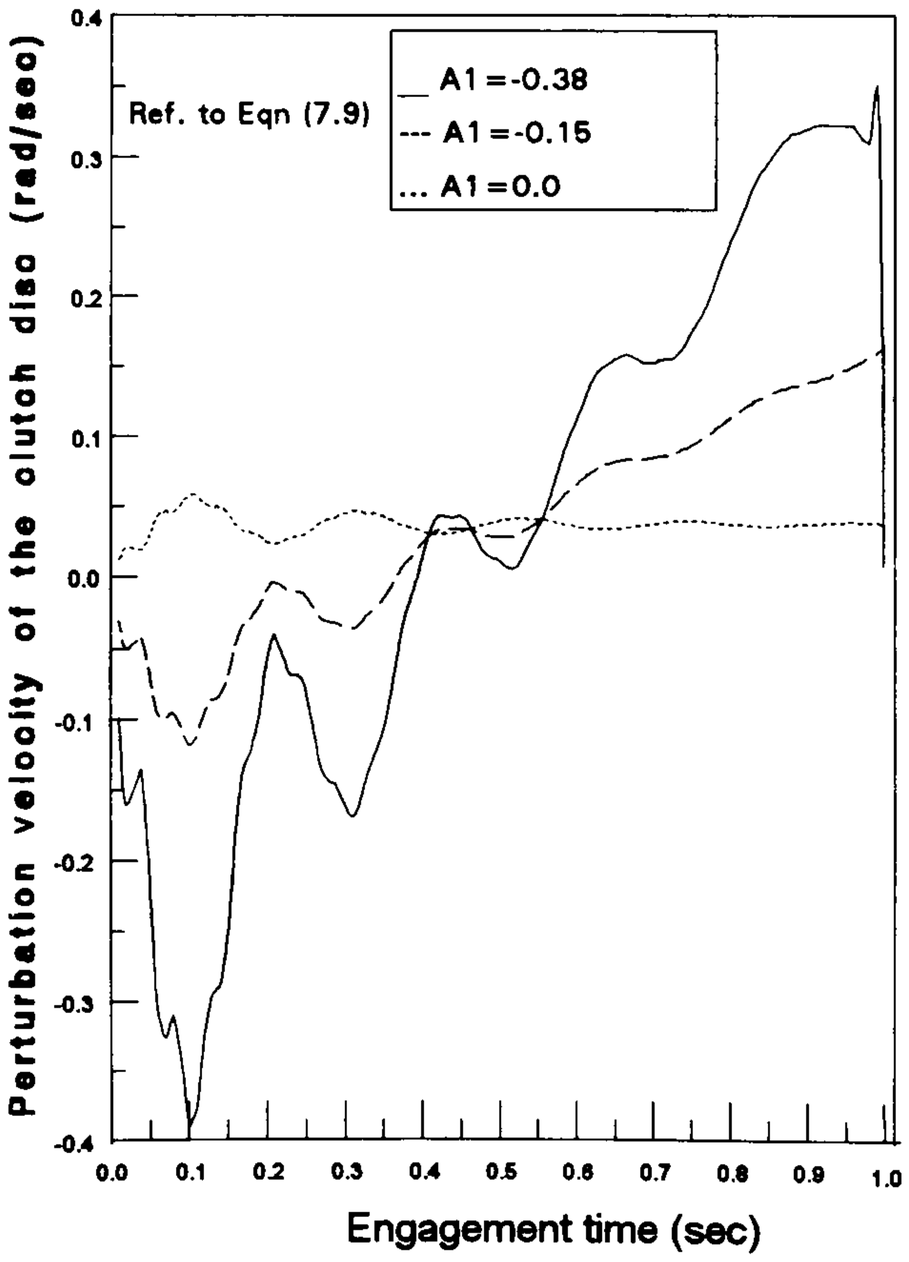

Fig (7.5) Effect of the gradient of the friction coefficient on the clutch judder

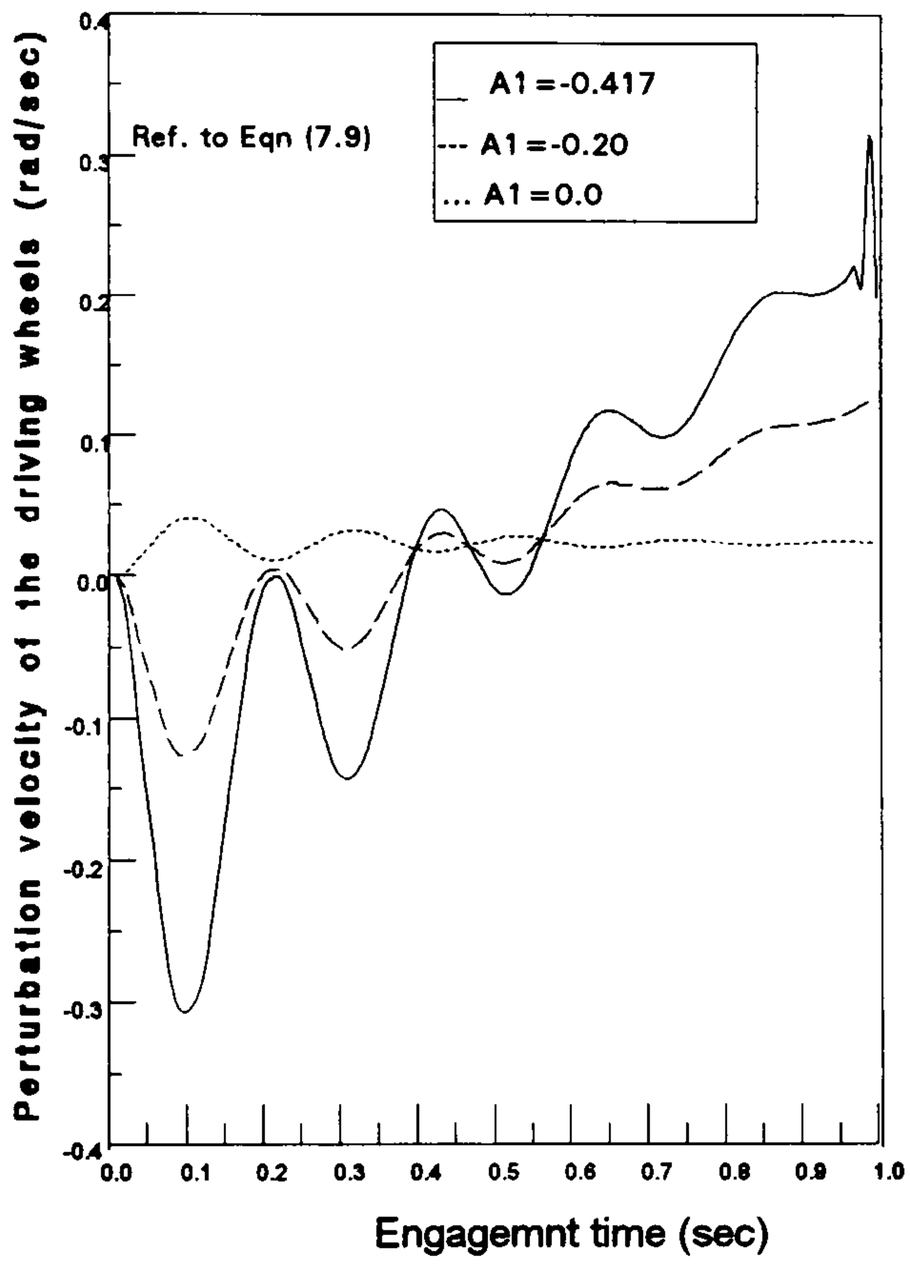

Fig (7.6) Effect of the gradient of the friction coefficient on the behaviour of the driving wheels

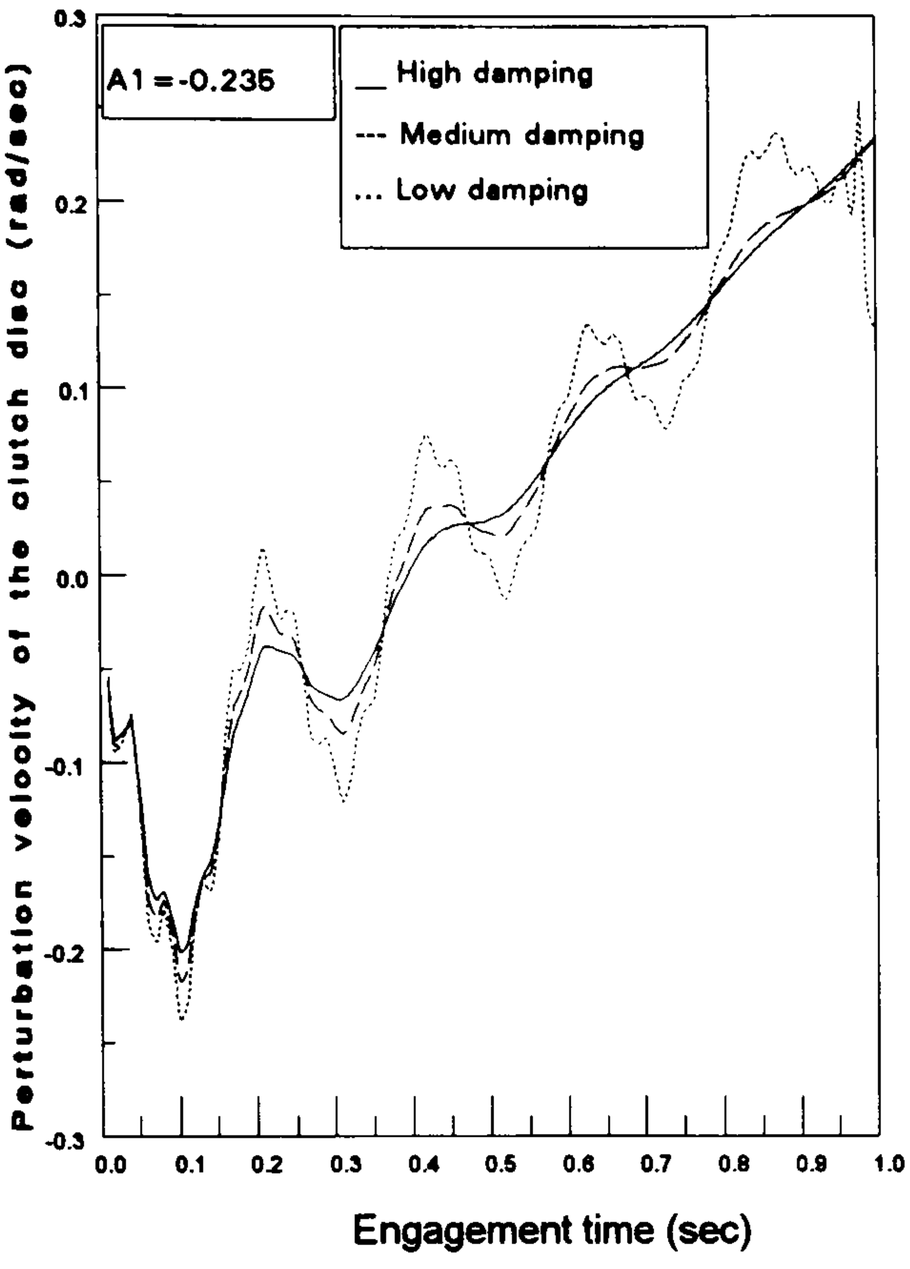

Fig (7.7) Effect of damping level on the clutch judder at negative gradient of friction coefficient.

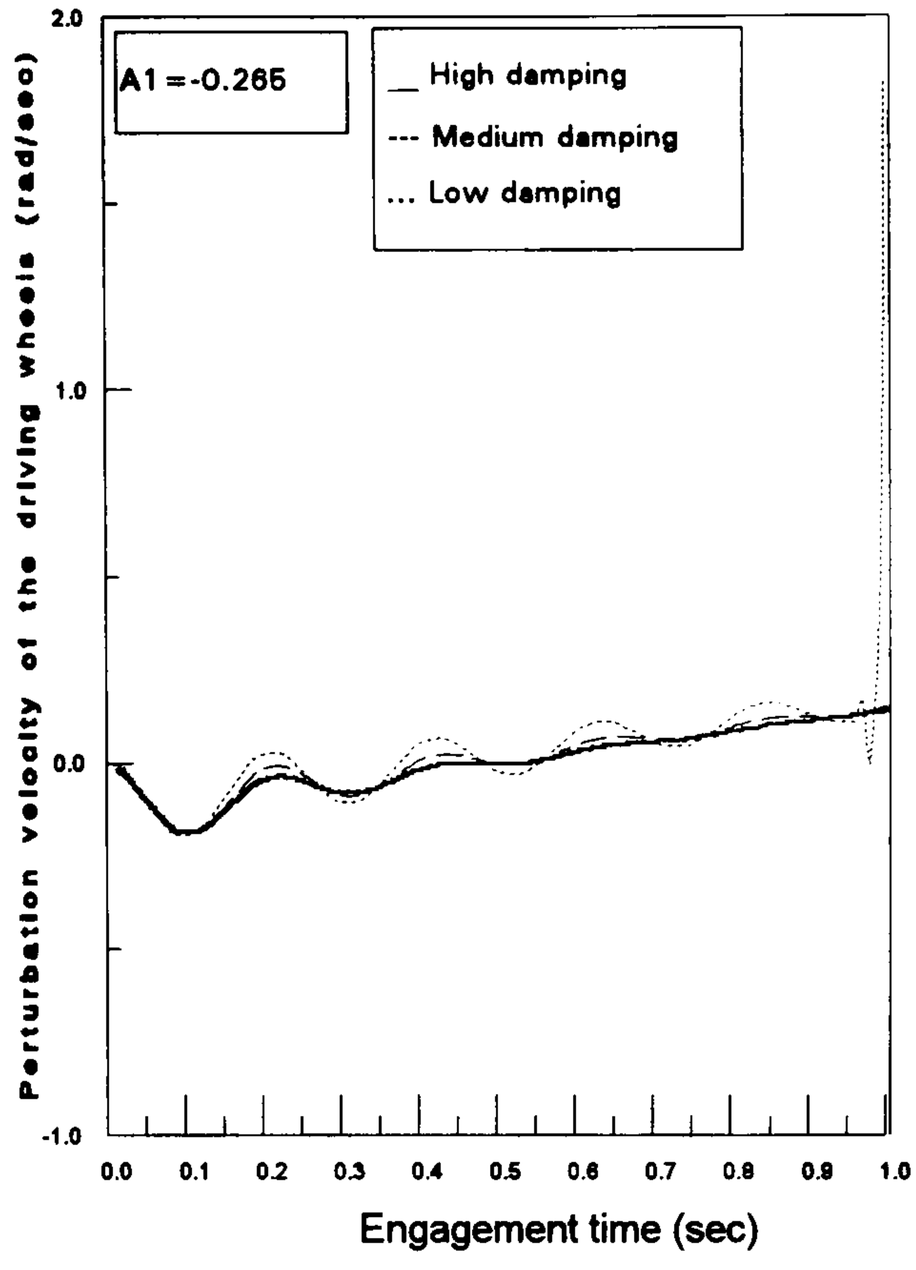

Fig (7.8) Effect of the damping level on the behaviour of the driving wheels at negative gradient of friction coefficient

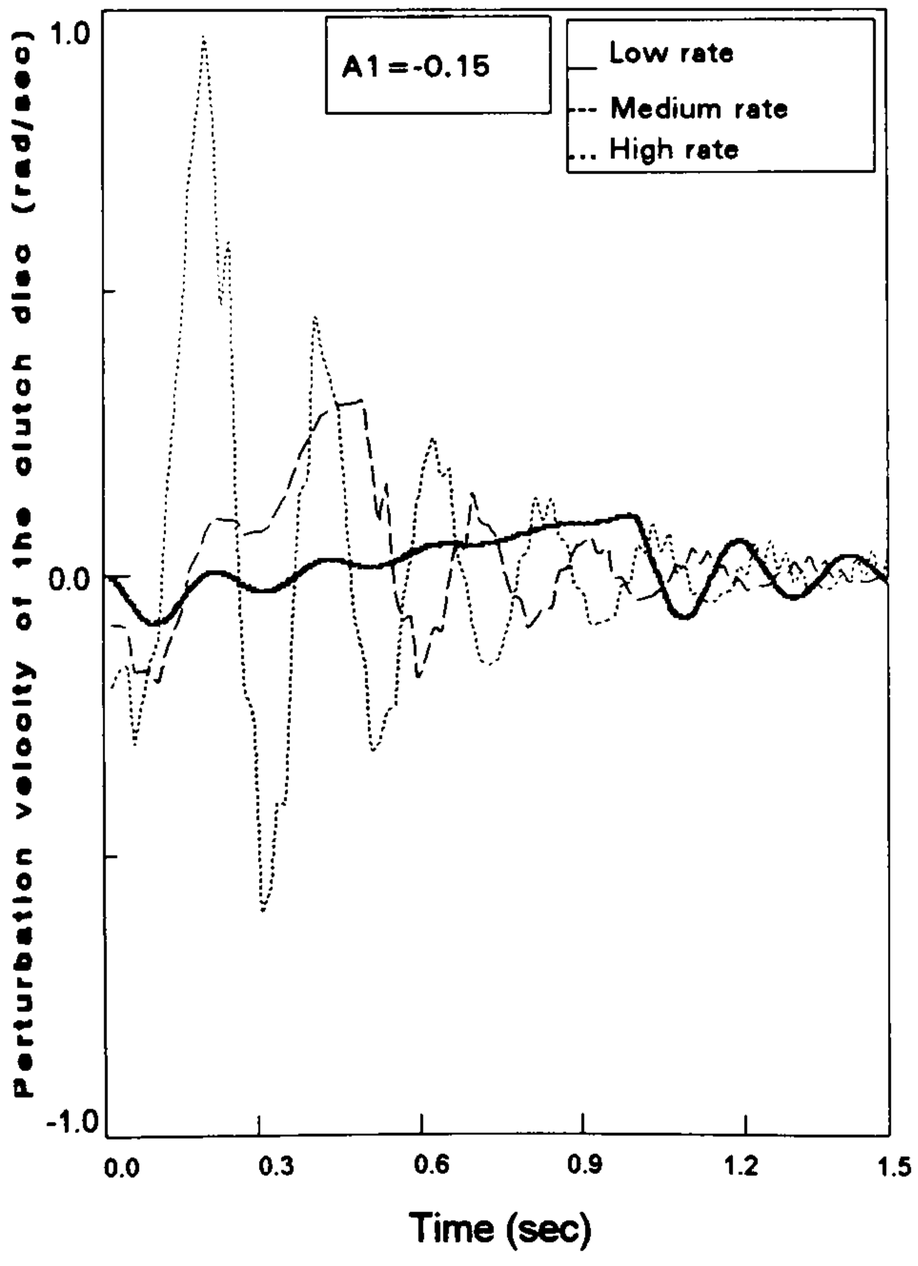

Fig (7.9) Effect of the engagement rate on the clutch judder

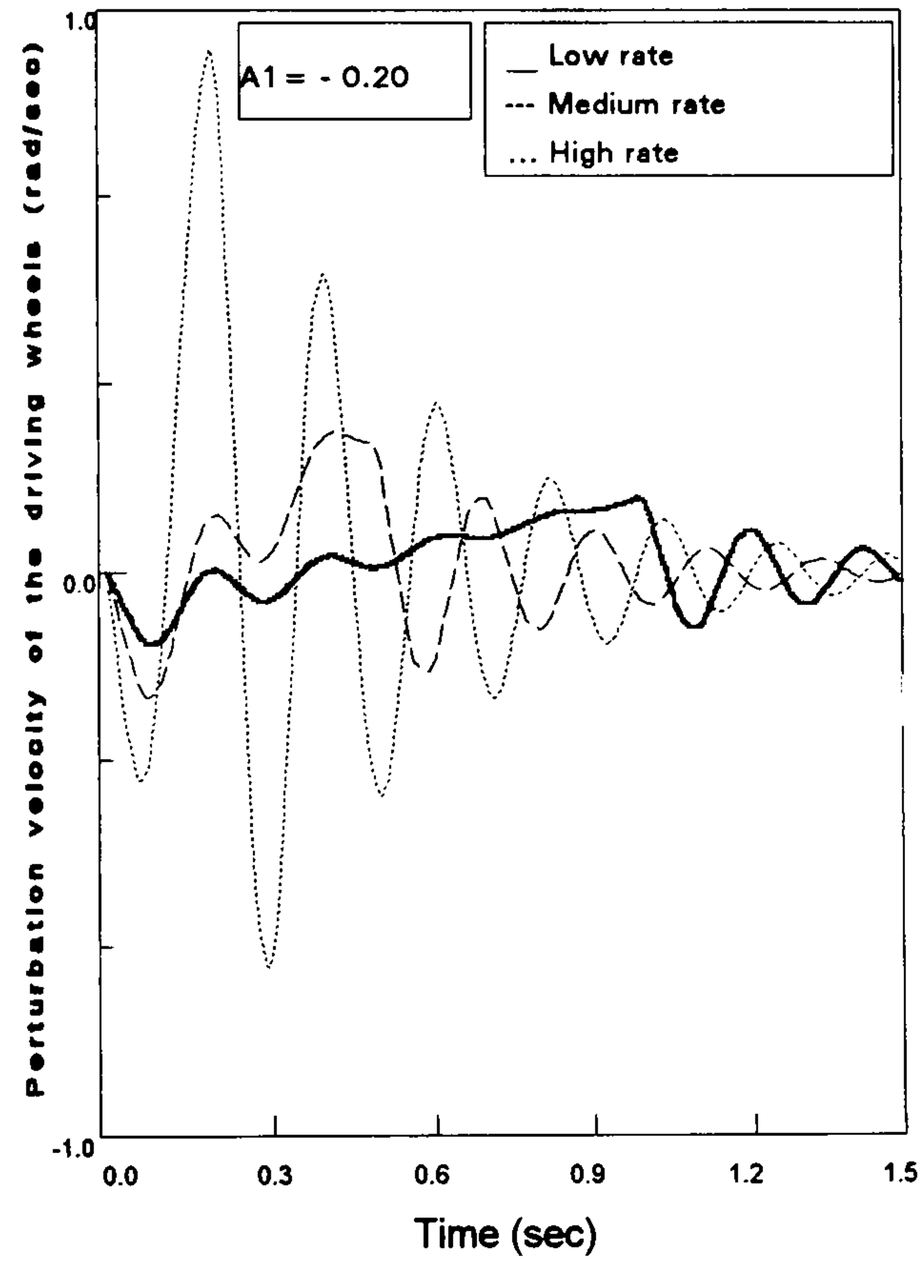

Fig (7.10) Effect of the engagement rate on the behaviour of the driving wheels

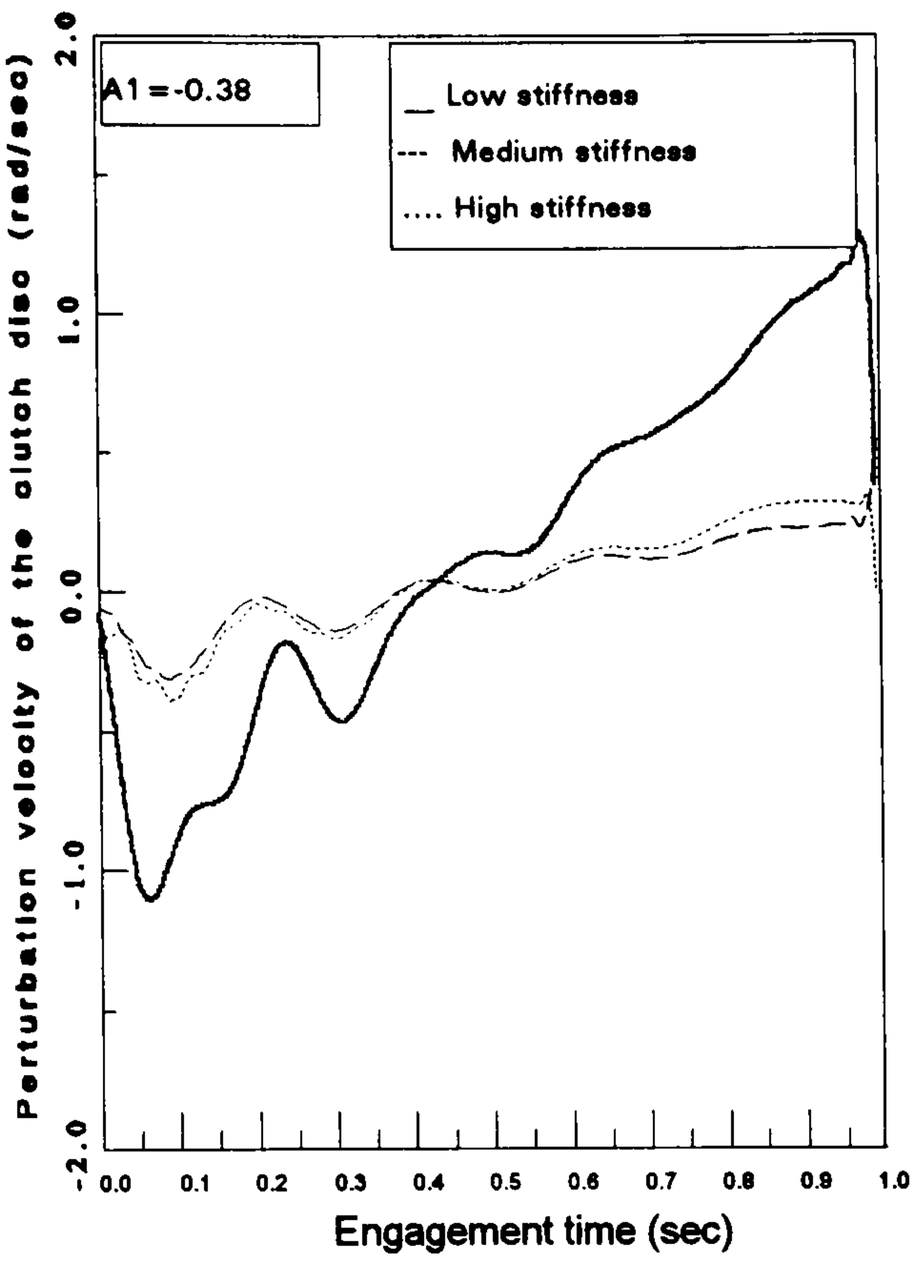

Fig (7.11) Effect of the axle shaft stiffness on the judder

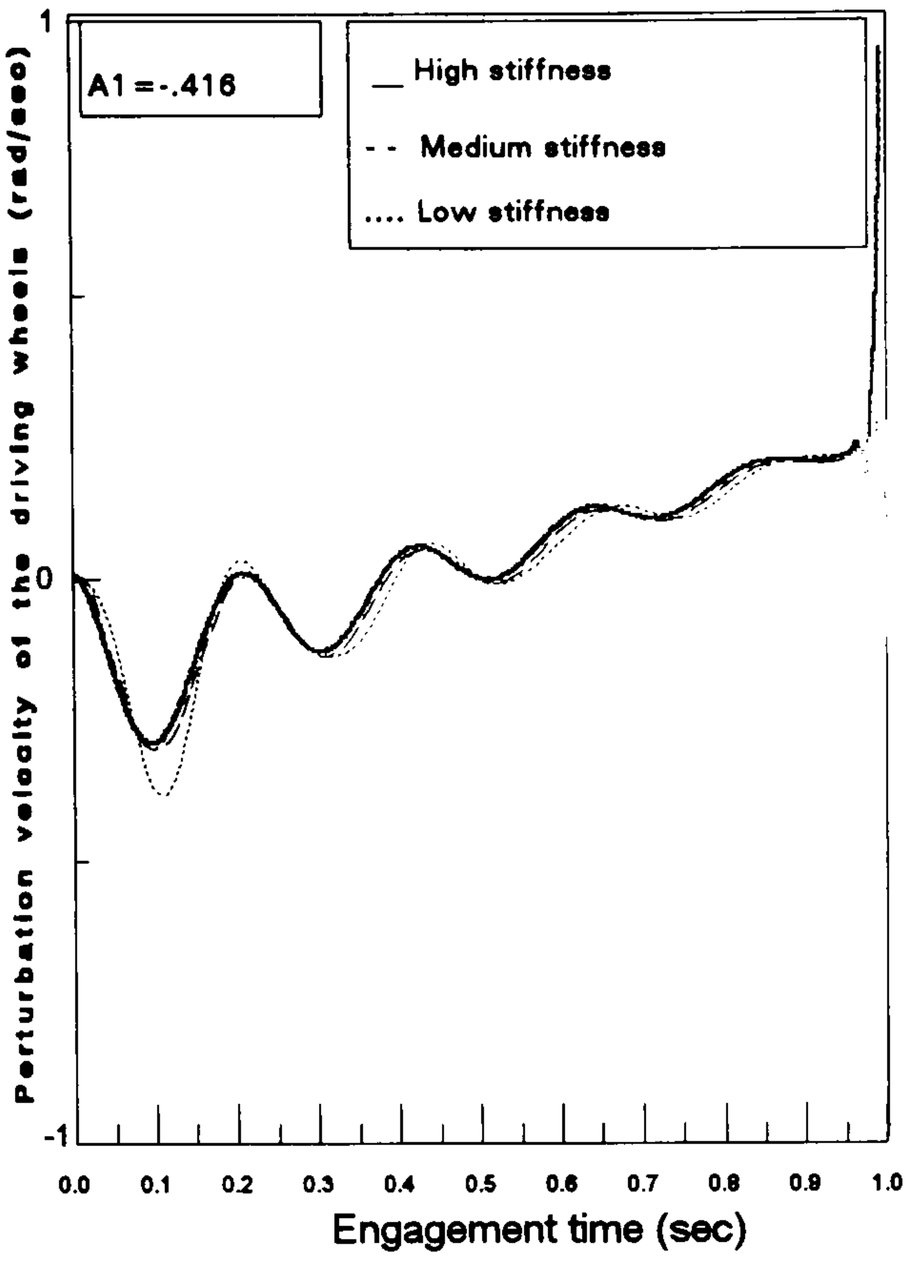

Fig (7.12) Effect of the axle shaft stiffness on the behaviour of the driving wheels

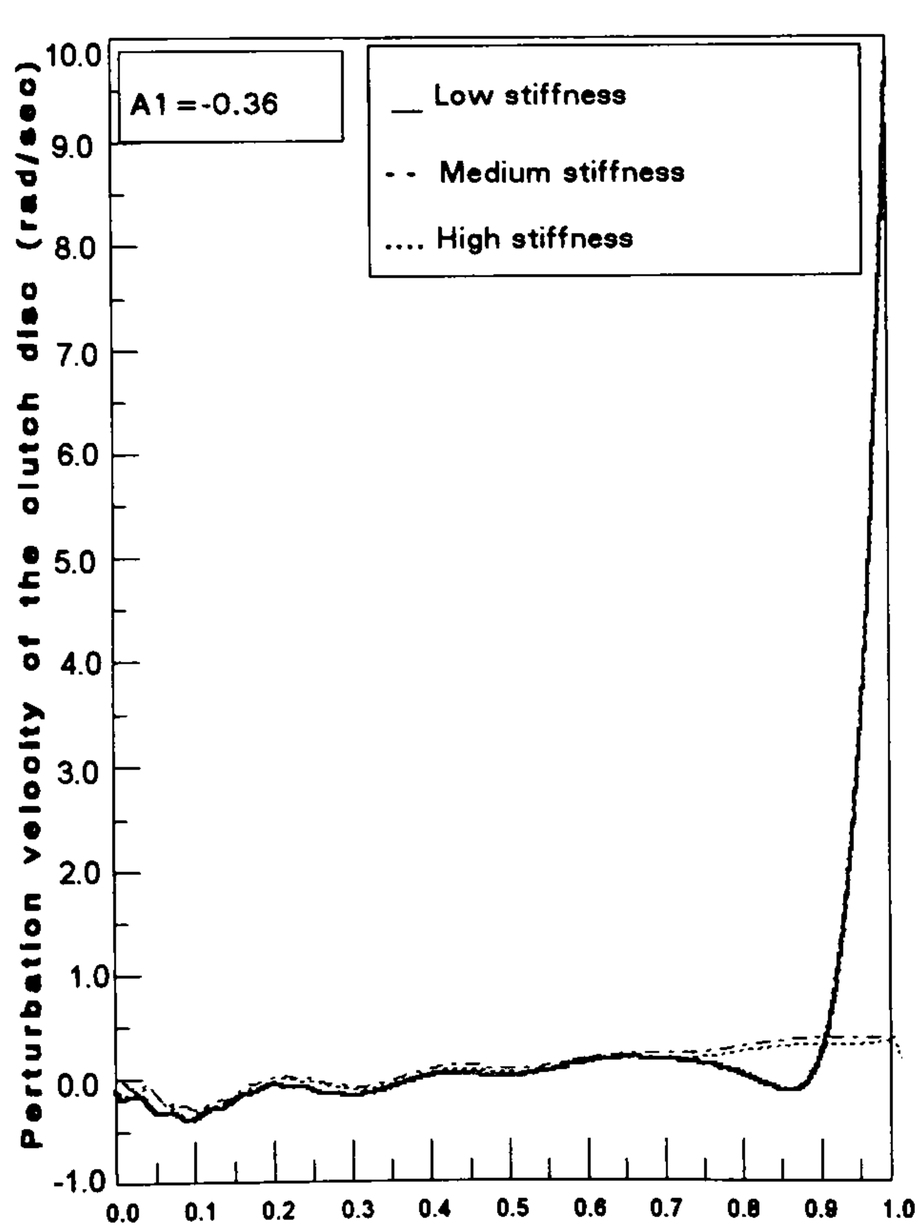

Fig (7.13) Effect of the clutch stiffness on the judder

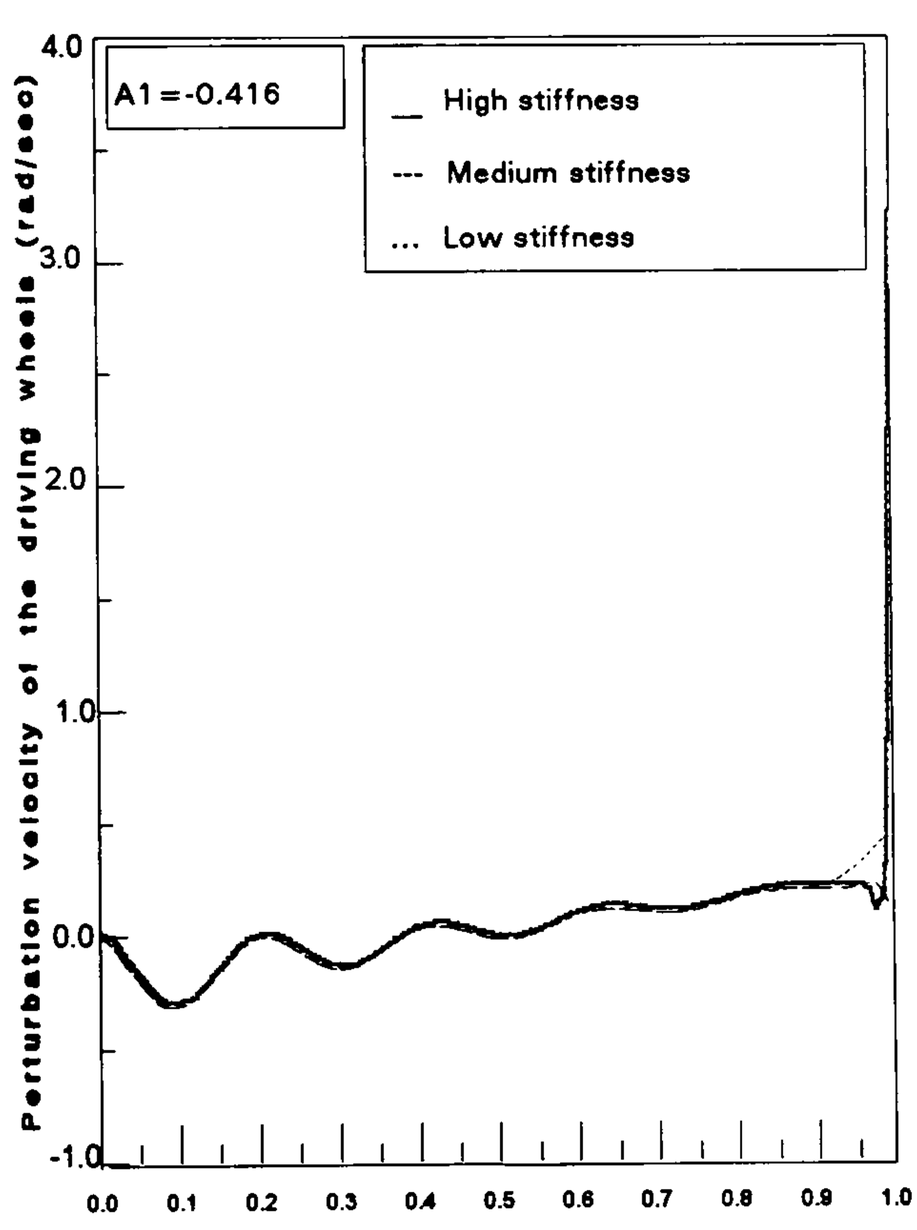

Fig (7.14) Effect of the clutch stiffness on the behaviour of the driving wheels

CHAPTER 8

COMPREHENSIVE MODEL OF DRIVELINE AND VEHICLE BODY VIBRATION SYSTEM

8.1-INTRODUCTION

The torsional motion of a vehicle driveline is coupled with the whole body motions of the vehicle because; (i) the torque variations at the axle will vary the drive forces at the ground and thus may act directly to generate longitudinal vibrations in the vehicle body, (ii) the torque variations at the transmission produce excitation in the roll direction on the engine/ transmission assembly, (iii) the drive torque reaction at the engine/transmission is transferred to the body structure and distributed between the front and rear suspensions, (iv) longitudinal and lateral loads are transferred into vertical loads in high accelerating torque and cornering conditions respectively.

This area of study is not well covered in the literature although there have been some attempts to derive mathematical models include driveline torsional motion and other motions of the vehicle components, see chapter 1.

The aim of this chapter is to establish a comprehensive mathematical model of vehicle driveline system vibrations with the body fore-aft and vertical vibrations and investigate the coupling of these vibrations, without details of other conditions such as handling or cornering of the vehicle.

8.2-TYRE MODEL

The tyre is modelled in this study based on the same principles used by Sharp and Jones [34] and Pacejka [69] which includes tyre longitudinal flexibility, modelled using longitudinal carcass stiffness, k_{13}, see Fig (8.1). The tyre is represented as having a massless circumferential band which is elastically connected to the carcass with the tread bands being subject to longitudinal forces 'F_1' at the road surface. These forces are non-linear functions of the wheel load and longitudinal slip. The polar moment of inertia of the wheel including a large portion of the tyre, J_{13}, may vibrate against the longitudinal stiffness of the lower section of the tyre near the contact region (tyre tread). On the other hand, it was found computationally advantageous to associate some inertia with the tyre tread bands, J_t. For the sake of

simplicity, it is assumed that the tyre has radial viscoelastic dampers between the rim and the tread bands with longitudinal and vertical damping coefficients, respectively c_{13} and c_{14}. Hence, the support force is transmitted to the vehicle body through the parallel spring-dashpot combination that simulates the inflation pressure and carcass forces.

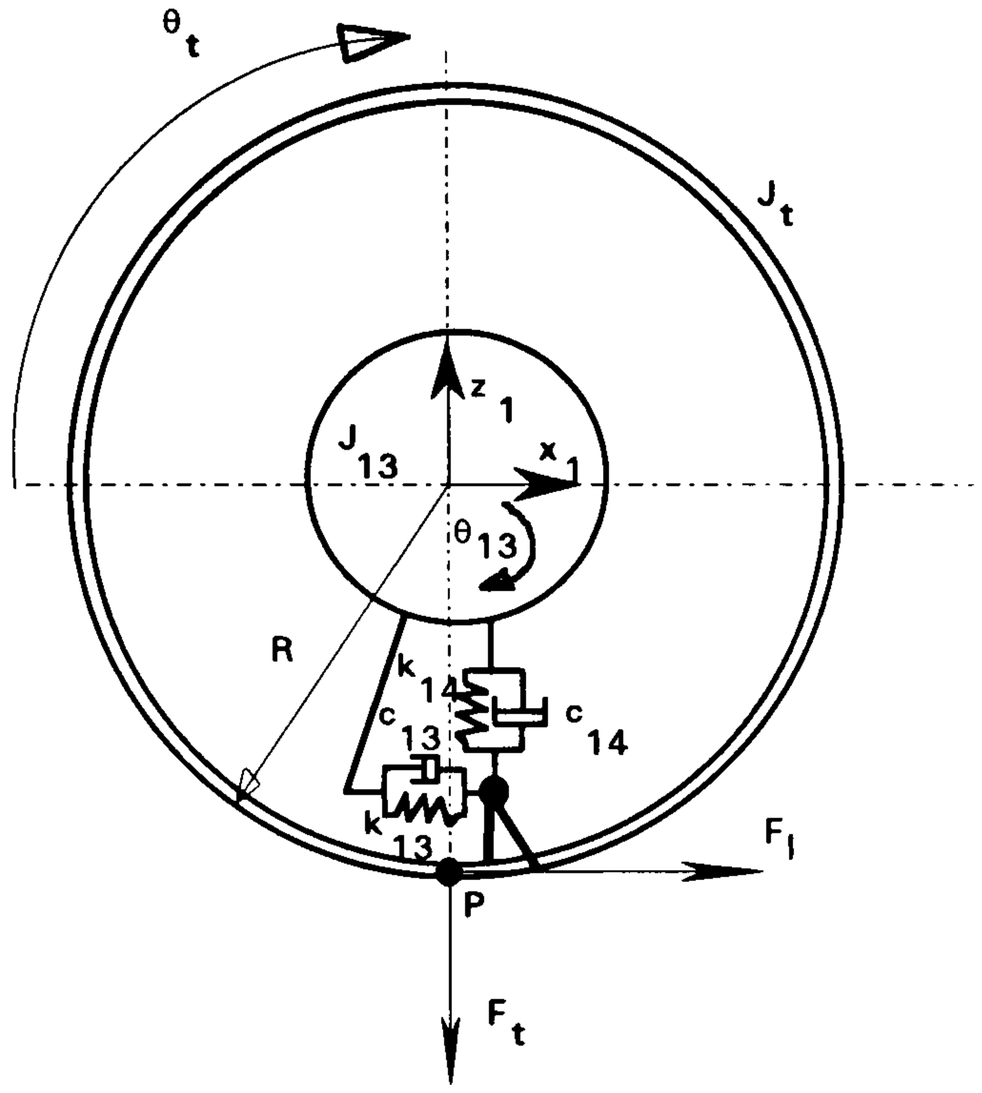

Fig (8.1) Tyre model

8.2.1-Longitudinal Force

In the free rolling condition, neither braking nor traction forces exist, the wheel angular oscillations, superimposed on the average forward rolling motion, are induced mainly by the interaction with fluctuations of the radial tyre deflection. When the wheel is braked or driven the point P, Fig (8.1), moves relative to the road in the longitudinal direction and the wheel has fore and aft slip, S. This slip is defined as the longitudinal velocity of the centre of the tyre contact relative to the road, i.e. forward velocity of point P, divided by the corresponding velocity of the wheel hub. Beside this longitudinal slip, the tyre may exhibit fore and aft deformations mainly of the carcass. The relative displacement of the lower portion of the tread band with respect to the rim ($R\theta_t$) is directly related to the slip force, $F_s = -k_{13}(R\theta_t)$. The longitudinal force associated with the slip, $-F_s$, is added to the force due to rolling resistance, $-F_r$,

already present during free rolling, and the viscoelastic damping force, $(-c_{13}R\dot{\theta}_t)$ to produce the total longitudinal force, F_l. The rolling resistance force expression [68] is;

$$F_r = A_r F_t \tag{8.1}$$

where A_r is the coefficient of tyre rolling resistance. The vertical tyre force, F_t, is transmitted through the vertical stiffness and damping coefficient of the tyre. The tyre is taken to have a linear vertical load / vertical deflection relationship. Assuming the tyre does not leave the ground, the vertical tyre force is;

$$F_t = k_{14}z_1 + c_{14}\dot{z}_1 \tag{8.2}$$

The total longitudinal force expression is;

$$F_l = -A_r(k_{14}z_1 + c_{14}\dot{z}_1) - R(k_{13}\theta_t + c_{13}\dot{\theta}_t) \tag{8.3}$$

Note that the longitudinal force is a function of the tyre degrees of freedom, z_1 and θ_t. This expression is significant because it specifies the variation of the longitudinal tyre/road contact force with the vertical and rotational oscillating motions of the tyre. Consequently, self-excited vibration of the system particularly under braking or traction conditions may result.

8.3-Coupled System Model

The coupled model is shown diagramatically in Figs (8.2a) and (8.2b). It consists of a part representing the torsional vibration of the driveline system from the engine to the driving axle, 12 DOF, Fig (8.2a), and a part representing the coupling motions of the tyre, suspension and vehicle body system, 6 DOF, Fig (8.2b). The two parts are associated together to produce the entire system model with 18 DOF. In this model, the two wheels of the vehicle perform the same movements, therefore they are condensed into a single wheel, thus imposing the restriction that the model can reproduce only symmetric motions of the real system [7,35]. The wheel motions have been restricted by vertical, longitudinal and torsional characteristics (stiffness and damping) of the tyres and the torsional flexibility of the driving axles. The total mass

of the vehicle is divided into two parts representing the unsprung mass, m_u, and vehicle body mass/sprung mass, m_b. The longitudinal and vertical motions of the unsprung mass are restricted by the longitudinal and vertical characteristics of the tyres and suspension. The longitudinal and vertical motions of the vehicle body mass are restricted by the longitudinal and vertical characteristics of the suspension. Because of the system has great complexity, the pitch movements of the vehicle body and axles and consequently, the torsional characteristics of the suspension have not been taken into consideration.

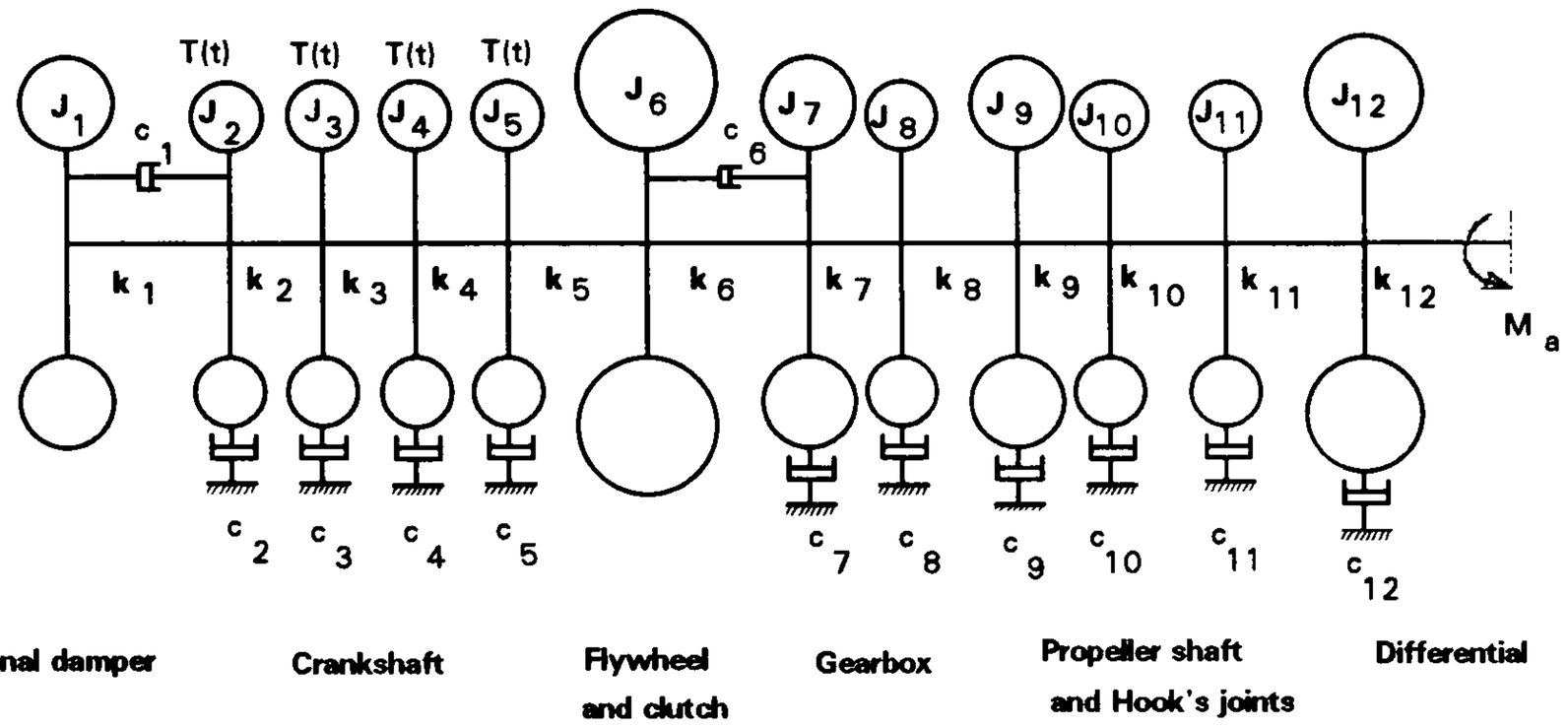

a: Transmission system model , torsional part

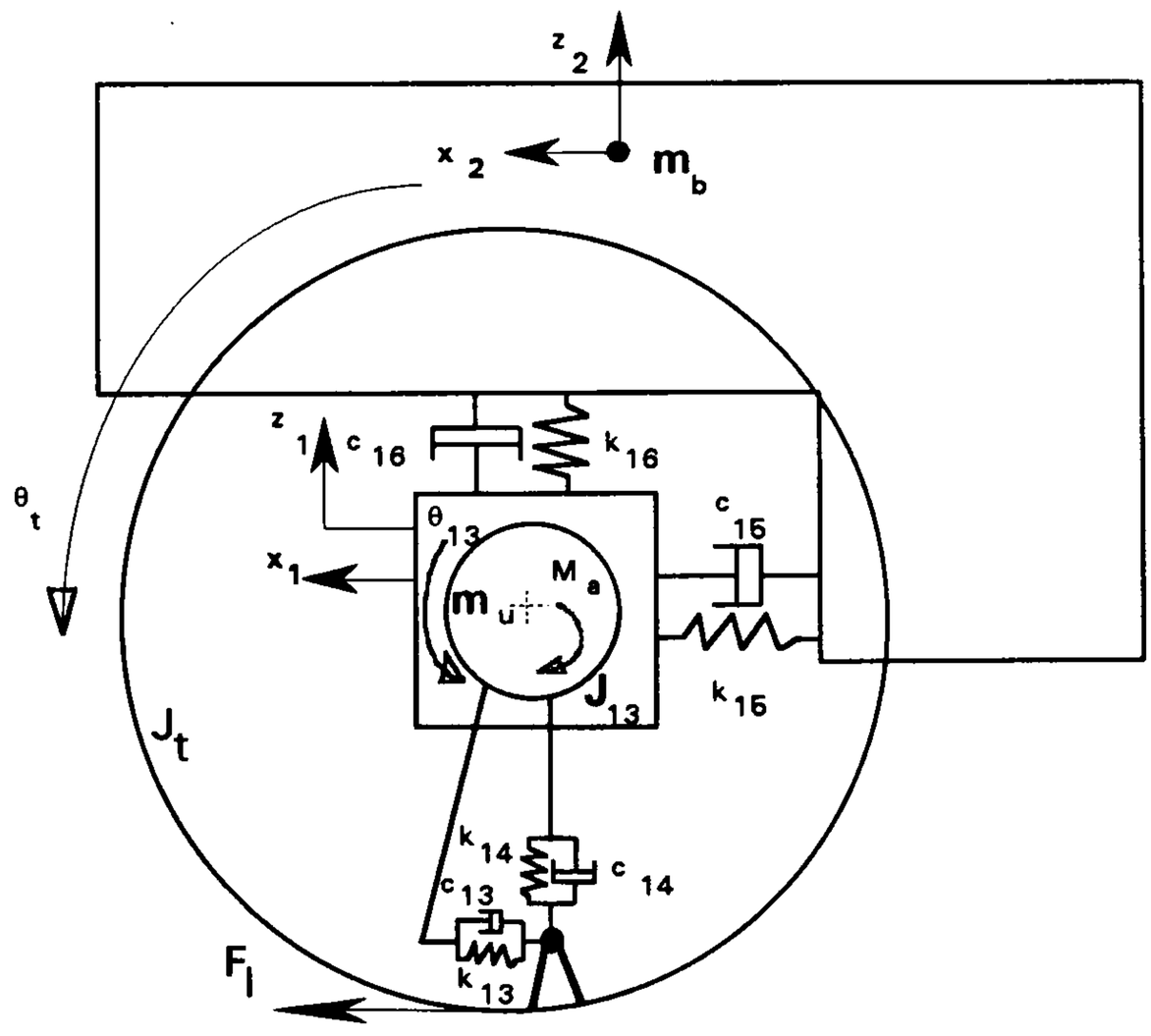

b: Tyre-Suspension-Body system model , coupled part

Fig (8.2) Coupled vibration system model

Typical numerical values of equivalent system parameters of a vehicle driveline system used in chapter 5 are used here in addition to the equivalent parameters of the vehicle body and suspension and tyres, Table (8.1).

Table (8.1) Typical data of equivalent parameters of a vehicle (nominal values)

Equivalent stiffness (N/m or N.m/rad)		Equivalent mass and moment of inertia (kg or kg m^2)		Equivalent system damping (Ns/m or N.m s/rad)	
Parameter	value	Parameter	value	Parameter	value
k_1	0.2×10^6	J_1	0.3	c_1	3
k_2	1×10^6	J_2	0.03	c_2	2
k_3	1×10^6	J_3	0.03	c_3	2
k_4	1×10^6	J_4	0.03	c_4	2
k_5	1×10^6	J_5	0.03	c_5	2
k_6	0.05×10^6	J_6	1.0	c_6	4.42
k_7	2×10^6	J_7	0.05	c_7	1
k_8	1×10^6	J_8	0.03	c_8	1
k_9	0.1×10^6	J_9	0.05	c_9	1
k_{10}	0.1×10^6	J_{10}	0.02	c_{10}	1.8
k_{11}	0.2×10^6	J_{11}	0.02	c_{11}	1.8
k_{12}	1×10^4	J_{12}	0.3	c_{12}	2
k_{13}	0.5×10^6	J_{13}	4	c_{13}	4000
k_{14}	0.4×10^6	J_t	0.12	c_{14}	600
k_{15}	1×10^8	m_u	180*	c_{15}	100000
k_{16}	9×10^4	m_b	1800	c_{16}	4000

* In the numerical analysis, m_u is taken as a single axle mass of 180 kg. The correct value should have been 90 kg

8.4-Equations of Motion

The equations of motion can be obtained by straightforward application of Newtonian or Lagrangian methods. The torsional part has not been changed from those mentioned in previous chapters, therefore, its equations are not mentioned here. These equations represent the torsional system's equations corresponding to the entire system degrees of freedom from 1 to 12, Fig (8.2a). For the tyre-suspension-body part, Fig (8.2b), the Lagrange's approach is used to drive the equations of motion which correspond to the entire system degrees of freedom from 13 into 18.

The inertia, elastic and dissipative forces come from the kinetic (K.E), strain (P.E) and dissipation (D.E) energy functions respectively. These expressions are;

$$K.E = \tfrac{1}{2} m_u (\dot{x}_1^2 + \dot{z}_1^2) + \tfrac{1}{2} J_{13} \dot{\theta}_{13}^2 + \tfrac{1}{2} J_t (\dot{\theta}_t + \dot{\theta}_{13})^2 + \tfrac{1}{2} m_b (\dot{x}_2^2 + \dot{z}_2^2) \qquad (8.4)$$

$$P.E = \tfrac{1}{2} k_{12} (\theta_{12} - \theta_{13})^2 + \tfrac{1}{2} k_{13} (R\theta_t)^2 + \tfrac{1}{2} k_{14} z_1^2 + \tfrac{1}{2} k_{15} (x_1 - x_2)^2 + \tfrac{1}{2} k_{16} (z_1 - z_2)^2 \qquad (8.5)$$

$$D.E = \tfrac{1}{2} c_{13} (R\dot{\theta}_t)^2 + \tfrac{1}{2} c_{14} \dot{z}_1^2 + \tfrac{1}{2} c_{15} (\dot{x}_1 - \dot{x}_2)^2 + \tfrac{1}{2} c_{16} (\dot{z}_1 - \dot{z}_2)^2 \qquad (8.6)$$

The generalised forces are obtained from virtual work done, δw, by all the forces whose effects have not been included in the energy expressions.

$$\delta w = -F_l R (\delta\theta_{13} + \delta\theta_t) + F_l \ \ \delta x_1 \qquad (8.7)$$

where, $\delta\theta_{13}, \delta\theta_t$ and δx_1 are virtual angular and longitudinal displacemets. The generalised force vector, {L}, induced by this force corresponding to degrees of freedom vector, $\{\theta_{13} \quad \theta_t \quad x_1 \quad z_1 \quad x_2 \quad z_2\}^T$, is;

$$\{L\} = \{-F_l R \quad -F_l R \quad F_l \quad 0 \quad 0 \quad 0\}^T \qquad (8.8)$$

From the Lagrange's equation, the equations of motion of the tyre-suspension-body part are;

$$(J_t + J_{13})\ddot{\theta}_{13} + J_t \ddot{\theta}_t + M_u = -F_l R \qquad (8.9)$$

$$J_t (\ddot{\theta}_t + \ddot{\theta}_{13}) + c_{13} R^2 \dot{\theta}_t + k_{13} R^2 \theta_t = -F_l R \qquad (8.10)$$

$$m_u \ddot{x}_1 + c_{15} (\dot{x}_1 - \dot{x}_2) + k_{15} (x_1 - x_2) = F_l \qquad (8.11)$$

$$m_u \ddot{z}_1 + c_{14} \dot{z}_1 + c_{16} (\dot{z}_1 - \dot{z}_2) + k_{14} z_1 + k_{16} (z_1 - z_2) = 0 \qquad (8.12)$$

$$m_b \ddot{x}_2 + c_{15} (\dot{x}_2 - \dot{x}_1) + k_{15} (x_2 - x_1) = 0 \qquad (8.13)$$

$$m_b \ddot{z}_2 + c_{16} (\dot{z}_2 - \dot{z}_1) + k_{16} (z_2 - z_1) = 0 \qquad (8.14)$$

where $M_u = k_{12}(\theta_{13} - \theta_{12})$

Eqns (8.9) into (8.14) represent the equations of motion corresponding to the entire system degrees of freedom from 13 into 18. These equations are associated with those of the torsional part to obtain the total equations of motion of the entire system which in matrix form are;

$$[M]\{\ddot{\phi}\} + [C]\{\dot{\phi}\} + [K]\{\phi\} = \{Q\} \qquad (8.15)$$

where [M], [C] and [K] are (18x18) inertia, damping and stiffness matrices of the entire system model respectively, {Q} is the generalised force vector and{ϕ} is (18x1) vector of nodal displacements (torsional, longitudinal or vertical). Note that the matrices [C] and [K] in the above equation contain terms relating to the tyre/road contact force.

8.5-Excitation Sources

The most important excitation sources of the system are; engine fluctuating torque, clutch friction torque and non-constant velocity joints. The generalised force vector contains components of these sources acting at the corresponding degrees of freedom of the entire system. These depends on the running conditions of the vehicle, i.e. steady or transient running. Refer to chapter 6 for more details of these components.

8.5.1-Steady Running

In steady state running, the (18x1) non-linear force vector {Q} includes; engine fluctuation torque, fluctuating torque from non-constant velocity joints and longitudinal tyre/road contact force. The effect of the friction torque due to clutch engagement is not included in the steady running since the clutch does not slip during normal running conditions. i.e. the generalised force vector is;

$$\{Q\} = \{T(t)\} + \{H(\phi)\} \qquad (8.16)$$

where

{T(t)} is the engine fluctuating torque vector, and

{H(ϕ)} is the vector of fluctuating torque coming from Hooke's joint.

8.5.2-Transient Running

It is well understood by most vehicle performance engineers that transient operation conditions are often one of the main cause of unwanted emissions and vibrations. Frequent stops and shifts and starts are the most common transient operating conditions. Therefore, the behaviour of the system during clutch engagement has been considered as a transient running condition of a vehicle. In the suggested model, the engine speed has been assumed constant, the first five degrees of freedom of the previous model were cancelled and the tyre-suspension-body part, Fig (8.2b), has not been changed. Fig (8.4) shows the torsional part of model during the clutch engagement. The same mathematical model as used for steady running conditions, is used. However, the value of J_6 depends on whether the clutch is fully engaged and not slipping, in which case it represents the combined inertia of engine flywheel, clutch cover and driven plate, or whether the clutch is slipping, in which case it represents the driven plate only. Also, the excitation torque vector does not include the engine fluctuating torque but the friction torque due to clutch engagement has been included, i.e. the generalised force vector is;

$$\{Q\} = \{M_f(\phi)\} + \{H(\phi)\} \tag{8.17}$$

where

$M_f(\phi)$ is the friction torque induced during clutch engagement $=2Fr\mu(\phi)$,

F is the time dependent clamping force,

r is the friction radius of clutch,

$\mu(\phi)$ is the coefficient of friction between the clutch friction plates, section 7.2.1

μ_o is the static friction coefficient,

ω is the mean sliding speed (mean engine speed - mean clutch disc speed),

ϕ_1 is the perturbation of the clutch disc and

A_1 is gradient of friction coefficient

Refer to chapter 7 for more details of the friction torque and its parameters.

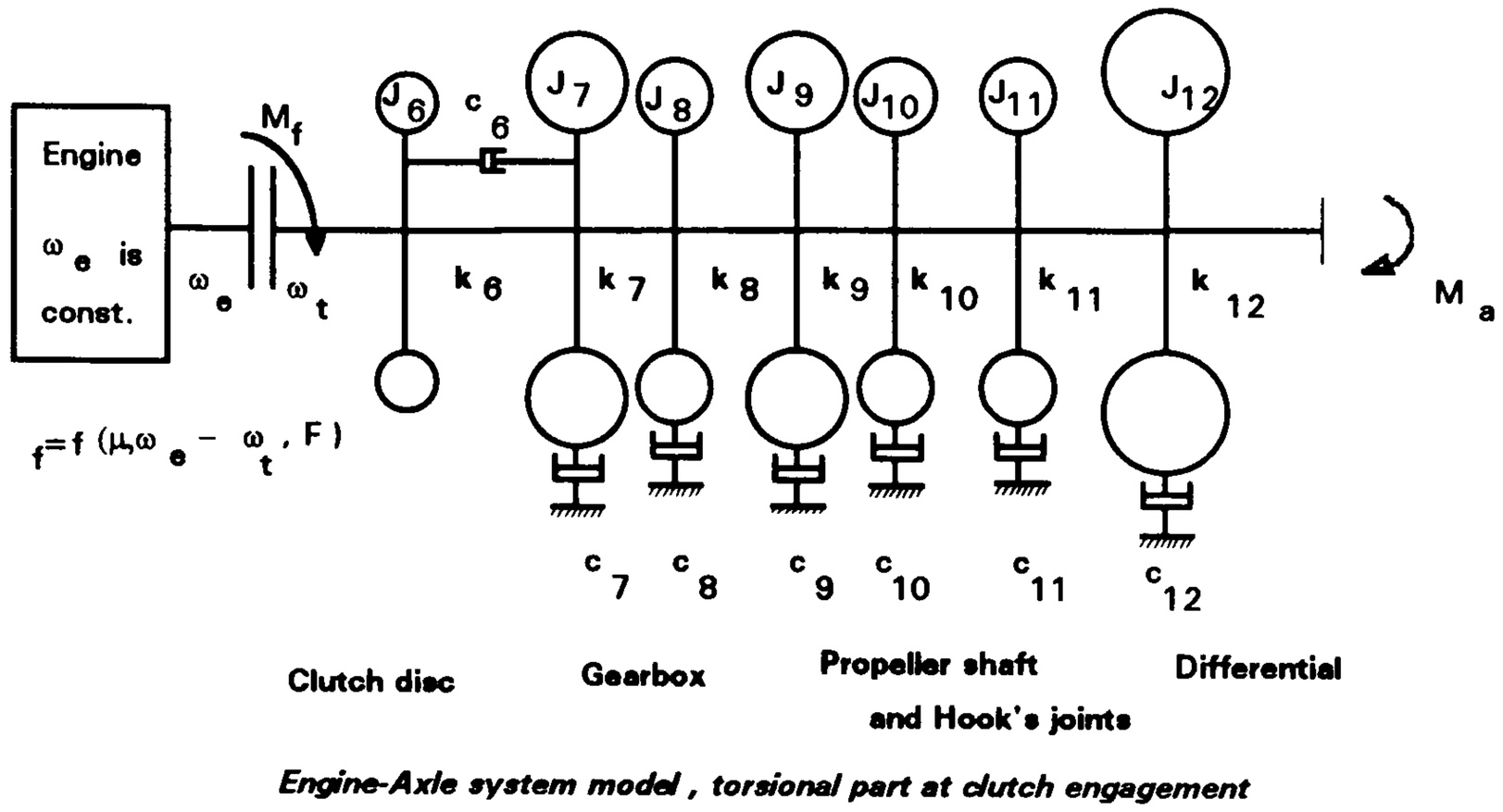

Engine-Axle system model , torsional part at clutch engagement

Fig (8.4) Torsional part model during the clutch engagement

8.6-Simulation

The Runge-Kutta numerical method has been again used to integrate the non-linear differential equations of motion (8.15) to obtain the time response of the system for different parameters values. These equations were transferred into a first order form by defining two (nx1) vectors $\{y_1\} = \{\phi\}$ and $\{y_2\} = \{\dot{\phi}\}$, where $\{y_1\}$is the displacement vector and $\{y_2\}$ is the velocity vector. Differentiating these two vectors yields;

$\{\dot{y}_1\} = \{\dot{\phi}\} = \{y_2\}$ and
$\{\dot{y}_2\} = \{\ddot{\phi}\}$

The equations of motion, (8.15), can be recognised as first-order vector differential equations;

$$\begin{Bmatrix} \dot{y}_1 \\ \dot{y}_2 \end{Bmatrix} = \begin{Bmatrix} \{y_2\} \\ M^{-1}(\{Q\} - [K]\{y_1\} - [C]\{y_2\}) \end{Bmatrix} \qquad (8.18)$$

with initial conditions $\begin{Bmatrix} y_1(o) \\ y_2(o) \end{Bmatrix} = \begin{Bmatrix} \phi_o \\ \dot{\phi}_o \end{Bmatrix}$

where

$$\{Q\} \begin{cases} = \{T(t)\} + \{H(y)\} & \text{in steady running} \\ = \{M_f(y)\} + \{H(y)\} & \text{in transient running} \end{cases} \qquad (8.19)$$

Eqn (8.18) is a first-order matrix differential equation which can be solved numerically to find the response vector {y(t)}. Here {y(t)} is the (2nx1) state vector, where the first nx1 elements correspond to the displacement vector,$\{\phi(t)\}$, and the second (nx1) elements correspond to the velocity vector, $\{\dot{\phi}(t)\}$.

8.7-Results and Discussion

A purpose-designed program, in FORTRAN, has been used to integrate the system of equation (8.18). The typical numerical values of the system parameters, shown in Table (8.1), have been used as nominal values or baseline values, in order to investigate the effect of different parameters on the system behaviour. Time responses of the torsional vibrations of the driving wheels and longitudinal vibrations of the vehicle body and rear axle are plotted in Figs (8.5) to (8.12) in the steady running condition and torsional vibration of the clutch disc is plotted in Figs (8.13) to (8.15) in transient running conditions.

8.7.1-Steady Running

The external excitation source which is considered in the steady running is the engine fluctuating torque, see chapter 3 Fig (3.4),. Some parameters of the system have been varied, around the nominal values, to investigate their effect on the system behaviour. The fluctuating velocity of the driving wheels and the vehicle body in response to engine fluctuating torque were obtained for different values of several important system parameters. As the driveline system, under steady conditions, runs at a constant speed, the excitation torque emanating from the engine was obtained at a particular engine speed, see chapter 3. The effect of Hooke's joints and system backlash has been discussed in separate study, chapter 6.

Figs (8.5) and (8.6) represent the velocity perturbation of the driving wheels torsional vibration and vehicle body and rear axle longitudinal vibrations respectively with the nominal parameters values. The system may become unstable for certain values of the system parameters such as decreasing system damping, compared to the nominal value, Figs (8.7) and (8.8). This flutter instability occurred because the energy dissipated by the damping of the system was less than the energy added to the system by the non-linear longitudinal force, Eqn (8.3). Increasing the tyre stiffness has stabilising effect on the torsional vibration of the driving wheel, Fig (8.9), and the longitudinal vibration of the vehicle body, Fig (8.10). Because the suspension longitudinal stiffness is relatively high, as expected the longitudinal vibrations of the axle and vehicle body are nearly identical, Figs (8.6) and (8.8). If this stiffness relatively low, the two motions are contrasted, Fig (8.11).

As the torsional response of the driving wheels, Figs (8.5), (8.7) and (8.9) and the longitudinal response of the vehicle body, Figs (8.6), and (8.10) have the same trend, it is confirmed that the torsional vibration of the driving wheels is valid as a measure of the fore-aft motion of the vehicle body (*shunt phenomenon*) in the model in which vehicle body motions are not included, as mentioned in chapter 7.

Figure (8.12) shows the effect of the axle torsional stiffness on the system behaviour. From this figure it can be seen that the vibration level increases with increasing the axle torsional stiffness.

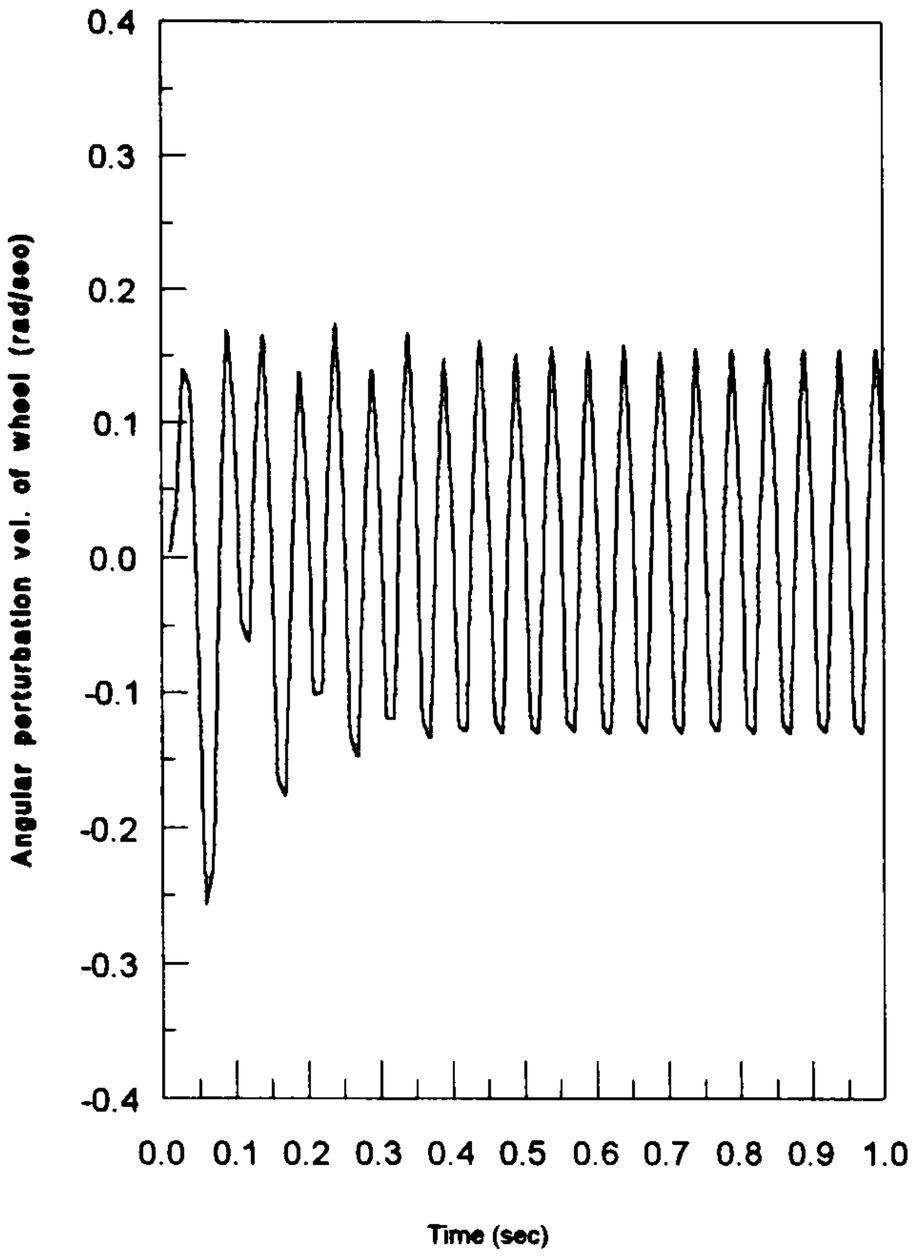

Fig (8.5) Torsional vibration of the driving wheels with nominal system parameter values

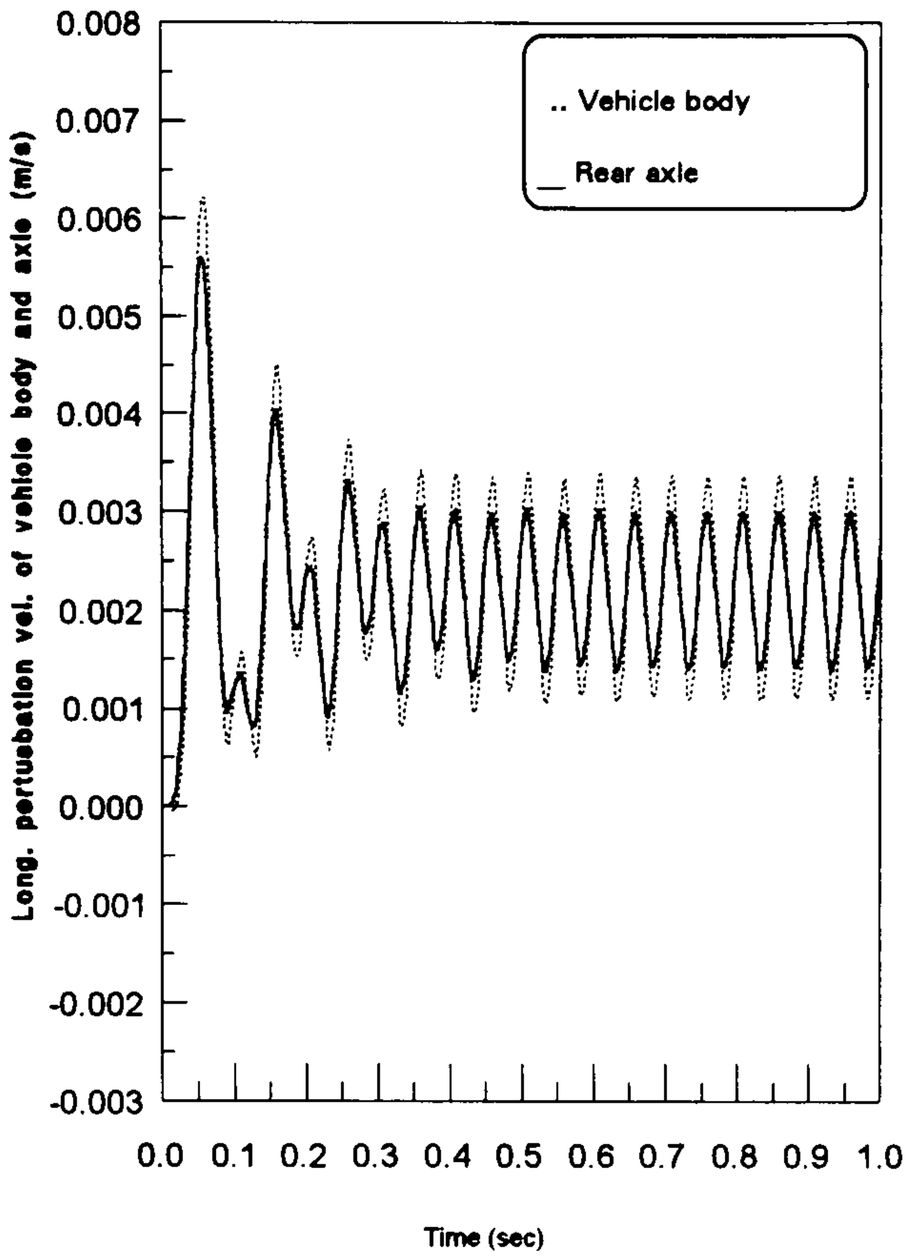

Fig (8.6) Longitudinal vibrations of the vehicle body and axle with nominal system parameter values

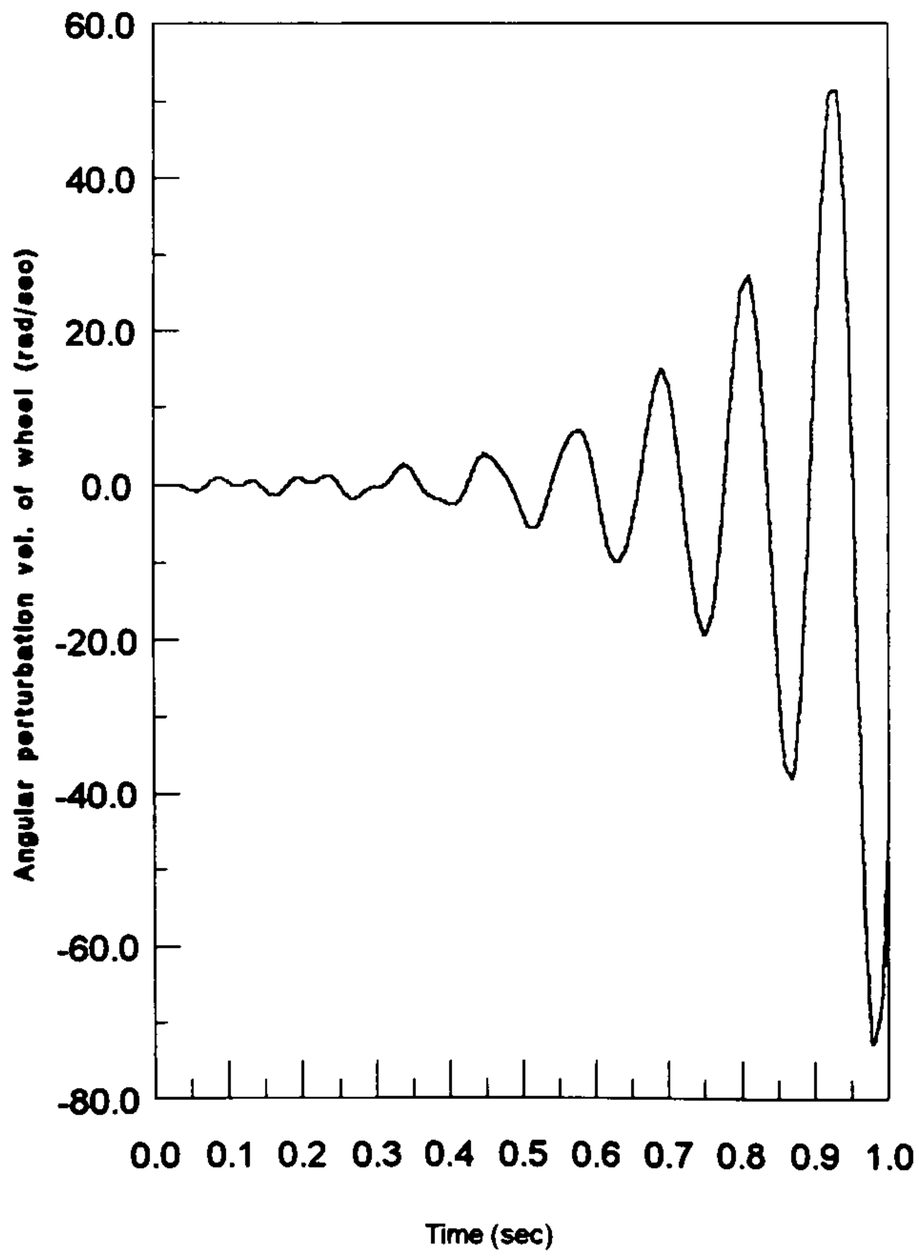

Fig (8.7) Torsional vibration of the driving wheels with low system damping (compared to the nominal values).

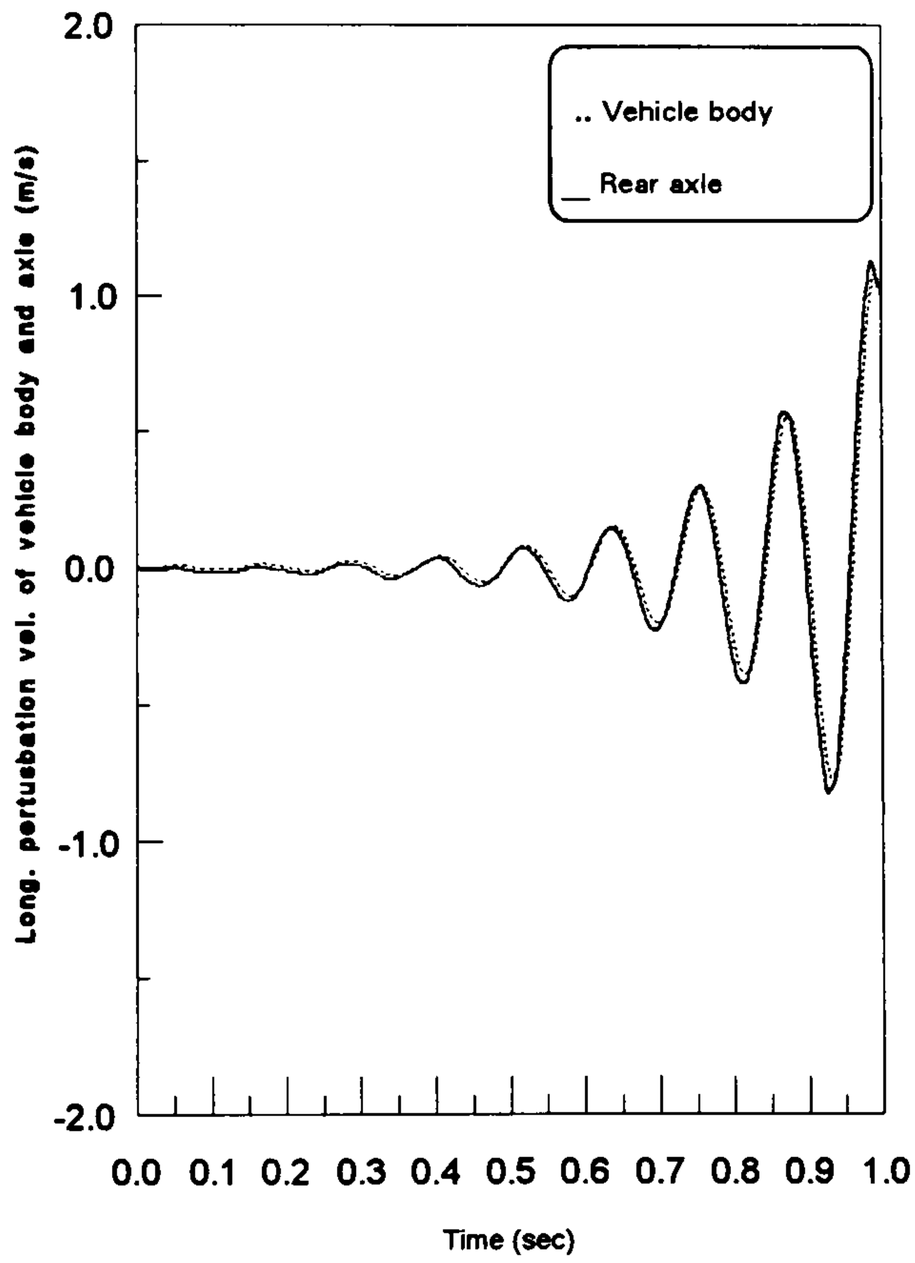

Fig (8.8) Longitudinal vibrations of the vehicle body and axle with low system damping (compared to the nominal values).

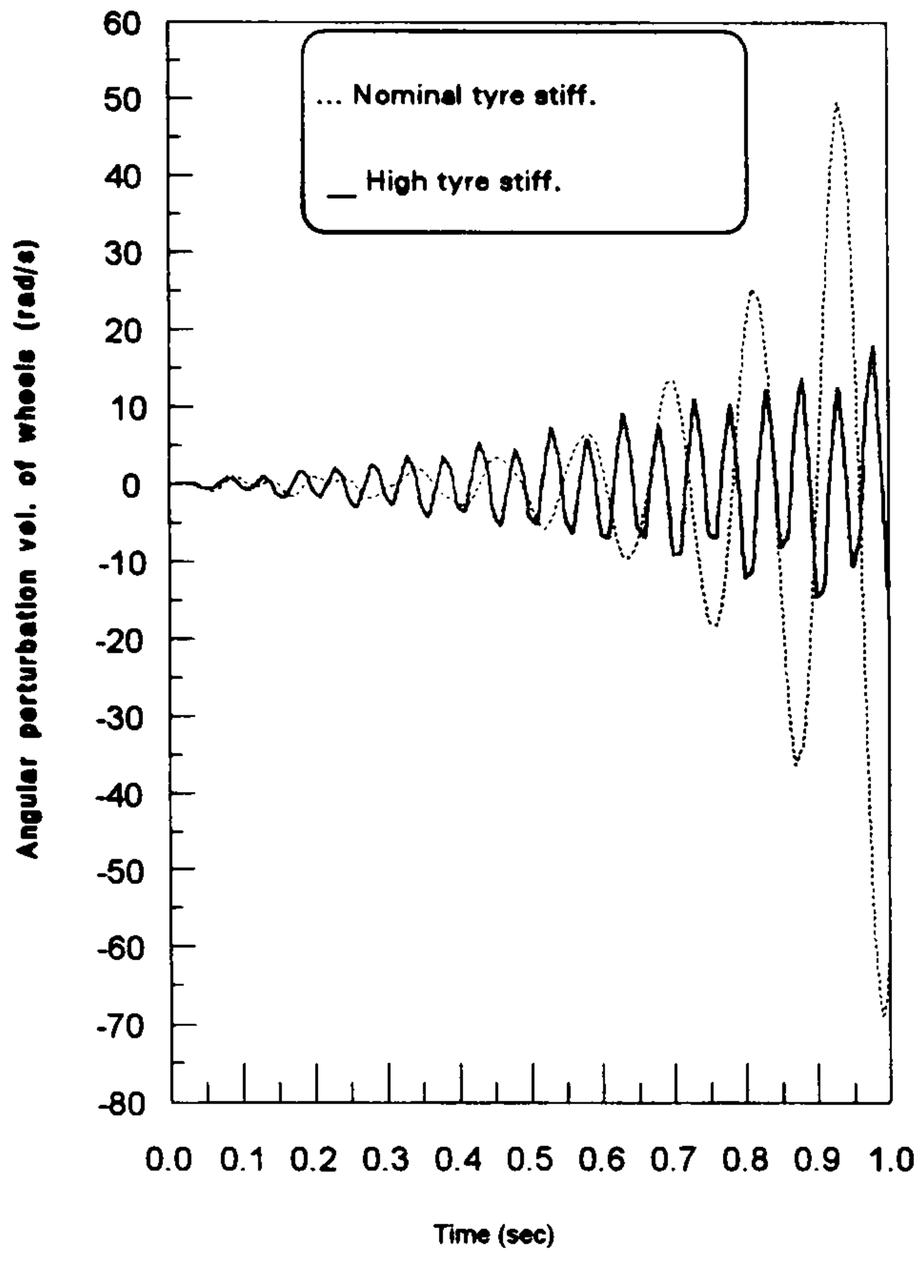

Fig (8.9) Torsional vibrations of the driving wheels with different tyre stiffness.

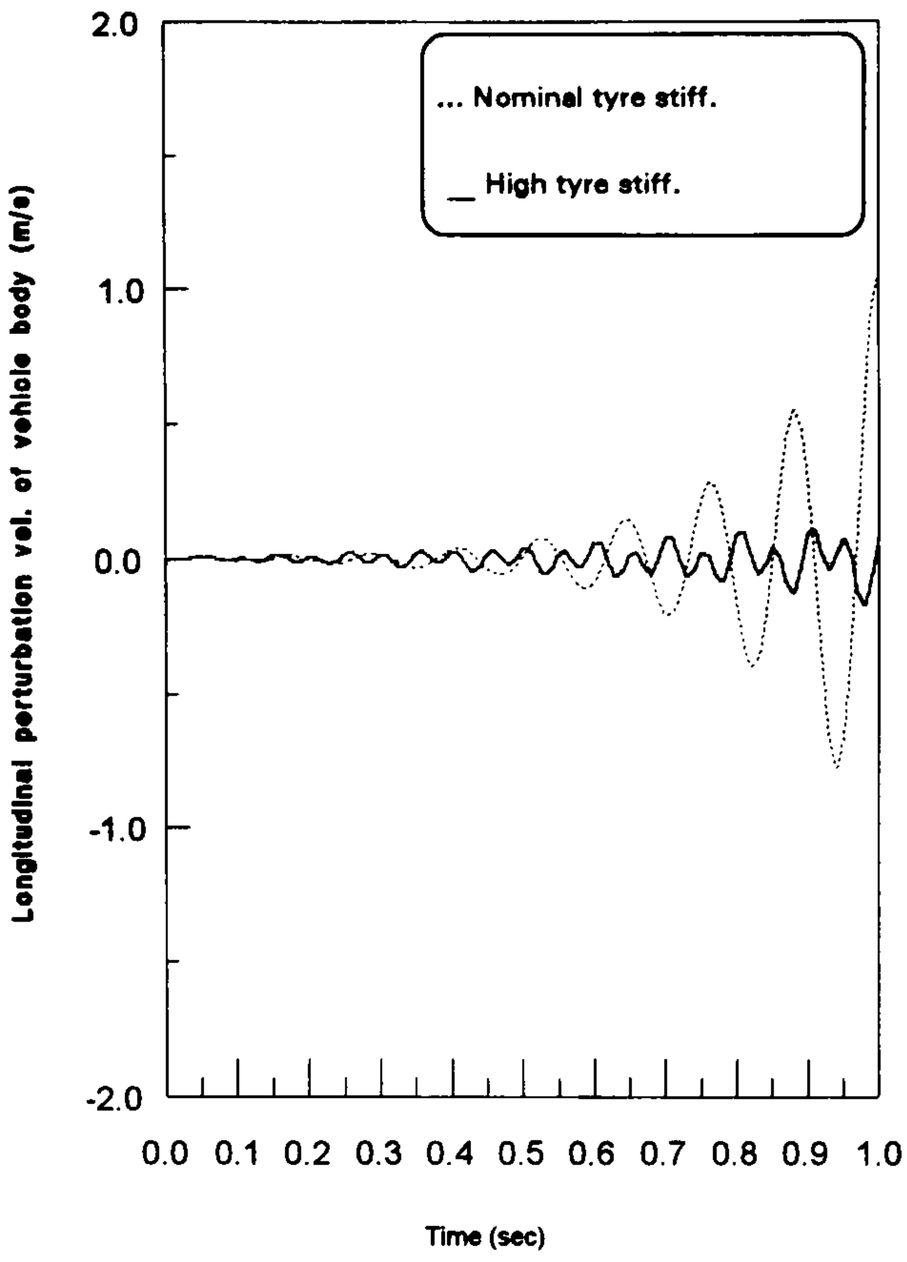

Fig (8.10) Longitudinal vibrations of the vehicle body with different tyre stiffness.

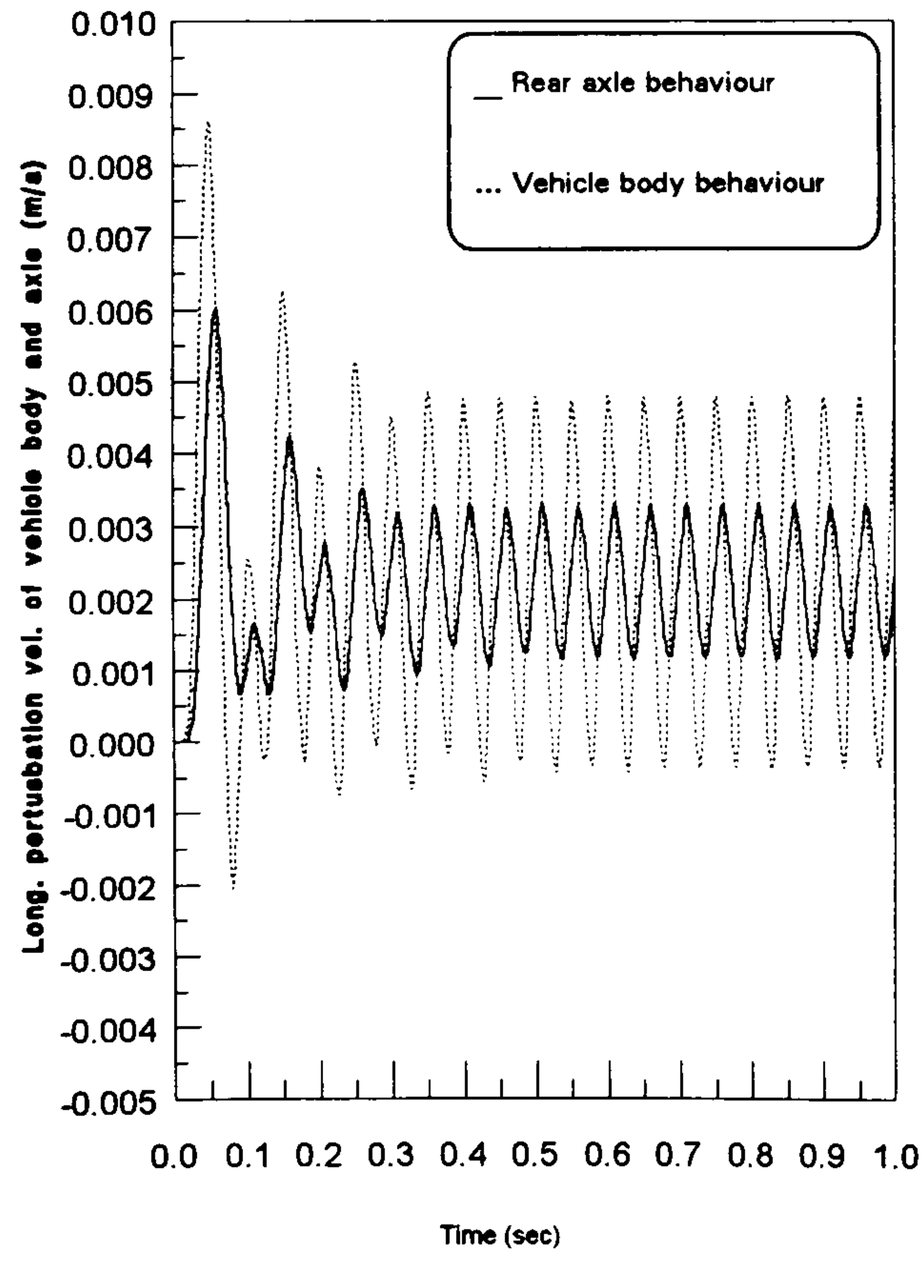

Fig (8.11) Longitudinal vibration of the vehicle body and rear axle with low longitudinal suspension stiffness (compared to the nominal value).

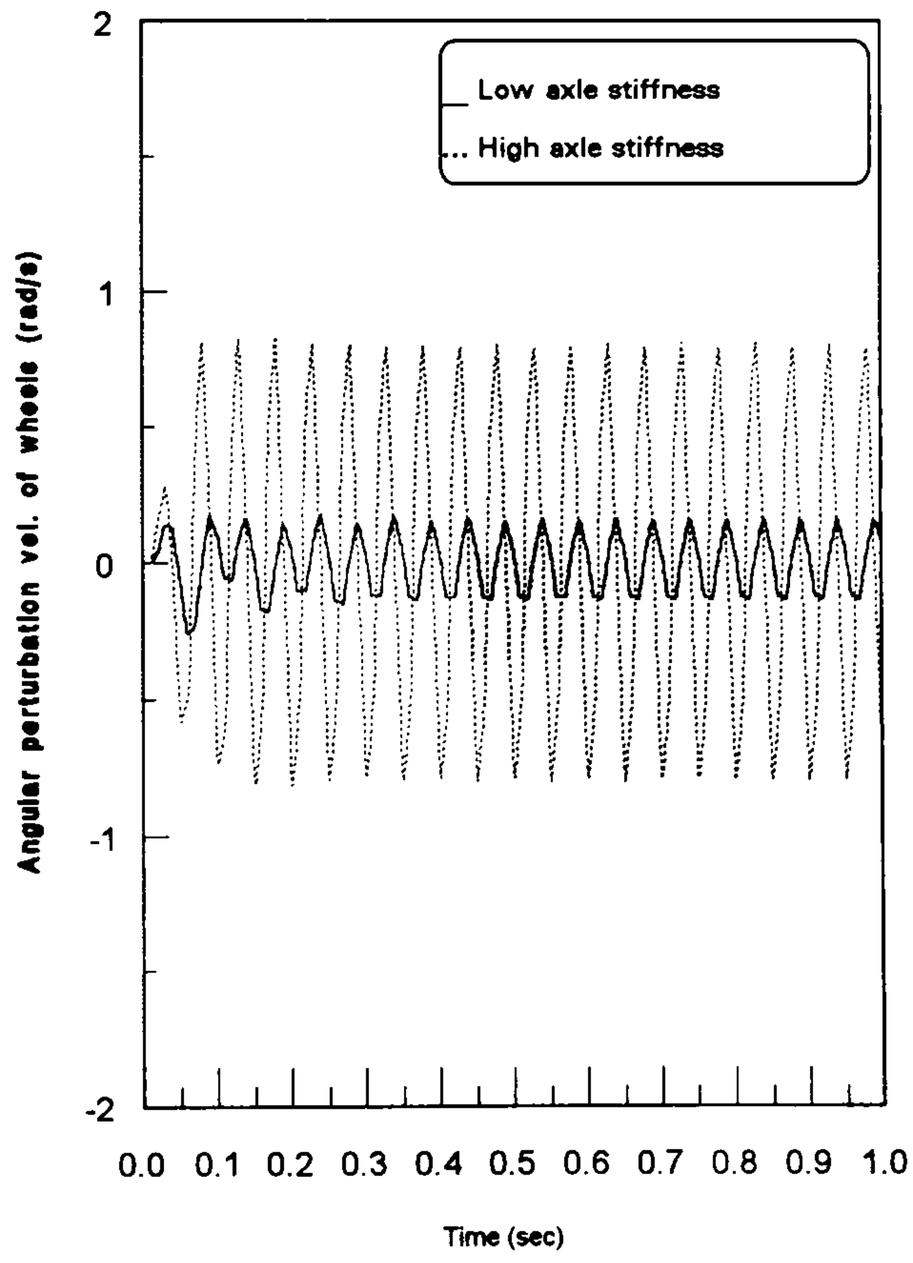

Fig (8.12) Effect of the axle stiffness on the system behaviour.

8.7.2-Transient Running

The same approach of simulation has been used to obtain the system behaviour during clutch engagement to confirm the model validity in the transient running conditions as well as in the steady running one. Figs (8.13) to (8.15) show the clutch disc time response for different gradients of friction coefficient and different system damping levels. Fig (8.13) shows that the system oscillates as a free damped vibratory system for zero and positive gradient values of friction coefficient, while for the negative gradient of the friction coefficient, the system may exhibit self excited vibrations and instability at a certain negative value of the gradient, Fig (8.14). On the other hand the system may be unstable even if the gradient of friction coefficient is zero when the system damping level decreases, Fig (8.15). These instabilities are because there are two sources of self excitation induced torque which provide energy to the system; clutch friction and tyre/road contact.

The obtained results confirm the same trends of the system behaviour as the investigation of the driveline system response during the clutch engagement, chapter 7.

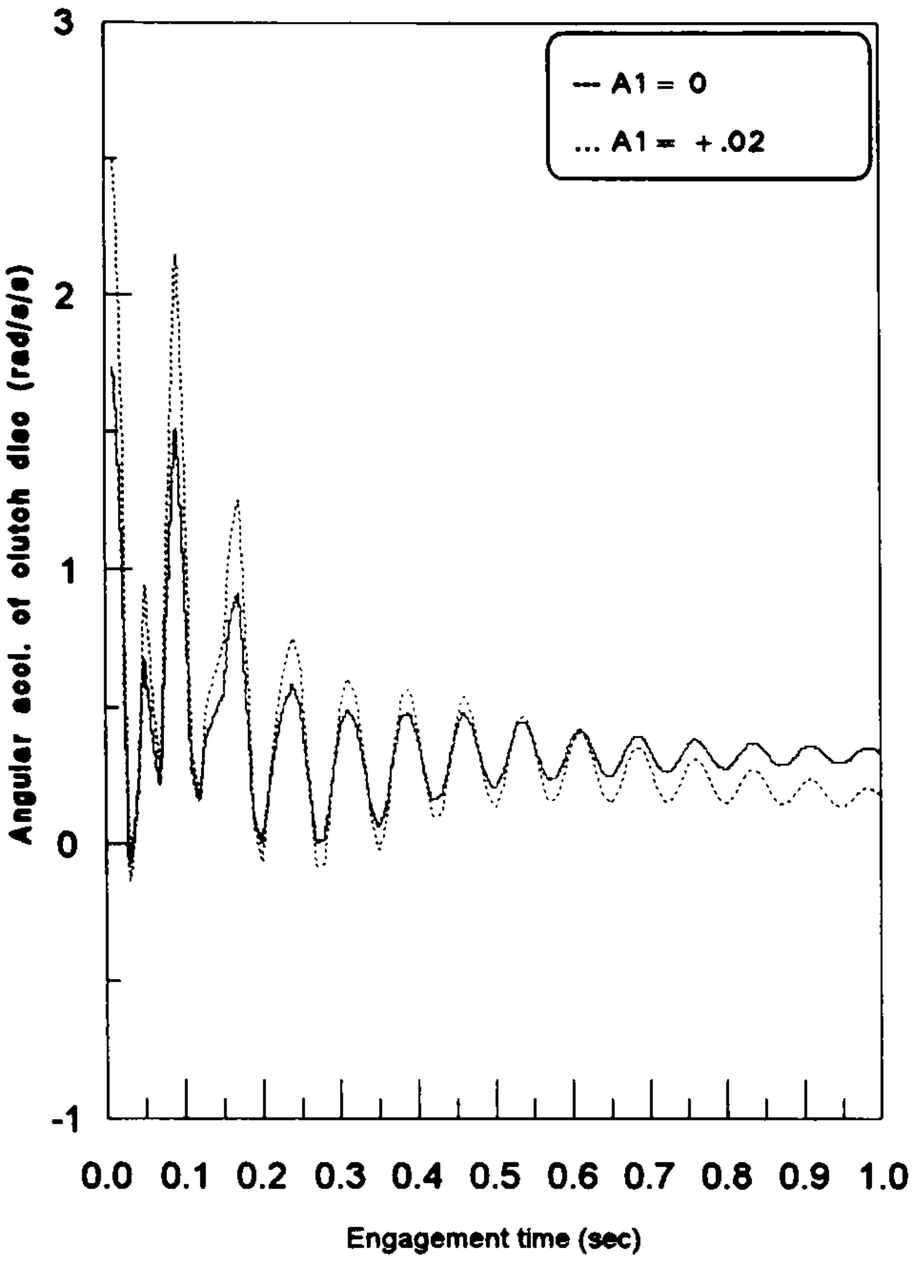

Fig (8.13) System response at zero and positive gradient of friction coefficient (A_1)

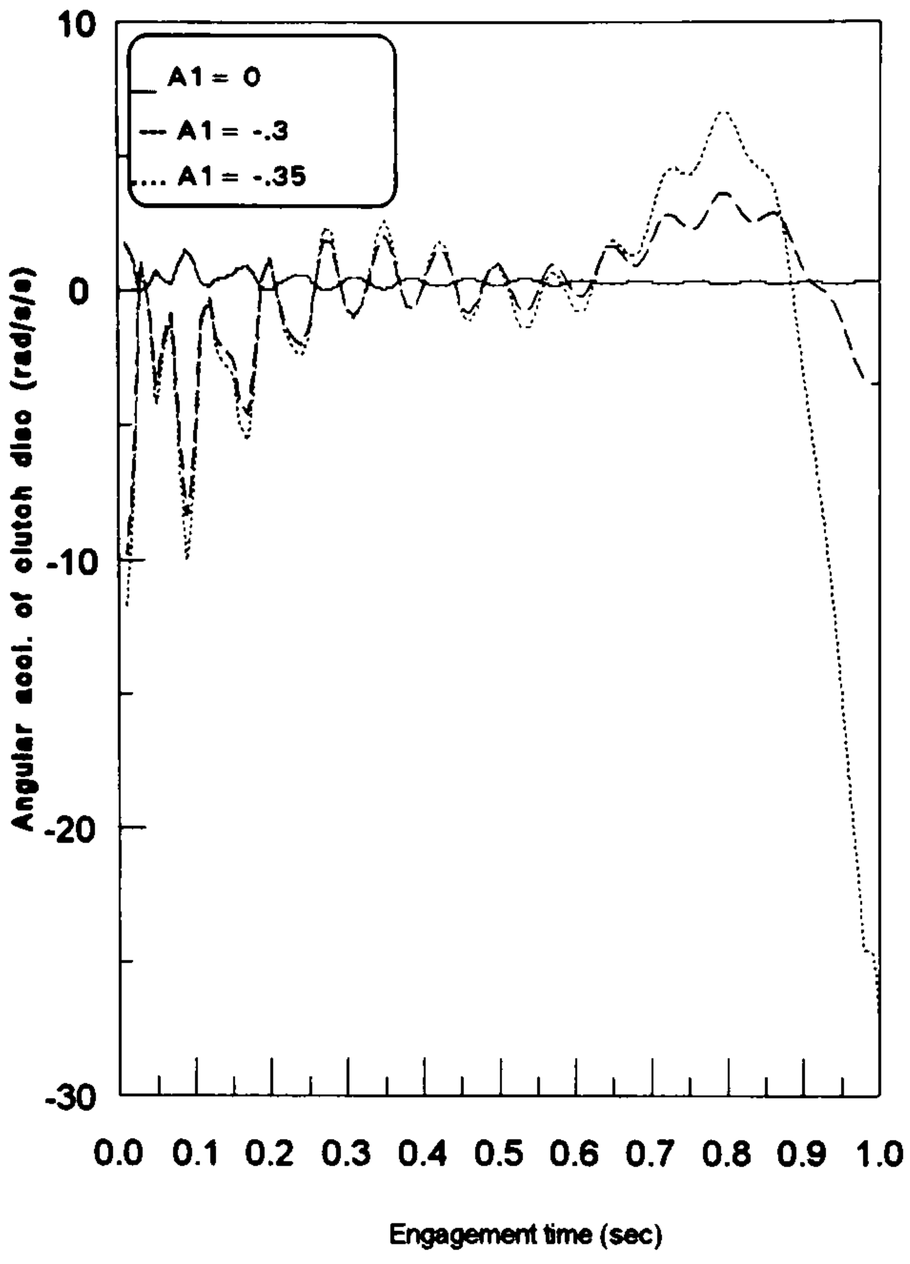

Fig (8.14) System response at different gradient of friction coefficient (A_1)

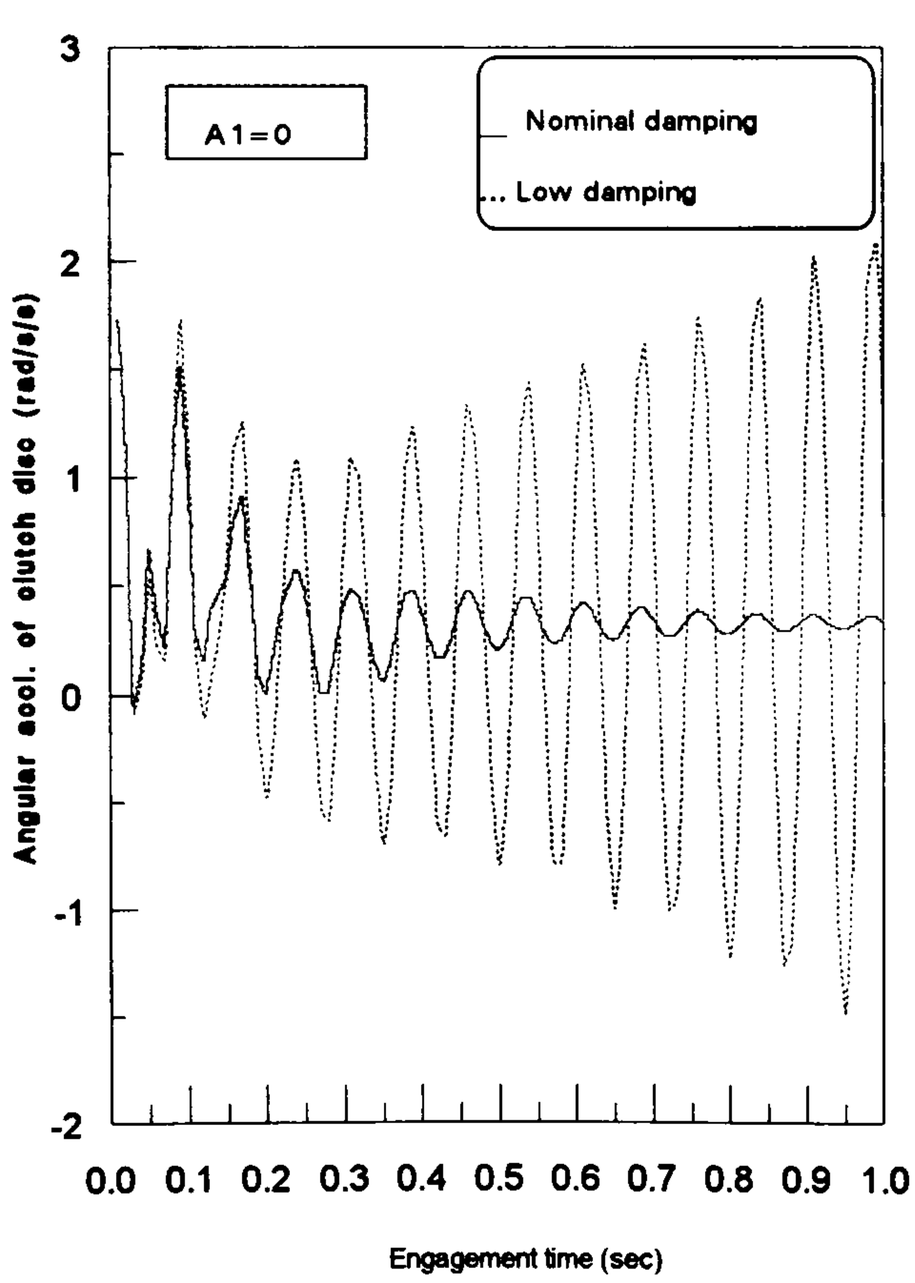

Fig (8.15) System response at zero gradient of friction coefficient and different levels of system damping

8.8-Summary

1. A mathematical model including torsional vibrations of the driveline system, vehicle body fore-aft vibrations and vertical vibrations has been developed in the last chapter to investigate and analyse the vibrational behaviour of the ways in which driveline can couple with other dynamic components. Two running conditions were investigated; steady running and transient running (during clutch engagement).

2. It was confirmed that the torsional vibrations of the driving wheels are valid as a measure of the fore-aft motion of the vehicle body (shunt phenomenon) in the model in which vehicle body motions were not included because the torsional motion of the wheel is directly related to the longitudinal motion of the vehicle.

3. The coupled model showed that two types of instabilities could occur depending on the system parameter values. The first was a self excited oscillation in the fore and aft direction of the vehicle which was heavily influenced by the tyre longitudinal force versus slip characteristics. The second was the torsional oscillation during clutch engagement discussed in chapter 7 which is coupled with the other body motions although not strongly.

4. Some parameters of the system, such as decreasing the axle stiffness, have a significant effect on reduction of the vibration level of the system. In general, high values of system damping tends to discourage self-excited vibrations and decreasing gradient of friction coefficient causes system instability.

5. This comprehensive model represents an important contribution of the work in this area of research in two ways. First, it clarifies understanding of the dynamic coupling between the rotational and translational components of the whole vehicle system. Second, it provides design information to tackle instability problems and to lead to reduction in overall vibration levels.

CHAPTER 9

GENERAL CONCLUSIONS AND FUTURE WORK

9.1-GENERAL CONCLUSIONS

This chapter attempts to draw together the conclusions obtained in each of the previous chapters.

9.1.1-Literature Review

In the literature, many of the problems associated with torsional vibrations and refinement in drivelines have been tackled through relatively simple, lumped mass models combined with experimental measurements. More recently, it has become increasingly common to use multibody system dynamics codes to develop more sophisticated models to assist understanding in ensuring high levels of refinement.

However, some problems remain, for example, coupling of torsional vibration of the driveline with suspension motions may causes shunt/shuffle problems. Although some simple lumped mass models have been derived, this problem is not yet fully understood.

Some vibrational phenomena such as shunt have been investigated through simple models incorporating engine throttle variations, although many of these phenomena arise due to clutch engagement. More understanding of the driveline system behaviour during clutch engagement is still required.

Although the transient operating condition of vehicles is one of the main causes of unwanted vibrations, publications concerned with the behaviour of driveline systems under these running conditions are relatively few. Therefore, more attention to the effects of transient behaviour is needed.

Parametric studies of the sensitivity of driveline system behaviour to changes in the design parameters have not proved satisfactory in providing guidelines for driveline designers in the early stages of the system design. Further work should be performed to analyse the sensitivity of driveline vibration problems to design parameter changes.

9.1.2-Driveline Components

In chapter 2, it was confirmed that the torsional vibration problems in the whole driveline system are closely related to the torsional vibration problems in the individual system components such as fluctuating engine torque, clutch judder, gearbox noise and fluctuating torque due to Hooke's joints. Therefore, it was concluded that it is not possible to understand the total system behaviour based on the behaviour of the individual component because they all interact dynamically. Hence, it is required to model the entire system to capture all the coupling effects.

9.1.3-Excitation Sources

Because it is crucial to the prediction of driveline behaviour since it provides the main forcing, a computer programme using MATLAB subroutines was developed to obtain this fluctuating torque for different engine parameters in chapter 3. The computer program was used throughout all later chapters for further study of the dynamic behaviour of the automotive driveline system.

9.1.4-Substructure Approach

In chapter 4, the substructure approach using the stiffness coupling technique, with combined use of residual flexibility and modal synthesis, was extended from two substructures to treat the general case with any number of substructures. The generalisation of this technique represents an important contribution to the study of complex, linear dynamic systems because it reduces the computational effort and time. This technique was embodied in a computer program, again using MATLAB subroutines, to facilitate its application to dynamic systems. This programme was subsequently used to study the driveline system vibration problems.

9.1.5-Linear System Model

In chapter 5, the total vehicle driveline system was analysed by deriving a model for the overall system based on an analysis of the separate components using the substructure approach. Using overall and substructured system models to study the behaviour of driveline systems indicated good agreement between results of the two

models. Using the substructure approach has shown that the natural frequencies and response of the vehicle driveline system in the range of normal vehicle operation may be obtained from considering only a few lower modes and residual flexibility of the higher modes of each component without significant error. This is very useful in reducing both the computational effort and time. There is good agreement between results for the overall system model and substructure model even for a few considered modes. This finding supports the effectiveness of the analysis technique (substructure technique) and feasibility of the computer programs for efficiently tackling problems of the dynamic behaviour of vehicle drivelines.

Unlike many other dynamic systems in which the forcing frequencies are fixed, by a constant running speed, the driveline vibration problem is more complicated because the engine speed varies over a wide range. Even at any given engine speed there are a range of forcing frequencies. Therefore, structural modifications aimed at changing the system natural frequencies to change the resonance of the torsional vibration of the driveline system are not really feasible in practice. However, because the system response is predictable, it opens up the opportunity in future to control this vibration using some sort of intelligent control system to control overall driveline system vibrations.

9.1.6-Effect of Non-linearities

A mathematical model of a vehicle driveline system including the important non-linear effects such as; backlash, non-linear spring stiffness, Hooke's joint and angularity of the propeller shaft was developed in chapter 6. The effect of backlash in the driveline system on the system torsional vibration levels is significant and, as expected, vibration levels increase as backlash increases. Hooke's joints in the driveline system were found to cause additional torsional vibration, however at the considered engine speed this vibration only became severe if the joint angle exceeded 15^{o}. The developed computer program may be used as a design tool to investigate the torsional vibrations of vehicle driveline systems including the effect of non-linear components.

The predicted results can be used to quantify the relative effects of different non-linearities and to rank their relative effects from a design viewpoint.

9.1.7-Engagement Problems

Clutch judder and shunt phenomena due to self excited torsional vibrations arising from the stick-slip phenomenon during engagement of the dry friction clutch were studied in chapter 7. It was found that these phenomena could be avoided by increasing the system damping or by decreasing the negative gradient of the friction coefficient. By increasing the axle shaft torsional stiffness and the clutch spring torsional stiffness, judder could be avoided.

This work, therefore, has lead to an improved understanding of these instabilities and to their relationship with design parameters. This modelling approach should be useful for tackling such refinement problems, examples of which still occur in practice. Because the dynamics of the system are predictable, it should in future be possible to control the torsional vibration instability during the engagement period using some sort of intelligent control system, sensing information related to the system and taking control action to modify the response into a subjectively acceptable form.

9.1.8-Comprehensive Driveline Model

A mathematical model including torsional vibrations of the driveline system, vehicle body fore-aft vibrations and vertical vibrations has been developed in the last chapter to investigate and analyse the vibrational behaviour of the ways in which driveline can couple with other dynamic components. Two running conditions were investigated; steady running and transient running (during clutch engagement). It was confirmed that the torsional vibrations of the driving wheels are valid as a measure of the fore-aft motion of the vehicle body (shunt phenomenon) in the model in which vehicle body motions were not included because the torsional motion of the wheel is directly related to the longitudinal motion of the vehicle.

The coupled model showed that two types of instabilities could occur depending on the system parameter values. The first was a self excited oscillation in the fore and aft

direction of the vehicle which was heavily influenced by the tyre longitudinal force versus slip characteristics. The second was the torsional oscillation during clutch engagement discussed in chapter 7 which is coupled with the other body motions although not strongly . In general, high values of system damping tend to discourage self-excited vibrations and increasing the negative gradient of friction coefficient causes system instability. Some parameters of the system, such as decreasing the axle stiffness, have a significant effect on reduction of the overall vibration level of the system.

This comprehensive model represents an important contribution of the work in this area of research in two ways. First, it clarifies understanding of the dynamic coupling between the rotational and translational components of the whole vehicle system. Second, it provides design information to tackle instability problems and to lead to reduction in overall vibration levels.

9.2-FUTURE WORK

From the author's point of view, the following work would to useful to extend this area of research;

1. The effect of the engine mountings on the driveline system behaviour should be included in the comprehensive model.

2. Details study of some component of the system such as the gearbox to include the gear rattle should be taken into consideration.

3. Different configurations of driveline system such as front wheel drive, four wheel drive , direct and indirect, etc.. gearbox should be considered.

4. A comprehensive model including all movements of the vehicle at different running conditions such as handling or cornering should be considered. Elasticity of chassis and torsional elasticity of the suspension should be taken into account.

5. Experimental work should be done to verify these theoretical results.

6. An optimisation technique should be incorporated in the computer program for optimising the system parameters to modify the system response. This will make it an even more useful design tool for the design of driveline systems.

7. An intelligent control system should be investigated which senses information related to the system and takes control action to modify the driveline system response during the engagement period.

REFERENCES

1. Gillespie, T. D., "Fundamentals of Vehicle Dynamics", Published by American Society of Automotive Engineering, Inc, 1992.

2. Chikamori, S. and Yoshikawa, N., "Noise and Vibration of Drive Train", JSAE Review, pp 51-62, Nov. 1980.

3. Hedges, J. L. and Butler, K. J., "A CAD System for the Analysis of Vehicle Driveline Noise", IMechE, C121/79, pp 39-46, 1979.

4. Mazziotti, P. J., "Dynamic Characteristics of Truck Driveline Systems", SAE, Paper No. 650189, pp 851-877, 1965.

5. Wu, H. L., et al, "A Study of the Torsional Vibration of Automotive Power Trains", Proc. of 2nd Int. pacific Conf. on Automotive Engng, Tokyo, pp 197-204, 7-10 Nov., 1983.

6. Birkett, C. A., et al, "Computer Simulation of Driveline Vibration Due to Universal Joints in Heavy and Medium Duty Truck", SAE SP-91/893, Paper No. 912700, pp 47-52, 1991.

7. Lu, Z. H., et al, "Theoretical Study of Structural Modification Control and Analytical Model Reduction of Torsional Vibration in FR-Type Automotive Power Drivetrain", XXV FISITA Congress, Technical Papers, Vehicle Dynamics, Beijing, pp 167-173, 17-21 Oct. 1994.

8. Crolla D. A, "Torsional Vibrations in Tractor Power-Take-off Drivelines", IMechE, C134/79, pp 91-97, 1979.

9. Crolla D. A., "Torsional Vibration Analysis of Tractor and Machine P.T.O. Drivelines", J. Agric. Engng. Res, Vol. 23, pp 259-272, 1978.

10. Bernard, D., et al, "Dynamic Modelling of the Transmission Line of an Agricultural Tractor", SAE, Paper No. 911779, pp 1-12, 1991.

11. Sykes, G. and Wyman, H. J., "The Dynamic Characteristics of Automobile Drivelines", Institution of Mechanical Engineering, C105, pp 102-111, 1971.

12. Ergun, S., "Torsional Vibrations of the Driveline of a Vehicle", MSc. Thesis, Granfield Institution of Technology, 1975.

13. Reik, W., "Torsional Vibrations in the Drive Train of Motor Vehicles, Principle Considerations", 4th International Symposium, Baden-Baden, pp 5-28, 20 April 1990.

14. Zhanoi, W., et al, "Research on the Coupling Power Train Torsional Vibration With Body Fore-Aft and Vertical Vibration of a 4x2 Vehicle", IMechE, C389/450, Vol. 2, Paper No. 925067, pp 219-223, 1992.

15. Parkins, D. W., "Automobile Drive-Line Vibration and Internal Noise", Annual Conf. of the stress Analysis Group of the Inst. of physics, "Stress, Vibration and Noise Analysis in Vehicles", pp 165-179.

16. Healy, S. P., et al, "An Experimental Study of Vehicle Driveline Vibrations", IMechE, Paper No. C132/79, pp 69-81, 1979.

17. Exner, W. and Amborn, P., "Noise and Vibration in the Driveline of Passenger Cars", IMechE Automotive Congress, Seminar 37, Paper No. C 427/37/025, 8 pages, 1991.

18. Tantot, G. and Chapon, S., "The Optimization of the Vibration of the Vibrational Dynamic Behaviour of Industrial Vehicle Power Trains", IMechE, C389/265, Vol. 2, Paper No. 925069, pp 231-238, 1992.

19. Stuecklschwaiger, W., et al, "Vibration Optimisation of Automotive Drivetrains", IMechE, Seminar 31, "Structural Dynamic Modelling", Vol. 1, pp 1-6, 1993.

20. Hong, C. W., "Dynamic Simulation of Road Vehicle Performance Under Transient Acceleration Conditions", Journal of Automotive Engineering, part D, proc Instn Mech Engs, Vol. 210, pp 11-21, 1996.

21. Ambrosi, G. and Orofino, L., "Automotive Driveline Vibration Analysis", XXIII, FISIA Congress, Torino (Haly), pp 2.507-2.515, 1990.

22. Ambrosi, G. and Orofino, L., "Driveline Vibration Simulation in a Four-Wheel Drive Vehicle. Total Vehicle Dynamics", IMechE, XXX IV FISITA Congress, London, Vol. 2, Paper No. 925088, C389/154, pp 105-115, 7-11 June 1992.

23. Schwibinger, P., et al, "Noise and Vibration Control Measures in the Powertrain of Passenger Cars", Proceeding of the 1991 Noise and Vibration Conference, Paper No. 911053, pp 123-131, 1991.

24. Fothergil, D.J. and Swierstra, N., "The Application of Non-Linear Displacements Modelling Techniques to an Automotive Driveline for the Investigation of Shunt", VDI Berichte, Nr 1007, pp 163-179, 1992.

25. Rooke, G.S., et al, "Computer Modelling of a vehicle Powertrain for Driveability Development", IMechE, Seminar 31, "Structural Dynamic Modelling", Vol. 1, pp 7-14, 1993.

26. Newcomb, T. P. and Spurr, R. T., "Clutch Judder", Proc. Int. Automobile Congress of FISITA, pp 1/16-1/18, 1972.

27. Lucas, G. and Mizon, R., "Clutch Manipulation During Engagement", Automotive Engineering, pp 81-85, April/May 1978.

28. Lucas, G. G. and Mizon, R., "A Modal of Clutch Engagement", IMechE, C147/79, pp 141-148, 1979.

29. Risbet, A., et al, "Engagement of Automobile Clutches: Experiments and Theory", Leeds-Lion Conference, Leeds, pp 285-292, 1982.

30. Maucher, P., "Clutch Chatter", 4th International Symposium, Baden-Baden, pp 109-124, 20 April 1990.

31. Kani, H., et al, "Analysis of the Friction Surface on Clutch Judder", JSAE Review, Vol. 13, No 1, pp 82-84, January 1992.

32. Szadkowski, A. and Morford, R. B., "Clutch Engagement Simulation: Engagement Without Throttle", SAE, Paper No. 920766, pp 103-117, 1992.

33. Sharp, R. S., "The Nature and Prevention of Axle Tramp", Proc. I Mech E, Vol. 184, No 3, pp 41-54, 1969-70.

34. Sharp, R. S. and Jones, C. J., "Self-Excited Vibrations of Truck Tandem Axle Suspension and Transmission System", Proc. 7th IAVSD Symposium on Dynamics of Vehicle on Roads and Tracks, Cambridge (UK), pp 66-80, Sept. 1981.

35. Sharp, R. S., "The Mechanics of Axle Tramping Vibrations", I Mech E, C137/84, pp 113-120, 1984.

36. Cranfiled Institute, Automotive Product Engineering, "Mechanical Engineering, Engines".

37. Okamura, K. S. and Shinno, A., "Dynamic Stiffness Matrix Method for the Three-Dimensional Analysis of Crankshaft Vibrations", IMechE International Conference, "Advances in the Control and Refinement of Vehicle Noise", C23/88, pp 95-108, March 1988.

38. Nagmatsu, A. and Nagaike, M., "Vibration Analysis of Movable Part of Internal Combustion Engine (Part 1 Crank Shaft)", JSME Bulletin, Vol. 24, No 198, pp 2141-2146, 1981.

39. Okamura, H., et al, "Simple Modelling and Analysis for Crankshaft Three-Dimensional Vibrations, part 1: Background and Application to Free Vibrations", Journal of Vibration and Acoustics, Vol. 117, pp 70-79, January 1995.

40. Morita, T. and Okamura, H., "Simple Modelling and Analysis for Crankshaft Three-Dimensional Vibrations, part 2: Application to an Operating Engine Crankshaft", Journal of Vibration and Acoustics, Vol. 117, pp 80-86, January 1995.

41. Okamura H, et al, "Experiments on the coupling and Transmission Behaviour of Crankshaft Torsional, Bending and longitudinal vibrations in High Speed Engines", Proc. of 2nd Int. pacific Conf. on Automotive Engng., Tokyo, pp 205-218, 7-10 Nov., 1983.

42. Welbourn, D. B., "Fundamental Knowledge of Gear Noise - A Survey", I Mech E, C117/79, pp 9-14, 1979.

43. Daly, K. J., and Smith, J. D., "Using Gratings in Driveline Noise Problems", IMechE, C118/79, pp 15-20, 1979.

44. Ozguven, H. N., "A Non-Linear Mathematical Model for Dynamic Analysis of Spur Gears Including Shaft and Bearing Dynamics", Journal of Sound and Vibration, Vol. 145, No 2, pp 239-260, 1991.

45. Brosey, T. G., et al, "Effect of Transmission Design on Gear Rattle and Shiftability", Int. J. of Vehicle Design, Vol. 7, No 1/2, pp 45-66, 1986.

46. Fudala, G.J., et al, "A system Approach to Reducing Gear rattle", SAE Technical Paper Series, Paper No 870396, PP 1-11, 1987.

47. Kato, M., et al, "Lateral-Torsional Coupled Vibrations of a Rotating Shaft Driven by a Universal Joint. (Derivation of Equations of Motion and Asymptotic Analysis)", JSME International Journal, Series III, Vol. 31, No 1, pp 68-74, 1988.

48. Kato, M. and Ota, H., "Lateral Excitation of a Rotating Shaft Driven by a Universal Joint With Friction", ASME Journal of Vibration and Acoustics, Vol. 112, pp 298-303, July 1990.

49. Otake, T., et al, "Prediction of Torsional Vibration Caused by Hook's Joint in Drive Train Total Vehicle Dynamics", IMechE XXX IV FISITA Congress, London, Vol. 1, Paper No. 925068, C389/223, pp 25-230, 7-11 June 1992.

50. Yamamoto, T., et al, "Efficiency of Constant Velocity Universal Joints", SAE International, “Automotive Transmissions and Drivelines”, SP-965, No 930906, pp 131-139, 1993.

51. Wilson, K. W, "Practical Solution of Torsional Vibration Problems", Chapman & Hall LTD, London, 3 rd Edition, Vol. 1, 1956.

52. Patterson, D., "Engine Torque and Balance Characteristics", SAE, Paper No. 821575, pp 51-57, 1982.

53. Nestorides, E. J., "A Handbook on Torsional Vibration", B.I.C.E.R.A. Research Laboratory, Cambridge University Press, 1958.

54. Nurhad, I. and Seireg, A., "Gear Noise Simulation Using a Displacement Based Finite Element Method", SAE Proceeding of the 4 th. Inter. Pacific Conference on Autom. Engng., Vol. 1, pp 201.1-201.5, 8-14 Nov., 1987.

55. Iida, H., et al, "Coupled Torsional-Flexural Vibration of a Shaft in a Geared System of Rotors (1 st Report)", JSME Bulletin, Vol. 23, No 186, pp 2111-2117, Dec. 1980.

56. Nevzt, H. and Houser, D., "Dynamic Analysis of High Speed Gears by Using Loaded Static Transmission Error", J. of Sound and Vibration, Vol. 125, No 1, pp 71-83, 1988.

57. Gilmartin, M., "Constant-Velocity Joints", Technical File No 50, Engineering, pp I-VIII, Feb. 1978.

58. Johnoson, D. A. and Willems, P. Y., "On the Necessary and Sufficient Conditions for Homokinetic Transmission in Chains of Cardan Joints", Journal of Mechanical Design, Transactions of the ASME, Vol. 115, pp 255-261, 1993.

59. Newton, K., et al, "The motor Vehicle", Butterworth, London, 10 th Edition, 1983.

60. Wilson, K. W., "Practical Solution of Torsional Vibration Problems", Chapman & Hall LTD, London, 3 rd Edition, Vol. 2, 1963.

61. Lim, B., et al, "Estimation of the Cylinder Pressure in a SI Engine Using the Variation of Crankshaft Speed", SAE, Paper No. 940145, pp 23-32, 1994.

62. Wu, J. S. and Chen, W. "Computer Method for Forced Torsional Vibration of Propulsive Shafting System of Marine Engine With and Without Damping", Journal of Ship Research, Vol. 26, No 3, pp 176-189, Sep. 1982.

63. Rizzoni, G., "Estimate of Indicated Torque from Crankshaft Speed Fluctuations: a Model for the Dynamics of the IC Engine", IEEE Transactions on Vehicular Technology, Vol. 38, No 3, pp 168-179, Aug. 1989.

64. Hurty, W. C., "Dynamic Analysis of Large Structures by Modal Synthesis Techniques", Computer and Structure Journal, Vol. 1, pp 535-563, 1971.

65. Hart, G. C., et al, "A Survey of Modal synthesis Methods", SAE National Aeronautic and Space Engineering Meeting, Los Angeles, California, Paper No. 710783, pp 1-7, 28-30 Sept. 1971.

66. Nagmatsu, A., et al, "Analysis of Vibration by Substructure Synthesis Method (Part 3, Application to Diesel Generator Package)", JSME Bulletin, Vol. 27, No 229, pp 1487-1492, 1984.

67. Ookuma, M. and Nagmatsu, A., "Analysis of Vibration by Substructure Synthesis Method (Part 4, Calculation of Residual Compliance Matrix)", JSME Bulletin, Vol. 28, No 239, pp 905-910, 1985.

68. Maher, A., et al, "On the Combined Use of Residual Flexibility and Modal Synthesis Techniques for Large Structures", 2 nd ASAT Conference, MTC, Cairo, Egypt, pp 597-607, 21-23 Apr. 1987.

69. Pacejka, H. B., "Tyre Factors and Front Wheel Vibrations", Int. Journal of Vehicle Design, Vol. 1, No 2, pp 97-119, 1980.

70. Duncan, A. E., "Application of Modal Modelling and Mount System Optimization to Light Duty Truck Ride Analysis", SAE Paper No. 811313, PP 4075-4090, 1981.

APPENDIX-A

COUPLING OF TWO SUBSTRUCTURES

A-1-INTRODUCTION

In this appendix, coupling of two substructures based on the stiffness coupling, with combined use of residual flexibility and modal synthesis, technique published in [68] is demonstrated. It is supposed that a structure composed of two substructures namely; sub-1 and sub-2. Each substructure is divided into two parts, namely, the interior region called the region "i" and interface or common region called "j" see Fig (A.1).

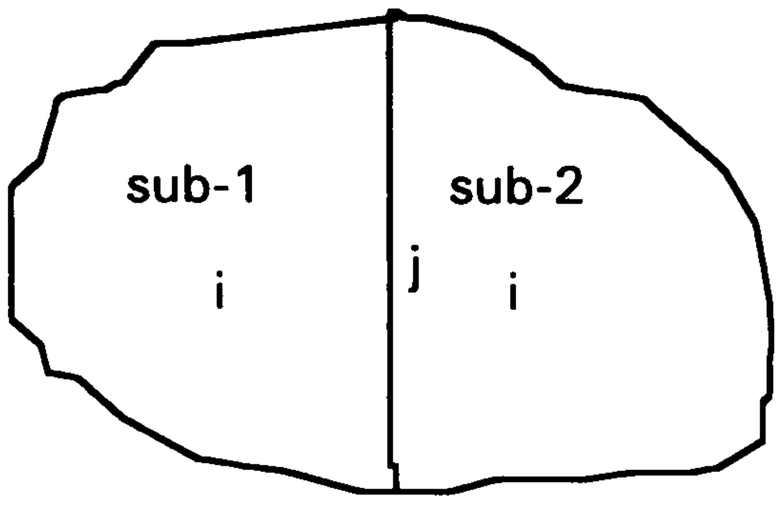

Fig (A.1) A structure composed of two substructures

The stiffness coupling method in which the structure is presented by a number of substructures connected through flexible links is suggested by Duncan [71] and developed to include the residual flexibility and modal synthesis by Maher, et al [68]. The method employs free component vibration modes. In other words the coupling is performed using physical flexible links between interface degrees of freedom represent the elastic connection at interface degrees of freedom "j" and/or fictitious link of flexibility equal to the sum of the residual flexibilities of both substructures at interface degrees of freedom, i.e. the residual flexibility from both substructures can be reduced to a single equivalent flexibility at the interface. Same notations of chapter 4 are used in this appendix.

A-2-EQUATION OF MOTION

The equation of motion of s th substructure is;

$$^{s}[M]\ ^{s}\{\ddot{x}\}+^{s}[C]\ ^{s}\{\dot{x}\}+^{s}[K]\ ^{s}\{x\}=^{s}\{F(t)\} \qquad (A.1)$$

where ${}^{s}[M]$, ${}^{s}[C]$ and ${}^{s}[K]$ are (NsxNs) mass, damping and stiffness matrices for s-th substructure respectively; ${}^{s}\{x\}$, ${}^{s}\{\dot{x}\}$ and ${}^{s}\{\ddot{x}\}$ are (Nsx1) vectors of nodal displacements, velocities and accelerations of s th substructure respectively and ${}^{s}\{F(t)\}$ is (Nsx1) vector of applied time-varying external load at nodal points of s th substructure.

The mass, damping and stiffness matrices can be split into sub matrices corresponding to interior and interface degrees of freedom, and the equation of motion of each substructure is ;

$$ {}^{s}\left[\begin{array}{c|c} [M_{ii}] & [M_{ij}] \\ \hline [M_{ji}] & [M_{jj}] \end{array}\right] {}^{s}\left\{\begin{array}{c} \ddot{x}_i \\ \hline \ddot{x}_j \end{array}\right\} + {}^{s}\left[\begin{array}{c|c} [C_{ii}] & [C_{ij}] \\ \hline [C_{ji}] & [C_{jj}] \end{array}\right] {}^{s}\left\{\begin{array}{c} \dot{x}_i \\ \hline \dot{x}_j \end{array}\right\} + {}^{s}\left[\begin{array}{c|c} [K_{ii}] & [K_{ij}] \\ \hline [K_{ji}] & [K_{jj}] \end{array}\right] {}^{s}\left\{\begin{array}{c} x_i \\ \hline x_j \end{array}\right\} = {}^{s}\left\{\begin{array}{c} F_i(t) \\ \hline F_j(t) \end{array}\right\} \qquad (A.2) $$

where ${}^{s}\{x_i\}$ is the displacement vector at the corresponding to internal degrees of freedom of s th substructure, ${}^{s}\{x_j\}$ is the displacement vector at the corresponding to interface degrees of freedom of s th substructure, ${}^{s}\{F_j\}$ is the load vector at the connection or interface degrees of freedom of s th of substructure, ${}^{s}\{F_i\}$ is the load vector at the internal degrees of freedom of s th substructure and Ns is the number of total DOFs of s th substructure.

A-3-UNCOUPLED EQUATIONS

The solution of the free undamped vibration of the s th substructure is performed to obtain a set of the normal mode shapes (ns) and corresponding natural frequencies. Then the uncoupled transformed equations of the s th substructure in terms of the modal co-ordinates, {y}, corresponding to retained modes, ns, can be obtained as;

$$ {}^{s}[m]_{ns}\ {}^{s}\{\ddot{y}\}_{ns} + {}^{s}[c]_{ns}\ {}^{s}\{\dot{y}\}_{ns} + {}^{s}[k]_{ns}\ {}^{s}\{y\}_{ns} = {}^{s}[\phi]_{ns}^{T}\ {}^{s}\{F(t)\} \qquad (A.3) $$

where ${}^{s}[m]_{ns} = {}^{s}[\phi]_{ns}^{T}\ {}^{s}[M]\ {}^{s}[\phi]_{ns}$ is the (nsxns) generalised mass matrix of the s-th substructure corresponding to retained modes, ns,

${}^s[c]_{ns}={}^s[\phi]_{ns}^T\ {}^s[C]\ {}^s[\phi]_{ns}$ is the (nsxns) generalised damping matrix of the s-th substructure corresponding to retained modes, ns,

${}^s[k]_{ns}={}^s[\phi]_{ns}^T\ {}^s[k]\ {}^s[\phi]_{ns}$ is the (nsxns) generalised stiffness matrix of the s-th substructure corresponding to retained modes, ns,

${}^s\{F(t)\} = \{{}^s\{F_i\}\quad {}^s\{F_j\}\}^T$ is the (Nsx1) total load vector of s th substructure and ${}^s[\phi]_{ns}$ is the (Nsxns) modal matrix of retained modes, ns, of s-th substructure.

The uncoupled equations corresponding to the interface degrees of freedom 'j' are;

$${}^s[m_j]_{ns}\ {}^s\{\ddot{y}_j\}_{ns}+{}^s[c_j]_{ns}\ {}^s\{\dot{y}_j\}_{ns}+{}^s[k_j]_{ns}\ {}^s\{y_j\}_{ns}={}^s[\phi_j]_{ns}^T\ {}^s\{F_j\} \qquad (A.4)$$

where; ${}^s[m_j]_{ns}$, ${}^s[c_j]_{ns}$ and ${}^s[k_j]_{ns}$ are generalised mass, damping and stiffness matrices corresponding to interface DOFs respectively.

The (jx1) interface displacement vector of s th substructure is;

$${}^s\{x_j\}={}^s[\phi_j]_{ns}\ {}^s\{y\}_{ns}+{}^s[G_j]_{sh}\ {}^s\{F_j\} \qquad (A.5)$$

where

${}^s[G_j]_{sh}$ is the (jxj) static residual flexibility matrix corresponding to the interface co-ordinates due to the omitted higher modes of s th substructure,

${}^s[\phi_j]_{ns}$ is the (jxns) matrix of the retained normal modes, ns, corresponding to the interface degrees of freedom "j" of s th substructure and

${}^s\{y\}_{ns}$ is the (nsx1) vector of retained modal modes, ns, of s th substructure.

A-4-COUPLING CONDITIONS

Both compatibility and equilibrium conditions at the interface region "j" of two substructures sub-1 and sub-2 must be satisfied for modal coupling, i.e.;

$$\begin{aligned} &{}^1\{x_j\}={}^2\{x_j\} \quad \text{and} \\ &{}^1\{F_j\}+{}^2\{F_j\}=0 \end{aligned} \qquad (A.6)$$

Applying the interface displacement vector expression, (A.5), for substructures 1 and 2 in the compatibility and equilibrium equations, (A.6), gives;

$$^{1}[\phi_j]_{n1}\ ^{1}\{y\}_{n1}+^{1}[G_j]_{sh}\ ^{1}\{F_j\}=^{2}[\phi_j]_{n2}\ ^{2}\{y\}_{n2}+^{2}[G_j]_{sh}\ ^{2}\{F_j\}$$

or

$$^{1}[\phi_j]_{n1}\ ^{1}\{y\}_{n1}-^{2}[\phi_j]_{n2}\ ^{2}\{y\}_{n2}=(^{2}[G_j]_{sh}+^{1}[G_j]_{sh})\ ^{2}\{F_j\}$$

So;

$$\left.\begin{aligned}&^{2}\{F_j\}=(^{2}[G_j]_{sh}+^{1}[G_j]_{sh})^{-1}\ (^{1}[\phi_j]_{n1}\ ^{1}\{y\}_{n1}-^{2}[\phi_j]_{n2}\ ^{2}\{y\}_{n2})=[k_j](^{1}[\phi_j]_{n1}\ ^{1}\{y\}_{n1}-^{2}[\phi_j]_{n2}\ ^{2}\{y\}_{n2})\\ &\text{and}\\ &^{1}\{F_j\}=(^{2}[G_j]_{sh}+^{1}[G_j]_{sh})^{-1}\ (^{2}[\phi_j]_{n2}\ ^{2}\{y\}_{n2}-^{1}[\phi_j]_{n1}\ ^{1}\{y\}_{n1})=[k_j](^{2}[\phi_j]_{n2}\ ^{2}\{y\}_{n2}-^{1}[\phi_j]_{n1}\ ^{1}\{y\}_{n1})\end{aligned}\right\} \quad (A.7)$$

where $[k_j]$ is the static residual stiffness matrix corresponding to the omitted higher modes (n_1+n_2) in both substructures sub 1 and sub 2 , $[k_j]=(^{1}[G_j]_{sh}+^{2}[G_j]_{sh})^{-1}$,

If there is an elastic connection with stiffness matrix $[k_c]$ between the substructures sub 1 and sub 2, the total equivalent flexibility connection matrix is the sum of residual flexibility corresponding to the omitted higher modes and the physical interface connection flexibility, i.e. $[k_j]$ is defined by this expression;

$$[k_j]=(^{1}[G_j]_{sh}+^{2}[G_j]_{sh}+[k_c]^{-1})^{-1} \quad (A.8)$$

Note that, if the flexibility of the interface connection is large compared to the residual flexibility due to the higher omitted modes, then the equivalent residual flexibility, $[k_j]$, is close to that of the interface connection alone and vice versa. The literature review of this subject shows that the residual flexibility has a significant effect on the results when it approaches the same value of the interface connection flexibility.

Modal couplings are performed by eliminating the terms of interface loads at connection from equations of motion through the compatibility relations as follow;

substituting the expressions of $^{1}\{F_j\}$ and $^{2}\{F_j\}$, Eqn (A.7), in these uncoupled equations for sub 1 and sub 2, i.e.;

$${}^{1}[m]_{n1}\ {}^{1}\{\ddot{y}\}_{n1}+{}^{1}[c]_{n1}\ {}^{1}\{\dot{y}\}_{n1}+{}^{1}[k]_{n1}\ {}^{1}\{y\}_{n1}={}^{1}[\phi_j]^{T}_{n1}\ {}^{1}\{F_j\}+{}^{1}[\phi_i]^{T}_{n1}\ {}^{1}\{F_i\} \qquad \text{and}$$

$${}^{2}[m]_{n2}\ {}^{2}\{\ddot{y}\}_{n2}+{}^{2}[c]_{n2}\ {}^{2}\{\dot{y}\}_{n2}+{}^{2}[k]_{n2}\ {}^{2}\{y\}_{n2}={}^{2}[\phi_j]^{T}_{n2}\ {}^{2}\{F_j\}+{}^{2}[\phi_i]^{T}_{n2}\ {}^{2}\{F_i\}$$

A-5-TOTAL SYSTEM EQUATIONS

Thus, replacing ${}^{1}\{F_j\}$ and ${}^{2}\{F_j\}$ by the above in the uncoupled equations of motions expressions and arrangement the equations, the total system equations are;

$$\left.\begin{array}{l}
\left[\begin{array}{c|c} {}^{1}[m]_{n1} & [0] \\ \hline [0] & {}^{2}[m]_{n2} \end{array}\right]\left\{\begin{array}{c} {}^{1}\{\ddot{y}\}_{n1} \\ \hline {}^{2}\{\ddot{y}\}_{n2} \end{array}\right\}+\left[\begin{array}{c|c} {}^{1}[c]_{n1} & [0] \\ \hline [0] & {}^{2}[c]_{n2} \end{array}\right]\left\{\begin{array}{c} {}^{1}\{\dot{y}\}_{n1} \\ \hline {}^{2}\{\dot{y}\}_{n2} \end{array}\right\}+ \\
\left[\begin{array}{c|c} {}^{1}[k]_{n1}+{}^{1}[\phi_j]^{T}_{n1}\ [k_j]\ {}^{1}[\phi_j]_{n1} & -{}^{1}[\phi_j]^{T}_{n1}\ [k_j]\ {}^{2}[\phi_j]_{n2} \\ \hline -{}^{2}[\phi_j]^{T}_{n2}\ [k_j]\ {}^{1}[\phi_j]_{n1} & {}^{2}[k]_{n2}+{}^{2}[\phi_j]^{T}_{n2}\ [k_j]\ {}^{2}[\phi_j]_{n2} \end{array}\right]\left\{\begin{array}{c} {}^{1}\{y\}_{n1} \\ \hline {}^{2}\{y\}_{n2} \end{array}\right\} \\
=\left\{\begin{array}{c} \{{}^{1}[\phi_i]^{T}_{n1}\{F_i\}_{n1}\} \\ \hline \{{}^{2}[\phi_i]^{T}_{n2}\{F_i\}_{n2}\} \end{array}\right\}
\end{array}\right\} \qquad (A.9)$$

These equations are now the analytical model of the whole system. Notice that, the necessary quantities to form these equations are obtained from dynamic analysis of the two substructures or experimental test of them. In other words, the behaviour of the entire structure has been obtained in terms of the behaviour of each substructure.

The recovery of the physical modal matrix for s-th substructure is accomplished by the transformation; ${}^{s}[x]={}^{s}[\phi]_{ns}\ {}^{s}[y]_{ns}$

where ${}^{s}[\phi]_{ns}$ is the (Ns x ns) modal matrix of the retained modes, ns, of s th substructure, ${}^{s}[x]$ is the (Ns x n) contribution matrix of s th substructure in the total physical modal matrix of the system and ${}^{s}[y]_{ns}$ is the (ns x n) matrix of mode shape of the total system equation corresponding to s th substructure.

The total modal matrix becomes;

$$[x]=\left[{}^{1}[x]\ \ {}^{2}[x]\right]^{T} \qquad (A.10)$$

Appendix B

Published Papers

PUBLISHED PAPERS

1. "**Analysis of Automotive Driveline Vibration Using a Sub-Structure Approach**", Bull. of the Faculty of Engng. & Tech., Minia, Egypt, Vol. 17, No 2 1995.

2. "**Investigation of the Clutch Judder and Shunt Phenomena**", Bull. of the Faculty. of Engng. & Tech., Minia, Egypt, Vol. 17, No. 2, 1995.

3. "**Investigation of Coupling of Vehicle Driveline Torsional Vibration with the Vehicle Body Vibration**", Seventh AMME Conference, Third International, Military Technical college, Cairo, Egypt, 28-30 May 1996.

4. "**Intelligent Control of Clutch Judder and Shunt Phenomena in Vehicle Drivelines**", International Journal of Vehicle Design, Vol. 17, No. 3, 1996, pp 318-332.

5. "**Coupling of Driveline and Body Vibration in Trucks**", SAE International Trucks & Bus Conference, Detroit MI, USA, 14-16 Oct. 1996.

6. "**Non-Linear Torsional Vibration of Vehicle Driveline Systems**", SAE Passenger Car Conference, Detroit MI, USA, 24-27 Feb. 1997.